



Terms and Conditions of Use of Digitised Theses from Trinity College Library Dublin

Copyright statement

All material supplied by Trinity College Library is protected by copyright (under the Copyright and Related Rights Act, 2000 as amended) and other relevant Intellectual Property Rights. By accessing and using a Digitised Thesis from Trinity College Library you acknowledge that all Intellectual Property Rights in any Works supplied are the sole and exclusive property of the copyright and/or other IPR holder. Specific copyright holders may not be explicitly identified. Use of materials from other sources within a thesis should not be construed as a claim over them.

A non-exclusive, non-transferable licence is hereby granted to those using or reproducing, in whole or in part, the material for valid purposes, providing the copyright owners are acknowledged using the normal conventions. Where specific permission to use material is required, this is identified and such permission must be sought from the copyright holder or agency cited.

Liability statement

By using a Digitised Thesis, I accept that Trinity College Dublin bears no legal responsibility for the accuracy, legality or comprehensiveness of materials contained within the thesis, and that Trinity College Dublin accepts no liability for indirect, consequential, or incidental, damages or losses arising from use of the thesis for whatever reason. Information located in a thesis may be subject to specific use constraints, details of which may not be explicitly described. It is the responsibility of potential and actual users to be aware of such constraints and to abide by them. By making use of material from a digitised thesis, you accept these copyright and disclaimer provisions. Where it is brought to the attention of Trinity College Library that there may be a breach of copyright or other restraint, it is the policy to withdraw or take down access to a thesis while the issue is being resolved.

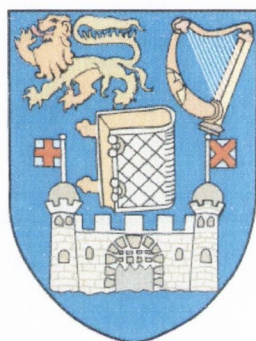
Access Agreement

By using a Digitised Thesis from Trinity College Library you are bound by the following Terms & Conditions. Please read them carefully.

I have read and I understand the following statement: All material supplied via a Digitised Thesis from Trinity College Library is protected by copyright and other intellectual property rights, and duplication or sale of all or part of any of a thesis is not permitted, except that material may be duplicated by you for your research use or for educational purposes in electronic or print form providing the copyright owners are acknowledged using the normal conventions. You must obtain permission for any other use. Electronic or print copies may not be offered, whether for sale or otherwise to anyone. This copy has been supplied on the understanding that it is copyright material and that no quotation from the thesis may be published without proper acknowledgement.

**CALIX[4]ARENE-BASED HOSTS FOR
LANTHANIDE AND ANION BINDING:
SYNTHESIS AND PHYSICAL STUDIES**

Eoin Quinlan

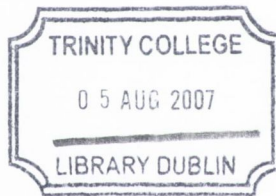


**School of Chemistry
Trinity College**

A thesis submitted to the University of Dublin for the degree of
Doctor of Philosophy

Based on research conducted under supervision of
Dr Susan E. Matthews & Prof. Thorfinnur Gunnlaugsson

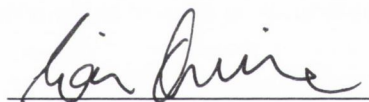
January 2007



THESIS
8162

Declaration

This thesis is submitted to the University of Dublin for the degree of Doctor of Philosophy and has not been previously submitted at this, or any other university for assessment or for any other degree. Except where stated, and reference or acknowledgement is given, this work is original and has been carried out by the author alone. I agree that the Library may freely lend or copy this thesis upon request.

A handwritten signature in black ink, appearing to read 'Eoin Quinlan', is written over a horizontal line.

Eoin Quinlan

Abstract

This thesis, entitled "Calix[4]arene-based hosts for lanthanide and anion binding: synthesis and physical studies" is divided into five chapters.

Chapter 1 provides an introduction to the chemistry of calix[4]arenes, an introduction to lanthanide-binding ligands, with emphasis on MRI application, and to anion sensing. The advantages to contrast agent development offered by the enhanced permeation and retention (EPR) effect of tumours is outlined. This chapter also describes the various intentions and aims of this work.

Chapter 2 provides detailed accounts of the methods which were used to derivatise the lower rim of calix[4]arene to achieve a binding array suitable for the complexation of lanthanide ions. A number of attempts to form lanthanide complexes using the ligands which have been synthesised are discussed, in addition to preliminary solution-state photochemical measurement which was undertaken.

Chapter 3 both develops and complements the work of Chapter 2 in discussing the efforts which were undertaken to incorporate upper-rim functionality into the hosts of the type outlined in Chapter 2. This was with the overall objective of incorporation of these species into biologically relevant macromolecules, with the objective of harnessing the benefits of the EPR effect of solid tumours.

Chapter 4 deals with the anion binding aspect of this project, specifically the synthesis and evaluation of a series of calix[4]arene-based semicarbazides. Various calix[4]arene-based and acyclic semicarbazides were synthesised and their anion-binding efficacy in DMSO solution was studied. These results, in addition to proposed binding modes elucidated by the preparation of several structural analogues are discussed.

Chapter 5, the final chapter, details experimental procedures which were developed for the synthesis and evaluation of the compounds and procedures which were discussed in the previous three chapters. Finally, references to the literature are provided.

The appendix provides crystallographic data obtained in the course of the work of Chapter 2 in addition to UV-Vis and derived titration data obtained from the studies in Chapter 4.

Acknowledgements

I have been fortunate to have been supported on this journey by excellent supervision. I am indebted to Dr Susan Matthews for giving me the opportunity to undertake this project. Her enthusiasm and ability to see the positives in everything have been invaluable. I am equally appreciative of the support of Prof. Thorri Gunnlaugsson, who stepped in later on, and was able to supply his own brand of enthusiasm, a brand new lab, and an array of UV instruments for the anion work. To both supervisors, I say a heart-felt thank you, and look forward to your continued friendship.

I wish to thank the executive of the School of Chemistry for use of departmental resources, the office staff (Corinne, Helen and Tess), Thanks to Dr John O'Brien for the countless NMR spectra, and Dr Manuel Reuther for the later stage urgent-characterisations. Thanks are also due to Dr Martin Feeney for the assistance with mass spectrometry. I appreciate also the help offered by Teresa McDonnell, Brendan Barry and Peggy Brehon with valuable technical assistance (and quibble-free equipment loans).

For the numerous crystal structures contained herein, a grateful special mention goes to Dr Tom McCabe.

I'd like to also thank Trinity College for a postgraduate award.

Debbie. Other half of the Matthews Group. Thank you for brightening up the lab over the years.

The old Top Lab was a pleasant place to work, not only because of the steady flow of water from the rafters, and the gentle breezy draft, but also due to those who shared the space. I thank Úna and Dorothy each for a few years worth of conversation and friendship, in particular in the first year or so.

And everyone in Thorri's group, past and present: Andrew, Ann-Marie, Céline, Célia, Christophe, Cidália, Claire, Danni, Doireann, Emma, Jennifer, Joe, Julie, Flo, Gary, Lin, Lisa, Niamh, Rebecca, Sally, Susan and Julien – for giving me a great atmosphere both in and outside of work. Thanks to Ruth and Estelle for admitting me to their lab, and showing me the ropes at UEA for six weeks. Thanks also to Shay for his enlightening discussions in the old lab.

To those friends who drank (coffee, usually) with me: Áine, Rowan, Hugh, Michael & Isabel – it's true that the time spent out of the lab is the most important, intellectually speaking.

To a few of those who have somehow found their lives complete without involvement of Trinity's School of Chemistry; I both wonder how this is possible, and thank you for friendship, lunches, and continued support during the production of this thesis: Elizabeth, Luke, Gráinne, James, Alan, Ruth, Blaize and Deirdre.

Finally. Thanks to the people who see me most, and at that, only ever outside of the lab – my family. In particular, thanks are due to my parents, Marian & Ronan for their constant support throughout my extended stay at big-school, and for realising they should refrain from asking about the progress of a thesis. Well that's that. I'm finished. Ask away.

Abbreviations used in this text

Å	ångström (1×10^{-10} m)
AcO ⁻	acetate (CH ₃ CO ₂ ⁻) anion
Boc	<i>tert</i> -butoxycarbonyl
BSA	bovine serum albumin
^t Bu	<i>tert</i> -butyl, -C(CH ₃) ₃
CMPO	<i>N,N</i> -diisobutylcarbamoymethyloctylphenyl phosphine oxide
CNS	central nervous system
COSY	correlation spectroscopy
d	doublet (NMR)
DCC	dicyclohexylcarbodiimide
DEPT	distortionless enhancement polarisation transfer
DMF	<i>N,N</i> -dimethylformamide
DMSO	dimethylsulfoxide
EPR	enhanced permeability and retention (effect)
equiv.	equivalent
ESMS	electrospray mass spectrometry
EtOAc	ethyl acetate
EtOH	ethanol
h	hour
HMBC	heteronuclear multiple bond correlation
HMQC	heteronuclear multiple quantum coherence
HSA	human serum albumin
HSQC	heteronuclear single quantum correlation
IR	infra red
<i>J</i>	coupling constant
m	multiplet (NMR)
m.p.	melting point
min	minute
mL	millilitre

MALDI-TOF	matrix-assisted laser desorption ionisation, time-of-flight
MRI	magnetic resonance imaging
NEt ₃	triethylamine
NMR	nuclear magnetic resonance
NMRD	nuclear magnetic resonance dispersion
ppm	parts per million
<i>pyr</i>	hydrogen pyrophosphate (HP ₂ O ₇ ³⁻) anion
q	quartet (NMR)
t	triplet (NMR)
TBA	tetra <i>n</i> -butylammonium
THF	tetrahydrofuran
TLC	thin-layer chromatography
UV-vis	ultraviolet-visible (spectroscopy)

Base units are abbreviated as their S.I. standards

Contents

Declaration	i
Abstract	ii
Acknowledgements	iii
Abbreviations used in this text	iv
Contents	vi
1.1 Calixarenes	1
1.2 The chemistry of calixarenes	3
1.3 Calixarenes as host molecules.....	7
1.3.1 Introduction to the host-guest concept	7
1.3.2 Calixarenes as hosts for neutral guests.....	8
1.3.3 Calixarenes as hosts for cationic guests	9
1.3.4 Calixarene hosts for f-elements	12
1.3.5 Hosts for anionic guests	18
1.3.6 Ditopic receptors.....	26
1.4 Macromolecule-bound calix[4]arenes	28
1.5 Enhanced Permeation and Retention (EPR)	30
1.6 Work described in this thesis	31
1.6.1 Chapter 2: Synthesis of cation-binding calix[4]arene derivatives.....	31
1.6.2 Chapter 3: Towards cation-binding calix[4]arene conjugates.....	32
1.6.3 Chapter 4: Synthesis and spectroscopic study of anion-binding calix[4]arene derivatives	33
2.1 Introduction.....	34
2.2 The Hard-Soft Acid-Base Concept.....	34
2.3 Development of a sarcosine-based calix[4]arene.....	35
2.3.1 Derivatisation of calix[4]arene ester	36
2.4 Formation of α -bromoamides	39
2.5 Preparation of flexible binding arrays at the lower rim	49
2.6 1,3-dialkylation reactions	50
2.7 Aminolysis of calixarene esters	55
2.7.1 Aminolysis using aliphatic amines	56
2.7.2 Lower-rim arrays with multiple amines	60

2.7.3	Synthesis of some calix[4]arene-based hydrazides	65
2.7.4	Diazotisation of calix[4]arene tetrahydrazide.....	67
2.7.5	Further aminolysis reactions.....	68
2.8	Lanthanide complex preparation	70
2.8.1	Luminescence titration of a Tb(III) complex	72
2.9	Conclusions.....	74
2.10	Future Work	74
3.1	Introduction.....	76
3.2	Synthetic requirements for macromolecular conjugation	76
3.3	Use of mono upper-rim substituted calix[4]arene	79
3.3.1	Stepwise syntheses using calix[4]arene	80
3.3.2	Use of benzoyl protecting groups	86
3.3.3	Introduction of functionality by diazo-coupling.....	88
3.3.4	Synthesis of allyl-functionalised calix[4]arene.....	89
3.3.5	Gutsche's Quinone Methide Route: Cyanomethyl calix[4]arene.....	93
3.3.6	Aminolysis of nitrated tetraester.....	95
3.3.7	Reduction of the nitro moiety.....	100
3.4	Conclusion	101
4.1	Introduction.....	102
4.2	Synthesis of ureas.....	104
4.3	Determination of binding constants, K.....	109
4.4	Assessment of anion binding affinity by ¹ H NMR methods.....	111
4.4.1	¹ H NMR titration of 126 with TBACl	112
4.4.2	NMR titration of 126 with dihydrogenphosphate.....	113
4.4.3	¹ H NMR titration of 125 with hydrogenpyrophosphate.....	115
4.5	Study of anion binding by UV-Vis titration.....	115
4.5.1	UV spectroscopy and the Beer-Lambert law	115
4.5.2	UV-Vis Titration of 125 with anionic guests	116
4.5.3	Determination of host-guest complex stoichiometry.....	122
4.5.4	A potential ditopic receptor for sodium halides	125
4.5.5	Study of 1,3-disubstituted receptor 131	127

4.5.6 Anion binding using acyclic amidoureas.....	130
4.6 Electrospray mass spectrometry study of host-guest interactions.....	136
4.7 Conclusions.....	138
4.8 Future Work.....	139
5.1 General Experimental Details.....	141
5.2 Nomenclature of calix[4]arenes.....	142
5.3 Synthetic Procedures.....	143
Appendix.....	184
(i) Crystallographic Data.....	184
(ii) UV-Vis Titration & Speciation Data.....	190

Publication arising from this thesis

Eoin Quinlan, Susan E. Matthews and Thorfinnur Gunnlaugsson

Anion sensing using colorimetric amidourea based receptors incorporated into a 1,3-disubstituted calix[4]arene.

Tetrahedron Lett., 2006, **47**, (52), 9333-9338

1.1 Calixarenes

Calixarenes are *meta*-cyclophanes, comprising cyclic oligomers of phenol, connected at their *meta* positions, which are derived from base-catalysed condensation reactions between certain phenols and formaldehyde. Their chemistry is vast and wide-ranging; finding uses across the breadth of supramolecular chemistry, from coordination chemistry^{1,2} to sensor chemistry.³ They have found application in areas including ion-channel mimetics⁴⁻⁶, catalysis⁷⁻⁹ and in the adhesives industry¹⁰⁻¹², while their syntheses and structural elucidation hold an important place in the history and development of modern organic chemistry, as will be outlined.

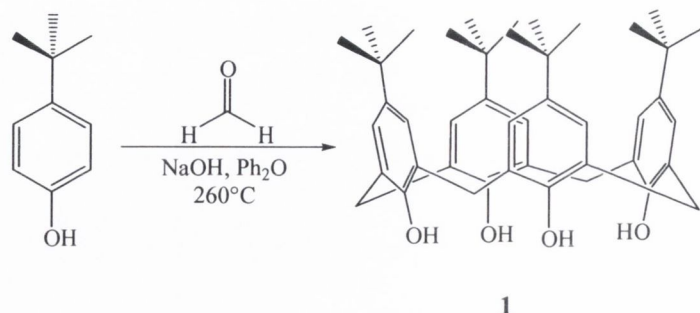
Phenol-formaldehyde chemistry has a long history, beginning in the laboratory of Adolph von Baeyer, in the 1870's. He heated an aqueous formaldehyde solution with phenol in a reaction which yielded a hard "resinous tar".^{13,14} Leo Baekeland, some decades later, famously adapted this process, and in doing so developed the first synthetic plastics, which became commercially known as Bakelite.¹⁵

The cyclic oligomers which we now know as calixarenes were prepared first by Zinke and Ziegler in 1944.¹⁶ Using a modified Bakelite procedure they prepared crystals from some *p*-alkyl phenols and formaldehyde, one of which gave an empirical analysis of C₁₁H₁₄O which was consistent with what is now recognised as *t*-butyl calix[4]arene. While Zinke proposed a cyclic structure for these compounds, proof was some time off. Hayes and Hunter prepared cyclic tetramers by a stepwise route, adopting a more rational approach¹⁷. Cornforth repeated Zinke's condensation reaction with both *t*-Bu phenol and *t*-Oct phenol, and in both cases two products formed, each with same empirical formula.^{18,19} Crystallographic studies of these products undertaken by Hodgkin, implied that the cyclic tetramer and octamer were the most likely, and that in each case they possessed fourfold axes of symmetry.

It was in 1978 that these cyclic oligomers were named. Gutsche, noting the non-planar, almost vase-shape of the molecules coined the term "calixarene", derived from the Greek "*calix*" (vase, or chalice), and the suffix -arene, denoting the system's aromatic nature.²⁰ In addition, the number of aromatic rings, *n* in the macrocycle can be denoted as "calix[*n*]arene". Although the focus of this thesis will be on calix[4]arene and its derivatives, each of the arrays where *n* = 4,5,6,7,8 are readily accessible^{21,22} and have been exploited for a variety of purposes including enzyme mimetics and host-guest chemistry^{14,23,24}. Each of the larger calixarenes up to *n* = 20 have also been reported to

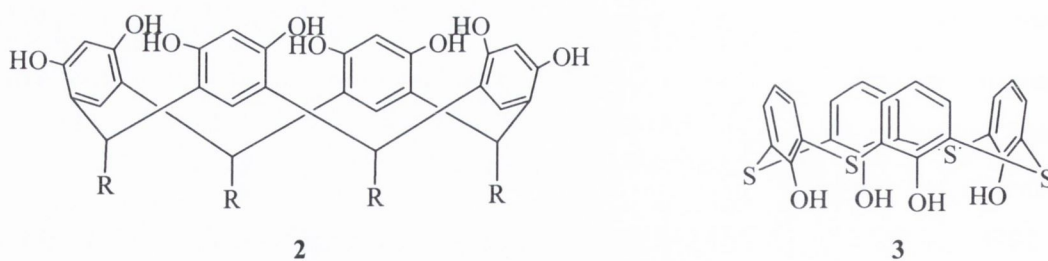
form in acid-catalysed and base-catalysed condensation reaction mixtures, and have been isolated using HPLC methods.²¹

^tButyl calix[4]arene and its formation conditions are shown in Scheme 1.1.



Scheme 1.1 – Base-catalysed formation of ^tbutyl calix[4]arene **1** from ^tBu phenol and formaldehyde.

This reaction proceeds in two stages; firstly the formation of an oligomer, which is carried out in the absence of solvent, followed by cyclisation of the oligomeric intermediate. The second step requires the high boiling point of diphenyl ether (259 °C) to affect the “cracking” or cyclisation step to occur. Lower boiling solvents such as xylenes (137-140 °C) may be used. This yields the cyclic octamer, calix[8]arene, while catalysis of the reaction in xylenes using KOH, in place of NaOH furnishes the hexamer, calix[6]arene. Calixarene analogues have also been prepared using other reaction conditions. Acid catalysed condensation of a 1,3-dihydroxybenzene (resorcinol) with aldehydes other than formaldehyde, yields the family of octahydroxy- compounds known as resorcin[4]arenes, such as **2**, while base-catalysed condensation of ^tBu phenol with elemental sulfur gives the thiacalix[4]arenes such as **3**.



Systematic IUPAC or Chemical Abstracts nomenclature for these large molecules is complicated, and as such is not routinely used. ^tButyl calix[4]arene, for example is classed as a [1_n] cyclophane, and as such, nomenclature as used for cyclophanes may be applied. Tetra ^tBu-calix[4]arene **1** is named as 5,11,17,23-tetrakis (1,1-dimethylethyl) pentacyclo [19.3.1.1^{3,7}.1^{9,13}.1^{15,19}] octacos-1(25),3,5,7(28),9,11,13(27),15,17,19(26),21,23- dodecane-25,26,27,28-tetraol. In accordance with Gutsche’s naming these molecules calixarenes, derivatives may be named according to the use of the parent term “calix[n]arene”.

Therefore, ^tbutyl calix[4]arene, is systematically known as 5,11,17,23-tetra-*tert*-butyl-25,26,27,28-tetrahydroxycalix[4]arene. This has become recognised, and is now suggested by Chemical Abstracts.²⁵

The calixarene platform offers three areas of distinct chemical reactivity, which will be discussed in the following section. The molecule is centred on a vacant annulus – the central unoccupied π -electron rich area which defines the three-dimensionality of calixarenes. The parts of varying reactivity as referred to in the text are shown in Figure 1.1.

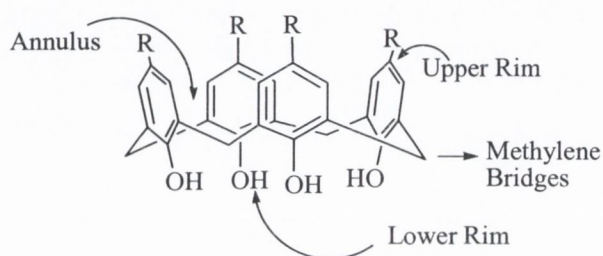


Figure 1.1- Regions of calix[4]arenes.

It is the versatility of these different types of reactivity which make the calixarenes exciting molecules for further exploitation and application. The following section will introduce some of the important aspects of the calixarenes unique chemistry.

1.2 The chemistry of calixarenes

The calixarenes offer several unique features which make them attractive for further derivatisation and use as host-species. Firstly, they provide an inherent pre-organisation which is greater than that found in other unfunctionalised macrocycles. For example, 1,4,7,10-tetraazacyclododecane (cyclen) is easily *N*-functionalised.²⁶⁻²⁸ However, it is upon interaction with a guest, such as a metal ion, that a host-guest cavity is formed by the puckering of the substituents. Calixarenes offer a more convergent array of hydroxyl moieties, allowing for greater directionality upon lower-rim functionalisation.

Secondly, calixarenes as mentioned above have areas of distinctly different reactivity. The upper or wide-rim is an array of aromatic protons, and as such is susceptible to reactions with electrophiles. Halogenation,²⁹⁻³¹ sulfonation,³²⁻³⁴ de-alkylation,³⁵ nitration,³⁶⁻³⁸ aminomethylation³⁹ and formylation⁴⁰⁻⁴³ reactions are possible and have been widely reported and reviewed, and these reactions allow for further derivatisations such as reduction (of the nitro group, for example), carboxylation, or metal catalysed cross-couplings (Heck⁴⁴, Stille⁴⁵ or Suzuki⁴⁶) to be achieved. The lower, narrow rim is also easily

derivatised, by Williamson ether synthesis, and as such its chemistry is dominated by alkylation and acylation reactions. Deprotonation is achieved using an appropriate base, and this is followed by nucleophilic reaction with an alkyl halide. This provides alkyl and ester derivatives. Acetylation and arylation reactions at the lower rim may be accomplished by Schotten-Baumann esterification. The chemistry of the bridging methylene moieties is relatively poorly exploited. It is benzylic in nature, and therefore amenable to deprotonation using strong bases, such as *n*-butyllithium.⁴⁷

Although these molecules have been named and reputed for their “vase” structure, this conformation is adopted by default only by calix[4]arenes which are unsubstituted at the lower rim. This can be attributed to a valuable hydrogen-bonding motif (Figure 1.2). Such hydrogen-bonding, in conjunction with their three-dimensional structure, is also responsible for the generally high melting points of unsubstituted calixarenes. This motif has been studied by IR spectroscopy, wherein the calixarenes show concentration-independent OH stretches at frequencies of between 3150 and 3200 cm^{-1} . Hydrogen bonding was interestingly also noted in a study by Cairns, wherein an acyclic tetramer of phenol moieties was seen to demonstrate a high degree of intramolecular hydrogen bonding. This led to the notion of the existence of coiled “pseudocalixarenes”, and “hemicalixarenes”,⁴⁸ where the latter is a hydrogen-bond stabilised dimer of the pre-formed oligomer.

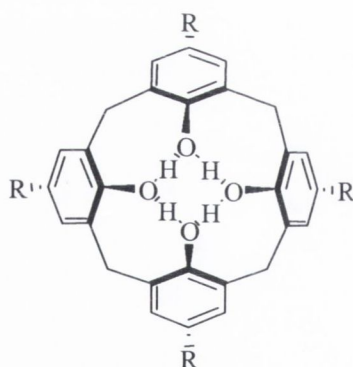


Figure 1.2 – “Circular” hydrogen bonding stabilisation of the cone conformation in calix[4]arene, viewed from below the annulus (CH_2 bridges exaggerated for clarity).

The circular hydrogen bonding motif also plays a key role in selective derivatisation of calix[4]arene. The choice of bases has a deciding effect on the outcome of the reaction stoichiometry. The different bases and their products are summarised in Figure 1.3.

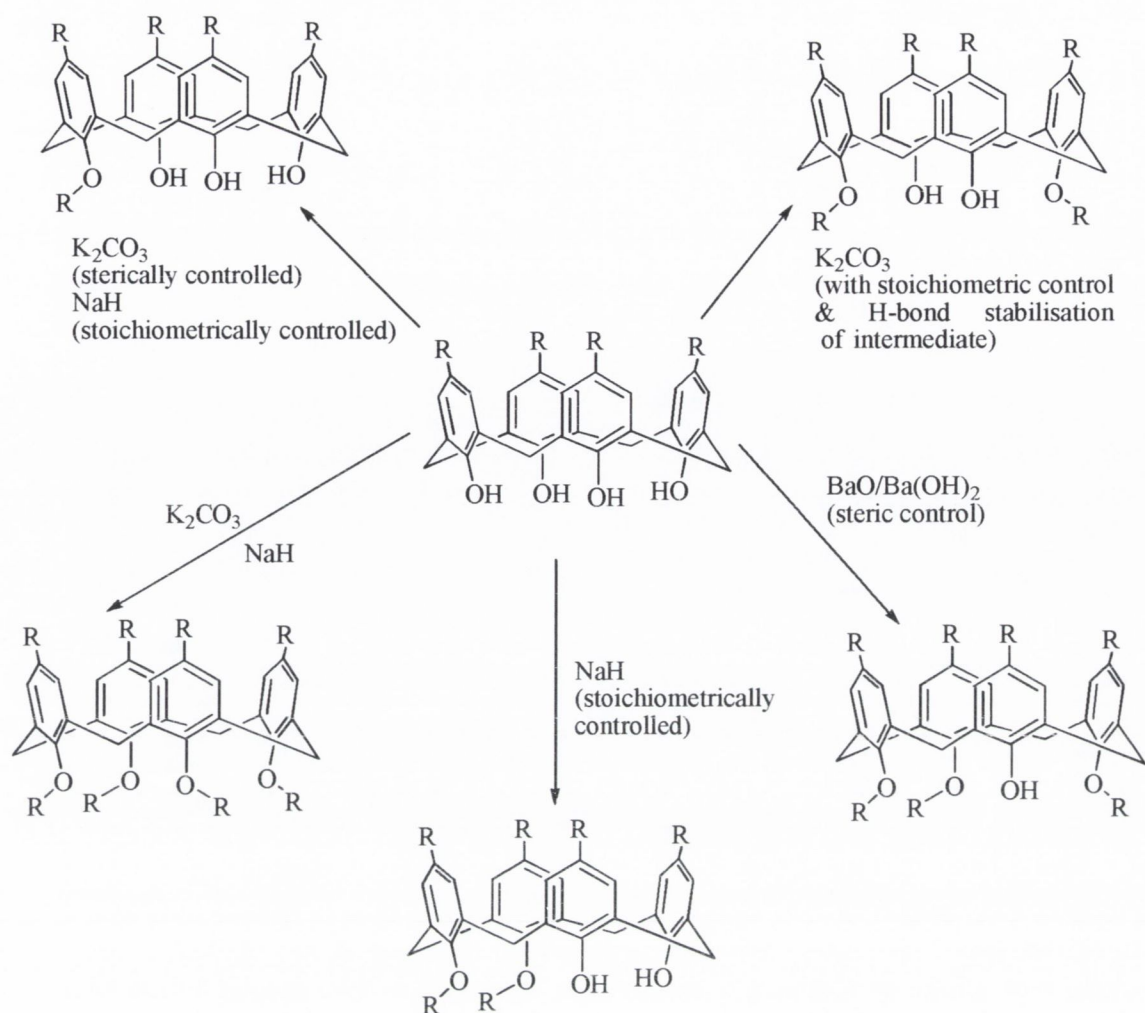


Figure 1.3 – Summary of substitution patterns achievable by variation of choice of alkylation base. Solvent may be interchangeable

Once a single deprotonation event has occurred, the mono-anion is stabilised by the neighbouring hydroxyl groups. Similarly, di-anions, both distal and proximal are stabilised in this manner. This is shown schematically in Figure 1.4.

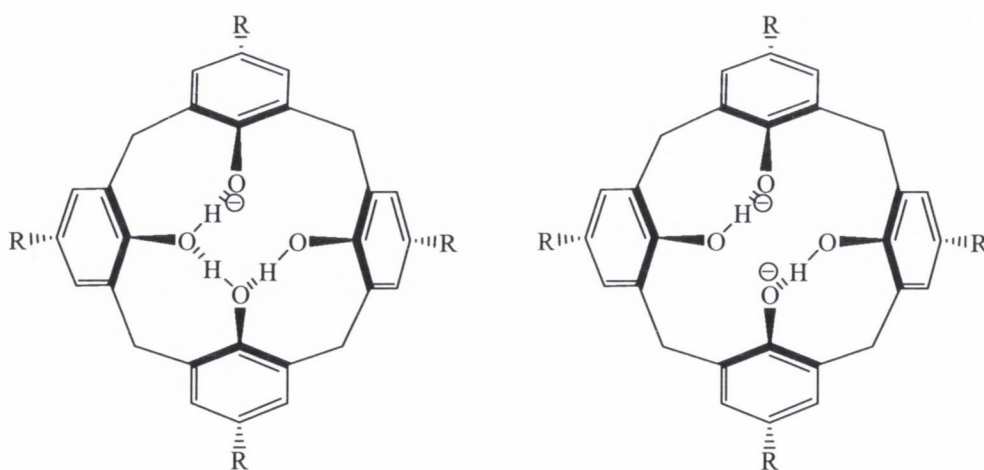


Figure 1.4 - Intramolecular stabilisation of deprotonated calix[4]arene by hydrogen bonding.

Once substitution has occurred at the lower rim, the hydrogen bonding motif is perturbed. The presence of small lower rim substituents, (smaller than *O*-propyl), can permit oxygen-through-the-annulus rotation, allowing for adoption of new conformations. The base which is used to deprotonate the calix[4]arene in alkylation reactions plays a deciding role in the conformation which is adopted. For example, alkylation using K_2CO_3 or Na_2CO_3 as a base will generally result in the formation of the product in the cone conformation, while Cs_2CO_3 will result almost exclusively in 1,3-alternate conformation.

The four conformations of calix[4]arene are illustrated in Figure 1.5, these are known as *cone*, *partial cone*, *1,3-alternate* and *1,2-alternate*. Conformational isomerism of unfunctionalised calix[4]arenes has been studied extensively by fluxional 1H NMR methods. Kammerer and co-workers, using a variety of *p*-alkylcalix[4]arenes, deduced that the cone formation converts rapidly on the NMR timescale at high temperature, forming a time-averaged cone and other conformations. A coalescence temperature of 45 °C was determined, at a rate of interconversions of 100 s^{-1} .

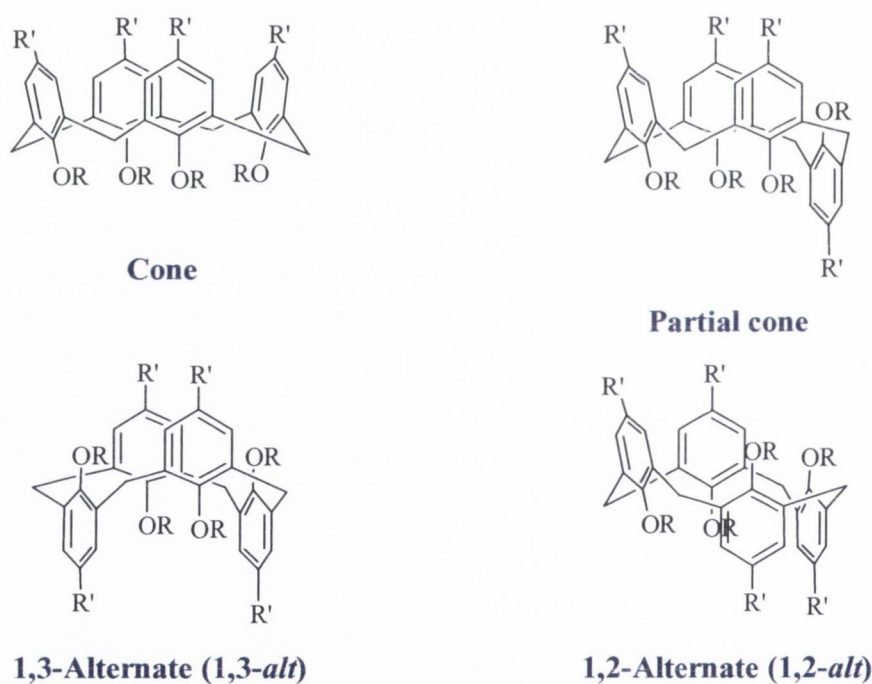


Figure 1.5 - Conformations of calix[4]arene, where R and R' denote arbitrary substituents

A feature common to each of the conformers is the high degree of symmetry. This means that the 1H NMR spectra have reduced complexity for molecules of these sizes. It is also on account of this symmetry that the 1H NMR signals for the bridging methylene protons can be used to unambiguously assign the conformation.

Table 1.1 - ^1H NMR patterns of bridging methylene protons in calix[4]arene, where the ^1H NMR signal in question appears generally between 2.5 and 5.5 ppm.¹⁴

Conformation	^1H NMR splitting pattern
Cone	Two doublets (consistent $J \approx 14$ Hz)
Partial cone	Two pairs of doublets or one pair of doublets, with one singlet
1,2-Alternate	One singlet and two doublets
1,3-Alternate	One singlet

To elaborate further in the case of the cone conformation, the bridging protons which are inside the annulus (*endo*) experience a significant ring current, and as such are shifted downfield relative to the external, *exo* protons. Geminal coupling between the *endo* and *exo* protons gives a doublet with coupling constant of approximately 14 Hz.

Having discussed the versatility of calix[4]arene chemistry, the following sections will outline some of the more noteworthy application of calixarenes in supramolecular chemistry.

1.3 Calixarenes as host molecules

1.3.1 Introduction to the host-guest concept

Supramolecular chemistry is concerned with chemistry which is “above” (Latin: *supra*), or beyond the covalent bond. As such, as supramolecular chemists we are interested in the development of architectures which are based on interactions other than covalent bonding. Host-guest chemistry draws much of its influence from Nature, and ultimately attempts to mimic Nature in its actions. The use of calixarenes as hosts extends from the generation of artificial ion-channel mimics to anion-regulation, a process which Nature has successfully achieved. Supramolecular chemistry thrives on the basic interactions which are shown in Figure 1.6. These include, but are not limited to: hydrogen bonding, electrostatic interactions, ion-dipole and van der Waal interactions.

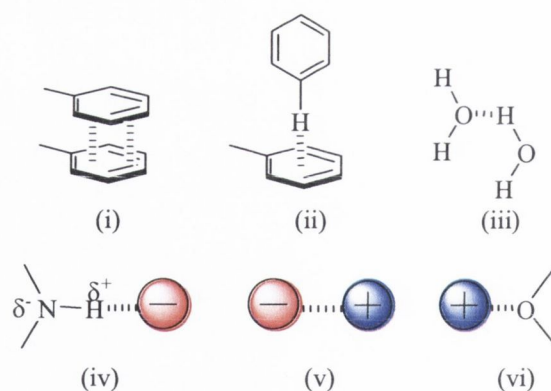


Figure 1.6 – The fundamental interactions of supramolecular systems: (i) π – π -stacking, (ii) face-edge π interaction (iii) hydrogen bonding (iv) anion-dipole (v) electrostatic (vi) cation-dipole

1.3.2 Calixarenes as hosts for neutral guests

The synthesis of *t*Bu calix[4]arene as described earlier proceeds very cleanly, with no isolated side-products. It is possible, when necessary, to purify the product by crystallisation from toluene. The crystals which have been prepared by this method have been shown to strongly bind the toluene molecules.⁴⁹ This can be attributed to the electron-rich annulus of calix[4]arenes which enables favourable interactions with electron-poor guests, such as the methyl moiety of toluene (Figure 1.7), and cations (Section 1.3.3). Single crystals which were obtained showed the existence of a clathrate, where the solvent was seen to be trapped within the structure of *t*-butylcalix[4]arene.

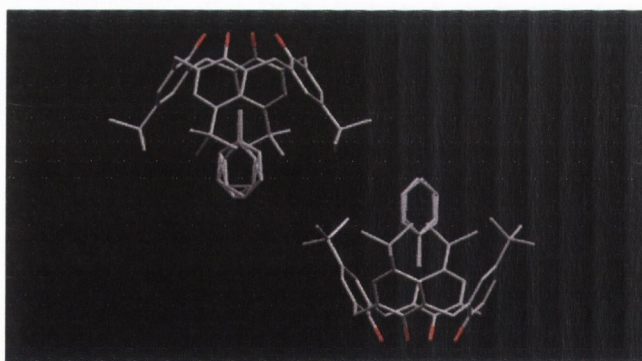


Figure 1.7- Crystal structure of *t*-butyl calix[4]arene as toluene inclusion complex⁵⁰

Ripmeester and co-workers have reported the inclusion by the cavity of calix[4]arene of several neutral guests, including mesitylene, menthol and azobenzene.⁵¹ They concluded that the *tert*-butyl calixarene was a versatile host, capable of forming a host-guest complex with any guest of appropriate size, and that multiple interactions were responsible for stability. A new solvent-free, “benign” approach to the preparation of the macrocycle has

recently been reported by Raston.⁵² The analogous *p*-cumylcalix[4]arene was prepared and its structure determined by X-ray crystallography.

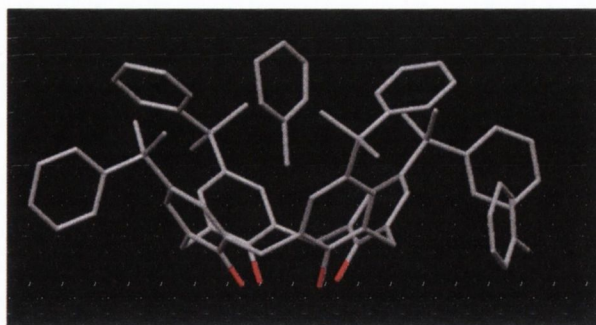


Figure 1.8 - *p*-Cumylcalix[4]arene prepared by Raston. Two toluene molecules can be seen: one in the hydrophobic cavity of the calix[4]arene, another occupying the interstitial space

In both cases, the toluene solvate is seen to occupy the cavity of the calixarene, with the methyl group pointing into the annulus. It has been reported that the toluene may be removed from host by heating under vacuum. Inclusion compounds have also been reported with DMF and chloroform. Calix[6]arene, for example, is reluctant to surrender its hold on chloroform, retaining the solvent after heating at 257 °C for 6 days at 1 mmHg pressure.²⁴ It is for this reason that it is accepted that accurate elemental analyses of calixarenes are often difficult to obtain.

The π -systems of calixarenes are also known to non-covalently interact with the electron rich systems of fullerenes such as C₆₀ and C₇₀. Several examples of inclusion and even solubilisation of fullerenes by calix[*n*]arene derivatives have been reported.^{53,54}

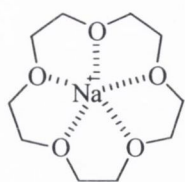
1.3.3 Calixarenes as hosts for cationic guests

As previously discussed, the arrays of functionality potentially offered by calix[4]arene derivatives are diverse. It is possible to fine-tune the reactivity by introduction of several reactive groups. The use of cation-binding moieties, for one example, has been well studied. The following section will outline some of the examples of calixarene-cation interactions which have featured in the literature to date.

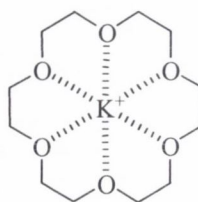
1.3.3.1 Alkali metal inclusion

Hosts for the small, polarised alkali metals are of tremendous importance, due to their ubiquitous physiological and environmental roles. The discovery of the crown ethers by Pedersen is regarded as being one of the key breakthroughs in host-guest chemistry.⁵⁵ The crown ethers owe their strong binding to the preorganised hard oxygen donor atoms interacting strongly with the hard alkali metals. A useful sensor, however must be able to

report on its detection, and thus crown ethers alone, lack the functional diversity required of a sensor, and they are frequently used to sequester and suppress Na^+ (**4**) or K^+ (**5**) ions in the presence of other potential host species.

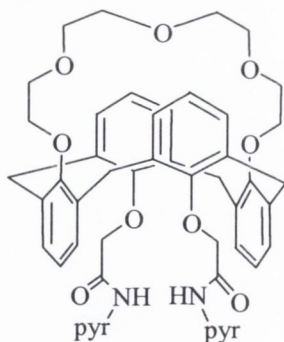


4



5

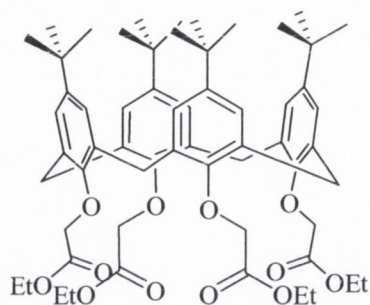
Given their strong affinity for metal ions which are of biological importance, crown ethers are highly cytotoxic, and have been reported to be toxic to the central nervous system.⁵⁶ To this end, incorporation of crown-like functionality into other macrocycles has been investigated. Calixarene-crown conjugates have been developed by several groups since the first report of a 'butyl calix[4]arene strapped at the lower rim by a pentamethyleneglycol unit in 1983 by the group of Ungaro.⁵⁷ Crowns and azacrowns have been incorporated into calix[4]arenes,⁵⁸⁻⁶⁰ systems based on the thiacalix[4]arene parent,^{61,62} ligands in the 1,3-*alt* conformation and have been a key part of some ditopic receptors⁶³. Receptor **6**, for example is a very recent report of a calix[4]crown in the 1,3-*alt* conformation.⁶⁴ In this example, Pb^{2+} is seen to be bound by the lower-rim carbonyl moieties, Ca^{2+} by the nitrogen atoms, while K^+ interacts solely with the crown moiety. Incorporation of a pyrene fluorophore (denoted as pyr) allows effective monitoring of change by absorbance and fluorescence spectroscopy.



6

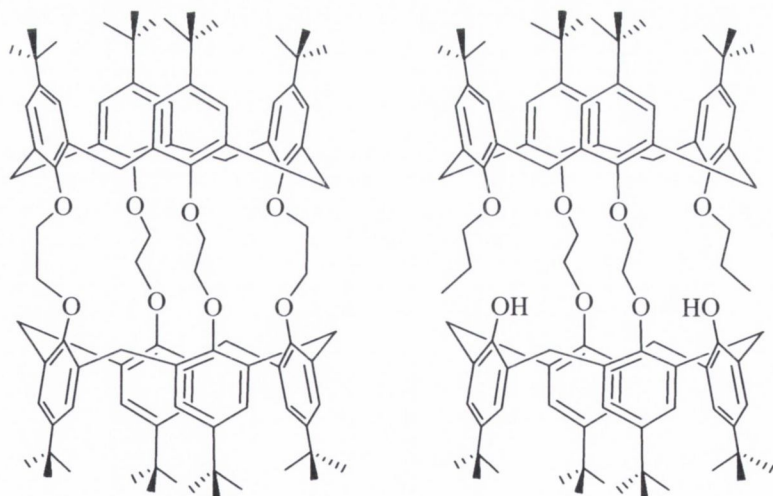
Calix[4]arene tetraethyl ester **7** was prepared in the 1980's by McKervey^{65,66}, and is held to be one of the hosts for Na^+ with greatest binding affinity. Indeed, its use as a sodium ionophore has led to its inclusion in the formulation of "Superglue", where it accelerates the adhesion time of the cyanoacrylate adhesive by sequestering the sodium ions that

would otherwise inhibit this process.^{10,12} Calixarenes have also been incorporated into electrodes, allowing for the monitoring of electrolytes in the blood.⁶⁷⁻⁷⁰



7

The contribution of Beer to the study of the uptake of simple cations by simple calixarene derivatives has been considerable.^{29,71-73} Calixtubes **8** and **9**, first reported by Beer in 1997 are tetra *O*-linked dimers of calixarene. Tubes such as **8**, form cryptand-like cavities between the lower rims of the calixarene units. These have been shown to form strong complexes with potassium. Later, calixsemitubes, wherein the calixarenes are connected at the 1,3-positions only, were also shown to have high affinity for K⁺, forming complexes with stability constants $K > 10^5$.⁷¹ This contrasts with the smaller Na⁺ and larger Rb⁺ ions for which the same ligand have $K = 20$ and $K = 30$ respectively, thus the ionophore is optimised for K⁺ only.



8

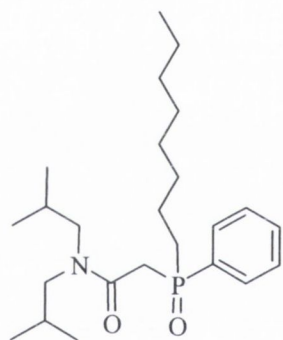
9

1.3.4 Calixarene hosts for *f*-elements

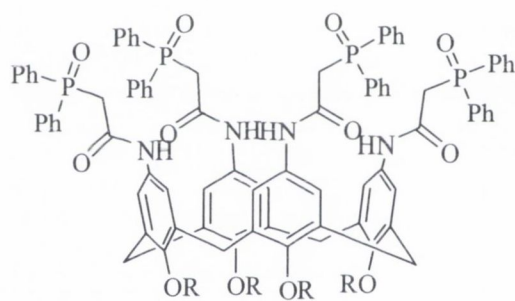
1.3.4.1 CMPO Calixarenes and TRUEX

Nuclear fuel processing produces a large amount of radioactive waste which must be either physically or chemically remediated prior to disposal. While vitrification of spent fuel (waste is concealed in glass and/or cement and is buried) has provided a method of disposal, calixarene and other related ionophores provide a method for extraction of toxic *f*-elements from water.

One proven method of chemically binding actinides requires the cooperation of three CMPO (*N,N*-diisobutylcarbamoylmethyloctylphenyl phosphine oxide) (**10**) moieties. This chelate is perceived to be one of the “classical” extractants for actinides, in the TRUEX (transuranium extraction) process.^{74,75} Calixarenes were subsequently employed to provide a preorganised scaffold on which to build CMPO analogues bearing multiple phosphino moieties. In doing so, a family of extractants such as **11** which are much more powerful than CMPO alone has been discovered.⁷⁶



10



11 (R = alkyl chain)

Prior to extraction, the CMPO derivatives are dissolved in nitrophenyl hexyl ether at a concentration of 10^{-2} – 10^{-3} M. Extraction then takes place in highly acidic conditions. The initial study, conducted by Böhmer showed high affinity for Th^{4+} in the case of CMPO calixarene.⁷⁶ These data are presented in Table 1.2. As can clearly be seen, the calix[4]arene-bound CMPO clearly demonstrates an enhancement in extraction capability. This appears to improve as the length of the alkyl chain R increases.

Table 1.2 - % Extraction of CMPO-calixarenes **11** compared with CMPO monomer **10**

	CMPO	R = C ₅ H ₁₁	R = C ₁₈ H ₃₇
Eu ³⁺	69.5	47	59
Th ⁴⁺	12.2	39	50

1.3.4.2 Luminescence study of calix[4]arene lanthanide complexes

Lanthanide ions are of great interest due to their photophysical and magnetic properties. It is the combination of the emission at long wavelengths, line-like emission and the long-lived excited states which gives rise to their potential usage as physiological probes and sensors.⁷⁷ This property has been extensively exploited within the literature by groups including those of Parker,^{78,79} Shinkai⁸⁰, Bünzli⁸¹ and within our own group, using various cyclic and acyclic ligand systems.⁸²⁻⁸⁷ However, to populate a lanthanide excited state, thus making the ion emissive, requires the introduction of an antenna. Systems based on macrocycles such as cyclen, become emissive only when they incorporate an antenna moiety (such as a quinoline, or naphthalene-containing “arm”). Alternatively, they may be used to sense aromatic molecules, as the guest may then be excited. Calix[4]arenes offer an electron-rich scaffold which may readily populate a lanthanide excited state, that is, the scaffold itself can act as an antenna without need for further sensitisation.

Shinkai and co-workers demonstrated the ability of a calix[4]arene to behave as an antenna moiety for Tb(III) (path A).⁸⁰ The same system when complexed with Eu(III) required an antenna such as a phenyl or biphenyl substituent (path B). Energy transfer pathways A and B are shown in Figure 1.9. Where the position occupied by the sensitizer is non-absorbing (a fourth piperidine moiety), emission is observed for Tb(III) only.

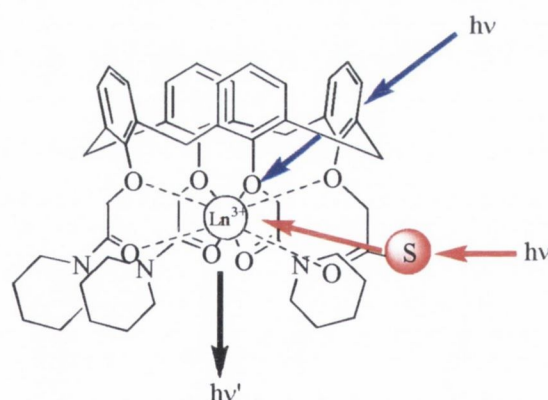


Figure 1.9 - Pathways of Ln³⁺ excitation in calix[4]arene derivative. S is a sensitizer moiety (phenyl or biphenyl). Blue lines denote Path A, red lines denote Path B.

A similar antenna effect was observed, again in the case of Tb(III) by the group of Ungaro, in the case of a tetra-*N,N*-diethylamide derivative of ^tBu calix[4]arene. This study noted the low molar absorptivity and poor quantum yield of emission observed in the case of Eu(III). This was attributed to deactivation of ligand excited states through a metal-to-ligand charge transfer mechanism.⁸⁸

1.3.4.3 Calixarenes as potential MRI contrast agents

1.3.4.3.1 Introduction to MRI and contrast agents

A contrast agent is a drug administered to a patient prior to medical imaging with the purpose of enhancing the resolution of the image. Magnetic resonance imaging (MRI) is a powerful, non-invasive imaging technique which relies on the proton NMR relaxation processes of the body's water, to gain insight into physiological processes. Since the advent of MRI, rapid diagnosis of tumours, stroke and diseases such as multiple sclerosis has become possible. The value of this method as a modern medical imaging technique lies in its ability to discern tissue types by measuring relaxation times of protons in physiological water.

Relaxation time is the time taken for a proton to return to its ground state following excitation by a radiofrequency pulse. There are two types of relaxation process which occur: T_1 and T_2 . T_1 is the spin-lattice or longitudinal relaxation time, while T_2 is the spin-spin or transverse relaxation time. For humans, T_1 and T_2 of fatty tissues are approximately 240 ms and 70 ms respectively, while for oxygenated blood they are 1350 ms and 200 ms respectively. In this case, stark differences in relaxation time allow for the difference to be clearly observed, and for an image to be derived. Unfortunately, the differences in T_1 and T_2 between neighbouring tissue types is not always adequate to provide precise contrast. What is required instead is a method of enhancing the T_1 and T_2 relaxation times. This is possible using an MRI contrast agent. The parameter by which contrast agents are assessed is their relaxivity, R_1 and R_2 , where $R_1=1/T_1$, and $R_2=1/T_2$. Therefore, faster relaxation is characterised by a short T_i and long R_i . A representative image showing the different types of scan and the effect of contrast administration is shown in Figure 1.10.⁸⁹

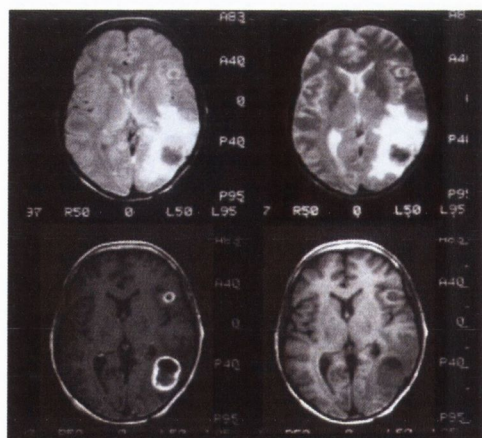
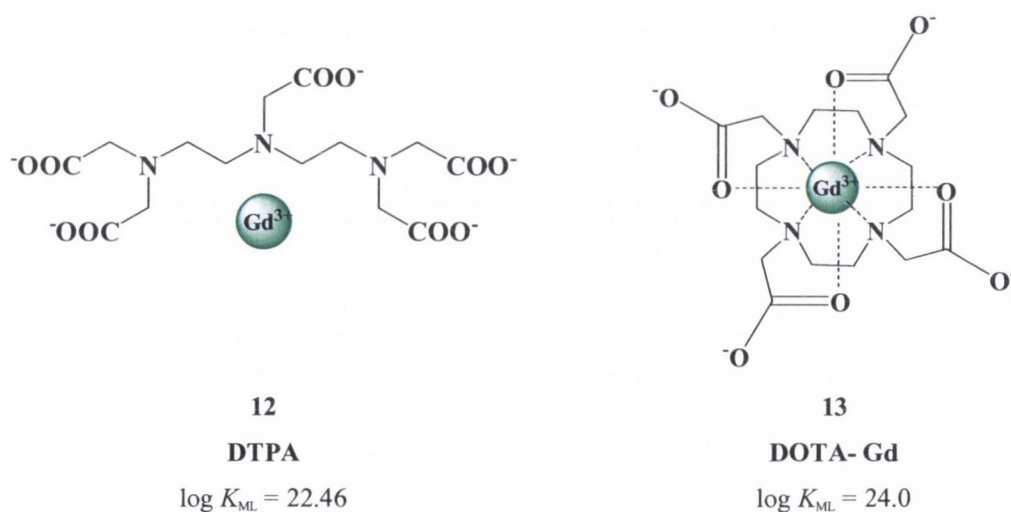


Figure 1.10 - Axial MR (Clockwise from upper left: Proton density, T_2 , T_1 , T_1 , post Gd.): Left posterior frontal and temporal enhancing masses with swelling consistent with tumour growth.

MRI contrast agents are typically paramagnetic in nature, that is, they possess unpaired electrons. This can be achieved using transition metal ions Mn(II), or Fe(II). In the case of the lanthanide ions, which have seven *f*-orbitals, seven unpaired electrons may be found in Gd(III). Gadolinium is a potentially toxic metal, and administering free gadolinium as hydrated gadolinium ions $[\text{Gd}(\text{H}_2\text{O})_8]^{3+}$ is not acceptable. Despite its high atomic number, its size approximates that of Na^+ and Ca^{2+} , due to the shielding effect of the lanthanide contraction. To this end, it is possible that its toxicity stems from blocking of sodium ion channels, or displacement of calcium in bone structure. Thorough toxicity studies on gadolinium are incomplete. Lanthanide ions have been studied extensively as ribonuclease mimics; therefore it is also possible that they may have adverse effects on the nuclear material. It is only by administration of Gd(III) in a safe form that it is practicable as an MRI contrast medium. This toxicity can be masked by preparation of a strong chelate which will bind the metal ion, will serve its relaxation purpose *in vivo*, and will be readily excreted intact.

Contrast agents have been prepared which have a variety of both acyclic and macrocyclic structures. These have only been able to reach the clinic by virtue of their strong binding affinities towards metal ions. A number of complexes and their respective stability constants are shown in Figure 1.11.



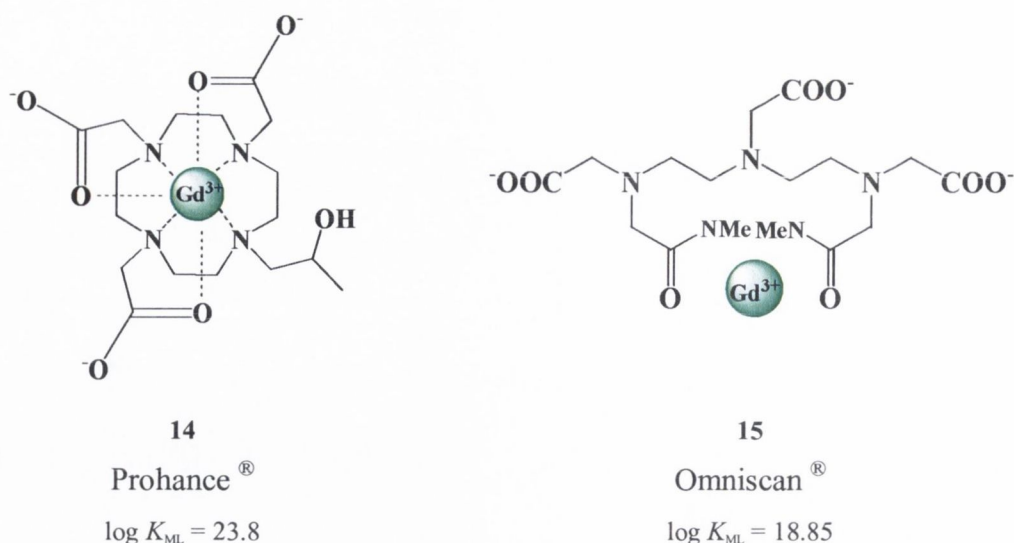
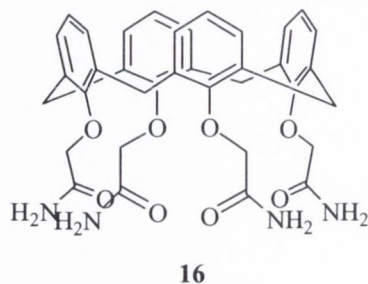


Figure 1.11 - Some acyclic DTPA (diethylenetriamine pentaacetic acid) and cyclic DOTA (1,4,7,10-tetraazacyclododecane-*N,N',N'',N'''*-tetra-acetic acid) Ligands

The use of calixarene chelates as potential MRI relaxation agents has also been investigated by a number of groups, while the conjugation of prior known contrast agents for both MRI and CT with calixarene derivatives has been the subject of a patent.⁹⁰

1.3.4.3.2 Application of calixarenes as MRI contrast agents

A promising assessment has been a trial of a calixarene/gadolinium complex as a T_1 relaxation agent, by Roundhill.⁹¹ A tetraacetamido substituted calixarene **16** was prepared and titrated with gadolinium(III) nitrate in a 9:1 DMSO/H₂O solution. T_1 rates were then measured by inversion-recovery at 400 MHz. Due to the linear dependence of solvent concentration on relaxation rate, the relaxivity could be determined, and was found to be $3.40 \text{ mM}^{-1} \text{ s}^{-1}$. The binding constant for the complex as calculated by UV-Vis titration was found to be $K = 1 \times 10^3 (\pm 1 \times 10^2) \text{ M}^{-1}$. These data represent a good relaxation agent, which unfortunately has poor affinity for the gadolinium ion. The authors note that the size of the cavity is expected to be adequate for gadolinium, and attribute the low affinity of the host towards the lanthanide to charge effects. It is noteworthy that the complex itself was not isolated.



The interaction between calixarenes and albumin proteins has been reported to some extent. Bryant studied a non-covalent interaction between a calixarene/Gd(III) complex and human serum albumin.⁹² These interactions were assessed using NMRD, and it was shown that upon addition of HSA, both R_1 and R_2 relaxivity values increased significantly. This was attributed to the increase in rotational correlation time of the complex caused by non-covalent interaction with HSA. Stability constants for their ligand were also more promising than those obtained by Roundhill. By calorimetric titration with $\text{Gd}(\text{NO}_3)_3$, the association was seen to be $K = 2 \times 10^5 \text{ M}^{-1}$, much more promising than the previous report. Again, however, the complex was not isolated. The NMRD results are outlined in Figure 1.12.

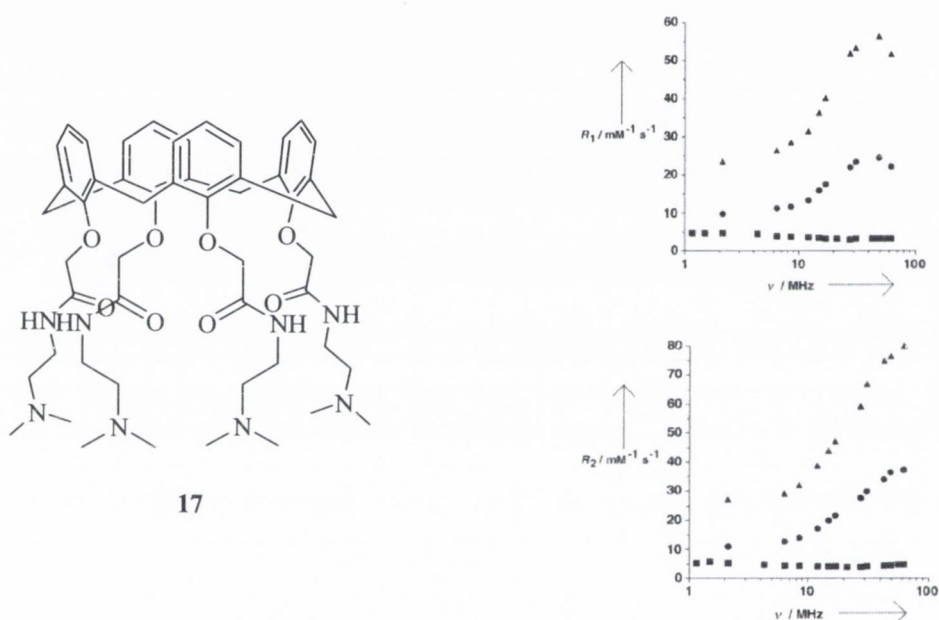


Figure 1.12 – Calixarene **17**, and ^1H NMRD profiles (traces: R_1 upper, R_2 lower, showing relaxivity of contrast agent as function of field frequency) of its Gd(III) complex in the absence (■) and in presence of 2% (●) and 10% (▲) HSA at 23 °C after subtraction of the HSA contribution.

A further study using calix[4]arene complexes with albumin was completed by Botta and co-workers.⁹³ Their ligand is endowed with high stability and relaxivity and NMRD was also used to assess binding affinity to albumin. Calixarene **17** was shown to have relaxivity of $9.6 \text{ mM}^{-1} \text{ s}^{-1}$, which was shown to be constant over five pH units from 4-9. This value is approximately twice that of $[\text{Gd}(\text{DOTA})(\text{H}_2\text{O})]^-$, which they proposed was due to a larger hydration of their species.

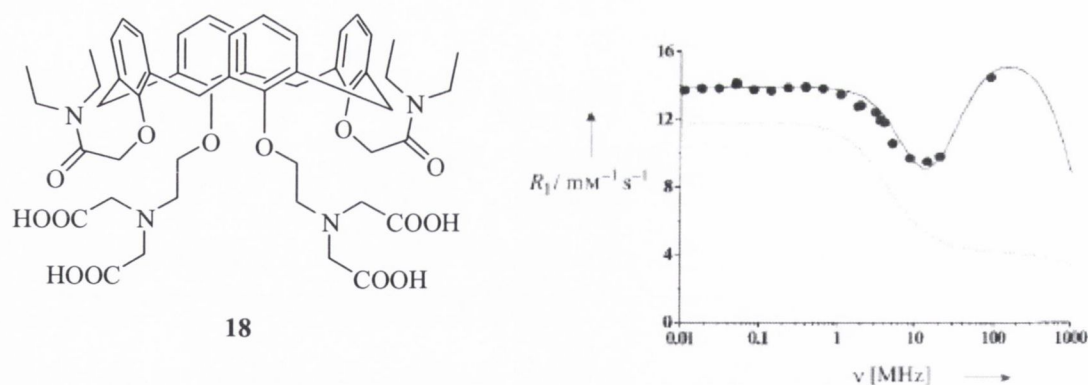


Figure 1.13 - Calixarene **18** and the ^1H NMRD profile of its Gd(III) complex in water at 25 °C. The dotted curve represents the calculated profile of the commercial $[\text{Gd}(\text{dota})]^-$

Further measurements using competitive relaxometry assigned a stability constant of $1 \times 10^{13} \text{ M}^{-1}$ to this Gd complex, again this is a marked increase on both previously reported compounds. Titration of this complex with HSA gave the expected enhancement of relaxivity at higher concentrations of HSA, up to a maximum value of $50 \text{ mM}^{-1}\text{s}^{-1}$ at 30 MHz.

1.3.4.4 Challenges in MRI contrast agent development

As shown in the previous sections, there has been some prior interest shown in the potential use of calixarenes as scaffolds for MRI agents. As these stand, the affinity towards lanthanides has been low, with binding constants of $K = 1 \times 10^3 \text{ M}^{-1}$ for the tetra amide synthesised by Roundhill discussed above. It was also postulated that the reason for poor binding by these amides may be charge effects, rather than size effects. For this purpose, preparation of ligands with multiple donor atoms, to diffuse the inherent charge of Gd(III) is desirable. In addition, each of the prior studies prepared their chelates in solution, and tested them as such; in none of these studies were the complexes collected or isolated, a feature which may be impeded by the low stability.

1.3.5 Hosts for anionic guests

In recent years the field of anion-binding has come to the fore of supramolecular chemistry. Anions are abundant in biology and the environment. From chloride regulation in the human body to the phosphates in detergents, and pertechnetate, a toxic, radioactive by-product of nuclear fuel production, the need to detect, quantify and extract anions is increasing. The challenges of anion coordination chemistry are demanding; complex anions such as oxoanions lack the spherical shape of cations, hence they require a more shape-complimentary receptor. In addition, anions are generally larger than their

isoelectronic cationic counterparts due to the lessened nuclear charge. Figure 1.14 shows the conformations of complex polyatomic anions phosphate, pyrophosphate and acetate.

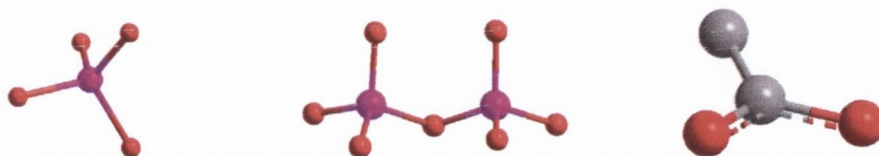
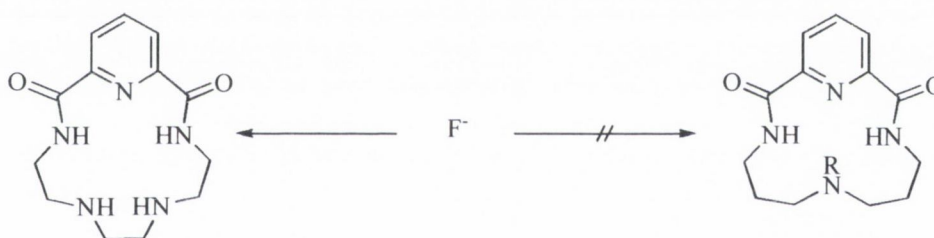


Figure 1.14 – Ball and stick representations of polyatomic anions phosphate, pyrophosphate and acetate

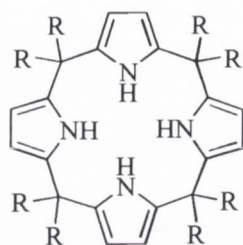
The electron density of anions makes them excellent hydrogen-bond acceptors. Polar NH, OH and SH bonds therefore are very attractive binding sites for anions and there are many examples of these species. Several anion-binding motifs have been developed within our group, based the thiourea and urea moieties, incorporated into naphthalimide⁹⁴⁻⁹⁶, norbornene⁹⁷ and anthracene⁹⁸⁻¹⁰⁰ frameworks. It is possible also to incorporate anion-recognition units into macrocycles, achieving a macrocyclic effect. The support for the strong binding of anions by macrocycles which incorporate amides, for example was recently confirmed by Rybak-Akimova, who asserted that in the case of fluoride, at least a 15-membered ring was required.¹⁰¹



Scheme 1.2 – Macrocyclic effect of anion complexation (R = H, Me)¹⁰¹

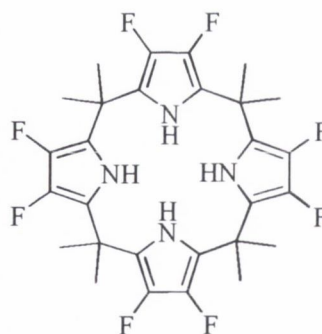
Binding by the 15-membered ring of fluoride proceeds with $K = 5.8 \times 10^2 \text{ M}^{-1}$, while no binding was observed in the case of the 14-membered analogue either in the presence (R = H) or absence (R = Me) of an NH donor moiety.

The N–H donors of calixpyrroles such as **19** and **20**, for example have proven excellent in anion binding studies by groups including those of Sessler¹⁰²⁻¹⁰⁴ and Gale.¹⁰⁵⁻¹⁰⁷



R = Alkyl, aromatic

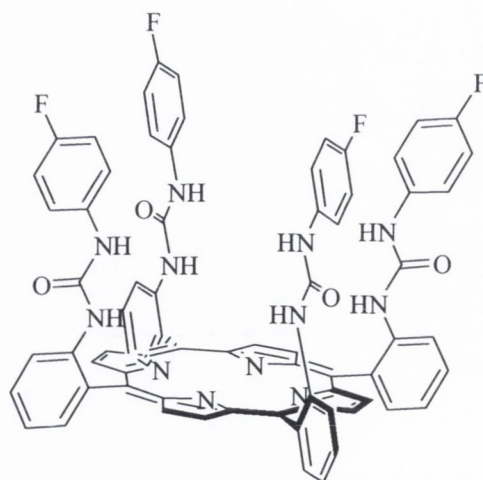
19



20

Unlike conjugated porphyrinic systems which remain relatively flattened, calixpyrroles adopt a flexible structure which allows them to adapt their shape and conformation to better accommodate guest species. Compound **20** was recently reported by Sessler¹⁰³ and was shown to bind Cl^- ($K_{\text{ass}} = 530,000 \text{ M}^{-1}$), acetate ($K_{\text{ass}} = 1,900,000 \text{ M}^{-1}$) and benzoate ($K_{\text{ass}} = 1,200,000 \text{ M}^{-1}$). Such high association constants can be attributed to the electron withdrawing nature of the fluorine moieties, in addition to the cooperative nature of the multiple N–H electron acceptors.

Rigidification and pre-organisation of hosts for anionic guests has been undertaken. This allows for the sensing of multi-dentate anions, and potentially for the detection of large halide species. This has for example been successfully achieved on expanded porphyrinic platforms. Porphyrin-immobilised hosts such as **21** have been synthesised and shown by electrochemical measurement to be selective for acetate and dihydrogenphosphate.¹⁰⁸⁻¹¹⁰ Its incorporation into an ion-selective electrode was undertaken. This was used for simple determination of acetate in aqueous solution.

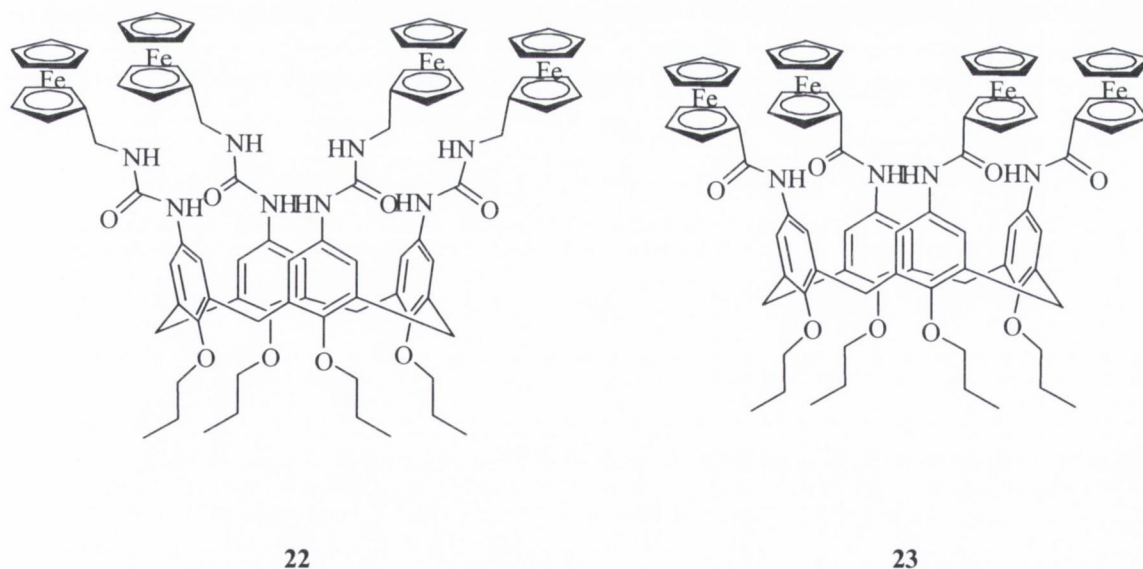


21

To date, “classical” calixarenes have been utilised as anion receptors through modification of both their upper or lower rims. Through appropriate derivatisation, it has also been possible to prepare some ditopic receptors (species which recognise both the anion and cation of an ion pair). The following section will provide a brief review of this chemistry.

1.3.5.1 Anion-Binding at the upper-rim of calix[4]arenes

Anion-recognition motifs at either rim have similar requirements; a charge or appropriate electron-accepting character, in addition to having a cavity of suitable size and shape. Metallocenes, for example have been very successfully incorporated into the upper-rim of calixarenes, providing neutral redox active centres, which supply an effective reporting system that can be monitored by electrochemical methods. Hosts **22** and **23** were prepared by Beer, incorporating the metallocene centres into a tetra amide and tetra-urea system, respectively. Tetraamide **23** was shown to bind BzO^- more strongly than the urea ($K_{\text{ass}} = 150 \text{ M}^{-1}$ for the urea **22**, $K_{\text{ass}} = 30 \text{ M}^{-1}$ for the tetra amide), while in both cases binding of H_2PO_4^- was seen to be strong ($K_{\text{ass}} = 150 \text{ M}^{-1}$ for urea, $K_{\text{ass}} = 120 \text{ M}^{-1}$ for amide). A distally disubstituted receptor was also prepared, incorporating ferrocenyl ureas. This system showed only weak binding for the anions tested ($K_{\text{ass}} < 50 \text{ M}^{-1}$).



Charged, cobaltocenium-based receptors were also prepared by the same group, again at the upper-rim, analogously to **22** and **23**. A distally disubstituted system was found to recognise both Cl^- and H_2PO_4^- with greater affinity than the tetrasubstituted cobaltocenium receptor.¹¹¹ However, it was shown that the tetrasubstituted analogue had *selectivity* for

H_2PO_4^- over Cl^- .¹¹² The data produced from ^1H NMR shift titrations in DMSO are presented below.

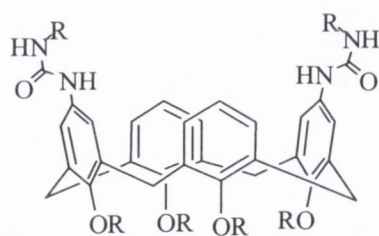
Table 1.3- Equilibrium constant data for bis- and tetra- cobaltocenium calix[4]arenes as measured in DMSO- d_6 data are stated as M^{-1} (*n.d.*: not determined).¹¹²

	Cl^-	Br^-	H_2PO_4^-	Adipate
Distal	5035	1860	2800	11510
Tetra	70	<i>n.d.</i>	1200	<i>n.d.</i>

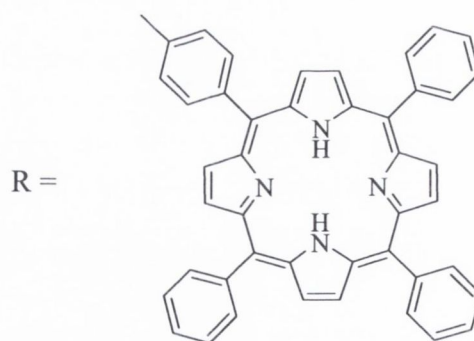
1.3.5.1.1 Anion Binding Using Calixarene-Urea Derivatives

In addition to the redox-active species already shown, the relative ease of modification of the calixarene scaffold has made possible the incorporation of neutral ureido moieties. This is achieved by creating a primary amine on the calixarene and by subsequent reaction with an isocyanate. Alternatively, the calixarene may be converted to its corresponding isocyanate using a phosgene synthon, and then reacted with a primary amine.

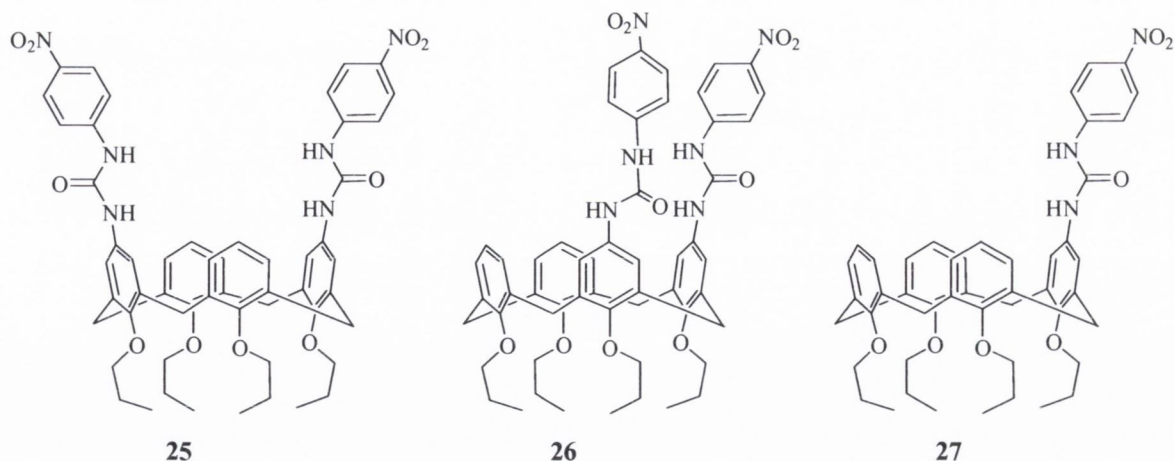
Stibor and Lhoták created a new class of porphyrinic conjugates for anion binding.¹¹³ Their mono amino-tetraphenylporphyrin was converted to its isocyanate and condensed with appropriate upper-rim amino calixarenes. The conjugated nature of the porphyrin moiety allows for incorporation of anions to be reported electronically and studied effectively by UV-vis spectroscopy. In the case of the distally disubstituted receptor **24**, binding constants for chloride and bromide anions were among their highest obtained values at $6.9 \times 10^5 \text{ M}^{-1}$ and $6.9 \times 10^4 \text{ M}^{-1}$ respectively, again indicating a very strong association.



24



Lhoták and Stibor have also prepared both distally (**25**) and proximally (**26**) di-substituted ureas, and monosubstituted **27**, with the objective of assessing stoichiometry of anion binding with respect to the calixarene functionalisation pattern.¹¹⁴



Binding constants for the associations between the hosts and a number of anions of different charges and shapes were determined by UV-Vis absorption spectroscopy. These values are tabulated in Table 1.4.

Table 1.4 – Binding constants (M^{-1}) observed for the binding of anions by hosts **25**, **26** and **27** determined by UV-Vis titration in CH_2Cl_2 at 298 K.

Anion	25	26	27
Cl^-	$> 10^6$	$\geq 10^5, \beta_{21} \geq 10^{11}$	5.3×10^4
Br^-	$> 10^6$	$\beta_{21} \geq 10^{10}$	1.2×10^4
I^-	1.7×10^5	$5 \times 10^3, \beta_{21} = 5 \times 10^9$	1.2×10^3
NO_3^-	4.1×10^5	$1 \times 10^4, \beta_{21} \geq 10^{10}$	6.9×10^3
BzO^-	$> 10^6$	$1 \times 10^5, \beta_{21} \geq 10^{10}$	6.2×10^5
AcO^-	$> 10^6$	$\beta_{21} \geq 10^9$	4.3×10^5

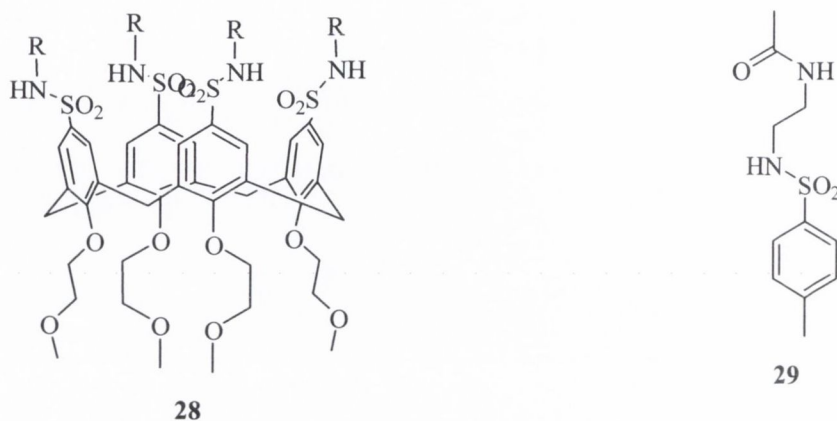
Job's plots were used to verify the existence of 2:1 stoichiometry in the case of **26**

It is clear from these data that the presence of two calix[4]arene-bound urea moieties enhances the binding affinity towards all anions. Such an effect is clearly evidenced in the proximally disubstituted **26** where a second binding event occurs, with very high binding overall binding constants.

1.3.5.1.2 Anion binding using calixarene-amide derivatives

Amides are also attractive functional groups, owing to their relative ease of synthesis (peptide coupling techniques). The amido moiety is electronically similar to the ureido functionality, possessing an acidic NH proton. It too, has been exploited by Beer, incorporating four ferrocenyl moieties at the upper-rim, coupled through an amide bond.

An early example of the use of amide moiety in calixarene-based anion binding was the construction of a series of sulfonamides by Reinhoudt. By comparing the macrocycle with a single monomer, this study also provides us with insight as to how the preorganisation offered by calix[4]arene enhances the potential binding affinity of a system.



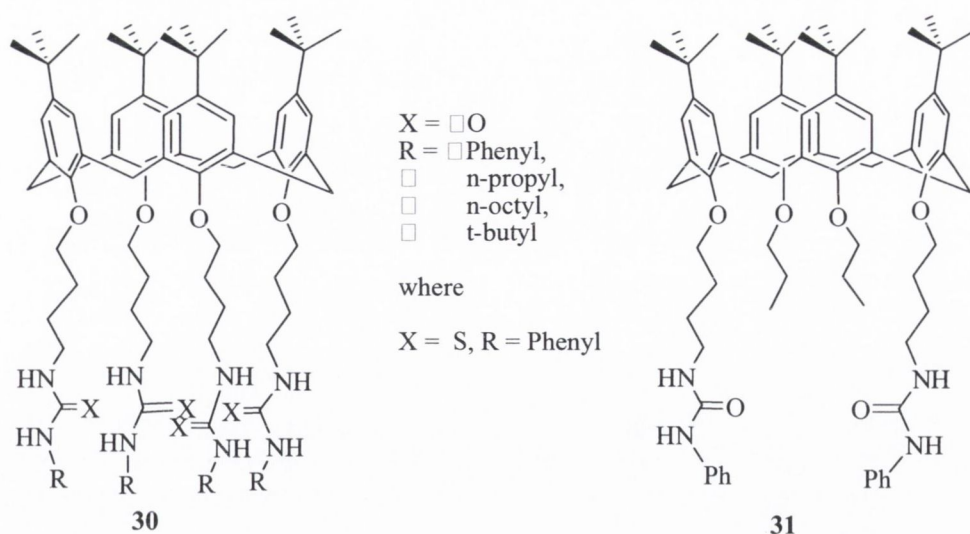
In the case of $R = \text{CH}_2\text{CH}_2\text{NHC(O)Me}$ **28**, the affinity towards tetrahedral HSO_4^- was strong, with $K = 103400 \text{ M}^{-1}$. This was in contrast with the monomer **29** which lacks the pre-organisation that is offered by the calix[4]arene scaffold and demonstrated an association constant value $K = 350 \text{ M}^{-1}$.¹¹⁵

1.3.5.2 Lower-Rim Modified calixarenes

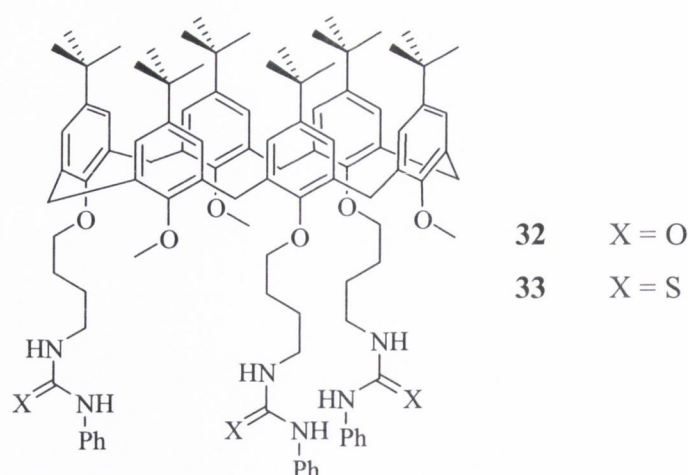
As discussed earlier, the lower rim is narrow, and due to the angular orientation of the phenol moieties, it is also convergent. This should offer preorganisation, which should, in turn, lead to a smaller binding cavity than would be possible at upper rim.

1.3.5.2.1 Modification with urea moieties at the lower rim

There are several examples of modification at the lower-rim to incorporate urea moieties for anion recognition, with one of the earliest successes being the work of Reinhoudt and co-workers, who prepared families such as **30** and **31**.¹¹⁶



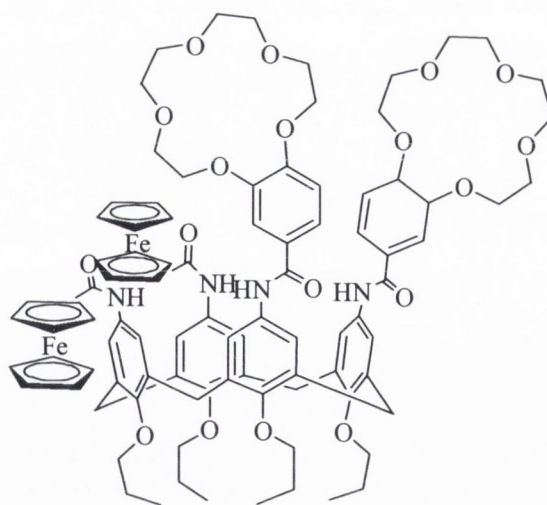
When the tetramer **30** was titrated with anionic guests, K_{ass} values were highest for Cl^- ; from 2660 M^{-1} for $R = \text{phenyl}$ to 2015 M^{-1} when $R = \text{t-butyl}$. This indicates the role played in the modification of the acidity of NH protons by the electron donating properties of the ureido substituents. The *n*-propyl urea, for example, was a poor host for all anions; for each of Cl^- , Br^- , I^- , CN^- , and NCS^- guests, K_{ass} did not exceed 25 M^{-1} . The use of the a bidentate phenlyurea host saw K_{ass} increase to 7105 and 2555 M^{-1} for Cl^- and Br^- respectively. This work was subsequently extended, and applied to calix[6]arene, which offers a larger annulus, and with a more flexible ring system with diminished hydrogen-bonding.¹¹⁷ It was shown that in 1,3,5-trimethoxy-2,4-6-trialkoxy-*p-tert*-butylcalix[6]arene derivatives **32** and **33**, the methoxy groups stabilise the cavity by $\text{C-H} \cdots \pi$ interactions, and this platform was used to provide a somewhat flattened cone upon which to build a larger anion-binding array, which can bind either spherical anions (480 M^{-1} for Cl^- , 1450 M^{-1} for Br^- , for **32**) or oxoanions with C_3 symmetry, such as benzene 1,3,5-tricarboxylate ($87,000 \text{ M}^{-1}$ for **32**). In the case of the thiourea, this binding is greatly enhanced, with K_{ass} of $290,000 \text{ M}^{-1}$ observed for binding of benzene-1,3,5-tricarboxylate by **33**.



1.3.6 Ditopic receptors

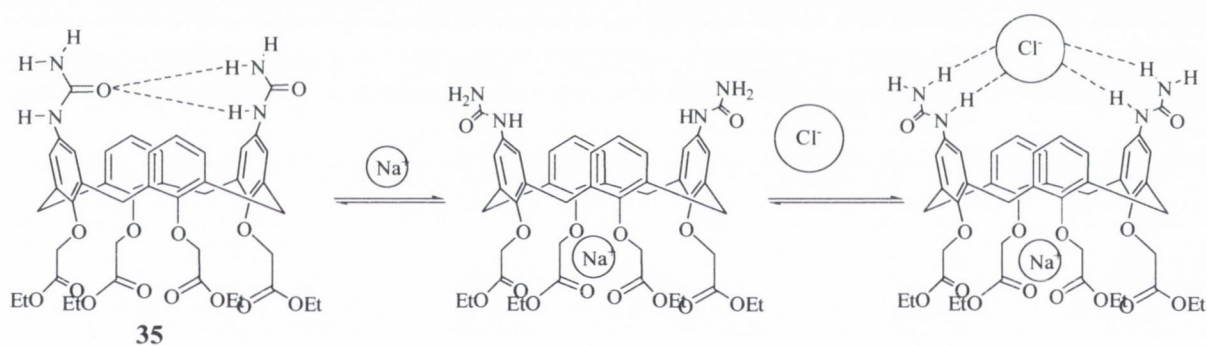
Ditopic receptors are bifunctional hosts which are capable of binding both anions and cations simultaneously at different sites. As for every anion in solution, there are corresponding cations, the development of effective ditopic receptors, capable of recognising native ion pairs is crucial to the furthering of research in the field of anion coordination chemistry. Calixarenes have played a part in the development of ditopic receptors. This is largely due to their inherent ditopic nature, whereby upper and lower rims give way to different types of chemistry, but also due to the large nature of cavities that may be formed on functionalisation. As a key aim of ditopic receptors is to achieve positive cooperativity between both cation and anion receptor moieties, calixarenes are ideally suited, due to their conformational flexibility.

The ferrocene-containing systems reported by Beer were applied to the design of ditopic receptors.¹¹⁸ Benzocrown-containing **34** was prepared, containing cation-binding crown moieties in a 1,2-disubstituted pattern. Amide moieties which bind anions are provided closer to the calixarene core, and the incorporation of ferrocene allows for electrochemical reporting. Upon complexation of 2Na^+ by **34**, the binding affinities towards chloride, benzoate and dihydrogenphosphate were seen to decrease. Complexation of K^+ , however, saw increased anion binding in the case of each anion. This was attributed to the formation of an intramolecular sandwiched complex wherein both crown moieties bound the K^+ , creating a sheltered cavity for anion complexation.



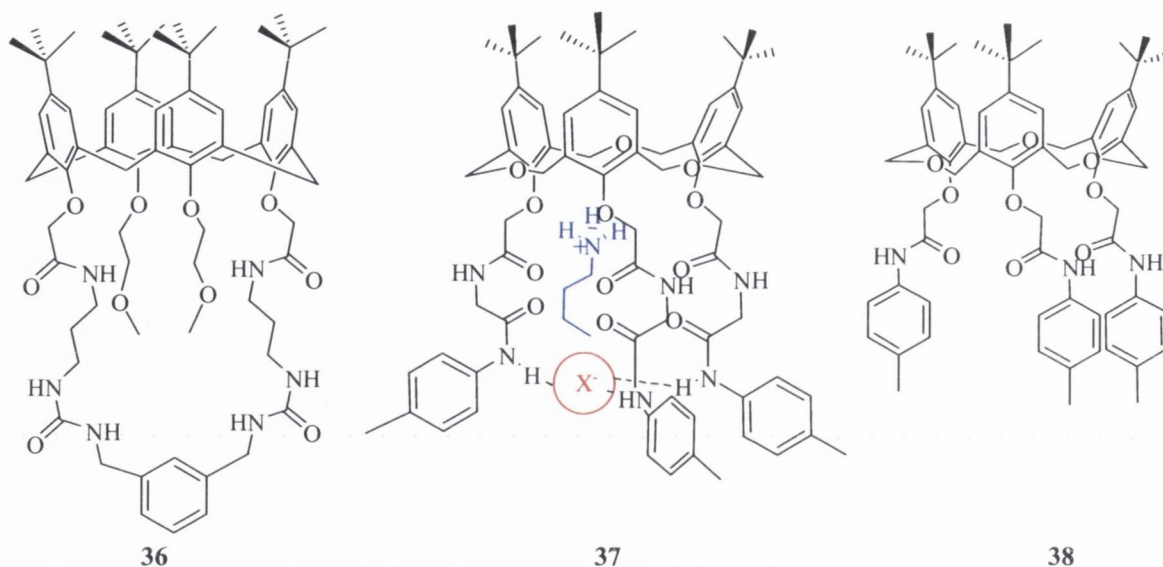
34

The Reinhoudt group introduced **35** shown in Scheme 1.3 a receptor which draws on the remarkable binding of Na^+ by the calix[4]arene tetraethyl ester.¹¹⁹ Incorporation of urea moieties at the upper rim allows for the simultaneous binding of chloride; the system is therefore capable of solubilising inorganic salts in organic solvents (**35** can fully solubilise NaCl , NaBr and NaI in CHCl_3).

Scheme 1.3 – Solubilisation of NaCl by calix[4]arene host **35**

Kilburn and co-workers reported **36** as an example of a potentially ditopic receptor.¹²⁰ The two thiourea moieties provide a strong anion-binding motif, while the upper cavity possesses electron rich oxygens, which would potentially bind cations. The cavity was found to bind large anions, such as the tetrahedral phenylphosphinate ($K = 24,000 \text{ M}^{-1}$), two equivalents of the smaller AcO^- ($K = 11,000 \text{ M}^{-1}$), and to a lesser extent diphenylphosphinate ($K = 1800 \text{ M}^{-1}$). Ditopicity was thought to be demonstrated in the final example, where K increased to 2200 in the presence of Na^+ . Hexahomotrioxacalix[3]arene derivatives **37** and **38** shown were reported in 2006 by the group of Yamato and was shown to have ditopic binding capability, where the phenolic and amido carbonyl oxygens

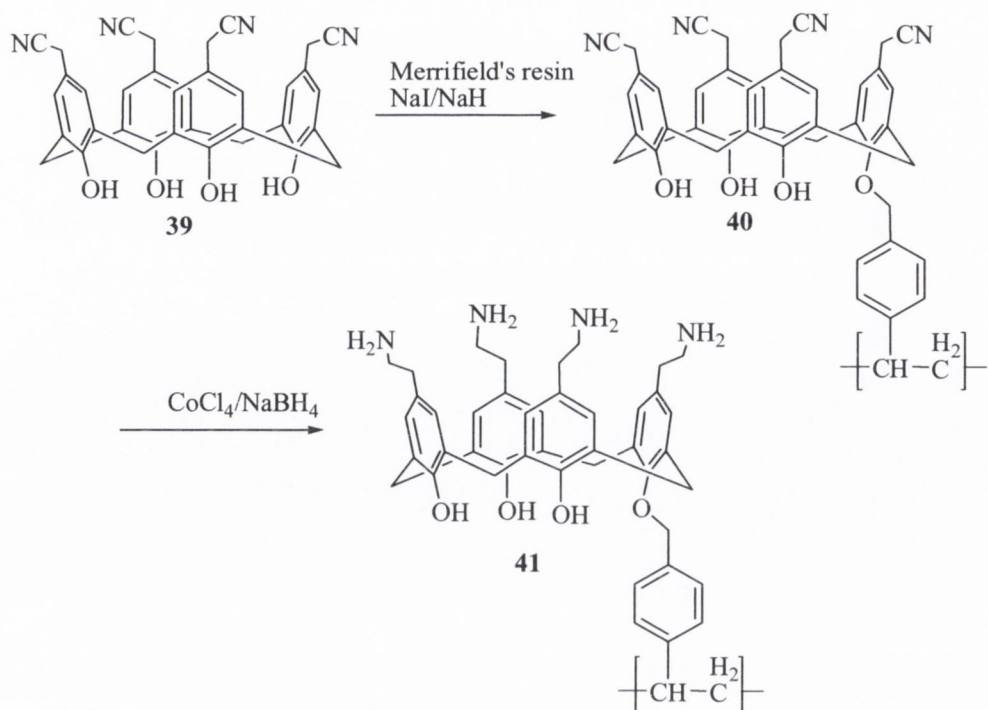
provided *n*-butylammonium binding ability, while the lower, amido NH protons supported binding of the corresponding Br^- or Cl^- anion.¹²¹



1.4 Macromolecule-bound calix[4]arenes

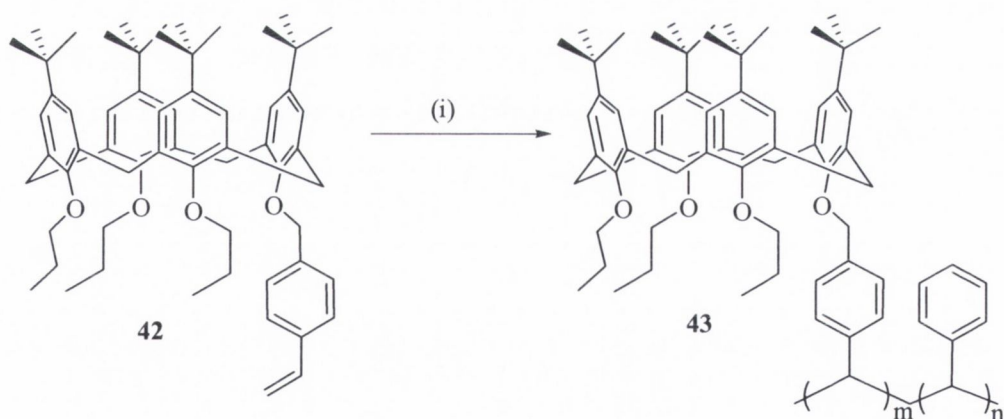
It is a fitting tribute that calixarenes, the synthesis of which parallels the preparation of the first commercial plastics (Bakelite), are now being incorporated into newer synthetic polymers such as poly(styrene) and Merrifield's resin. Further applications beyond synthetic resins have included the preparation of conjugates of calix[4]arenes with nanoparticles¹²². Such conjugate preparations offer the advantage of heterogeneous sensing by allowing for the incorporation of ionophores into electrodes, or by further immobilisation upon solid supports. The following section will outline some of the first examples of covalently bound macromolecule calix[4]arene conjugates.

The electrophilic nature of the benzylic carbon of Merrifield's resin is ideal for attack by the phenoxide ion of deprotonated calix[4]arene. Yilmaz and co-workers have recently reported the synthesis of a Merrifield resin-bound calixarene for use as a chromium(VI) extractant.¹²³ The monomeric calix[4]arene derivative gave a pH dependent extraction profile; at low pH (1.5), 13.5% of Cr(VI) was seen to be taken up by the host, while at higher pH (4.5) this was reduced to 4.8%. Upon conjugation of the ionophore to Merrifield's resin, Cr(VI) extraction was greatly enhanced: 91% at low pH, which was reduced to 9.8% at higher pH. The synthesis of this polymer-bound ionophore is outlined in Scheme 1.4.



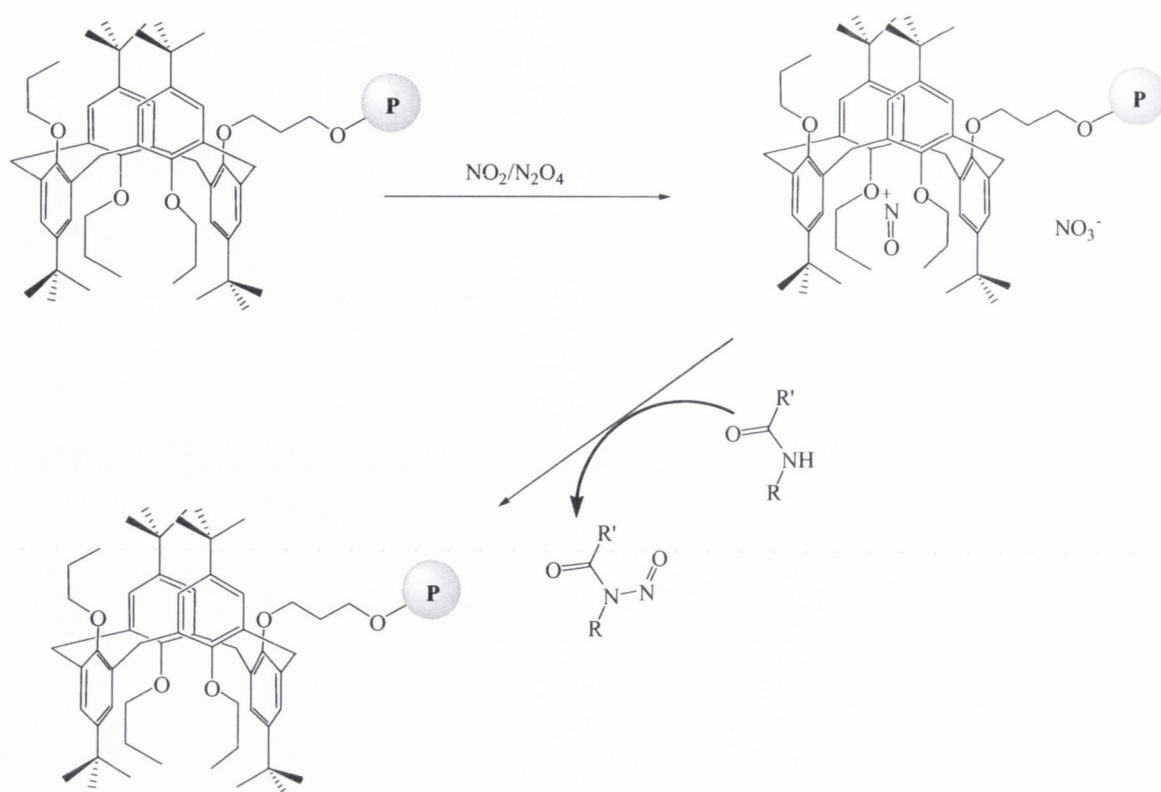
Scheme 1.4 – Incorporation of cyanomethylcalix[4]arene into Merrifield's resin and subsequent reduction.¹²³

Another example, proposed by Prata merges two strategies; the alkylation of calix[4]arene using a polymer such as Merrifield's resin, and the polymerisation of a calix[4]arene synthon.^{124,125} The latter in this case begins with alkylation at the lower rim to incorporate a styrene moiety. Polymerisation of this styryl calixarene with styrene using a benzoic anhydride activator furnished the copolymer shown in Scheme 1.5.



Scheme 1.5 – (i): styrene, acacia powder, NaCl/H₂O, Bz₂O, PhCl, 80°C

Polymer-supported calix[4]arenes were proposed by Rudkevich and co-workers, as sensors for NO₂/N₂O₄, and were used to entrap NO⁺ within their cavities.¹²⁶ This PEG-bound calix[4]arene/NO⁺ complex was further used to affect *N*-nitrosation of secondary amides.



Scheme 1.6 – Fixation of $\text{NO}_2/\text{N}_2\text{O}_4$ by polymer-immobilised calix[4]arene derivative and subsequent release of NO^+ in *N*-nitrosation reactions. (P) denotes polyethylene glycol 5000.¹²⁶

1.5 Enhanced Permeation and Retention (EPR)

As has been outlined in previous sections, calix[4]arene derivatives show significant potential as contrast agents for MRI. Many of the current efforts in contrast agent development, however, are directed towards of macromolecular bound or associated systems.¹²⁷ The purpose of this approach is two-fold. Firstly, tumorous cells possess leaky vasculature, compared to normal cells. This means that molecules can readily enter the tumour cells. In addition to this “enhanced permeation”, tumours also have poorly developed lymphatic systems. The result of the combination of these two factors is the uptake of macromolecules which are not readily cleared from the tumours and hence accumulate within the tumour mass.^{128,129} In the case of MRI contrast agents, this effect may be exploited either by the tethering of the drug to a macromolecule, or using a drug-containing macromolecule.¹³⁰ The EPR effect therefore leads to the accrual of a high concentration of contrast agent within the region of interest.

The second advantage to be gained from attachment of contrast agents to macromolecules is in the reduced rotational correlational time (τ). Larger molecules rotate and tumble more slowly than small molecules. Maximum relaxivity (thus the efficacy of contrast agents) is

limited, due to the Solomon-Bloembergen equations, by the rotational correlation time, τ_R (the average rotational time of the macromolecule in solution). For the contrast agents mentioned above, this is short, at approximately 2×10^{-10} s. This relationship is outlined in Equation 1.2, where η is the microviscosity of the sample (and is assumed similar to the macroviscosity of the solution) and k_B is Boltzmann's constant.^{131,132}

$$\tau_R = \frac{4\pi r_{\text{eff}}^3 \eta}{3k_B T} \quad \text{Equation 1.2}$$

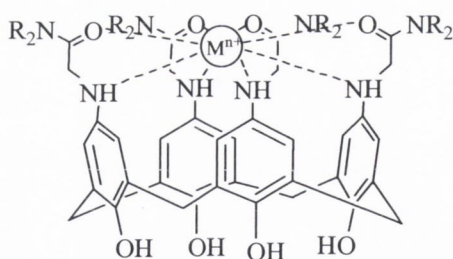
Conjugation to a macromolecule will therefore lead to an increase in the effective radius of the complex. The result of this is an increase in τ (a slower rotation rate). The effect that this has is that a larger number of water molecules are affected by the paramagnetic centre, through second and outer-sphere effects. This results in a greater enhancement in relaxation, and ultimately improved contrast in the image.^{133,134}

1.6 Work described in this thesis

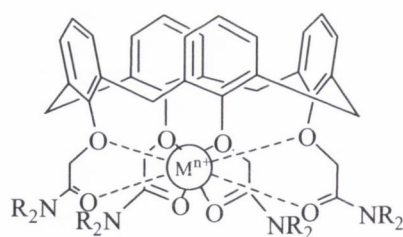
The aim of this thesis has been to combine the versatile chemistry of calixarenes and the recent innovations in the development of MRI contrast agents to prepare macromolecule-bound calix[4]arene derivatives for use as potential image enhancers. This requires the construction of a strong chelate and a covalent linkage for attachment to a macromolecular backbone. The following section will summarise the rational approach undertaken in this design.

1.6.1 Chapter 2: Synthesis of cation-binding calix[4]arene derivatives

Hitherto, as outlined, the appending of calix[4]arenes to macromolecules has generally been achieved by conjugation reactions at the lower rim. This has left the upper rim free and unfunctionalised. The lower rim, it was believed, would offer a more convergent lanthanide-binding array than that at the upper-rim. It was hoped that this preorganisation may allow stronger binding than that which would be possible at the upper rim. Upper and lower-rim cavities are illustrated schematically as **44** and **45** respectively.

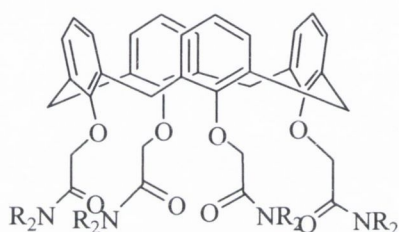


44

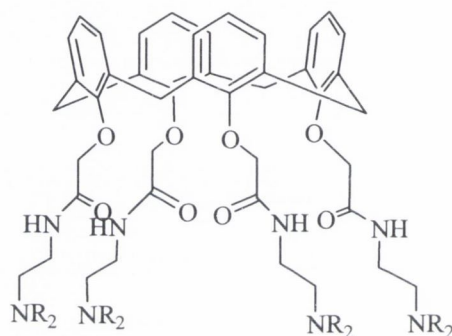


45

The potential lanthanide hosts described in this thesis are based on the motifs **46** and **47**, where R groups include piperidine, morpholine and simple alkyl groups. The incorporation of some simple amino acid moieties will also be discussed.



46

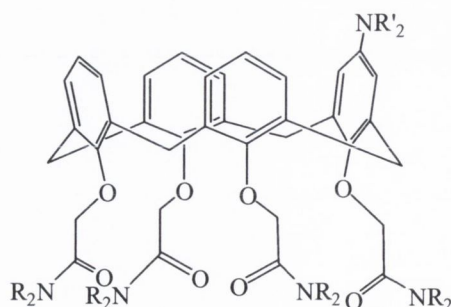


47

Chapter 2 describes several approaches to the preparation of chelates are described with intention of isolating any formed complex, in contrast with several literature precedents where solution-phase studies were possible by generation of the complexes *in situ*. Solution-state studies of some of the compounds prepared will also be reported.

1.6.2 Chapter 3: Towards cation-binding calix[4]arene conjugates

Chapter 3 outlines the approaches which were taken to incorporate functionality at a single position of the upper rim, that is to prepare chelates such as **48**.



48

Compounds such as **48** are under investigation for their potential be incorporated into larger architectures such as that schematically indicated in Figure 1.15, where the linker of primary interest is a urea or thiourea moiety. This may be accessible by conversion of the amino group to an isocyanate or isothiocyanate.

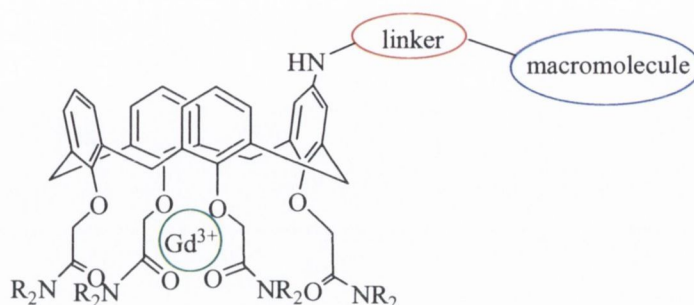


Figure 1.15 – Potential motif for covalent attachment of calix[4]arene derivative to a macromolecule

1.6.3 Chapter 4: Synthesis and spectroscopic study of anion-binding calix[4]arene derivatives

Chapter 4 describes the synthesis and study of the anion-complexation ability of a family of novel calix[4]arenes, based on the schematic molecule shown in Figure 1.16. The unique chemistry of calix[4]arenes has been exploited to provide arrays based on containing different numbers and different arrangements of anion-binding moieties. These contain the semicarbazide moiety which has not previously been exploited in the field of anion recognition using calix[4]arene derivatives.

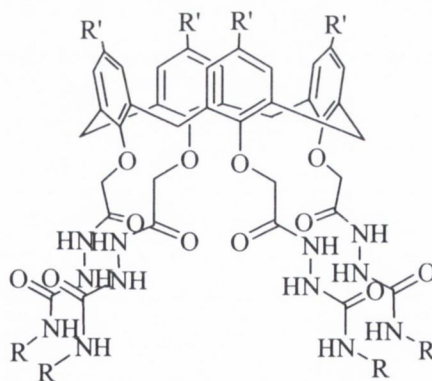


Figure 1.16 - Schematic target for anion-sensing using calix[4]arene derivatives

2.1 Introduction

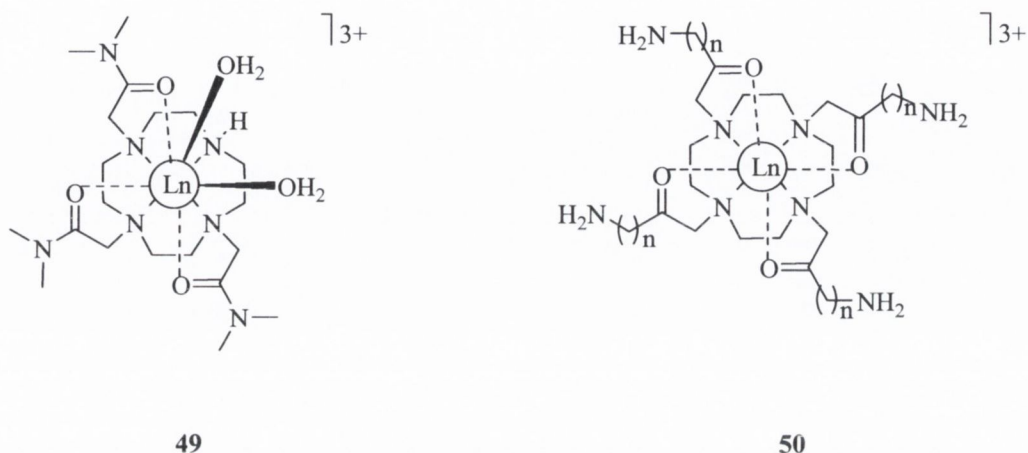
As discussed in Chapter 1, the use of calix[4]arenes as ionophores is long-established, and they have been particularly well studied for alkali earth metals.^{135,136} Calix[4]arene tetraethyl ester **7**, for example, is regarded as one of the best known artificial hosts for sodium ions, while affinity for potassium ions is also appreciable.^{65,66} Moderate functionalisation, which is generally straightforward, allows for the introduction of donor groups which can fine-tune the selectivity of the ionophore towards its guest. This chapter will outline the various attempts made to optimise the binding affinity of the lower-rim of calix[4]arene towards lanthanide ions, with the intention of developing efficient chelates for potential MRI application. Several approaches which were taken toward the introduction of amide functionality are described. The formation of complexes of metal ions with the ligands which were synthesised will also be discussed.

2.2 The Hard-Soft Acid-Base Concept

In constructing a metal-binding ligand, in which the metal behaves as a Lewis acid, and the ligand as a Lewis base, the interaction between the metal and ligand can be described as “hard” or “soft” (HSAB).¹³⁷ Hard acids are the smaller ions, with high charge states and include H^+ , alkali metal ions, some early transition metal ions and lanthanides. Hard bases, include ammonia, hydroxide moieties, carboxylates and the smaller halides – these, like hard acids are small, with localised, weakly polarisable charge. Soft acids are generally larger metal ions, with less charge density, including Cd^{2+} , Pt^{2+} and Hg^{2+} ions. Soft bases include sulfides, hydrides, and larger halides such as I^- . The rationale behind the HSAB theory is qualitative rather than quantitative; as an empirical observation, hard acids bind hard bases, while soft acids bind soft bases. With a hard acid in mind, such as Na^+ , for example it is therefore not surprising that it is readily bound by carboxylates, esters, oxygen-rich crown ethers and amides. Similarly, Hg^{2+} ions are readily bound using ligands which contain thiols – this is an example of a *soft-soft* acid-base interaction.

Lanthanide ions are hard acids, due to their small atomic radii and high charge density. Consequently, we expect Ln(III) to be bound efficiently using hard bases, such as carboxylates and amides. As shown in Chapter 1, the efficient MRI contrast agents DOTA and DTPA, in addition to the classic chelating agent EDTA, have carboxylate moieties, possessing significant Lewis basicity at the coordinating oxygen atoms. Strong binding constants ($\log K_{ML}$ in the region 22-24) have been reported for the complexation of these

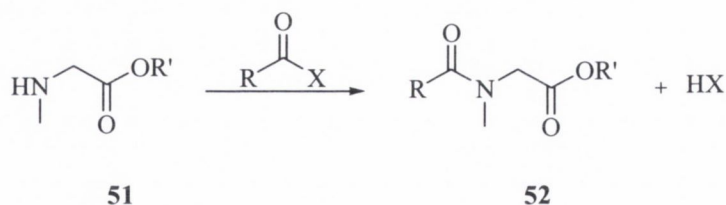
ligands with lanthanide ions.¹³⁸ Within our own group, considerable success has been enjoyed in creating cyclen-based systems such as **49** and **50** which contain amide functionality.^{139,140} These have been developed for several applications, including the hydrolytic cleavage of RNA and as lanthanide luminescent probes.



Given the affinity possessed by amides towards lanthanide ions, as shown here and as discussed in Chapter 1, it was decided to develop methods for the preparation of amide-containing calix[4]arenes, as amido functionality can be introduced by the use of a number of peptide-coupling techniques. This Chapter will detail these undertakings.

2.3 Development of a sarcosine-based calix[4]arene

N-Methyl glycine, or sarcosine, **3** is a simple secondary amine. When incorporated in to an amide bond, it provides a tertiary amide, as shown in Scheme 2.1.



Scheme 2.1 Formation of tertiary amide from secondary amine.

Initially, such tertiary-amide containing calixarenes were chosen for development due to the slow rotation that tertiary amides possess. This motif was also chosen due to the preorganisation that it would provide in a potential MRI contrast agent. Once the complex has formed, it is anticipated that the lower, non-amido carbonyl moiety would also be bound to the guest ion, due to the self assembling, templating effect of the metal ion. It is this property which complicates the ¹H NMR spectra of tertiary amides. Rotation proceeds at a rate slower than the NMR timescale,¹⁴¹ and frequently two isomers, or rotamers can be

seen in ^1H NMR spectra. The presence of rotamers is confirmed by recording the spectrum at elevated (50 – 70 °C) temperature, allowing the energy barrier for rotation to be overcome. This may, however cause loss of fine structure in the ^1H NMR spectrum.

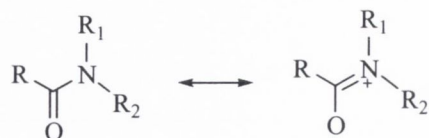
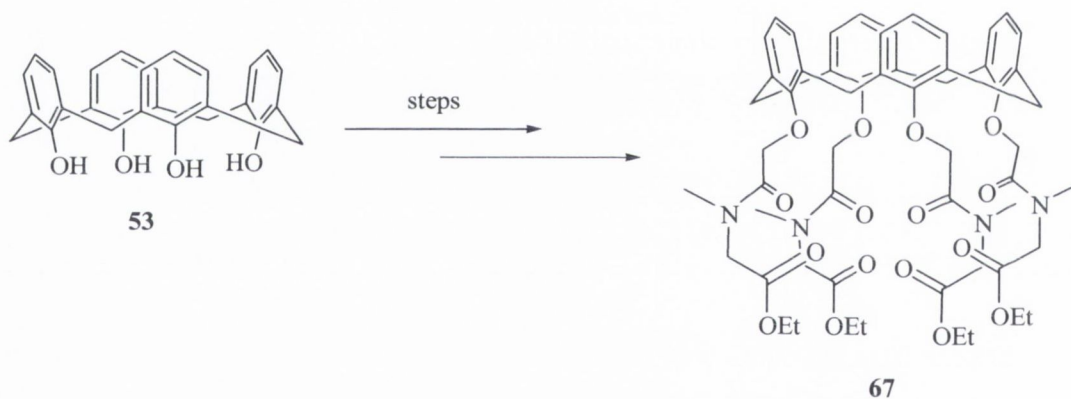


Figure 2.1 – Restriction of rotation about the amide bond in highly *N*-substituted systems due to double-bond character in the C-N bond inducing p-orbital overlap.

As has been discussed in Chapter 1, there are several techniques at our disposal for the incorporation of functionality into the lower-rim of calix[4]arenes. Once these transformations have occurred, it is possible to introduce further functionalisation by additional derivatisation reactions. Targets such as **67**, as shown in Scheme 2.2, are therefore of interest in this project, as they will potentially enable the binding of lanthanides in a hard-acidic binding array, which is fortified by the preorganisation offered by both the calix[4]arene scaffold and the aforementioned rigid tertiary-amides.



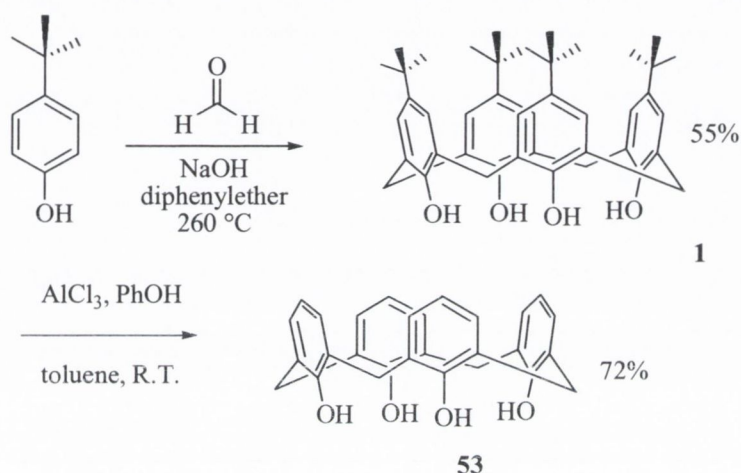
Scheme 2.2 – Target sarcosine-containing calix[4]arene ligand.

2.3.1 Derivatisation of calix[4]arene ester

Though it is commercially available, calix[4]arene is expensive. It was therefore prepared according to a literature procedure, which is shown in Scheme 2.3.²⁵ This was achieved by first preparing the parent tetra *tert*-butyl calix[4]arene **1** by a base-catalysed condensation reaction between 4-*tert*-butyl phenol and formaldehyde. This occurs in two stages. Firstly, the reactants are gently heated to initiate the condensation, and to form a polymeric “precursor” to the *tert*-butyl calix[4]arene. The precursor is then heated in refluxing diphenyl ether to >260 °C for several hours. This heating is responsible for the formation

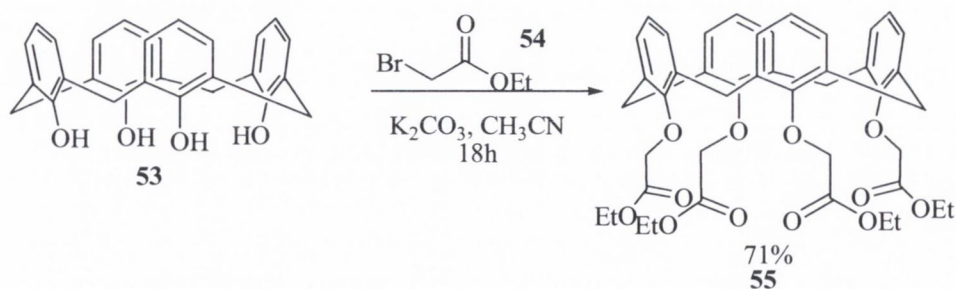
of the cyclic tetramer. Following cooling, the product is precipitated using ethyl acetate and collected with suction filtration. Several washes with further ethyl acetate, acetic acid and water provide the desired product **6**, in 55% yield, requiring no additional purification steps.

Cleavage of the *tert*-butyl moieties of **6** can be accomplished by a retro Friedel-Crafts reaction,³⁵ using aluminium(III) chloride in a large excess, in the presence of phenol. The reaction occurs in toluene, which, in conjunction with phenol acts as a Friedel-Crafts acceptor of the ^tBu groups. This is outlined in Scheme 2.,



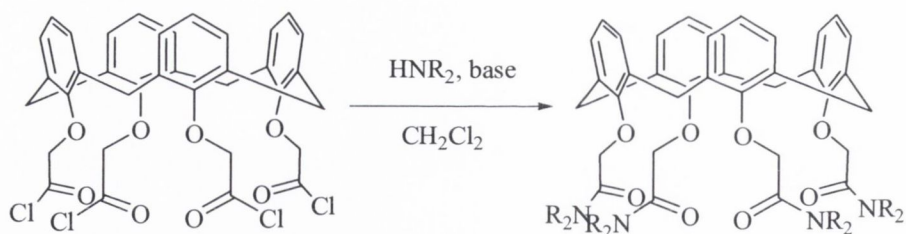
Scheme 2.3- Preparation of ^tBu calix[4]arene **1**, and calix[4]arene, **53**.

The first approach taken was to prepare the tetraethyl ester of calix[4]arene⁶⁶ and to further derivatise the ester by peptide coupling techniques. Alkylation of calix[4]arene using ethyl bromoacetate to yield the tetra ester was first attempted, as illustrated in Scheme 2., forming the desired product, **55** as a crystalline solid in 71% yield.



Scheme 2.4 - Esterification of calix[4]arene in cone conformation.

The conversion of the tetraester, **55** to the corresponding acid chloride is attractive, as this intermediate should then be amenable to reaction with an amine, such as sarcosine ethyl ester hydrochloride to furnish the corresponding amide. This is as illustrated in Scheme 2.5.



56

Scheme 2.5 – Reaction of acid chloride of calix[4]arene with a secondary amine to yield the corresponding tetra-tertiary amide.

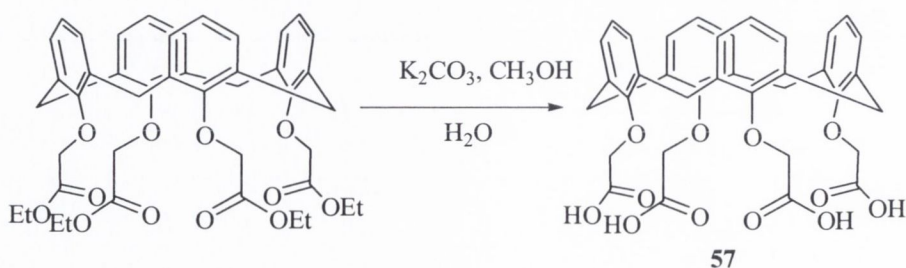
This reaction was attempted using a variety of conditions, varying the acid chloride precursor, solvent and base, as shown in Table 2.1. In each case, the acid chloride was not isolated prior to reaction with the amine. Rather, it was brought to dryness under vacuum and then introduced to a solution of the amine in CH_2Cl_2 .

Table 2.5 –Reaction conditions attempted for direct conversion of ester to amide.

Acid Chloride Synthon	Solvent	Base	Result
SOCl_2	neat	1 equiv. NEt_3	No product
$(\text{COCl})_2$	neat	1 equiv. NEt_3	No product
SOCl_2	CH_2Cl_2	2 equiv. NEt_3	No product

On a number of occasions, these reactions were attempted, as listed in Table 2.5 with a catalytic amount of DMF. This has been shown to be an effective catalyst for the formation of acid chlorides from carboxyl derivatives.¹⁴² The result of these reactions was as before, showing no formation of the products.

Alkaline hydrolysis of the ester moieties of **55** was then carried out, using either tetramethylammonium hydroxide or potassium carbonate. This yielded the corresponding carboxylic acid, as outlined in Scheme 2.6. Attempts to convert this acid to the corresponding tetra acid chloride, and to subsequently treat this with sarcosine ethyl ester were also unsuccessful, under a variety of base and solvent conditions.



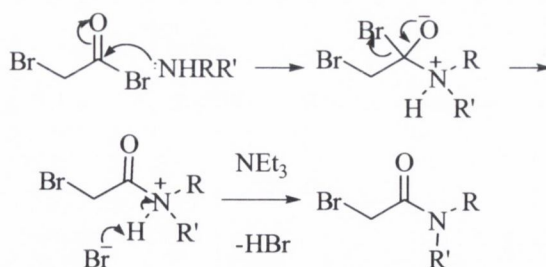
Scheme 2.6 - Hydrolysis of ester moieties of calix[4]arene tetraethyl ester, **55**

The use of peptide coupling agent, dicyclohexylcarbodiimide (DCC) was also investigated. DCC is a useful coupling agent due to the insolubility of the by-product of its reaction, dicyclohexylurea (DCU), which can therefore be removed by filtration. Reaction of calix[4]arene tetra carboxylic acid with DCC and sarcosine ethyl ester hydrochloride in either CH_2Cl_2 or 1,4-dioxane, in the presence of triethylamine gave a visible DCU precipitate, which indicated the progression of the reaction, that is, that the active ester was forming and was being displaced by an amine. The product however could not be isolated further from this reaction, and due to sensitisation issues, the approach was not further pursued.

Due to these difficulties, it was decided to focus attention on the introduction of pre-formed amide functionality, using α -bromoamides, which could be used to alkylate the calixarene to give the desired amide linkage. The following section will detail the syntheses of the α -bromoamides which were synthesised in the course of this work.

2.4 Formation of α -bromoamides

Given the failure of attempts to form the amide bond on the calixarene, it was logical to adopt a convergent synthesis, requiring the calixarene to be alkylated with an amide-containing unit. The synthesis of these alkylators was straightforward, requiring the reaction of one equivalent of bromoacetyl bromide with an amine in the presence of a base such as NEt_3 to scavenge the HBr generated. The base was successfully altered from triethylamine, to solid NaHCO_3 (which had the advantage that it was removed by filtration) though it was not advantageous in terms of yield or purification to use any base other than triethylamine (which was removed by washing). The mechanism of formation of these compounds occurs is outlined in Scheme 2.7.



Scheme 2.7 – General mechanism of formation of α -bromoamide.

The product of this reaction is then reacted with calix[4]arene in a classical base-catalysed Williamson ether synthesis. Similar compounds are obtained by use of chloroacetyl chloride, and are utilised within the Gunnlaugsson group for the alkylation of cyclen.^{26,27}

However for the functionalisation of the phenolic moiety of the calixarenes, the bromo leaving group was preferred.

Preparation of the sarcosinyl α -bromoamide, ethyl 2-(2-bromo-*N*-methylacetamido)acetate **58** was undertaken in this manner, analogous to the synthesis of the α -chloroamide of the methyl ester which had previously been reported.¹⁴³ This yielded the product as an oil which was satisfactorily characterised, with accurate mass spectrometry (ES+) showing two peaks of equal intensity, separated by 2 units, which is characteristic of a monobrominated molecule. As expected, the presence of a tertiary amide complicated the ^1H NMR spectrum, due to the aforementioned rotamers, as shown in Figure 2.2.

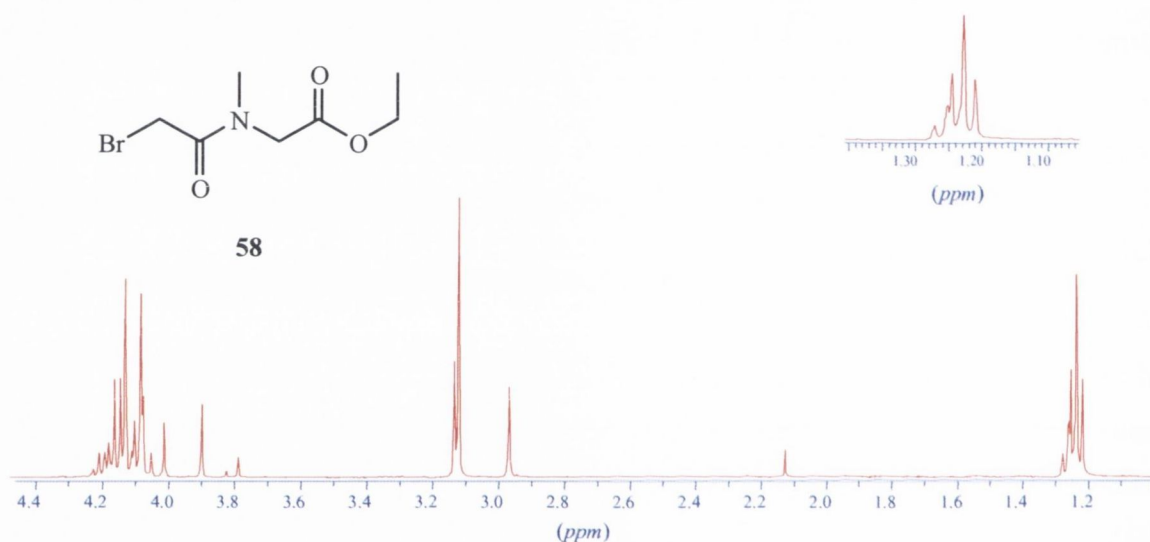
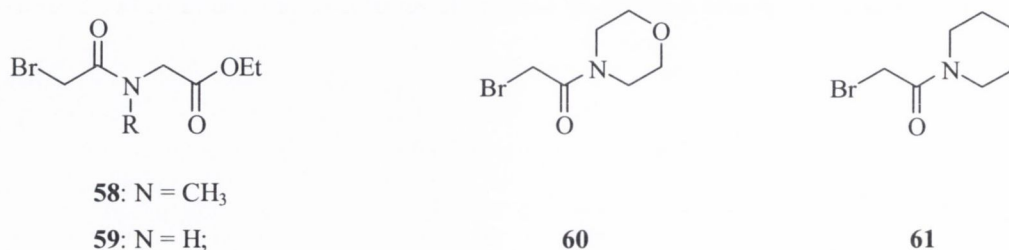
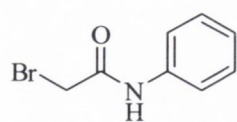


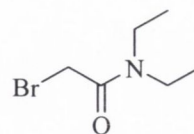
Figure 2.2 – ^1H NMR (400 MHz, CDCl_3) spectrum of sarcosine bromoamide **58**.

Purification of the oil, when required, was achieved by distillation at reduced pressure where necessary. Column chromatography on silica, with elution in 100% ethyl acetate was also employed as a method of purification. However, in most cases, the bromoamides were used without purification, with no adverse effect on the next stage of the reaction. Yields were therefore assumed to be quantitative. The synthesis of the following α -bromoamides was successfully achieved using the outlined methodology.



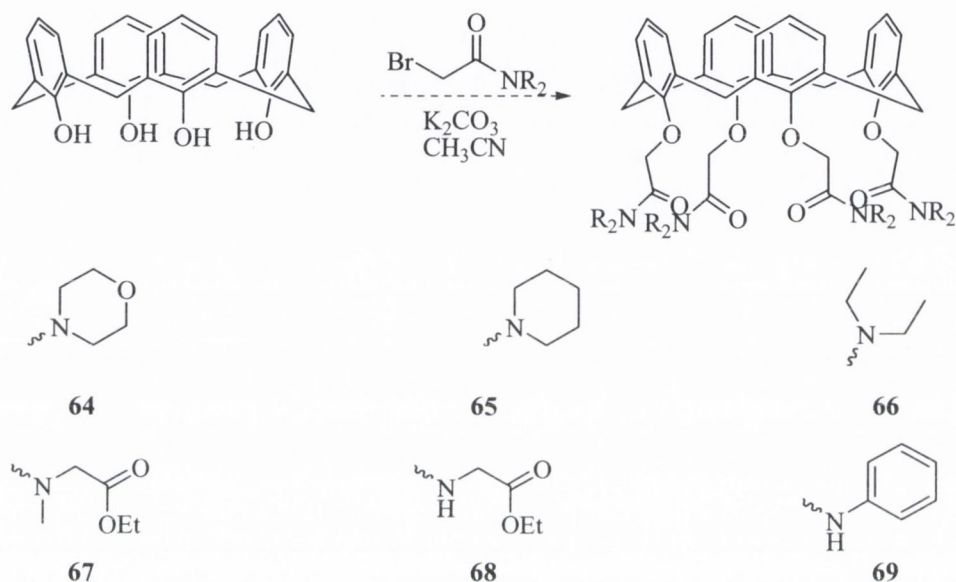


62



63

In each case, the bromoamides **10-15** were seen to react with calix[4]arene **7**, as shown in Scheme 2.8.



Scheme 2.8 – Intended alkylation of calix[4]arene using α -bromoamide with R derivatives shown.

In the case of alkylation using **58**, the sarcosine analogue, isolation of the product, **67** met with difficulty, and on only one occasion was the desired ligand obtained. The reaction was repeated numerous times, varying the reaction conditions, including addition of iodide which is expected to mediate a Finkelstein halogen exchange reaction. However, this was without success. Solvent variations did not appear to play a significant role either, with similar impure products forming from reactions conducted in acetone, CH₃CN, 2-butanone and DMF. Use of different carbonate bases (K₂CO₃, Na₂CO₃) also showed no difference in the formation of the product. While it was believed that the product was present, purification was difficult. Column chromatography (SiO₂) was attempted in a variety of polar solvents (CH₂Cl₂/MeOH 95:5, MeCN 100%), each time failing to yield the product. Size-exclusion chromatography, using Sephadex (LH-20, lipophilic), eluting the solution in CH₂Cl₂, again failed to give the desired product.

The sample of **67** which was successfully isolated was obtained by precipitation of a crude solid from a CH_2Cl_2 solution using both ethyl acetate and diethyl ether, followed by collection by suction filtration and recrystallisation from hot ethanol. The ^1H NMR spectrum was complicated, as expected, due to the existence of rotamers. This complexity was nevertheless significantly alleviated upon recording the spectrum at elevated temperature. The variable-temperature NMR spectra, which were recorded at 30 °C, 50 °C, and 70 °C respectively are shown in Figure 2.3

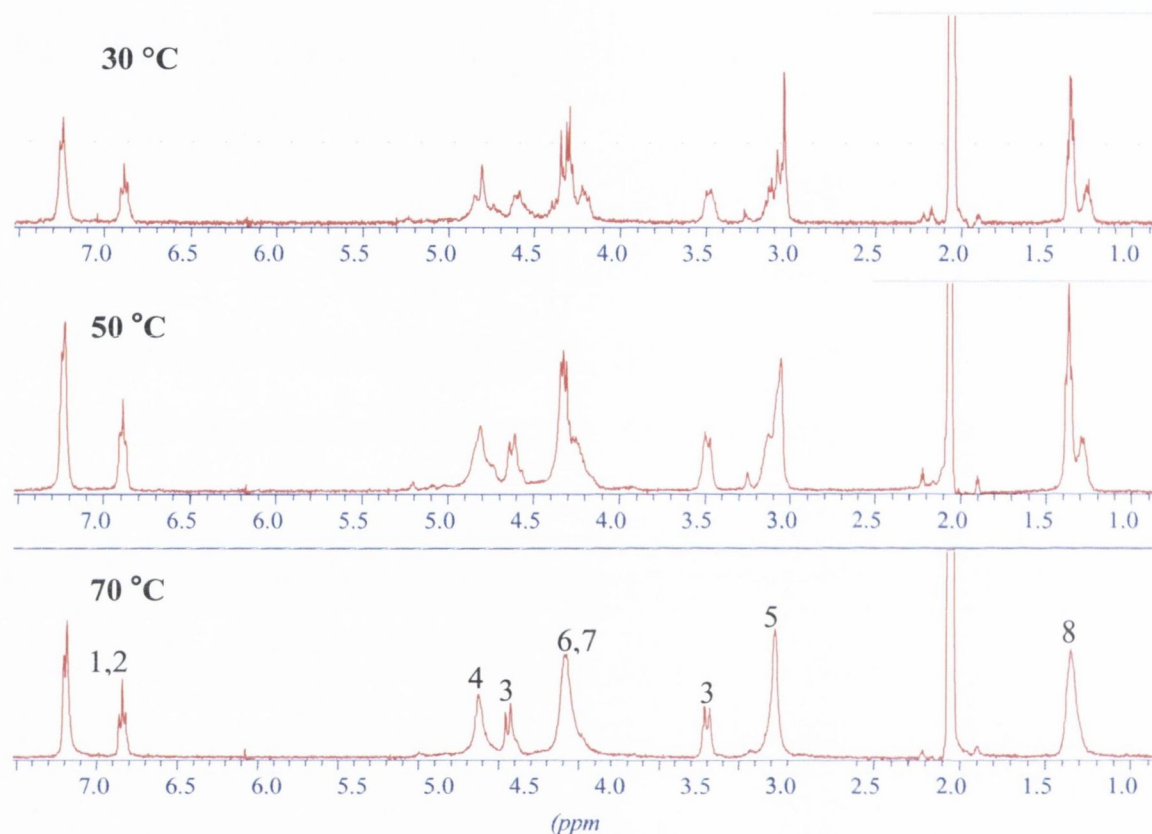
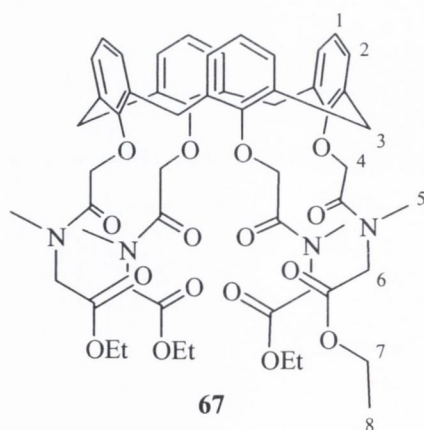


Figure 2.3 – ^1H NMR spectra (400 MHz, $\text{CD}_3\text{CO}_2\text{D}$) of **67** at 30 °C, 50 °C and 70 °C respectively, showing coalescence of rotameric signals upon heating.



The splitting of the CH₃ signals of the ethyl ester is most clearly resolved upon heating, where upon heating from 50 °C to 70 °C, the rotamers become one broad singlet (resolution of the expected triplet is lost at high temperature) which resonates at 1.35 ppm. The “quartet” signal corresponding to the adjacent CH₂ is not clearly visible at lower temperatures, yet appears to be centred around 4.3 ppm. Upon heating, this merges with other signals to give a broad singlet (4.31 ppm) with integration of 16H, this is assigned to both the ethyl moiety and the CH₂ moiety α- to both amide and ester moieties. This assignment was confirmed by HMBC experiments which showed the singlet at 4.31 to be coupled to two environments of CH₂, at 49.1 and 61.1 ppm. While the fine structure is lost upon heating, the overall simplification of the spectrum is indicative of formation of the desired product. The corresponding quartet of the ethyl moiety is seen to coalesce with the *N*-methyl moiety. The calixarene doublets are clearly visible at 4.64 and 3.47 ppm, indicating the fixed cone conformation of the molecule. This is also indicative of substitution of the calixarene parent. Notably, the aromatic signals are unperturbed by heating. This is due to their remote location relative to the point of rotation. As the DEPT NMR experiment could not be carried out at high temperature, full resolution of the ¹³C signals could not be carried out. The HMQC spectrum, illustrated in Figure 2.4, shows these correlations.

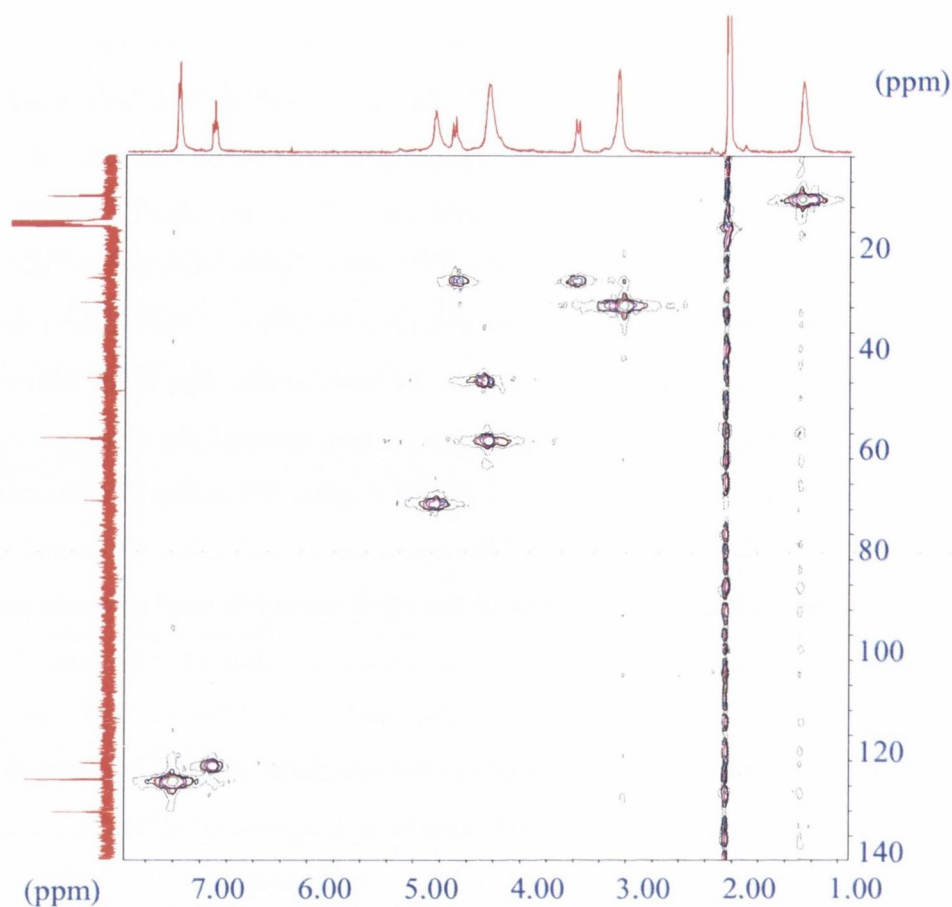
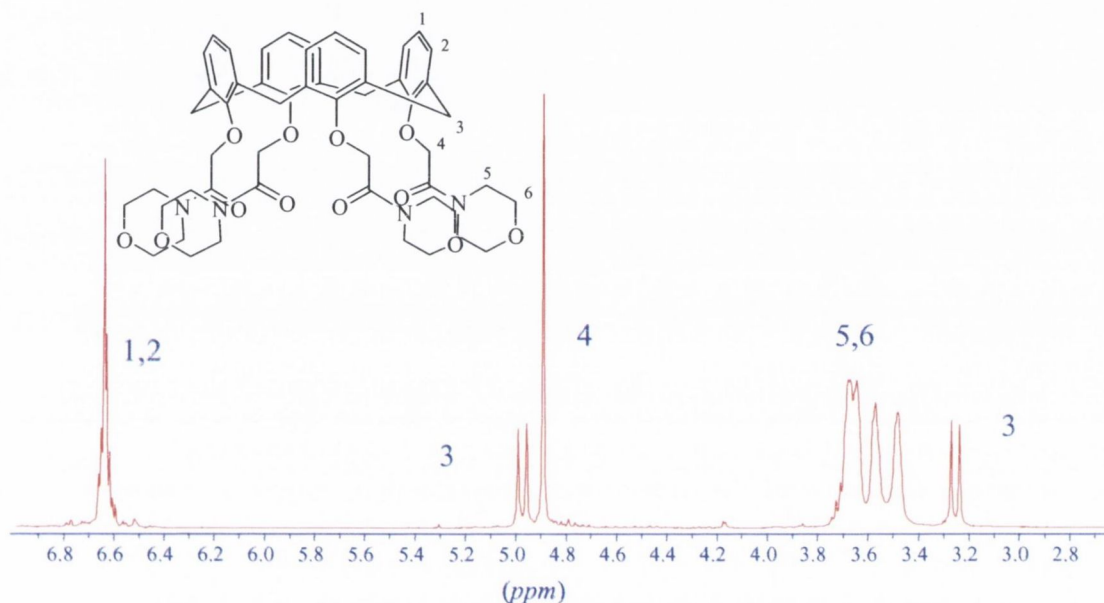
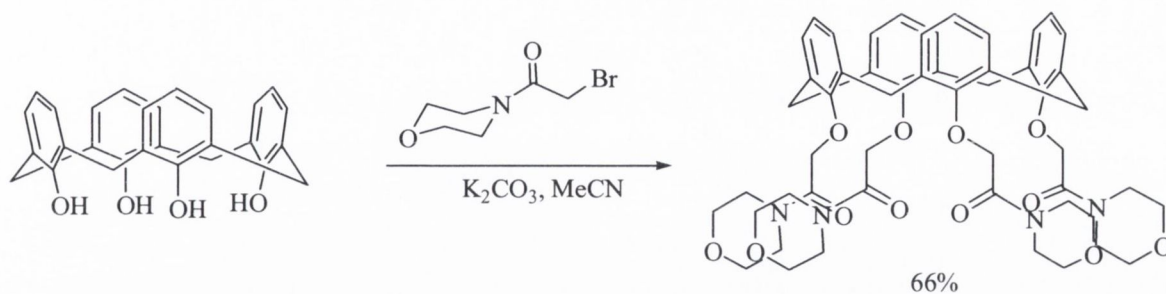


Figure 2.4 – HMBC of sarcosinyl calix[4]arene **67** (9.4 T, 70 °C, CD₃CO₂D).

However, with some other α -bromoamides more successful results were readily obtained and their spectra more simplified. The α -bromoamides **60** and **61**, containing morpholine and piperidine respectively, were selected as they allowed for the introduction of diverse amines. Morpholine was chosen due to the presence of the oxygen, which may potentially act as a hydrogen bond acceptor, in outer-sphere MRI contrast application. The piperidine analogue was prepared as a control for analysis of the effect which this additional oxygen may provide.

The alkylation of calix[4]arene using both α -bromoamides **60** and **61** was straightforward; using a small excess (5.0 equiv.) of the appropriate α -bromoamide with respect to calix[4]arene, in acetonitrile, with excess K₂CO₃ as a base. Workup required evaporation of the solvents to dryness, followed by uptake of the residue into CH₂Cl₂ and washing with water. Evaporation of the organic phase gave an oil which was stirred in diethyl ether, and which precipitated the crude product. This was then purified by crystallisation from CH₂Cl₂/EtOH, giving **64** and **65** in 66% and 49% yields, respectively. The retention of the

cone conformation by this ligand is confirmed by the characteristic two-doublet pattern observed in the ^1H NMR spectrum, which is shown in Figure 2.5.



The C_4 symmetry of this molecule is immediately apparent from the simplicity of the spectrum. The aromatic protons coalesce to a multiplet, centred at 6.50 ppm, while the calixarene bridging doublets are at 4.98 ppm and 3.26 ppm respectively. The methylene protons α - to the phenolic oxygens are represented as a singlet at 4.90 ppm, while the morpholine protons are seen as four different environments between 3.69 ppm and 3.49 ppm which correspond to each of the different axial (A) and equatorial (E) protons, as shown in Figure 2.6.

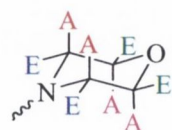


Figure 2.6 – Two types of both axial (A) and equatorial (E) proton environments in morpholine derivatives.

The geminal (axial to equatorial) coupling constants were not obtainable from this spectrum. However, the spectrum is unambiguously simple, for such a ligand.

The ^1H NMR spectrum (400 MHz, CDCl_3), shown in Figure 2.7, obtained in the case of the piperidine analogue **18** was also unambiguously assigned to the desired structure. The aromatic protons and spacer protons resonate clearly at 6.62 and 4.90 respectively, while the calixarene doublets are seen, once again, as distinct doublets at 5.11 and 3.26. The aliphatic protons are seen in four different environments; two broad singlets at 3.53 and 3.43 which can be attributed to the protons adjacent to the nitrogen in both *cis*- and *trans*-environments. The remaining methylene protons are seen in a 1:2 ratio at 1.63 and 1.55 ppm, respectively.

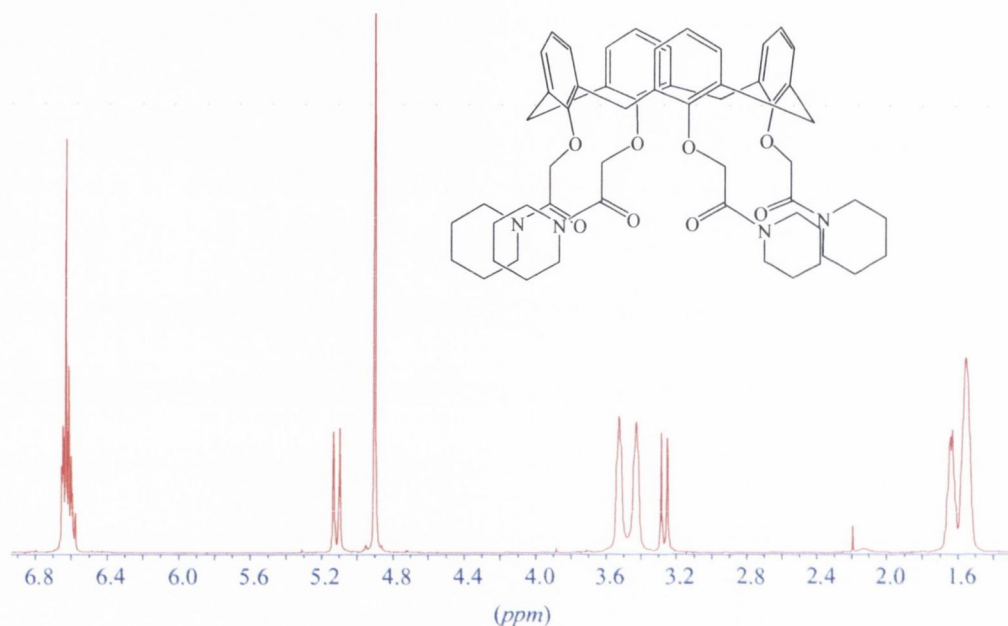


Figure 2.7 - ^1H NMR (400 MHz, CDCl_3) of tetrapiperidinyl **65**.

In this case, crystals which were suitable for X-ray crystallographic studies were grown for both compounds. Both samples were crystallised overnight from $\text{CH}_2\text{Cl}_2/\text{CH}_3\text{OH}$ solutions. For **64**, the crystals diffracted only weakly, and no structural data could be obtained. In the case of **65**, the crystal structure, as solved by Dr Tom McCabe of the School of Chemistry, Trinity College Dublin is shown in Figure 2.8. Further crystallographic data for all structures are detailed in Appendix 1.

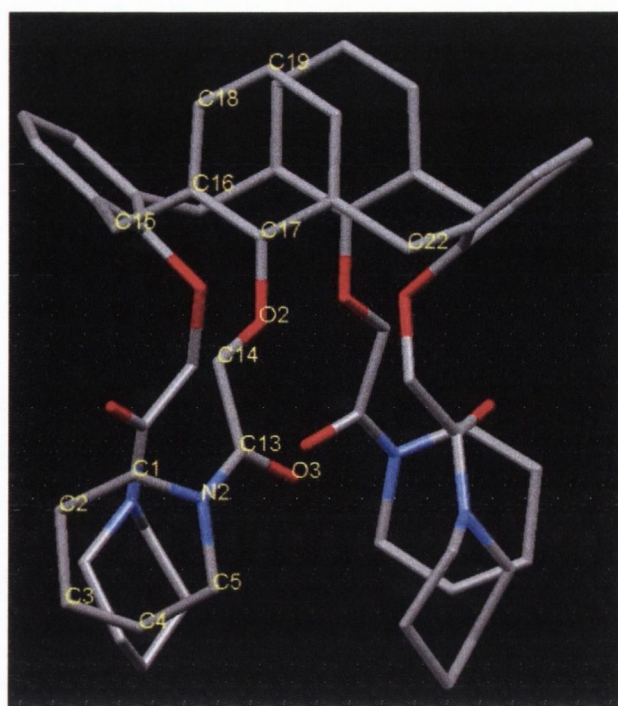


Figure 2.8 – X-ray crystal structure of **65**. Hydrogen atoms have been omitted for clarity.

As is clear from the crystal structure, the calixarene has a pronounced “flattened-cone” where two of opposite aromatic rings are “flattened” out, while the others are pinched together and are essentially parallel (a more extreme “pinched cone” will be seen in **75**). Using internuclear distances as determined from the crystallographic coordinates, the “pinched” rings lie 5.08 Å apart, while the “flattened” rings are 9.86 Å apart.

Selected bond angles and distances are detailed in Table 2.6.

Table 2.6 – Selected bond lengths and angles for **65**.

Bond		Length (Å)	Bond			Angle(°)
C19	C18	1.375(6)	C3	C2	C1	110.4(5)
C18	C16	1.398(7)	C4	C3	C2	111.0(4)
C16	C17	1.402(6)	C2	C1	N2	109.0(4)
C17	O2	1.391(5)	C1	N2	C5	113.1(4)
O2	C14	1.389(5)	C5	N2	C13	120.5(5)
C14	C13	1.499(8)	N2	C13	O3	120.9(5)
C13	O3	1.169(7)	O3	C13	C14	121.2(4)
C13	N2	1.339(6)	C13	C14	O2	110.7(4)
N2	C1	1.393(7)	C21	C22	C23	107.1(3)
C1	C2	1.472(8)	C25	C15	C16	114.6(3)

C2	C3	1.521(8)
C3	C4	1.431(8)
C4	C5	1.514(9)
C5	N2	1.483(8)
C16	C15	1.535(6)
C22	C21	1.511(6)

A view of the packing in the solid state, along the c^* crystallographic axis, as determined from this study is shown in Figure 2.9. A ribbon-like packing array can be seen, whereby the calix[4]arene aromatic core and the aliphatic piperidine moieties alternate in a head-to-tail fashion. Contact between the aliphatic protons and the protons α - to the phenolic oxygen is observed in this structure.

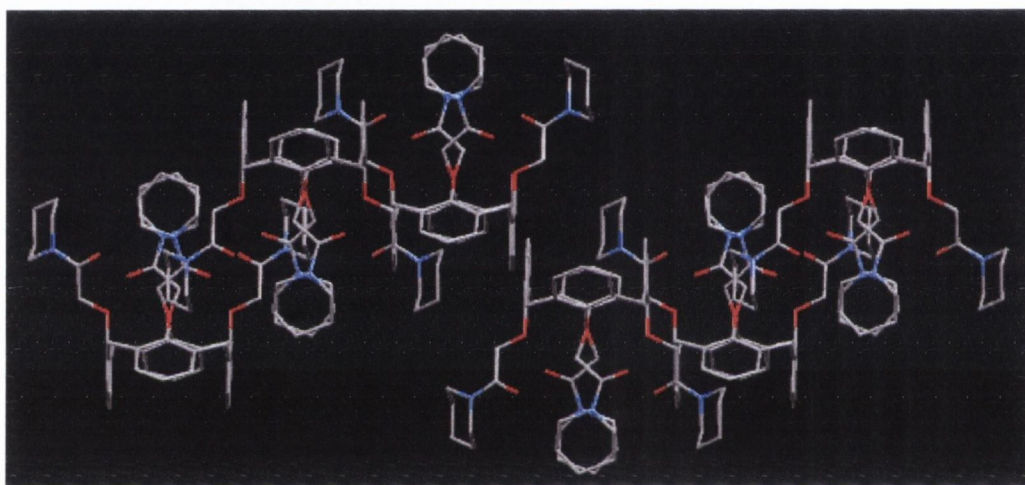


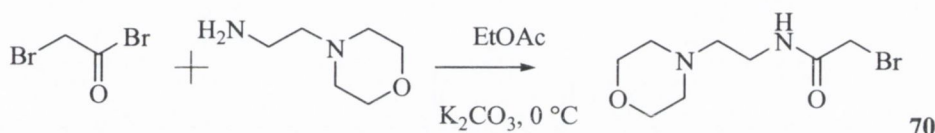
Figure 2.9 - Packing diagram as viewed along c^* crystallographic axis of structure of 65

The solid state structure of this ligand has allowed insight to be obtained into the size (approximately 6.4 Å diagonally between coordinating amido carbonyl oxygens) of the cavity, and possible binding modes which may occur upon inclusion of a metallic guest. Coordination of the metal by both phenolic and amido carbonyls is feasible, however it is possible that the piperidinyl or morpholinyl ring may impart strain on the system, thus lowering the binding affinities towards metals. Synthesis of some more flexible binding motifs was to be undertaken; it was believed that introduction of spacer moieties may provide this flexibility.

2.5 Preparation of flexible binding arrays at the lower rim

While the previous section has outlined the preparation of some potential ligands, it was decided to incorporate a larger cavity to the calixarene. The extension of the morpholinyl and piperidinyl compounds to incorporate a spacer moiety would potentially allow more flexible assembly of a host-guest complex. The synthesis of the required α -bromoamides was therefore undertaken, and alkylation carried out. The following section will outline these efforts.

Firstly, α -bromoamides such as that of 4-(2-aminoethyl)morpholine **70** were prepared according to the conditions shown in Scheme 2.10



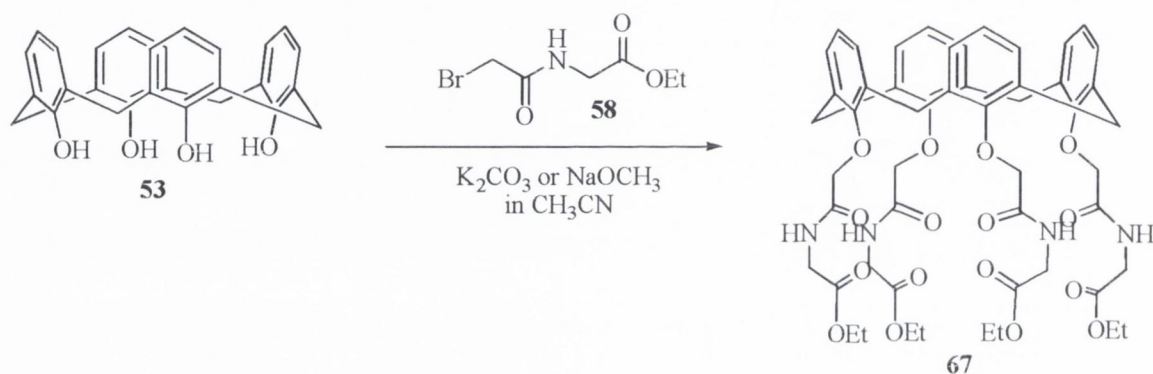
Scheme 2.10 - Synthesis of 2-bromo-*N*-(2-morpholinoethyl)acetamide **70**.

This strategy was attempted in analogy to work performed within the Gunnlaugsson group by Vigui er on some similar cyclen systems.¹⁴⁴ The α -bromoamide **70** was prepared quantitatively as its hydrobromide salt by stirring both reagents in ethyl acetate at 0 °C over solid potassium carbonate. The use of a heterogeneous base offered further simplification of the work-up of this type compound; the solids were filtered off once the reaction had reached completion, and the solvent washed with water. Drying of the organic layer (Na_2SO_4) and removal of the solvent gave a solid which was identified as the pure product by ^1H NMR spectroscopy. This method was utilised in the synthesis of morpholine, piperidine and *N,N*-diethyl analogues. The morpholine bromoamide **70** was then subjected to standard calixarene alkylation procedure, by stirring at reflux with calix[4]arene and base in CH_3CN overnight. To compensate for the use of a salt and the subsequent formation of HBr , a further equivalent of base (K_2CO_3) was then added. Work-up using the standard procedure of washing the residues with water or acid/base workup however, failed to isolate the products; thick emulsions repeatedly formed upon washing the solvent mixtures with water. The reaction was repeated, with prior liberation of the free α -bromoamide (the salt was taken up in CH_2Cl_2 , washed with K_2CO_3 and reduced to an oil). When this was used as an alkylator in subsequent reactions, the desired product was again not isolated. Similar difficulties were met with in the alkylation of calixarene with the *N,N*-diethyl analogue. As a result, the synthesis by this method of these ethyl-spaced

compounds was deferred. A more expedient route to these desired compounds was later developed which avoided the isolation issues which were encountered with this reaction. This will be discussed in Section 2.7.2.

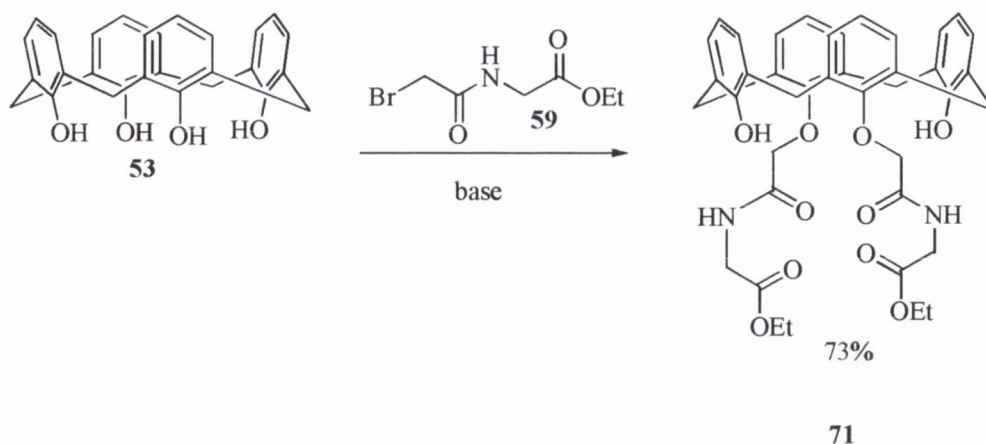
2.6 1,3-dialkylation reactions

The α -bromoamide **59** (derived from glycine ethyl ester hydrochloride) and **62** (from aniline) were successfully prepared by the standard method, using NEt_3 in CH_2Cl_2 . Both of these alkylators were used to alkylate calix[4]arene **55** with the intention of preparing tetra-amide containing scaffolds. These reactions were carried out in the normal manner, using a slight excess of alkylator in CH_3CN in the presence of K_2CO_3 , as is shown in Scheme 2.11.



Scheme 2.11 – Intended alkylation of calix[4]arene with glycinyln bromoamide.

In the case of the glycine analogue, the reaction did not proceed past the 1,3-dialkylated calixarene **71**; two distal phenolic moieties had been alkylated. This reaction was repeated using longer reaction times and more forcing conditions (the stronger base NaOMe was used), to try to drive the reaction to tetrasubstitution. In each case, again only formation of the disubstituted product was observed. This is illustrated in Scheme 2.11, where either NaOCH_3 or K_2CO_3 provided the same 1,3-disubstituted product.



Scheme 2.12 – Formation of 1,3-disubstituted glycinylic **71** calix[4]arene.

However, the product was formed in good yield of 73%, with high purity. Following evaporation of the solvents and washing with water, the product was precipitated by stirring in ethanol. The ^1H NMR spectrum, confirming disubstitution in a distal arrangement is shown in Figure 2.10.

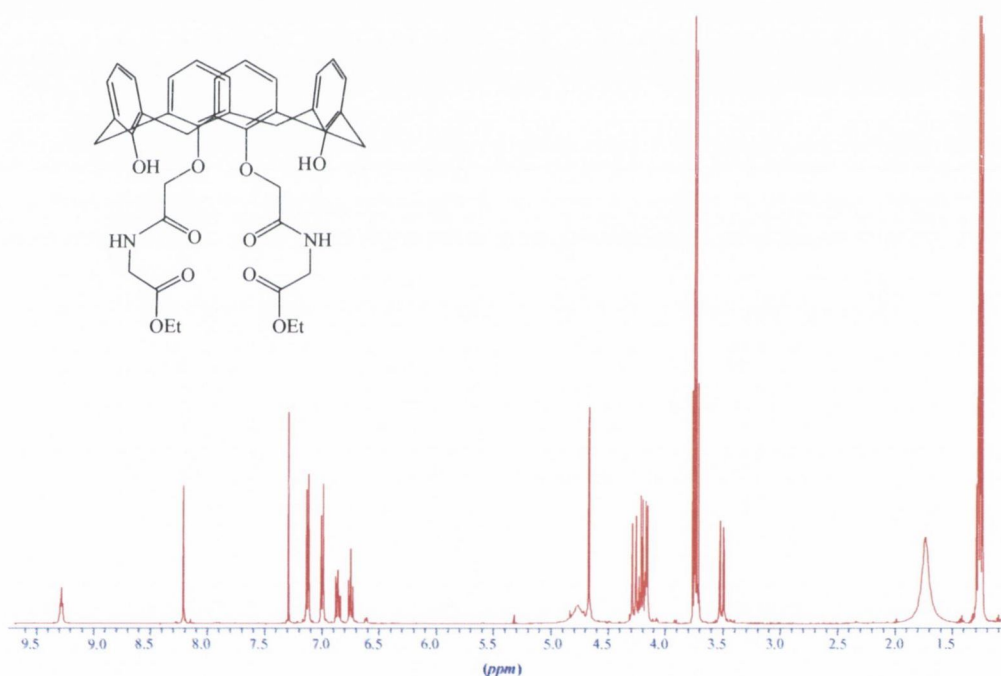
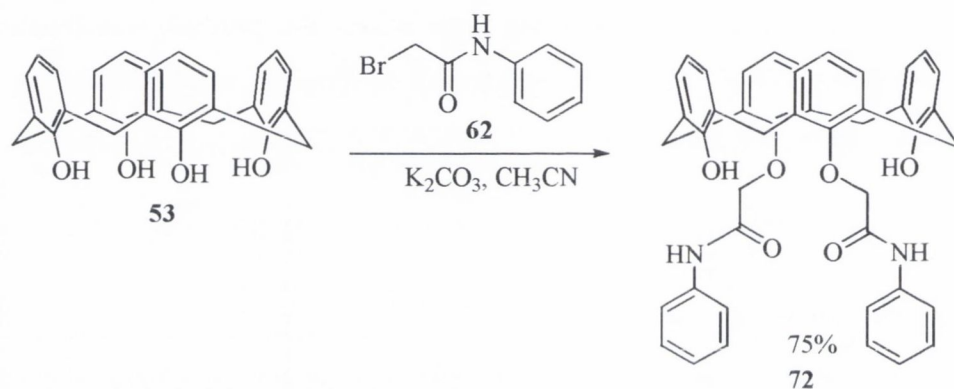


Figure 2.10 - ^1H NMR spectrum of distally disubstituted glycinylic calix[4]arene **71** (400 MHz, CDCl_3).

The singlets downfield, at 9.28 and 8.23 ppm provide the initial confirmation of disubstitution; each integrating to 2H, indicating two NH (substitution) and two OH (unsubstituted phenols) protons respectively. The aromatic region shows two doublet-triplet pairs (AB systems), corresponding to the upper-rim protons of the two different lower-rim environments. The CH_2 spacers, in addition to calix doublets (which confirm the cone conformation), and ethyl moieties are also in agreement by integration, with this proposed structure. In contrast, proximal disubstitution (which would result upon

alkylating adjacent phenolic rings) would result in three environments for bridging methylene protons: (i) between two unsubstituted rings; (ii) between two substituted rings; and (iii) between the substituted and unsubstituted rings.

A further, unexpected example of disubstitution was observed when exhaustive alkylation using 2-bromoacetanilide **62** was attempted (Scheme 2.13). Instead of obtaining a tetrasubstituted product, the reaction was seen to proceed only to the distally disubstituted product **72**. Attempts to drive this reaction to completion using a stronger base (KO^tBu) again saw the formation of the single, disubstituted product.



Scheme 2.13 - Formation of 1,3-disubstituted acetanilidyl calix[4]arene.

Inspection of the ¹H NMR (400 MHz, CDCl₃) spectrum of this product saw similar substitution patterns observed to those seen in the glycine analogue.

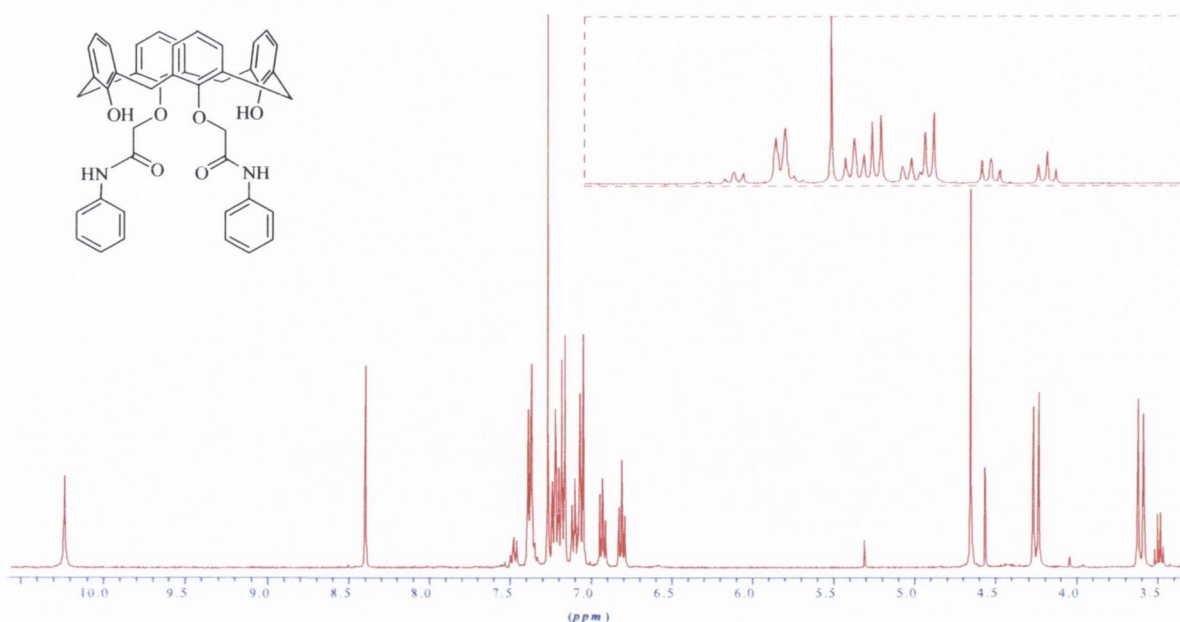


Figure 2.11 – ^1H NMR spectrum of 1,3-disubstituted acetanilidyl calix[4]arene **72** (400 MHz, CDCl_3), inset shows the aromatic region.

Phenolic OH and amide NH protons again resonate downfield, integrating to two protons each. The aromatic region is somewhat more crowded than before, due to the phenyl substituents on the nitrogen. The region is nonetheless easily distinguishable. The two doublet-triplet pairs are clearly visible, this indicates disubstitution. The methylene protons α - to the carbonyl spacer is agreement, integrating to four protons, while the cone conformation is confirmed by two doublets, which is further confirmation of the distal disubstitution pattern in **72**.

Single crystals which were suitable for X-ray diffraction studies were grown by slow evaporation of CH_2Cl_2 from a MeOH suspension of the compound. The structure as obtained by Dr Tom McCabe is shown in Figure 2.12. Selected bond angles as determined by this study are shown in Table 2.7.

The unit cell consists of a pair of ligands, which are oriented in a head-to-tail fashion, relative to each other. Hydrogen bonding of the free hydroxyl moieties with the substituted phenolic oxygen is also apparent in the crystal structure. This provides the molecule with further stabilisation. This weak interaction, however is unlikely to be a stabilising force preventing further substitution. It is therefore proposed that the bulk and planarity of the phenyl component of the pendant substituent prevents the tri- and ultimately the tetra-substituted compounds from forming.

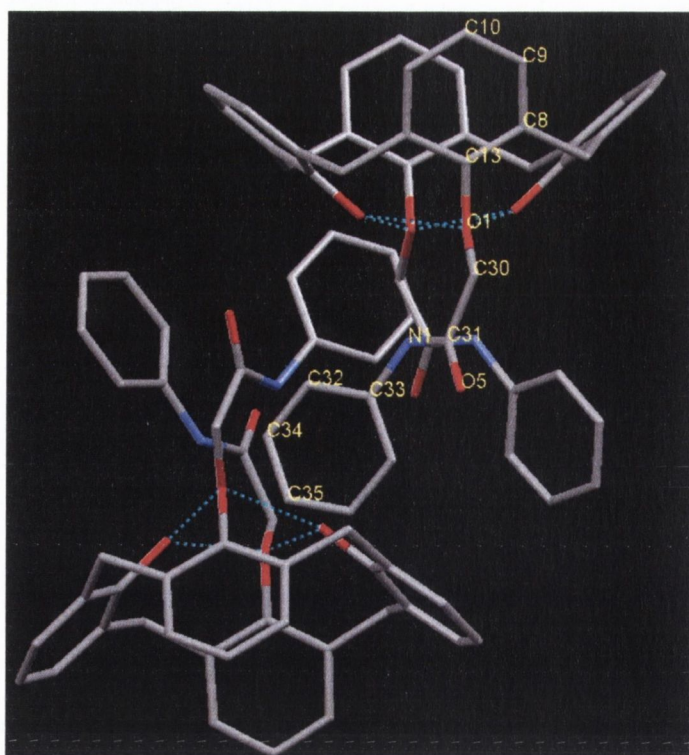


Figure 2.12 – Unit cell of 1,3-dianiline calixarene derivative **72**. Selected atoms are labelled in yellow, intramolecular hydrogen bonding between phenolic moieties is indicated by blue dotted lines.

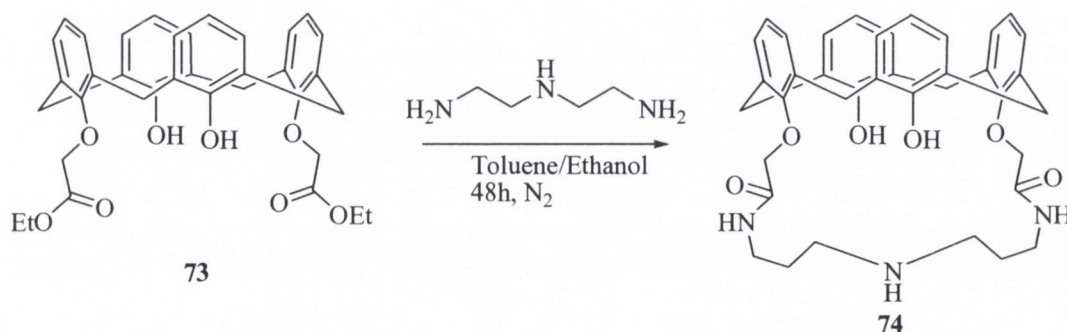
Table 2.7 - Bond angles observed in X-ray crystallographic study of **72**

Bond		Length (Å)	Bond			Angle(°)	
O1	C30	1.431(3)	C10	C9	C8	120.8(2)	
N1	C33	1.423(3)	C13	O1	C30	115.22(17)	
C9	C8	1.392(3)	O1	C30	C31	110.9(2)	
C8	C13	1.384(3)	C30	C31	O5	118.6(2)	
C34	C35	1.375(4)	O5	C31	N1	125.2(2)	
C33	C32	1.385(4)	N1	C33	C43	122.2(2)	
C32	C34	1.382(4)	C33	C43	C36	119.2(3)	
C31	O5	1.224(3)	C12	C14	C15	112.24(19)	
C31	N1	1.347(3)	Bond			Torsion Angle(°)	
C30	C31	1.512(3)	C26	C25	C27	C1	-104.29
C13	O1	1.415(3)	C26	C21	C20	C19	97.26
C10	C9	1.382(4)					

Having explored some inadvertent 1,3-disubstitution reactions, attention was drawn to the literature of 1,3-dialkylations where the aminolysis of some 1,3-disubstituted calix[4]arenes has been recently reported.¹⁴⁵ The following section will outline the successes achieved using the aminolysis reaction to introduce amide functionality into tetrasubstituted systems.

2.7 Aminolysis of calixarene esters

In the aminolysis reaction, an ester is reacted with an amine, yielding an amide. This is analogous to hydrolysis, which yields a carboxylic acid, by attack of aqueous hydroxide on an ester substrate. Aminolysis occurs upon optimisation of amine nucleophilicity, ester leaving-group and steric control such that the amine has access to the ester. Aminolysis of calixarene esters has been relatively poorly exploited, with some exceptions, such as the work of Wu and co-workers who studied the reaction of esters of both calix[4]arene and the parent *tert*-butyl calix[4]arene.¹⁴⁶ In this study, partial and complete aminolysis of the precursor esters was achieved using different solvents, amines and by addition of an additional base. Wu continued these studies, preparing some novel intramolecular bridges by aminolysis using ethylenediamine.¹⁴⁷ Aminolysis required five equivalents of amine to take place, and at that, two proximal moieties were bridged. Use of higher equivalents (>20) saw the bridging between both pairs of proximal esters (1,2 and 3,4). A further example of aminolysis was reported in 2004, by Kim, and co-workers, where a distally di-substituted ester of calix[4]arene was reacted with diethylenetriamine in toluene/ethanol.¹⁴⁵ This yielded, in a single-step, a calix-azacrown type structure, which found application in Pb^{2+} complexation. The diamide product was isolated by trituration in methanol, with no further purification necessary.



Scheme 2.14 – Formation of calix/azacrown conjugate reported by Lee and co-workers¹⁴⁵.

While these studies were carried out using simple aliphatic, primary amines, it was decided to investigate whether this methodology could be extended to larger amines, and perhaps to

study some reactions with secondary amines, to produce tertiary amides. The mechanism of ester aminolysis is detailed in Figure 2.13.

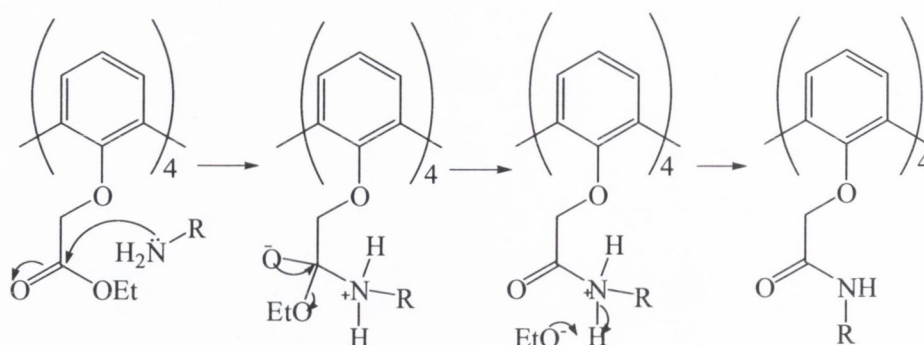


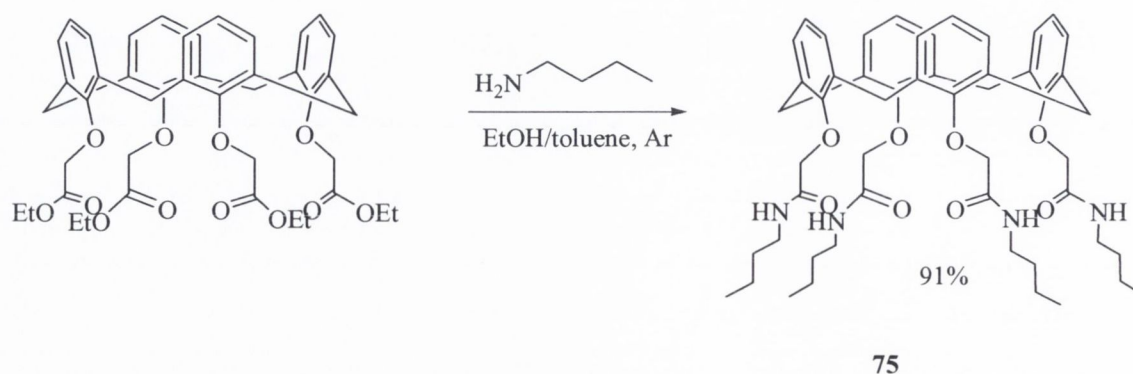
Figure 2.13 - Mechanism aminolysis of **55** – single monomer of calix[4]arene tetramer shown for clarity.

The attack on the carbonyl is by the nucleophilic amine, which proceeds analogous to ester hydrolysis, yielding the desired amide, with elimination of a molecule of ethanol. Initially, use of small amines was to be investigated.

2.7.1 Aminolysis using aliphatic amines

Calix[4]arene tetraethyl ester **55** is readily accessible, and when synthesised using K_2CO_3 as a base, is formed exclusively in the cone conformation. Reaction of calix[4]arene tetraethyl ester **55** and butylamine in a mixture of toluene/ethanol (50:50 v/v) at reflux temperature for 5 days yielded the desired tetrabutylamide **75**. 1H NMR spectroscopy confirmed the retention of the cone conformation, though the size of lower-rim substituents at the point prior to this reaction would be prohibitive to rotation through the annulus.

Single, orthorhombic crystals of this product which were suitable for X-ray analysis were grown by evaporation of CH_2Cl_2 from a CH_3OH suspension. The structure was determined by X-ray crystallography, by Dr Tom McCabe, and is shown in Figure 2.14.



Scheme 2.15 – Aminolysis of **55** using butylamine.

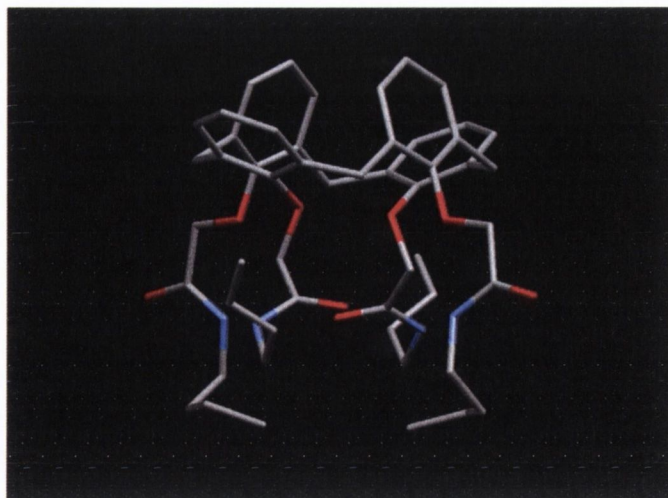


Figure 2.14 –X-ray crystal structure of tetrabutyl amide **75** in the cone conformation.

An example of a “pinched-cone” conformation was observed; the pairs of opposing phenyl groups angled away from the annulus, and pinched into the annulus.¹⁴⁸ Selected bond angles representative of one of the monomers of the tetramer are detailed in Table 2.8.

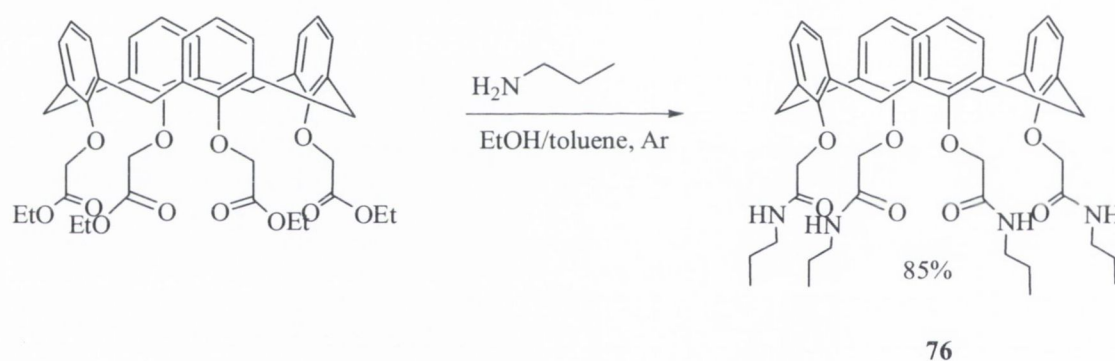
Table 2.8 - Selected bond lengths and angles of **75**.

Bond	Length (Å)	Bond	Angle(°)
O1 C32	1.426(3)	C23 C22 C27	118.2(2)
N4 C37	1.451(3)	C27 O1 C32	112.71(16)
C39 C40	1.511(5)	O1 C32 C33	111.14(18)
C38 C39	1.516(5)	C32 C33 O5	118.7(2)
C37 C38	1.504(4)	C32 C33 N4	116.70(19)
C33 O5	1.235(3)	C33 N4 C37	122.72(19)
C33 C32	1.502(3)	N4 C37 C38	113.7(2)
C33 N4	1.319(3)	C37 C38 C39	114.8(2)
C27 O1	1.389(3)	C38 C39 C40	114.4(3)
C23 C22	1.390(3)	C21 C22 C27	121.4(2)
C22 C27	1.393(3)	C27 C26 C28	120.8(2)
C21 C22	1.517(3)		

Following the promising results obtained with a simple, alkyl system, attention was then turned to analogues of this structure; to attempt to shorten the alkyl chain, and thus reduce

the hydrophobicity of the system. The potential role of the alkyl chains, such as potential interdigitation, in the solid state may then be observed.

The synthesis of the simple tetrapropylamide of calixarene, by any method, had not been reported before. Due to the low boiling point of the starting amine (39 °C), the reaction was initially attempted in a sealed tube in ethanol, where the temperature of the closed system was allowed to reach 120 °C. Isolation of the products of this reaction returned the starting material. The reaction was then attempted using standard reflux conditions, with a large excess of amine. A solution of the calixarene ester **55** in EtOH/toluene (50:50 v/v), was treated with propylamine (100 equivalents) and the mixture heated at reflux, under argon for 3 days. Following analysis by TLC (100% CH₂Cl₂), additional propylamine (100 equivalents) was then added and the mixture heated for a further two days. Isolation of the product required evaporation of solvent and amine, followed by trituration with methanol to give the desired product, which was fully characterised.



Scheme 2.16- Aminolysis of calix[4]arene ester **55** using propylamine.

Again, the C_4 symmetry of the compound was immediately apparent upon inspection of the ¹H NMR spectrum (400 MHz, CDCl₃). The NH protons are visible at 7.37 ppm, while the aromatic protons resonate at 6.63 ppm, and the calixarene doublets overlapped with other protons in both cases. The *endo*, more downfield doublet is seen to overlap with the singlet of the O-CH₂-C(O) protons. This resonates around 3.90 ppm, while the *exo* was seen to overlap with a CH₂ quartet from the propyl moiety around 3.25 ppm. The second methylene group is obscured by the solvent residual water, and resonates as a multiplet at 1.61 ppm. The terminal CH₃ is seen as a clearly resolved triplet at 0.94 ppm.

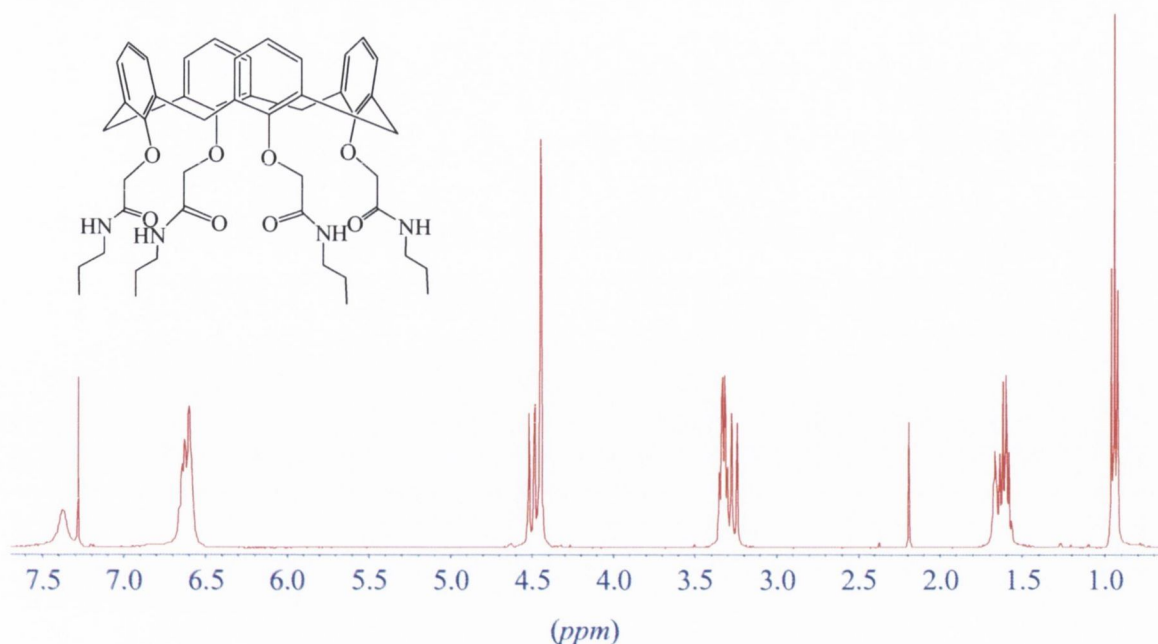


Figure 2.15 – ^1H NMR spectrum of tetrapropylamide of calix[4]arene **76** (400 MHz, CDCl_3).

Single crystals of this compound were grown by slow evaporation of a concentrated MeOH solution. These proved appropriate for X-ray diffraction, and the structure, as determined by Dr Tom McCabe is shown in Fig 2.16.

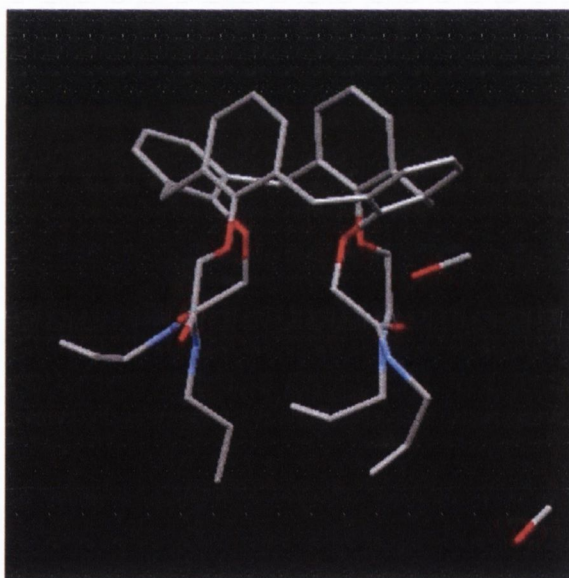


Figure 2.16 - Single crystal X-ray structure and stick diagram of **76** showing cone conformation of tetrapropylamide. Methanol molecule also indicated.

The refinement of the data of this crystal structure proved difficult; the data were weak, and the thermal ellipsoids of the terminal C-C bonds proved unstable, therefore the terminal C-C bonds have varying lengths between 1.004 Å and 1.462 Å. Selected bond lengths and angles determined are shown in Table 2.5.

Table 2.9 - Selected Bond Angles of tetrapropylamide **76**.

Bond		Length (Å)	Bond			Angle(°)
C20	C19	1.494(7)	C43	C44	C45	113.6(14)
C20	C25	1.409(7)	C44	C45	N2	114.5(7)
C20	C21	1.390(7)	C45	N2	C33	124.5(5)
C25	O4	1.393(6)	N2	C33	O5	124.4(5)
O4	C32	1.441(6)	O5	C33	C32	119.1(5)
C32	C33	1.497(7)	C33	C32	O4	109.5(4)
C33	O5	1.246(6)	C32	O4	C25	115.0(3)
C33	N2	1.322(7)	C25	C20	C19	123.3(4)
N2	C45	1.440(8)	C20	C19	C17	112.0(4)
C45	C44	1.4639(11)	C20	C21	C22	121.9(5)
C44	C43	1.463(18)				

Two methanol molecules are clearly visible within the structure. Again, this compound adopts the pinched cone conformation, with distal aromatic rings either directed towards or away from the annulus. Despite the weak statistics of this crystal, it unambiguously confirms the spectral characterisation.

2.7.2 Lower-rim arrays with multiple amines

With the success enjoyed in the case of simple aliphatic primary amines propylamine and butylamine, it was decided to investigate the use of more diversely functionalised amines in the aminolysis reaction. A series of ethylenediamine spaced amines such as those described in Figure 2.17 was chosen. These reactions follow on from some of the α -bromo amides which were synthesised and were discussed earlier. In the example of the piperazine analogue, this direct aminolysis approach eliminates the need for circuitous protection of the free ring-nitrogen, which would be required in synthesis of an α -bromoamide.

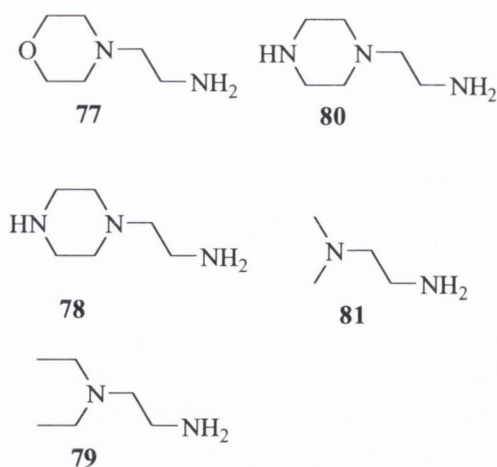
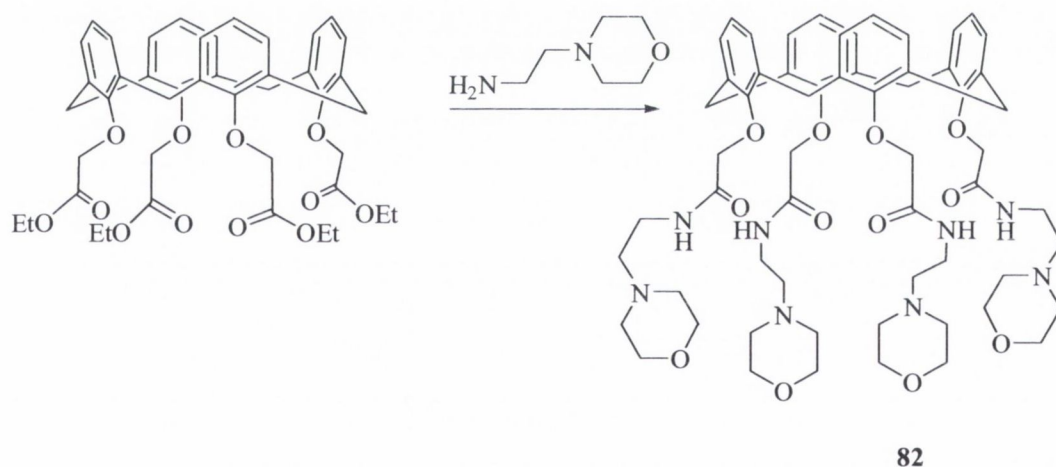


Figure 2.17 - amines used in aminolysis of **55** to provide flexible ethyl-spaced binding array

In light of a literature procedure for the synthesis of the *N,N*-dimethyl analogue,⁹² the calixarene tetraethyl ester was stirred overnight in neat amine, at room temperature, under an atmosphere of argon. In the case of the morpholine analogue, the starting amine is a low-melting (26 °C) solid, therefore this reaction was controlled at 35 °C. In each case, excess amine was removed by high-vacuum distillation. The synthesis of the morpholinyl analogue **82**, obtained by treatment of **55** with **77**, is outlined in Scheme 2.17.



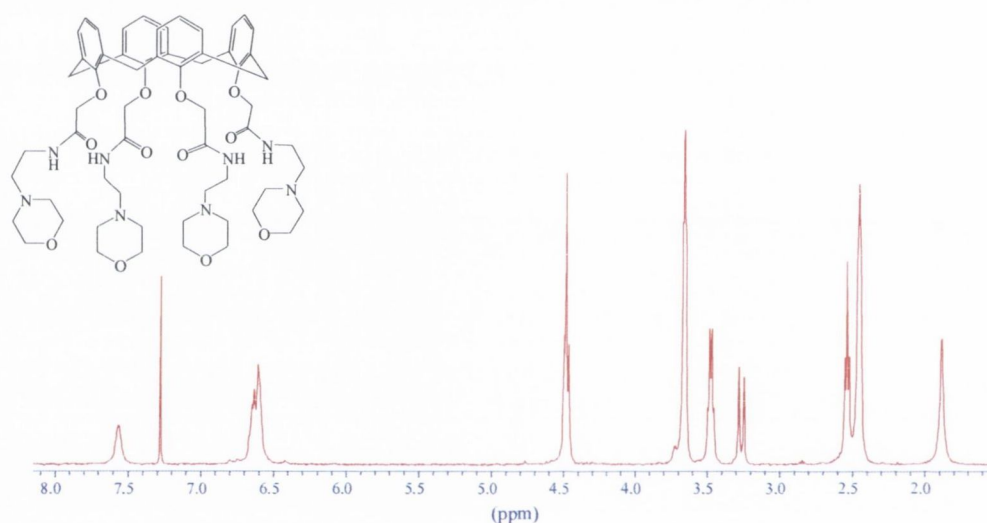
Scheme 2.17 – Aminolysis of calix[4]arene tetraethylester using 2-aminoethylmorpholine.

The approach was useful for several ligands, incorporating piperazine, pyridine, *N,N*-diethylamine, the conditions and yields of which are tabulated in Table 2.6. The known *N,N*-dimethyl analogue was also synthesised.

Table 2.10 - Yields of ligands A-E formed by direct aminolysis of calix[4]arene tetraethyl ester **55**.

Product	Amine used	Solvent	Time (h)	Yield
82	4-(2-Aminoethyl)morpholine	none	18h	89%
83	1-(2-Aminoethyl)piperazine	none	18h	44%
84	1-(2-Aminoethyl)piperidine	none	18h	78%
85	<i>N,N</i> -Diethylethylenediamine	none	18h	62%
17	<i>N,N</i> -Dimethylethylenediamine	none	18h	88%

In each case, the crude residue which resulted was triturated with diethyl ether until white solids were formed, stirred for 1 h, and then filtered with suction to give the desired compound in moderate yield. No further purification stage was necessary for any of these compounds. A representative ^1H NMR spectrum of the family is outlined in Figure 2.18.

**Figure 2.18** – ^1H NMR spectrum of **82** (400 MHz, CDCl_3).

The calix[4]arene methylene bridges are visible, resonating at 4.48 ppm and 3.26 ppm for the *endo*- and *exo*- environments respectively. The 4.48 ppm doublet appears overlapped with the CH_2 singlet corresponding to the attachment point to the calixarene. Morpholine protons at 2.54 and 2.46 are seen as broadened signals, no axial and equatorial coupling patterns could be determined from this spectrum.

The surprising result from this synthesis was that compounds **82** and **83**, which are the morpholinyl and piperazinyl analogues respectively, were found to be soluble in water. A ^1H NMR spectrum of **82** was recorded in D_2O , but the peaks were broad and not as clearly resolved as that recorded in CDCl_3 . This spectrum is nonetheless shown in Figure 2.19.

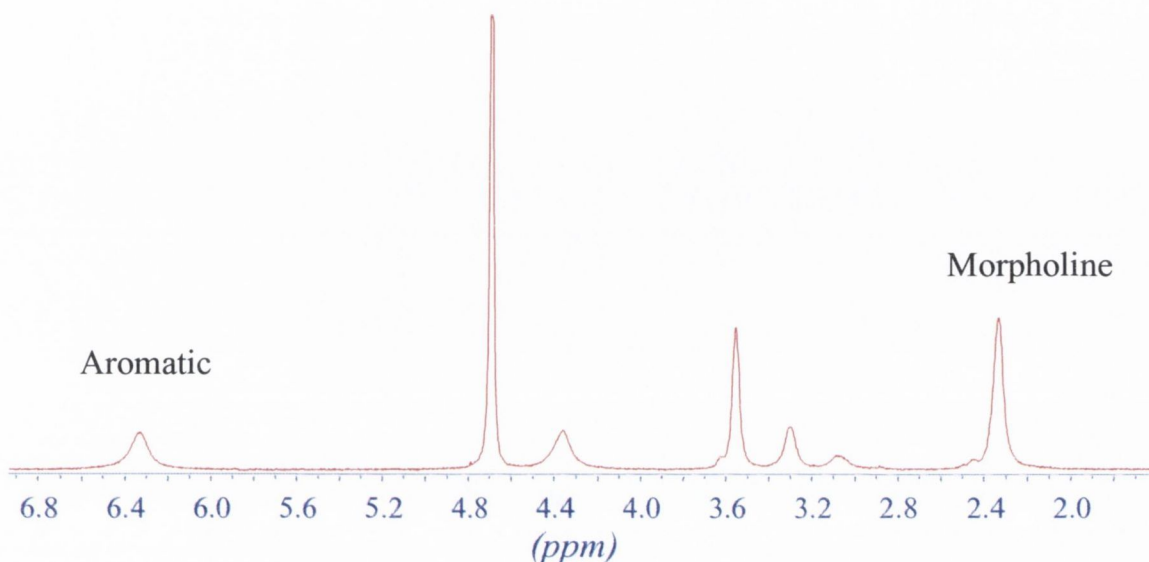


Figure 2.19 – ^1H NMR spectrum recorded in D_2O of tetramorpholinyl calix[4]arene **82** (400 MHz).

The spectrum can be roughly assigned, with peaks present in the aromatic region corresponding to the calix[4]arene scaffold, and aliphatic resonances in agreement with the previously solved high-resolution spectrum.

A crystal suitable for X-ray crystallography was grown of the piperidinyl analogue (**84**), from a mixture of CH_2Cl_2 and diisopropyl ether. This is shown in Figure 2.21, with bond angles and lengths detailed in Figure 2.20. This crystal structure also comes with the caveat that the solvent molecule has induced disorder into a single piperidinyl moiety. Repeated attempts by crystallographer, Dr Tom McCabe to refine this disorder were unsuccessful. The structure, however provides valuable insight into the solid-state structure of this ligand.

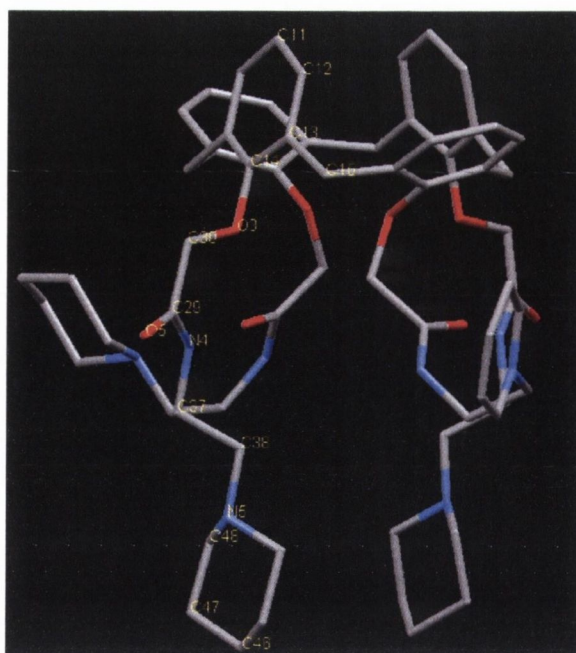


Figure 2.20 – Crystal structure of **84** showing pinched cone conformation; solvent molecule omitted for clarity. Piperidine moiety to right seen as planar due to solvent-induced disorder and intraplanar vibration

Table 2.11 – Selected bond lengths and angles for **84**

Bond	Length (Å)	Bond	Angle(°)
C11 C12	1.377(12)	C11 C12 C13	121.3(8)
C12 C13	1.387(10)	C12 C13 C15	118.2(7)
C13 C15	1.525(11)	C13 C14 O3	118.9(7)
C13 C14	1.387(10)	C14 O3 C30	113.9(5)
C14 O3	1.393(8)	O3 C30 C29	111.8(6)
O3 C30	1.354(7)	C30 C29 O5	120.8(6)
C30 C29	1.543(10)	C30 C29 N4	114.8(6)
C29 O5	1.233(9)	C29 N4 C37	124.6(6)
C29 N4	1.299(9)	N4 C37 C38	108.7(6)
N4 C37	1.439(9)	C37 C38 N5	109.2(6)
C37 C38	1.543(11)	N5 C44 C45	108.9(8)
C38 N5	1.482(10)	C44 C45 C46	109.6(9)
N5 C48	1.436(11)	C45 C46 C47	112.4(9)
C48 C47	1.565(13)		
C47 C46	1.447(15)		

The packing of these molecules in the solid state was also observed, and is indicated in Figure 2.21.

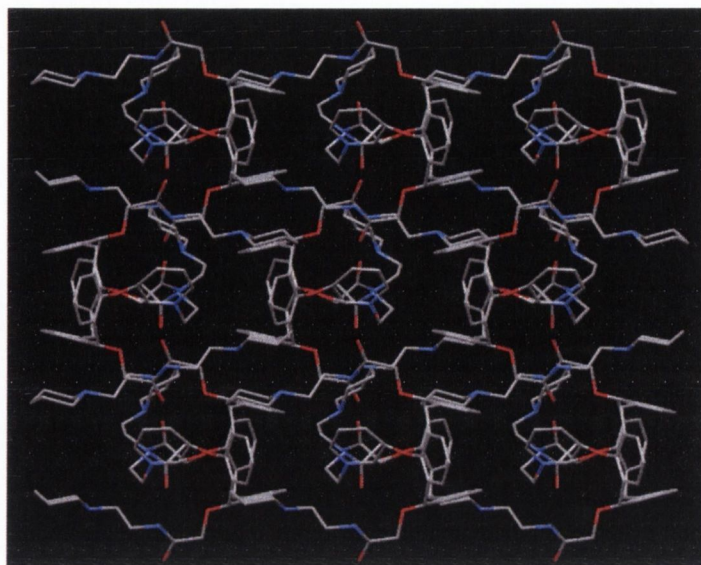


Figure 2.21 - View along a* crystallographic axis of crystal packing in **84**.

Intramolecular hydrogen bonding between the carbonyl and amido protons is observed in the crystal structure. This occurs between proximal units of the calixarene. The carbonyl moieties of those amides which donate hydrogen bonds are seen to accept hydrogen bonds from neighbouring molecules, that is, that there is also intermolecular hydrogen bonding occurring in this structure.

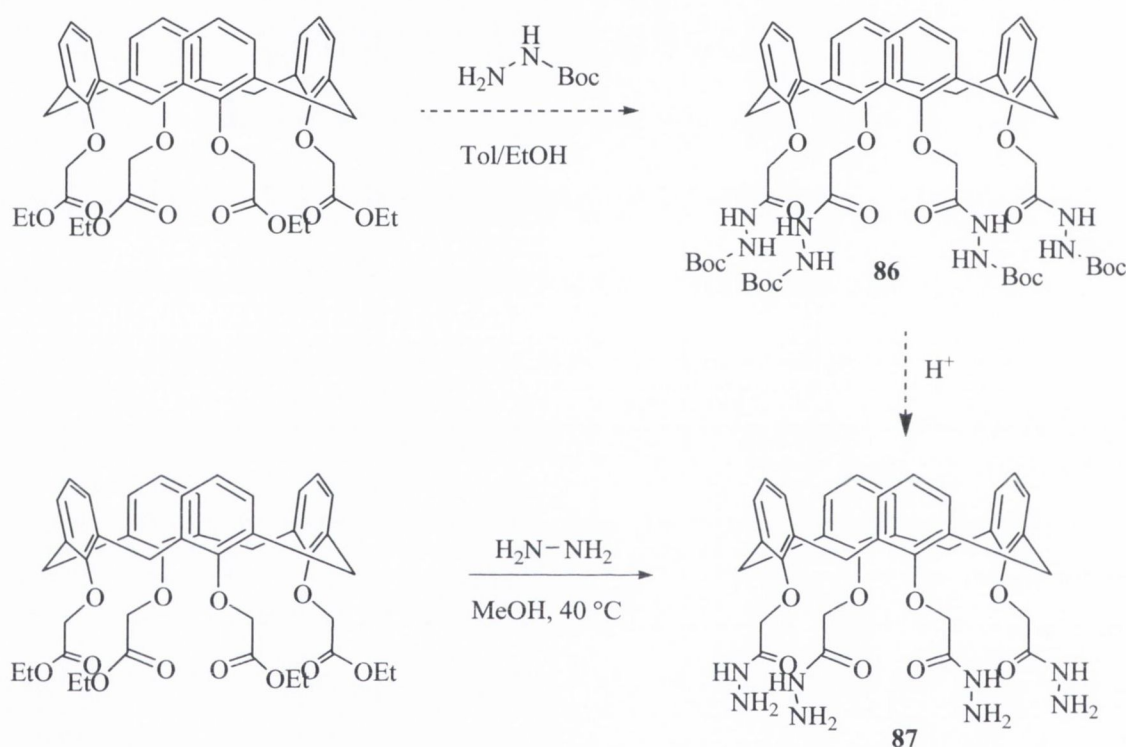
These compounds are readily accessible in good yield, and provided further support for the technique of aminolysis. Incorporation of large, multifunctional amines had proceeded as desired, as had the introduction of simple aliphatic species. Attempts at complexation of lanthanide ions using these molecules will be discussed in Section 2.7. At this point, having synthesised complex systems, attention was diverted to simple, yet useful species: those prepared using hydrazine derivatives.

2.7.3 Synthesis of some calix[4]arene-based hydrazides

The use of the primary amino group as a nucleophile for aminolysis had proved successful and useful. Hydrazine, $\text{H}_2\text{N-NH}_2$ contains two such amino moieties, thus attack by a hydrazine synthon on an ester would create the desired amide bond, leaving the second amino group for further functionalisation. Initially this synthesis was attempted using a mono-*tert*-butoxycarbonyl (Boc) protected derivative of hydrazine, *tert*-butyl carbazate. The intention was to then cleave the Boc group using trifluoroacetic acid (TFA), to yield a tetrahydrazide. Aminolysis of the tetraethyl ester in toluene/ethanol at reflux over 4 days

gave no formation of the desired product. However, changing from the protected hydrazine to hydrazine hydrate gave the desired hydrazide in a reaction that took only 30 minutes in methanol. Hydrazine is small enough not to affect dimerisation or bridging within the calix[4]arene derivative.

The pure hydrazide, 25,26,27,28-tetrakis[(hydrazidocarbonylmethyl)oxy]calix[4]arene was isolated in near-quantitative yield by evaporation of methanol and excess hydrazine. Purification required triturating the compound with further methanol and washing with water. Both the attempted and successful routes to this compound are outlined in Scheme 2.18.

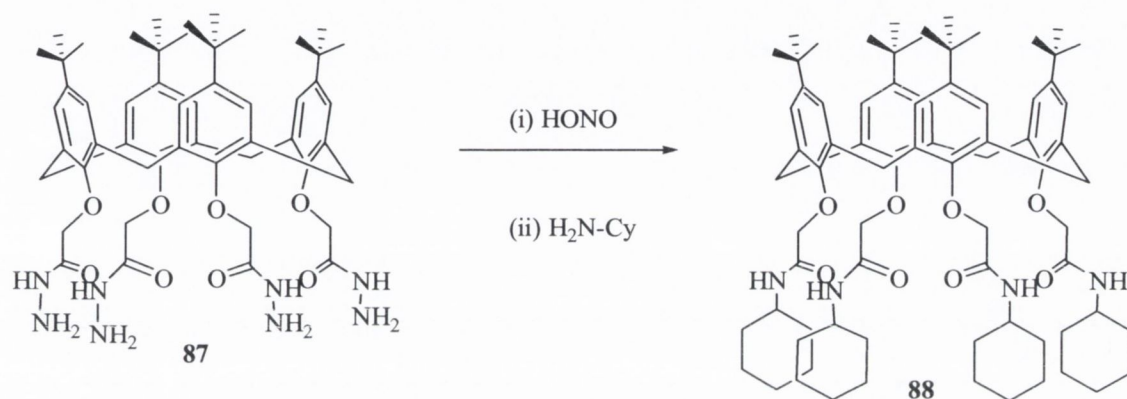


Scheme 2.18 – Routes to the formation of calix hydrazide.

With the hydrazide in hand, several potential aspects of its chemistry were worth pursuing; Firstly, investigation of whether the $\text{NH}-\text{NH}_2$ functionality would provide a binding array for the accommodation of metals. Secondly, utilisation of the free amino moiety in diazotisation reactions, forming an azide which could potentially be displaced by an amine to form an amide. In addition, reaction of the free amine with isocyanates to form ureas was of great interest, in light of recent success enjoyed in the Gunnlaugsson group from the use of ureas as anion-binding motifs. This final aspect and its results will be discussed in Chapter 4.

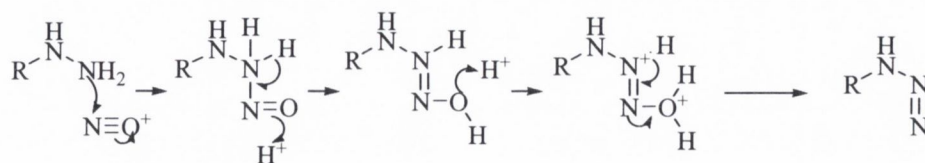
2.7.4 Diazotisation of calix[4]arene tetrahydrazide

While the hydrazide which was formed has not been previously been reported, the hydrazide of the parent 'butyl calix[4]arene was previously synthesised and its diazotisation and subsequent reaction with simple amines has been investigated.¹⁴⁹ This led to the formation of benzyl and cyclohexylamides, as shown in Scheme 2.23. It was intended to prepare some more diverse amides using this methodology (such as the problematic sarcosine derivative, which was unsuccessful using other methods).



Scheme 2.19 –Previously accomplished synthesis of a tetracyclohexylamide by a diazotisation method.¹⁴⁹

Diazotisation requires generation of nitrous acid *in situ*, which will then generate the diazonium salt (in the case of a hydrazine, this generates an azide). The azide is then displaced by an amine to form an amide. Diazonium salts are very reactive and prone to explosion when dry. Consequentially, the reactions must be carried out at low temperature, where the temperature must not rise above 5 °C. Nitrous acid is generated by protonation of a nitrite (either sodium nitrite or an alkyl nitrite). The use of sodium nitrite is preferable, as alkyl nitrites have undesirable health effects when in use. When an organic nitrite must be employed, (for example, for solubility reasons), *tert*-butyl nitrite is advantageous, as its side-product, 'BuOH, is stable. The product of protonation, NO⁺ then attacks the lone pair of an amine and dehydration then follows. This mechanism is outlined in Scheme 2.20.



Scheme 2.20 - Mechanism of formation of azide from hydrazide.

Initially, it was decided to use 'butyl nitrite, in accordance with a method already utilised within the Matthews group for functionalisation of a porphyrin.¹⁵⁰ Treatment of an acetic

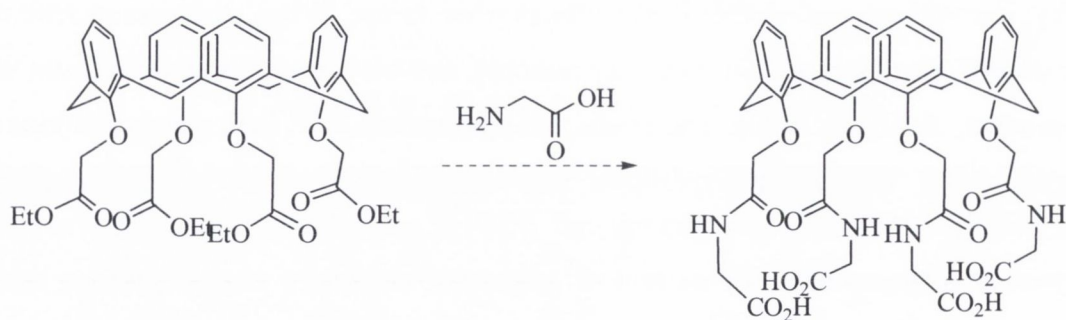
acid solution of the calix-hydrazide with 5 M HCl and an excess of *t*Bu-nitrite was performed to prepare the azide. Extraction of the azide into chloroform, followed by treating the organic layer with sarcosine did not see the formation of any product. Instead, thick emulsions were seen to form, indicating that solubility of these compounds was an issue.

The solubility problem stemmed from the use of aqueous HCl. While the starting material was soluble in acetic acid, it was seen to partially precipitate upon the addition of aqueous HCl. Furthermore, upon cooling to diazotisation temperature, the conditions would be more conducive to precipitation. It was therefore decided to repeat this reaction using commercially available HCl in an organic solvent (4 M in 1,4-dioxane). Furthermore, the reaction itself must be carried out in a neutral solvent (DMF).

Despite various attempts considering the issues with solvents and the conditions mentioned above, the reaction failed to proceed when using either sarcosine ethyl ester or glycine ethyl ester hydrochloride, no products were obtained, or detectable by electrospray mass spectrometry. The reaction was repeated using propylamine, a simple amine which we had earlier proven to be synthetically accessible by the aminolysis reaction. Again, no reaction occurred. It was decided not to pursue this reaction further.

2.7.5 Further aminolysis reactions

Given the relative success which was realised using the aminolysis technique, it was decided to attempt to prepare the glycinyl and sarcosyl derivatised calix[4]arenes using this approach, such as that outlined in Scheme 2.21.



89

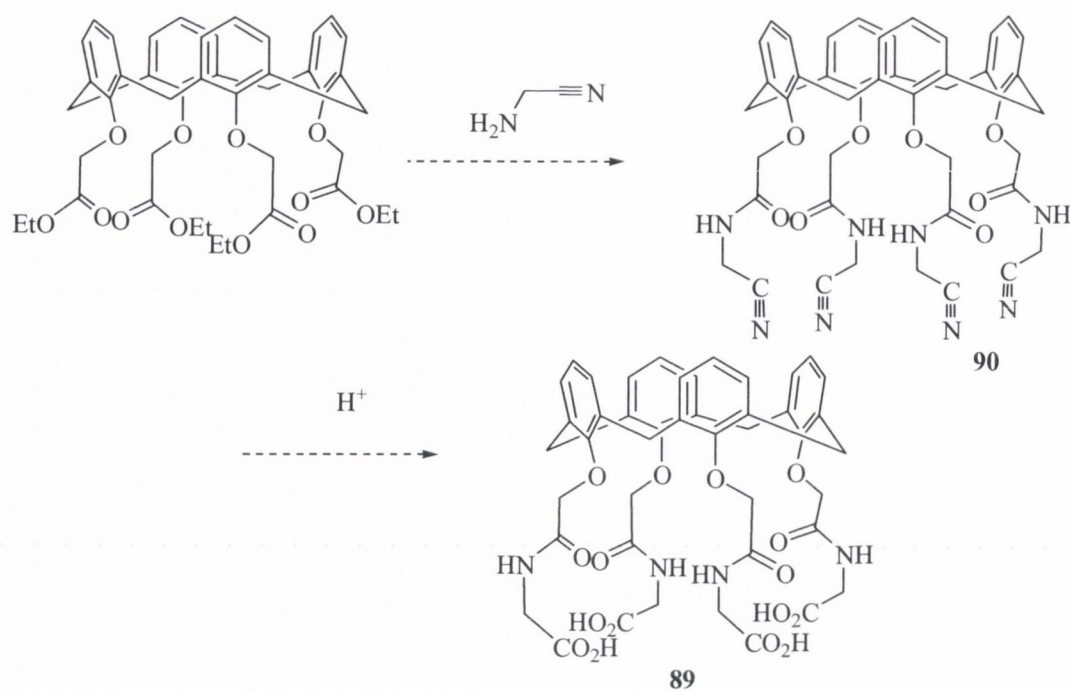
Scheme 2.21 – Potential aminolytic route to tetraglycinyl calix[4]arene.

Initially, glycine was allowed to stir at reflux with calix[4]arene tetraethyl ester overnight in ethanol. However, no reaction was observed. This was attributed to the insolubility of

glycine in alcoholic solvents. No appropriate solvent mixture could be found which was appropriate for both calixarene ester and glycine. Following prolonged reaction at reflux temperature, only starting material was observed. Attempted reaction of these two materials without solvent was then undertaken. While the melting point of calix[4]arene tetraethyl ester is moderate, glycine underwent rapid decomposition, turning black. This was therefore not further pursued. Aminolysis using sarcosine was equally unsuccessful, however this is most likely due to hindrance of the nitrogen centre by the *N*-methyl moiety. It is an inherent property of the aminolysis reaction that the attacking amine must be both nucleophilic and sterically accessible. Reacting the corresponding ethyl esters of either glycine or sarcosine with calix[4]arene tetraethyl esters was also ineffective. In addition, aminolysis of calixarene tetraester using either morpholine or piperidine to achieve the ligands **64** and **65** which were obtained by the α -bromoamide route was unsuccessful, despite their nucleophilicity. This is again attributed to steric hindrance about the amino nitrogen.

A final approach was attempted, which, if proved successful would be attractive for the rapid synthesis of a variety of hosts. This involved aminolysis using aminoacetonitrile, $\text{H}_2\text{NCH}_2\text{CN}$. As aminoacetonitrile was commercially unavailable in free form, it was purchased as its hydrogensulfate salt. It was envisaged that the tetranitrile which would form could be hydrolysed to the corresponding carboxylic acid, which would be the glycine product. This is illustrated in Scheme 2.22. Indeed, the versatility of the cyano group would also enable its reduction to a further free NH_2 moiety.

Aminolysis was attempted in the presence of excess aminoacetonitrile in the presence of a corresponding amount of base (NEt_3). Subjecting this mixture to the optimised aminolysis conditions (heating at reflux overnight with calix[4]arene tetraethyl ester in ethanol) proved unsuccessful, with no product observed in the ^1H NMR spectrum. Only the starting calixarene derivative was isolated from the reaction.



Scheme 2.22 - Aminolysis route to tetraglycynyl calix[4]arene **89** proceeding through nitrile stage.

While this final approach to the glycine analogue was unsuccessful, it is envisaged that it is viable. Should this method be optimised in the future, it will provide a rapid route not only to the glycine derivative, but also to β -amino acid analogues, and to longer chain derivatives.

2.8 Lanthanide complex preparation

Attempts to prepare lanthanide complexes of the ligands synthesised in the course of this work were undertaken. Complexation involved heating the ligand with the triflate (CF_3SO_3^-) salt of a lanthanide ion in acetonitrile at reflux for 16 h. This was then concentrated at reduced pressure to approximately 20% volume, upon which it was poured into vigorously stirring, sodium-dried diethyl ether. The precipitate which formed was repeatedly filtered until the mother liquor remained clear. The solid residue was then analysed by electrospray mass spectrometry (ESMS).

In the case of complexation with Gd(III), ESMS is a straightforward technique at our disposal which allows characterisation. Gadolinium induces fast relaxation in NMR, which is too rapid to allow a proper NMR signal to occur. While this property of Gd(III) is desirable for MRI applications, it serves as a hindrance in the characterisation of potential relaxation enhancing compounds. ^1H NMR spectra of Gd(III) complexes which were acquired consisted of only a single broad peak which was attributed to broadening of all

signals in addition to the solvent signal. Electrospray mass spectra of each of the complexes **64.Gd** and **65.Gd** were recorded in acetonitrile, however in each case, the free ligand was also observed. In addition to this, the characteristic gadolinium splitting pattern which agreed with **64.Gd** was observed for each case. This splitting pattern serves as confirmation of the complex presence, as accurate mass could not be obtained. The spectra obtained for these complexes are indicated in Fig 2.22. It must also be noted that mass spectrometry is not quantitative, but rather qualitative. The intensity of signals depends on extent of ionisation, rather than the relative concentration. Complexes of Gd(III) have distinctive isotopic distributions, thus the distribution of the mass intensities at an appropriate mass may be considered a “fingerprint” of the desired complex.

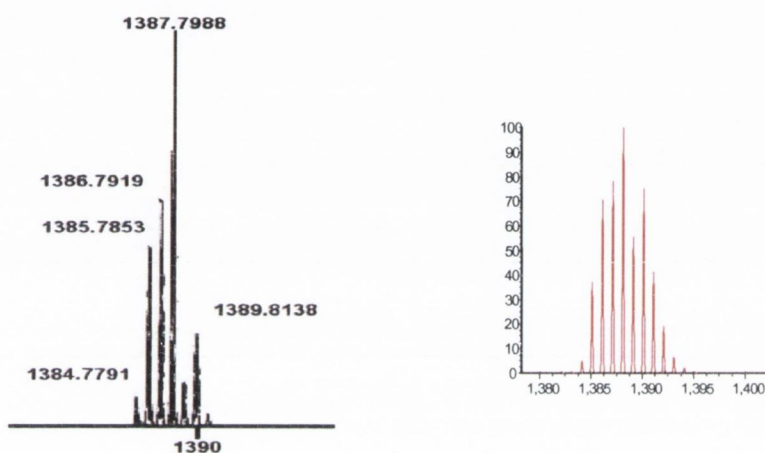


Figure 2.22 - Electrospray mass spectrum (experimental) and predicted isotopic distribution for **64.Gd(OTf)₂**. Complexation of the tetrahydrazide of lanthanides was attempted, using Eu(III) triflate, chloride and perchlorate. In the case of triflate and chloride, the complexations were attempted in acetonitrile. Chloride salts were purchased in hydrated forms, therefore triethyl orthoformate was used to scavenge the water from solution.^{80,151} However, this tetrahydrazide is very insoluble in most organic solvents, including acetonitrile. Even in the presence of the lanthanide triflate, a cloudy suspension persisted. Use of europium(III) perchlorate required a mixed solvent system, as the salt is only available commercially as an aqueous solution. The ligand was dispersed in acetonitrile, and to the solution was added Eu(ClO₄)₃. A clear, colourless solution formed instantly, which indicated interaction between host and guest. Upon evaporation of the solvents, a glassy solid formed. No complex could be detected by ES mass spectrometry, while ¹H NMR did not show the expected shifting of signals. A further method attempted for the incorporation of lanthanide ions was their delivery as DMSO solvates. This method has been used for calixarene derivatives by Beer and co-workers¹⁵², and is based on a method reported by

Ramalingham and Soundararajan.¹⁵³ In this procedure, lanthanide nitrates are crystallised from a mixture of methanol and DMSO, and the resulting salt is then used for further study. When these salts were used instead of the triflates, perchlorates or oxides, complexation was not observed.

Given the high water solubility of the neutral ethyl-spaced morpholinyl and piperazinyl ligands, it was decided to prepare some model Ln(III) complexes of these ligands to assess their respective abilities to bind gadolinium. The model metals chosen were Eu(III) and Tb(III). Gadolinium is not routinely used in preliminary measurements, which are often photophysical. To excite the metal centre of a Gd(III) containing complex, as is normally carried out in fluorescence spectroscopy, requires the use of laser pulses to assess the luminescence behaviour of the metal centres. The model metals flank gadolinium in the lanthanide series, thus by studying their properties, an insight into the potential behaviour of the Gd(III) analogue may be obtained. The structures of complexes are believed to be such as that shown in Figure 2.23.

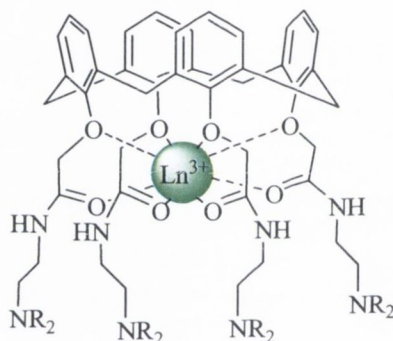


Figure 2.23 - Representative complex formed with Ln³⁺ (the counter-ions are variable, and have been omitted for clarity).

The ligand will provide eight donor atoms; four phenolic ether moieties, and four amido carbonyl oxygen atoms. This will satisfy eight of the coordination sites of the Ln³⁺. This is as expected, and is seen in ligands such as DOTA. In both cases, the ninth and final coordination site is expected to be occupied by a single metal-bound water molecule. As difficulty was had with isolation of these complexes, it was therefore decided to undertake a preliminary solution-state study of the binding by these ligands, specifically the morpholine-containing analogue **82**.

2.8.1 Luminescence titration of a Tb(III) complex

The previous section has outlined the attempts which were undertaken to prepare lanthanide complexes, and the measures which were taken with the intention of isolating

these species. Mass spectrometry and some of the NMR results indicated these complexes were indeed forming, hence it became necessary to study these interactions in solution. As outlined in Chapter 1, the calixarene scaffold provides an antenna for the population of the excited state of Tb(III), while excitation of Eu(III) requires the use of a further sensitising moiety. It was decided to harness this property with respect to the water-soluble ligand **82**. Phosphorescence titrations were carried out between Tb(III) (delivered as its non-coordinating, perchlorate salt) and **82**. This involved the measuring the phosphorescence intensity of the metal centre following excitation of the calixarene (271 nm). Measurements were conducted in constant ionic strength (NEt₄ClO₄, $I = 0.1$ M); keeping I intentionally high to minimise the effects of ionisation of the guest during equilibration. Phosphate buffering at pH = 6.5 saw the precipitation of the metal guest from solution, therefore the solution was buffered using 2-morpholinoethanesulfonic acid (MES). Upon addition of successive aliquots of guest to **82**, the morpholine analogue, emission of the Tb(III) ion was switched on. With increasing concentration of Tb(III), the emission continued to rise, giving rise to the spectra shown in Figure 2.24; the inset showing the change in phosphorescence intensity of the $J = 5$ band.

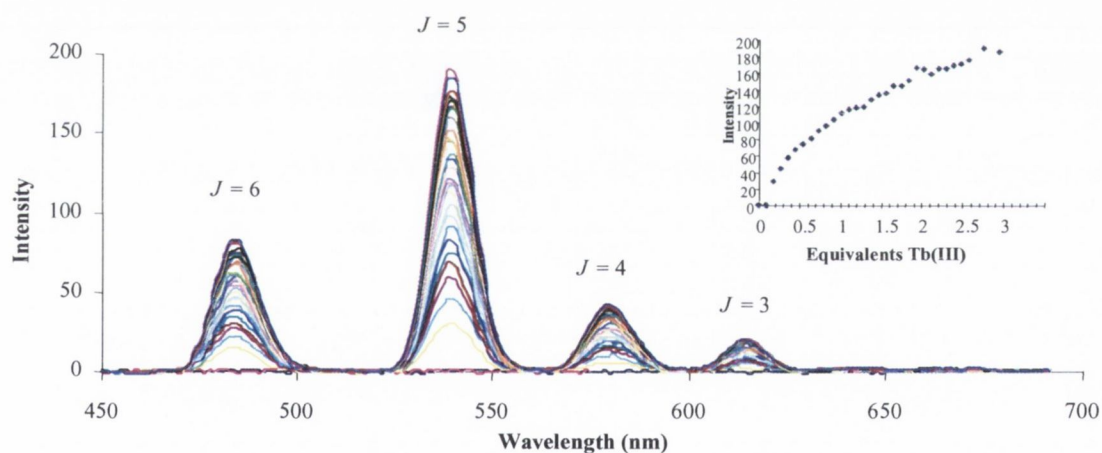


Figure 2.24 - Phosphorescence spectrum obtained upon titration of **82** with Tb(III)

From these spectra, it can be clearly seen that Tb(III) emission intensity increases as the concentration of the lanthanide ion increases. It can be therefore asserted that the complex is forming in solution, as it is the absorbance at 271 nm (the aromatic system of the calixarene moiety) which is being excited, and which populates the Tb(III) metal ion excited state. The concentration of ion does not appear to equilibrate at the expected value of 1. A similar effect was seen when solutions were prepared to contain different amounts

of guest and allowed to equilibrate overnight. The titration was undertaken in the absence of buffer, and again, no plateau was observed. At this point, this study is to be seen as a preliminary confirmation of the complexation using ligands of this type. Full solution-state study and data-fitting will be further investigated in the future.

2.9 Conclusions

In this chapter, the synthesis of a number of calix[4]arene derivatives has been discussed. This was undertaken with the intention of preparing strong metal chelates for the binding of lanthanides. For MRI contrast application, this was ultimately to be gadolinium(III). The approaches taken for the introduction of functionality to accommodate hard Lewis acids has been discussed, as have the preliminary studies which were undertaken using model metals, both europium and terbium for solid-state study, and terbium alone in solution.

Synthetically, significant advances have been made, preparing amides in a number of different routes. This began with the coupling of carboxylic acids with amines on the calix[4]arene framework, then focused performing this coupling step prior to alkylation of calix[4]arene. This gave positive results, and saw the preparation of ligands such as piperidine and morpholine derivatives, while the isolation of the elusive sarcosinyl compound remained as an issue of purification. In a slightly retrograde step, the reaction of esters with amines was once again examined, post-alkylation. This culminated in the one-step aminolysis of the readily accessible calix[4]arene tetraethyl ester using a variety of amines. While this has been shown to be of great synthetic utility for the amines discussed, it can feasibly be extended to any primary amino-group containing compound. Finally, preliminary electrospray mass spectrometry and phosphorescence titration studies have indicated the complexation by these species of some lanthanide ions of interest.

2.10 Future Work

This study has developed the methods of derivatisation of calix[4]arene with regards to incorporation of amide functionality. Aminolyses of calix[4]arene esters has proven remarkably successful on numerous occasions, and it is envisaged that the use of this technique will be extended to further amines and to the development of the optimum conditions for the direct incorporation of amino acids, and for the nitrile synthons shown.

Further study of complexation conditions should be undertaken, with emphasis on the use of Tb(III), rather than Eu(III) as a model for photophysical studies. This will allow, through harnessing of the antenna effect offered by the electron rich calixarene core, for the

population of the lanthanide excited state and for its solution photochemistry to be further probed.

Imminent collaboration with Prof. Françoise Arnaud-Neu of Université Louis Pasteur, Strasbourg will allow high-throughput screening of the potential hosts which have been synthesised herein, against a range of lanthanide, actinide and transition metal ions.

3.1 Introduction

As discussed in Chapter 1, the ultimate objective of this thesis was the preparation of calix[4]arene derivatives with diverse functionality at the lower-rim, which, at the same time, retain upper-rim functionality for subsequent preparation of a calixarene-macromolecule conjugate. This will allow for the exploitation of both the enhanced permeability and retention (EPR) effect, for targeting purposes, and would provide an increase in rotational correlation time. As discussed in Chapter 1, both of these factors are expected to enhance MRI contrast efficacy. In Chapter 2, strategies which enabled the incorporation of metal-binding sites to the lower rim of calix[4]arene were discussed. This chapter will outline the various approaches employed in the preparation of lower-rim substituted precursors with upper-rim functionality, with the aim of preparing the aforementioned calix[4]arene-macromolecule conjugates.

3.2 Synthetic requirements for macromolecular conjugation

Covalent attachment of small bioactive or drug molecules to polymers^{128-130,154}, bio-macromolecules,¹⁵⁴⁻¹⁵⁷ or nanoparticles^{158,159} is well established in the areas of pharmaceuticals and drug delivery.¹⁶⁰ Attachment of smaller molecules to proteins may allow site-specific targeting of drugs or sensors, and as such, there are many protocols for their incorporation which are available.^{127,160,161} A key application of these techniques, for example, is the labelling of proteins by conjugation with dyes or haptens.^{162,163} These methods rely on the existence of reactive groups within macromolecules which are available for derivatisation, such as the ϵ -amino group of lysine, which itself is not involved in peptide bond formation, the S-H bond of the cysteine residue, or carboxylic acid moieties which are available for binding, such as those in the dicarboxylic amino acids aspartic acid¹⁶⁴ and glutamic acid. An attractive macromolecule for the attachment of smaller molecules is human serum albumin, an abundant blood-pool protein. Albumins possess up to 60 lysine moieties, with the frequently used model, bovine-serum albumin (BSA) has been found to have 59 free lysines,¹⁶⁵ each comprising a free ϵ -terminal amino moiety. This contrasts with bovine insulin which contains a single lysine residue, while avidin, found in egg whites, contains 36 lysine groups.¹⁶⁶ The nucleophilicity of this free amino moiety at pH > 8.0 can be exploited in reactions towards electrophiles, thus allowing loading of multiple smaller molecules onto each albumin molecule.

In each case, the reaction between a protein and a smaller molecule of interest must be carried out in an appropriate buffer, in the presence of ionic strength. A water-miscible co-solvent, such as DMSO or DMF may be used where required, and modifications are generally conducted below room temperature. Once the conjugate is formed, standard protein purification techniques, including dialysis or gel-permeation chromatography are undertaken to afford the pure conjugate.¹⁶⁰ A summary of some of the synthetic protocols for the covalent modification of these functional groups is outlined in cartoon format in Figure 3.1.

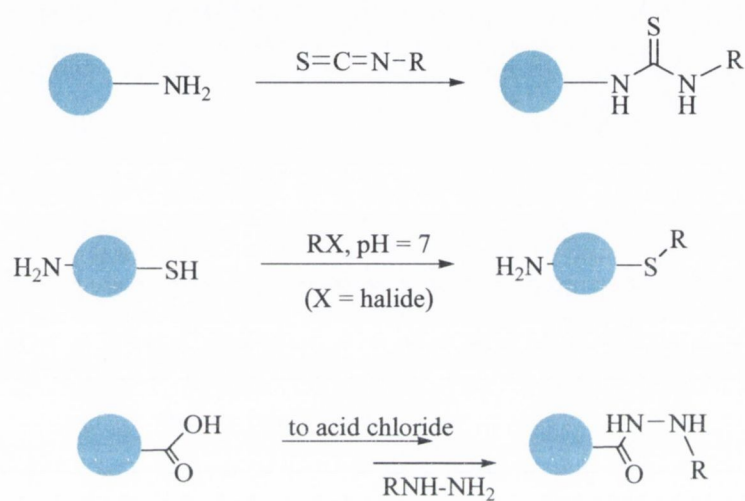
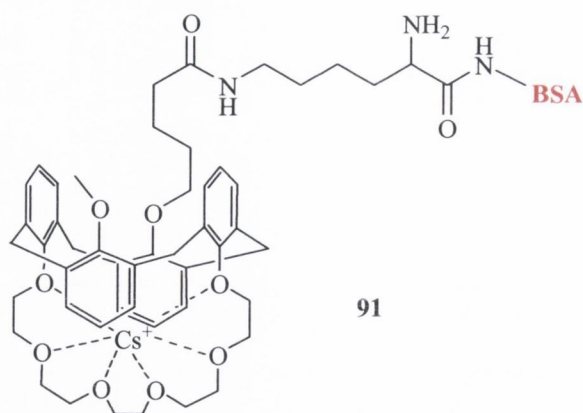
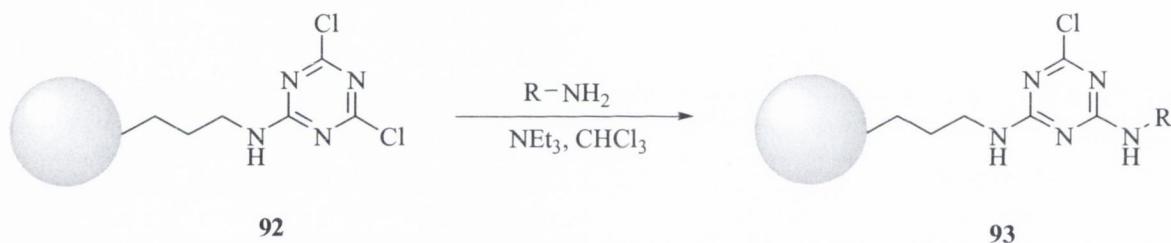


Figure 3.1 - Schematic representation of some methods for preparing protein conjugates, where the macromolecule is represented as a blue circle, showing free reactive functional groups.

Despite their substantial exploitation as hosts, the attachment of calixarenes to biomacromolecules has received relatively little attention. Reinhoudt and co-workers, in 1999 synthesised some calix[4]arene-based Ac^{3+} chelates, and undertook a study of their conjugation to both mouse and human serum albumins.¹⁶⁷ Conjugation by means of an isothiocyanate moiety and cystamine linker, forming a thiourea linker, was found to be inefficient, with only 6 hosts attached to the albumin, and was attributed to the low solubility of the calix[4]arene chelate in water. More recently, Hagège and co-workers have incorporated a calix[4]arene in the 1,3-*alt* conformation into BSA, with the objective of preparation of immunogens for the generation of antibodies towards Cs^+ ions.¹⁶⁸ The motif depicted (**91**) was prepared, and was shown using MALDI-ToF mass spectrometry and spectrophotometric experiments to load albumin in coupling ratios of between 8 ± 2 and 36 ± 2 calixarenes per albumin.



Calix[4]arene has also been bound successfully to nanoparticles, such as the covalent attachment of CMPO-functionalised calix[4]arene to magnetic particles. This has been pioneered by Böhmer and co-workers. In the case of attachment to magnetic silica particles, commercially available, pre-functionalised particles bearing 4,6-dichloro-1,3,5-triazin-2-yl (DCT) moieties (**92**) were treated with a calix[4]arene bearing four CMPO (*N,N*-diisobutylcarbamoylmethyloctylphenyl phosphine oxide) moieties at the upper rim, with ω -aminoalkyl substituents at the lower rim. Substitution of the DCT ring with the amino moieties to yield **93** is indicated in Scheme 3.1.¹⁶⁹

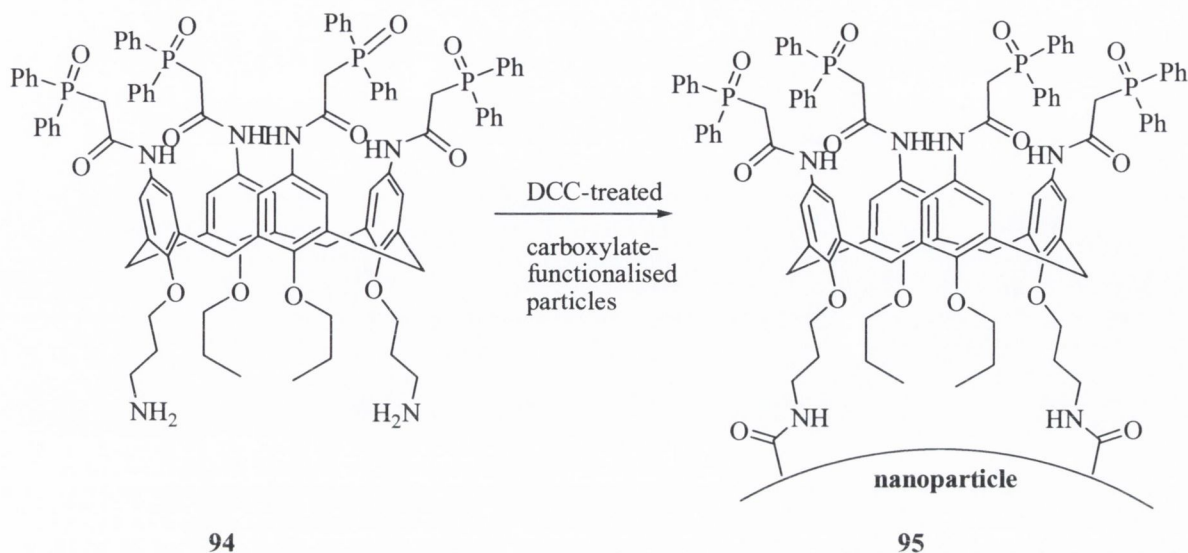


Scheme 3.1 - Functionalisation of DCT-functionalised silica particles, where R represents the CMPO-functionalised calix[4]arene derivative.¹⁶⁹

This strategy was successfully adopted in the case of mono, 1,3-di-, and tetra- substituted calix[4]arenes, each similarly bearing aminopropyl moieties at the lower rim, and CMPO functionality at the upper rim. Such covalent attachment was found to distinctly enhance the extraction of actinides from acidic solution when compared to analogous single-chain CMPO functionalised calixarenes.¹⁶⁹

A further example, using carboxylic acid functionalised silica particles was reported. Again, these modifications were to the lower rim; the upper-rim bore CMPO functionality for lanthanide and actinide extraction, while attachment to a nanoparticle was achieved through covalent attachment at the lower rim using the peptide coupling agent, DCC.¹⁷⁰ This is shown in Scheme 3.2. The calixarene-nanoparticle conjugate **95** was shown to

extract actinides efficiently from simulated nuclear waste streams, encapsulating between 78% and 92% of the metal ions.¹⁷⁰



Scheme 3.2 - Grafting of CMPO calix[4]arene to carboxylate functionalised SiO_2 particles.¹⁷⁰

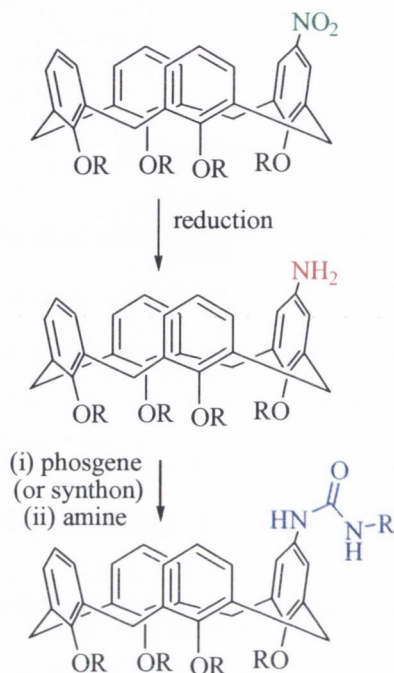
The above examples have shown how calix[4]arene derivatives may be covalently incorporated into larger macromolecules, with the objective of either site-specific drug delivery, or surface immobilisation, as is seen for the nanoparticle attachment. The following sections of this chapter will outline our the efforts undertaken in the course of this study in the development of calix[4]arene derivatives for macromolecular conjugation

3.3 Use of mono upper-rim substituted calix[4]arene

As evidenced above by Böhmer's seminal work in the attachment of calixarene derivatives to silica particles, calixarenes provide a scaffold which can be essentially ditopic in nature. However, this work, to date has focused on attachment through the lower-rim. It is our intention however, to build a single attachment point at the upper rim, while maintaining a strong binding array at the lower rim.

As discussed in Chapter 1, the lower-rim can be derivatised to allow for accommodation of a host ion such as a lanthanide ion, while the upper-rim can be derivatised to incorporate reactive functionality for protein conjugation. Considering the principal options for further derivatisation to be amines, carboxylates and thiols, it was decided to focus attention on the incorporation of an amino group into the upper rim. This can, in theory, be achieved by nitration of calix[4]arene, and by subsequent reduction of the nitro group to form the

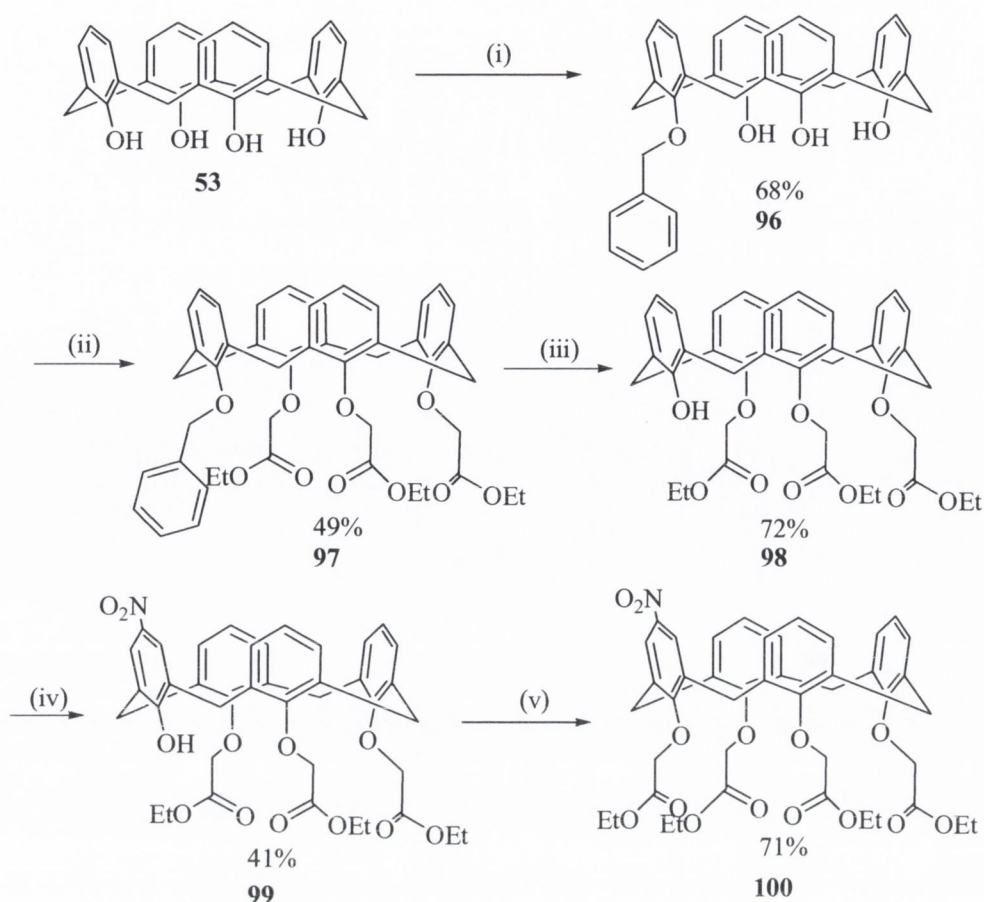
desired aniline, as outlined in Scheme 3.3. The resulting amino moiety may then be used for conjugation purposes either by reacting with an acid chloride to form an amide linkage, or by conversion to an isocyanate or isothiocyanate as precursors to the corresponding urea or thiourea tether.



Scheme 3.3 – Proposed route to a calix[4]arene-based synthon for bioconjugation, where variable R substituents will provide appropriate metal-binding arrays. Reduction methods and selection of R will be discussed.

3.3.1 Stepwise syntheses using calix[4]arene

Beer and co-workers prepared a number of ditopic receptors incorporating a ruthenium-bipyridine motif into a calix[4]arene.¹⁷¹⁻¹⁷³ In doing so, protocols were developed which afforded a singly nitrated calixarene with tetraester functionality. Chen and co-workers prepared a similar mononitrated tetracarboxylic derivative for the binding of actinides, specifically Ac-225.¹⁷⁴ Incorporation of an isothiocyanato moiety at the upper rim was performed, with the intention of labelling monoclonal antibodies. Further elaboration by the same group, of this work, has not been reported since the initial report in 1999. The synthesis of the mononitrated tetraester was repeated in the course of this work, and is outlined in Scheme 3.4.



Scheme 3.4 Stepwise route to mononitrated tetraethyl ester of calix[4]arene. Reagents and conditions: (i) K_2CO_3 , BnBr, CH_3CN (reflux). (ii) K_2CO_3 , $BrCH_2CO_2Et$, CH_3CN (reflux). (iii) $NH_4(HCOO)$, Pd/C , $EtOH$ (reflux). (iv) HNO_3/HCl in water/ $EtOH$, r.t. (v) K_2CO_3 , $BrCH_2CO_2Et$, CH_3CN (reflux).

This five-stage, linear synthesis which invokes a protection-deprotection strategy that was employed affords the final product in a low yield of 7%. The first stage, which introduces a single benzyl moiety to calix[4]arene **53** providing **96** in 68% yield. This serves as a good example of how single functionalisation at the lower rim of the C_4 macrocycle induces desymmetrisation, yielding a product with C_2 symmetry. This compound is prepared by standard alkylation procedure for calixarene, using K_2CO_3 and a corresponding electrophilic alkylator. In this case, the alkylating agent is benzyl bromide. Workup of this reaction was as for most alkylations: solvents were evaporated to yield an oil containing remaining benzyl bromide and K_2CO_3 . Partitioning this residue between CH_2Cl_2 and water allowed the excess base to be removed by washing. Removal of the organic solvent under reduced pressure left an oil which was stirred in diethyl ether. This yielded a white precipitate which was shown by 1H NMR to be the product. It was then purified by crystallisation from CH_3CN to yield a crystalline solid in 68% yield. The 1H NMR (400 MHz, $CDCl_3$) spectrum is shown in Figure 3.2.

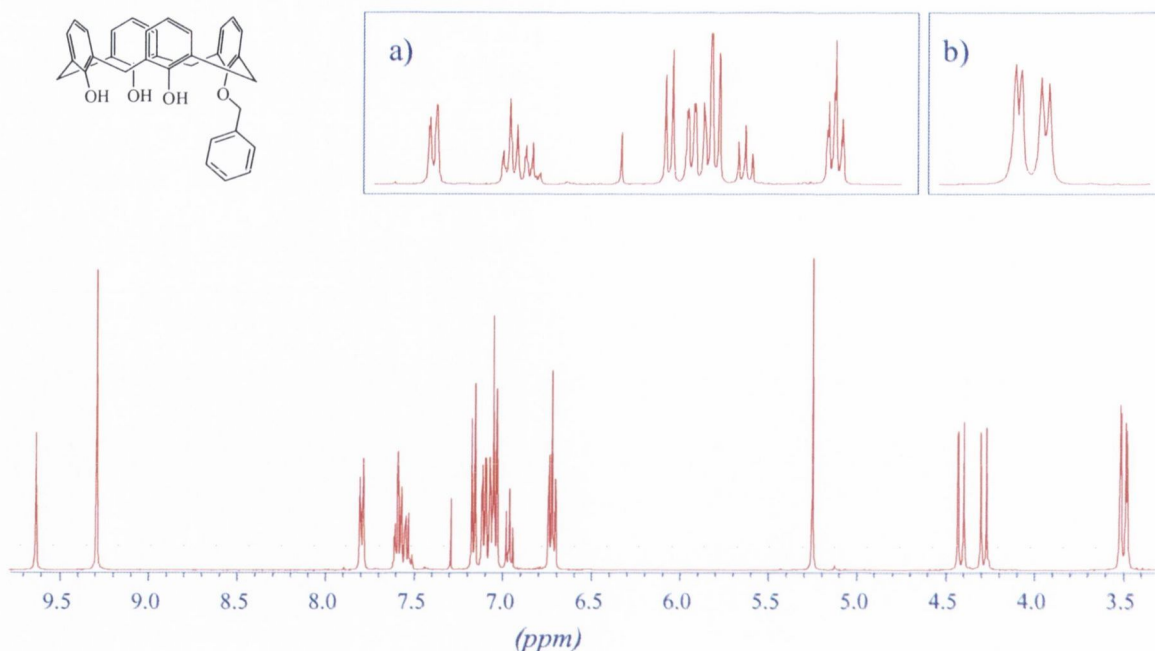


Figure 3.2 – ^1H NMR spectrum of monobenzyl calix[4]arene **3.7** (400 MHz, CDCl_3). Inset a) showing the expanded aromatic region 7.7–6.3 ppm, inset b) shows the two overlapping calix[4]arene doublets at approx. 3.5 ppm.

At this point it is useful to note the implications to the ^1H NMR spectrum induced by functionalisation at a single point. The splitting of the calixarene doublets upfield is noticeable, and now four doublets between 4.5 and 3.5 ppm can be seen, instead of the two which are seen for tetrasubstituted calix[4]arene derivatives. This can be attributed to the symmetry pattern as indicated in Figure 3.3.

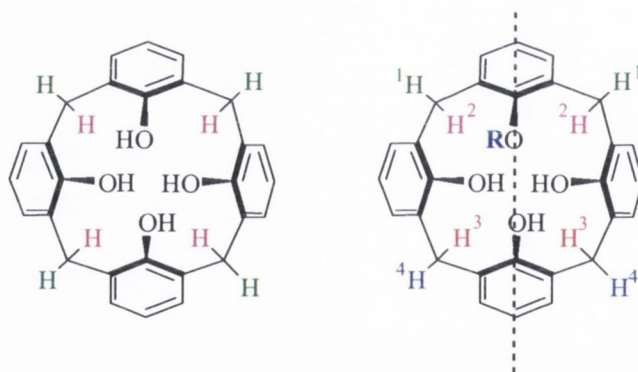
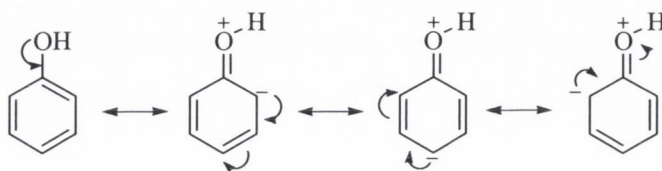


Figure 3.3 – $C_4 \rightarrow C_2$ Desymmetrisation of calix[4]arene induced by monofunctionalisation where four different environments of proton resonance are depicted.

As seen in the schematic Figure 3.5, there now exist four environments of bridging proton: the *endo* and *exo* protons at the position adjacent to the functionalised ring (H^1 and H^2), and the second methylene position, distal from the functionalised ring (H^3 and H^4). Again this environment has both *endo*- and *exo*- protons. In each case, geminal coupling is seen (as for the C_4 analogue), which splits the signals to doublets with expected high coupling

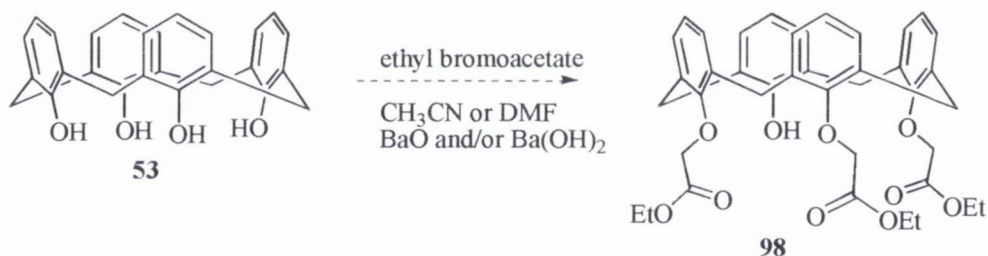
constants of 13 – 14 Hz. These doublets integrate in the expected 2:2:2+2 ratio, where the third resonance shows overlapping doublets. The aromatic region of the calix[4]arene core is desymmetrised, resulting in three environments, in addition to the further complication added by the benzyl moiety. Further downfield, the OH protons now resonate in a 2:1 ratio, indicating conclusively that a single OH position has been substituted. A peak at 5.24 ppm which integrates to two protons corresponds to the benzyl CH₂ protons, again, confirmation of a single benzyl group. It should be further noted that the schematic shown in Figure 3.5 applies throughout this stepwise synthesis for all C₂ intermediates herein, through to the trisubstituted calix[4]arene and for the tetrasubstituted ester with single functionality. Further examples of desymmetrised ¹H NMR spectra will be seen in Section 3.3.6.

The three remaining phenol positions were alkylated using ethyl bromoacetate in CH₃CN, again with K₂CO₃ as a base. The workup was analogous to that for the benzyl derivative, except that diethyl ether was used to precipitate unreacted starting material. The product, which remained in the ether was then isolated by concentrating the ether to an oil under reduced pressure. The resultant oil was stirred with ethanol to precipitate the desired product, **97** which was collected by suction filtration in 49% yield. The benzyl group was subsequently removed, again as reported by Cooper, using ammonium formate and Pd/C in ethanol.¹⁷⁵ This method allows simple hydrogenolysis, and is used in situations where retention of chirality is not required. Use of formate allows H₂ to be generated *in situ*, thus affording a safe and efficient method of cleavage of the benzyl moiety to yield **98** in 72% yield. Step (iv), nitration of calix[4]arene at a single position, is of particular interest, as it highlights the selective nitration of the *p*-hydroxy ring of the calixarene. This can be attributed to the distribution of charge in phenol, the canonical forms of which are shown in Scheme 3.5. In canonical forms where the partial negative charge lies on the *ortho*-positions, substitution cannot occur as this position is occupied by the methylene bridges of calixarene. Therefore, under standard conditions, electrophilic attack is ensured exclusively at the *para*- position, since phenol units are more reactive than phenol ether or ester units.²³



Scheme 3.5 - Distribution of charge in phenol.

The compound to be nitrated is dissolved in CH_2Cl_2 and stirred vigorously (or shaken) with an aqueous solution of NH_4NO_3 and HCl , with acetic anhydride acting as a phase-transfer catalyst. This step yields **99** in 40% yield with no side products isolated. The remaining hydroxyl moiety was then alkylated by reacting overnight with excess ethyl bromoacetate. This reaction was carried in refluxing CH_3CN using K_2CO_3 as a base. Evaporation of the solvent, gave a residue which was worked up analogously to **97** and **98** to yield an oil which was stirred in 2-propanol to give a fine yellow crystalline powder, **100** in 71% yield. Despite being able to isolate the desired singly nitrated tetraester, with the benzyl protection-deprotection strategy, it was desirable to eliminate this stage, and proceed with direct trialkylation using ethyl bromoacetate. This has been reported by a number of groups, using barium salts in place of the usual potassium carbonate base. The use of a base containing a large metal ion, such as Ba(II) allows exploitation of a template effect in the alkylation. CaH_2 has also been reported to be successful in synthesis of trialkylated calixarene derivatives, but with the stipulation that the ester moieties will likely undergo hydrolysis, yielding the analogous tricarboxylic acid.¹⁷⁴ We therefore set about using Ba(OH)_2 and BaO , both separately and in combination, to catalyse and template this reaction. This is outlined in Scheme 3.6.



Scheme 3.6– Direct trialkylation of calix[4]arene catalysed by barium(II) salts.

Several days of heating the reactions containing Ba(II) salts in CH_3CN or DMF yielded brightly coloured (blue or green) suspensions. When these were subjected to standard workup, the colour dissipated upon vigorous shaking with aqueous solutions, giving yellow organic solutions, which when analysed by ^1H NMR and ESMS did not contain the desired trisubstituted calix[4]arene. Attempts to nonetheless purify the crude products, such as that indicated in Figure 3.4, (prepared using BaO alone) by column chromatography (SiO_2) were unsuccessful.

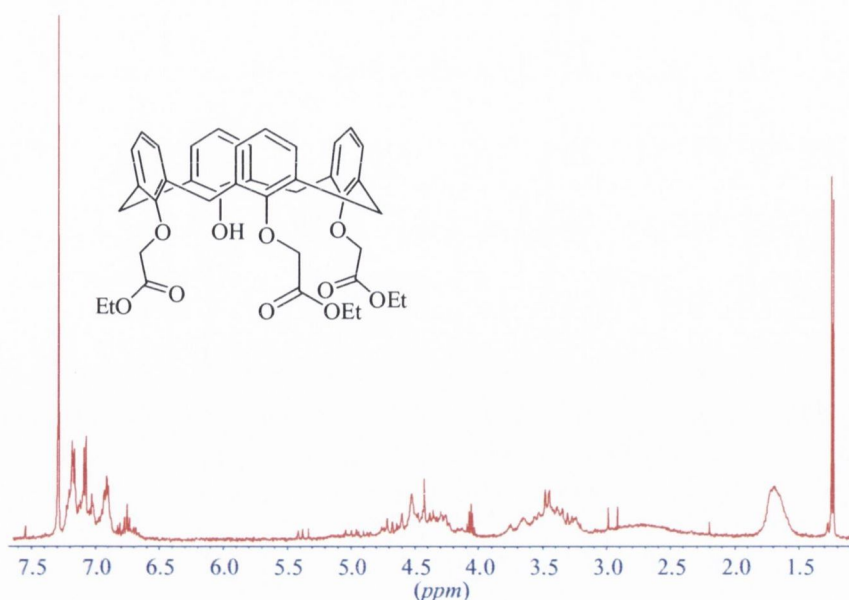
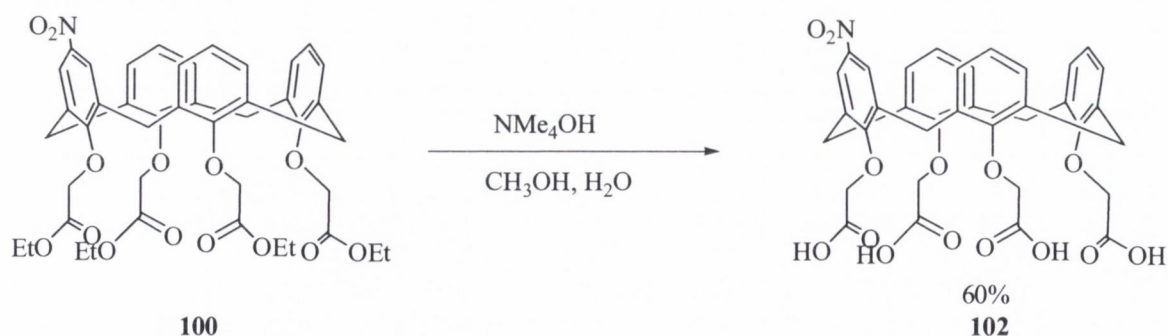


Figure 3.4 - Mixture resulting from attempted trialkylation of calix[4]arene using BaO/ethyl bromoacetate.

Alkaline hydrolysis of the ester moieties of **3.10** to their carboxylic acid equivalents was thus attempted. This was to allow for further amide bond formation, analogous to as set out in Chapter 2. This was initially attempted using NMe_4OH , as it had been reported that using NaOH or KOH can lead to the formation of inclusion complexes¹⁷⁴ (as discussed in Chapter 1, species such as the lower-rim ester and amides are known as excellent Na^+ and K^+ ionophores). Final isolation of the compound was met with difficulty and it became necessary to use column chromatography to isolate the pure compound. Elution of the tetracarboxylic acid on SiO_2 , in 5% CH_3OH in CH_2Cl_2 v/v, afforded an oil, which when stirred in CH_3OH gave the final product as a crystalline solid. This hydrolysis reaction is outlined in Scheme 3.7.



Scheme 3.7 – Hydrolysis of the ethyl ester moieties of **100** to carboxylic acid equivalents

With the nitrated tetracarboxylic acid (**102**) in hand, albeit by an unavoidable protection-deprotection linear synthesis, peptide coupling reactions at this carboxyl terminus were attempted. These were analogous to the reactions of the non-nitrated calix[4]arene

derivative discussed in Chapter 2, and are tabulated in Table 3.1 In no case was the desired product isolated when analysed by ^1H NMR spectroscopy.

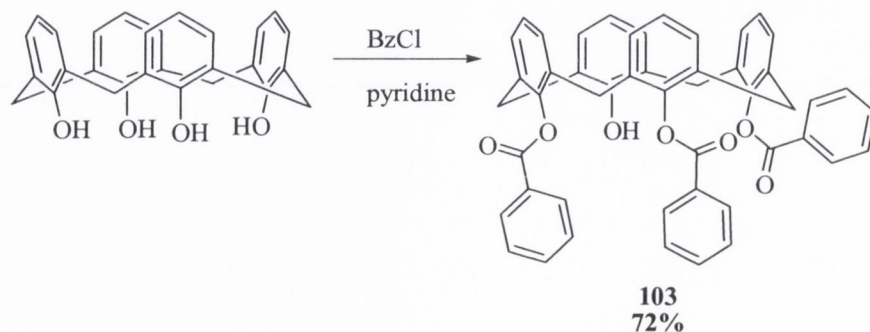
Table 3.1 - Reaction conditions for the formation of amide bonds between **102** and sarcosine ethyl ester.

Attempt	Conditions
1	DCC, sarcosine ethyl ester hydrochloride, <i>N,N</i> -diisopropylethylamine, CH_2Cl_2 , R.T.
2	SOCl_2 , sarcosine ethyl ester hydrochloride, NEt_3 , CH_2Cl_2 (dry), R.T.
3	$(\text{COCl})_2$, sarcosine ethyl ester hydrochloride, DBU, CH_2Cl_2 , $0^\circ \rightarrow \text{R.T.}$

In each case outlined above, only the starting material, **3.11** was recovered. It was therefore decided to prepare the nitrated calix[4]arene derivative without lower rim functionalisation. The intention here was that this may then be alkylated with the α -bromoamides which were outlined in Chapter 2. The following sections will discuss the strategies which were undertaken to introduce a single nitro group at the upper rims of both calix[4]arene and ^tBu -calix[4]arene.

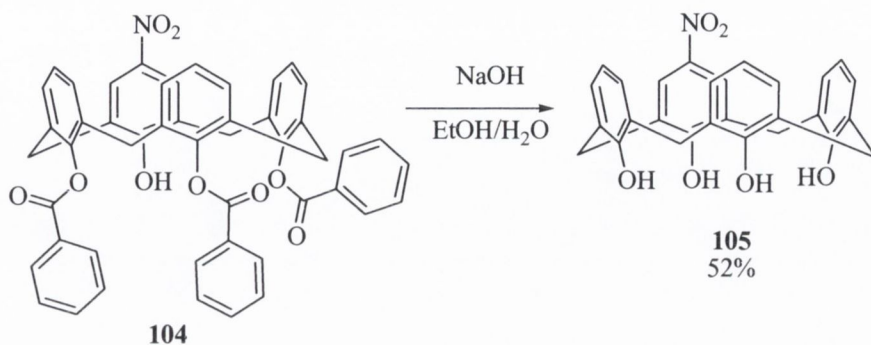
3.3.2 Use of benzoyl protecting groups

Two further approaches involving a protection strategy were subsequently attempted. Firstly, we attempted single nitration of the upper rim by protection of the lower-rim with benzoyl moieties, as reported by Wang and colleagues.¹⁷⁶ It had been shown by Gutsche, that the bulk of the benzoyl group allows for easy trisubstitution in pyridine.³⁵ Indeed, even upon exposure of calix[4]arene to excess benzoylating conditions for prolonged periods does not allow for tetrasubstitution. In addition, benzoyl moieties are relatively easily cleaved by alkaline ester hydrolysis. The introduction of these moieties proceeded in good yield of 72% according to Scheme 3.8.



Scheme 3.8 - Benzoylation of calix[4]arene at the lower rim.

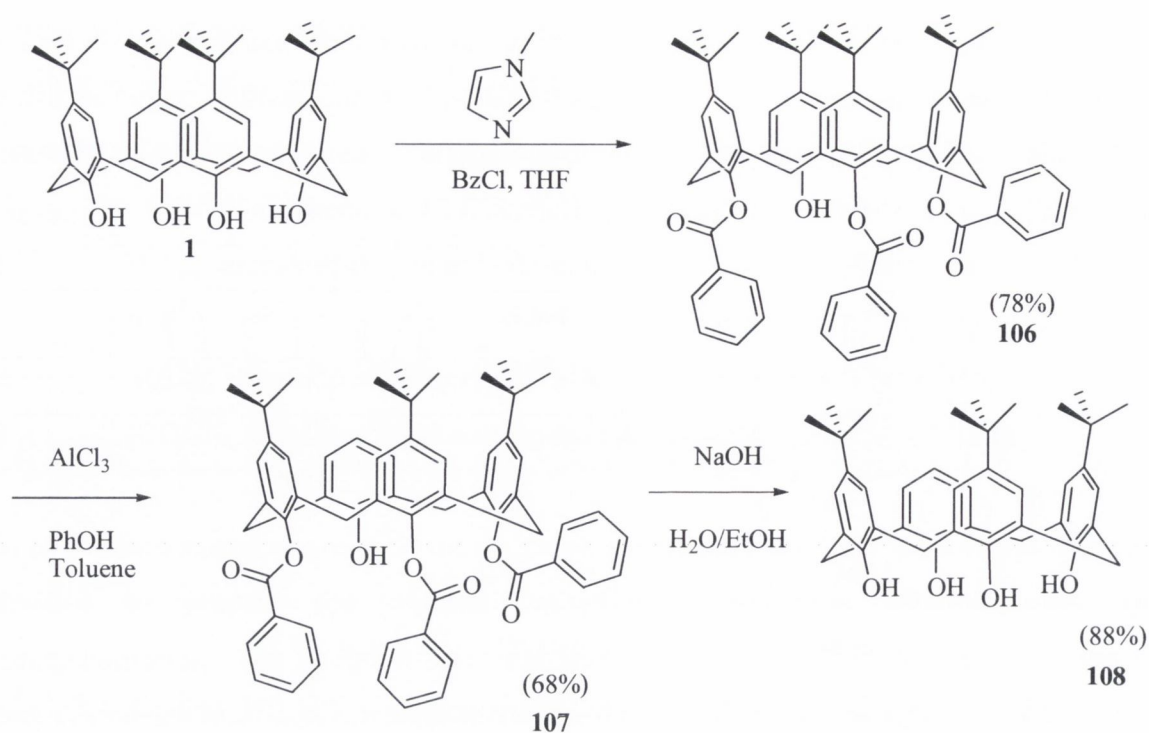
Again, this compound has a single unsubstituted phenol within the macrocycle, allows for single nitration at the upper rim. This transformation was successfully achieved using HNO_3 and AcOH . Cleavage of the benzoyl moieties using NaOH in EtOH/water successfully yielded the singly nitrated calix[4]arene, **3.34**, as shown in Scheme 3.9.



Scheme 3.9 – Alkaline hydrolysis of benzoyl groups of 3.33

When **3.34** was subjected to alkylation (ethyl bromoacetate in CH_3CN , using K_2CO_3 as a base), the desired product was not formed. As this methodology also required stepwise synthesis, and was not seen as advantageous to the synthesis of nitrated tetraester **3.10**, further alkylations or reactions of this compound were not undertaken.

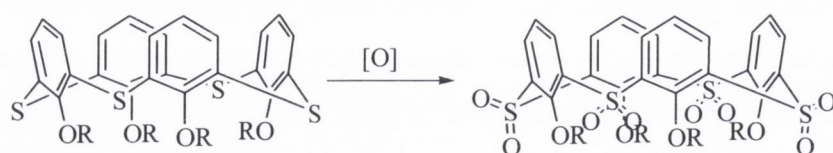
Upper-rim nitration was extended to the ^tBu-calix[4]arene parent, whereby a single ^tBu moiety would be effectively replaced with a nitro group. A method has been reported for removal of a single ^tBu moiety, again following a stepwise synthesis.¹⁷⁷ It was decided to attempt this method, and to subsequently investigate nitration at the single de-^tBu moiety. The synthesis of this compound is shown in Scheme 3.10. In each step, the reaction proceeded cleanly, providing the desired compounds which were characterised in agreement with the literature.¹⁷⁷ It should be noted however, that the first stage, whereby benzoyl moieties are introduced, was prepared using dry THF in place of the literature reported toluene. This fortuitous substitution of solvent yielded the product exactly as reported in the literature, with a higher yield of 78% in place of the reported 70%.

Scheme 3.10 - Preparation of tri-*t*Bu-calix[4]arene.

With this molecule in hand, a similar biphasic nitration, analogous to that carried out on the de-*tert*-butyl compound was attempted. Nitration using either ammonium nitrate or nitric acid failed to provide the desired nitrated compounds when analysed by ^1H NMR.

3.3.3 Introduction of functionality by diazo-coupling

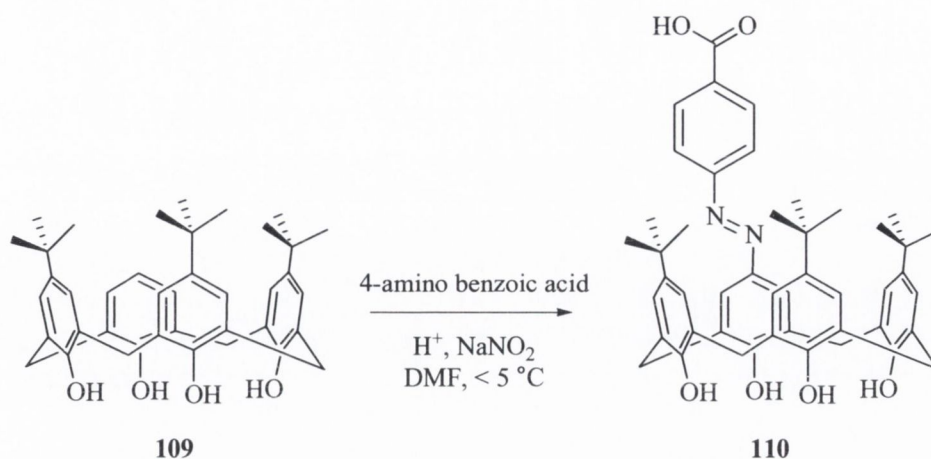
Groups working on the thiacalix[4]arene parent which was introduced in Chapter 1, wherein the methylene bridges have been replaced with epithio bridges, face the issue of oxidation of the sulfur bridges to sulfoxides and sulfones, as indicated in Scheme 3.11 when attempting to derivatise the upper rim using mineral acids and nitrates.¹⁷⁸



Scheme 3.11 - Oxidation of epithio bridges of thiacalix[4]arene to sulfones equivalents.

To this end, the incorporation of amino moieties into thiacalix[4]arene has been achieved by first introducing an azo group, followed by reduction to the amine.¹⁷⁹ We attempted this reaction using the tri-*t*Bu calix[4]arene synthesised in Section 3.3.2. This is shown in Scheme 3.12 The reaction involves preparation, at low temperature of a diazonium salt of

4-aminobenzoic acid, and addition of a solution this compound to a DMF solution of the tris-*t*-Bu-calix[4]arene.



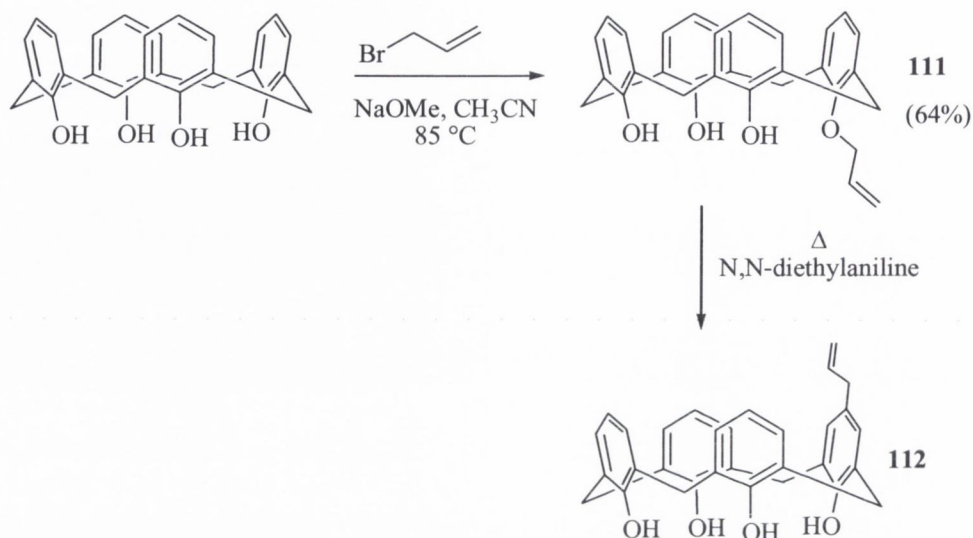
Scheme 3.12 - Preparation of upper-rim azo substituted calix[4]arenes.

This reaction was successful when forming the azo moiety using 4-aminobenzoic acid. Reduction of the azo moiety was then investigated. The compound was heated in water at 90 °C with NaOH and Na₂S₂O₄ for 1 hour, following which the resulting yellow precipitate was collected by filtration. Due to slow filtration of the aqueous solution, this compound was exposed to the atmosphere and turned to a black oil before it could be characterised. This problem had been reported in the original procedure for thiacalixarene; to overcome this, the authors prepared an imine *in situ* to give an air-stable product.¹⁷⁹ When we attempted analogous *in situ* introduction of Boc protection, this also resulted in a green-black oil which could not be successfully characterised. The reduction was once again attempted, and the product immediately extracted with CH₂Cl₂. This also led to decomposition of the products. This strategy was not pursued further, instead, attention was turned to the use of the allyl group, a potentially versatile synthon.

3.3.4 Synthesis of allyl-functionalised calix[4]arene

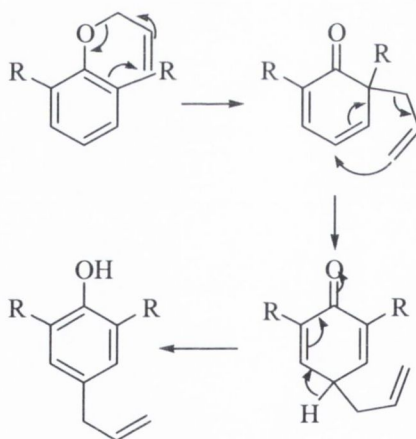
Gutsche and co-workers have pioneered the synthesis of lower and upper rim derivatives, and perhaps one of their most interesting modifications was the moving of a substituent from the lower to upper rim. This was affected by a Cope-Claisen rearrangement.³⁵ As this reaction was reported to give a single reactive substituent (an allyl group) at the upper rim, we therefore set about repeating this work to apply it to our own objectives. Monoallyl calix[4]arene (**3.17**) was prepared by alkylation of calix[4]arene in CH₃CN with allyl bromide, using NaOCH₃ as a base. This reaction, controlled stoichiometrically, provided no side products and yielded the desired product in 64% yield. Heating the 5-allyl

calix[4]arene in *N,N*-diethylaniline for 4 hours gave a clear pink solution, which when poured into 1 M HCl gave the desired product as a grey precipitate, which was collected by suction filtration. The preparation of both allyl derivatives is indicated in Scheme 3.13.



Scheme 3.13 - Preparation of monoallyl calix[4]arene at both lower and upper rims.

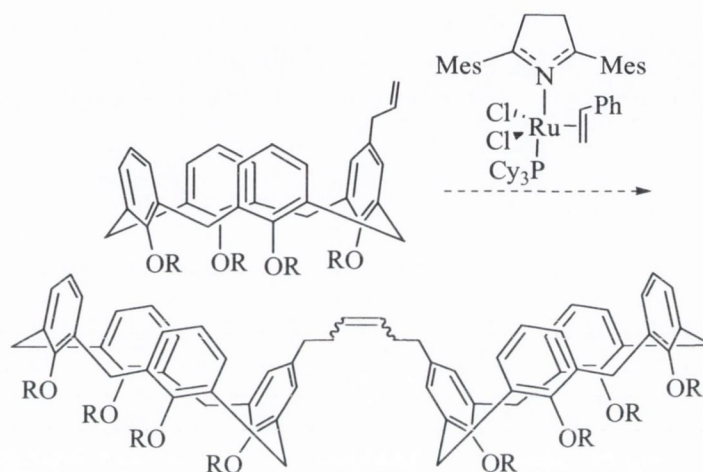
The outline mechanism of the sigmatropic, Cope-Claisen rearrangement is shown in Scheme 3.14.



Scheme 3.14 – Mechanism of the Cope-Claisen Rearrangement of 5-allyloxy calix[4]arene **111** to form **112** (single ring shown for clarity, R represents remaining calix[4]arene).

This reaction was performed a number of times, however on several occasions, the product underwent decomposition to a dark red oil. We considered this calixarene derivative to be a valuable synthetic intermediate, as chemistry may be carried out at the lower rim while upper rim functionality is maintained at a single position.

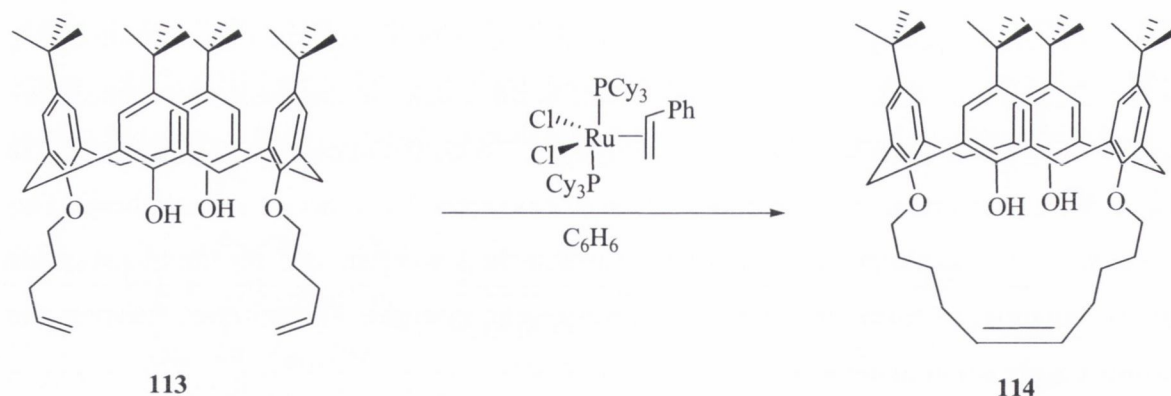
While upper-rim phenylene and vinylene groups have been exploited as cross-coupling synthons, this application requires synthesis of boronic acid or halogenated intermediates, followed by tin or palladium catalysed couplings.⁴⁶ With the upper rim allyl derivative in hand, it was decided to attempt dimerisation of calixarene by direct cross metathesis. This route will allow exploration of simple reactions at the lower rim, and for the investigation of the potential to form large binuclear macrocyclic systems. The outlined reaction and product is shown in Scheme 3.15.



Scheme 3.15 - Desired metathesis of allylcalix[4]arene using Grubbs' 2nd generation catalyst (stereochemistry at the double bond is arbitrary).

Grubbs catalyst is renowned for its synthetic versatility, allowing organic chemists to perform the metathesis transformation without the need for glove-box level anhydrous conditions that are required for organometallic reagents which affect similar transformations.^{180,181} Initially, protection of the lower-rim was undertaken prior to attempting metathesis. Alkylation was chosen as the first attempt, as this would provide a more attractive product for further derivatisation, enabling ester hydrolysis or reduction, and further reactions to be undertaken. Exhaustive alkylation with ethyl bromoacetate in CH₃CN was unsuccessful, so a more simple acylation reaction, for the purpose of temporary protection of the phenolic oxygens was attempted. Neither acylation with acyl chloride or acetic anhydride with pyridine afforded desired acylated products.

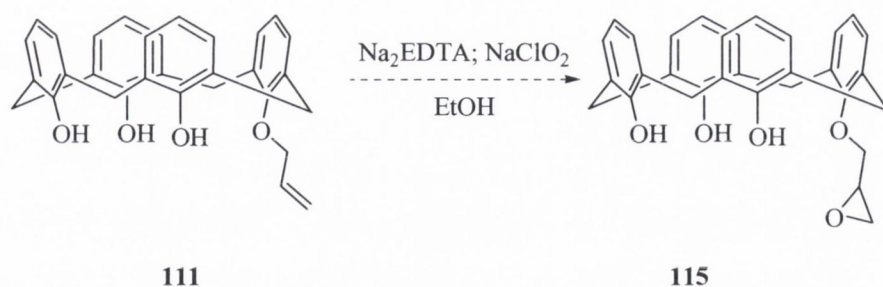
The metathesis reaction was next attempted with free phenolic OH groups, in light of a method reported by McKerverey and co-workers wherein Grubbs catalyst (first generation) was employed in the formation of a lower rim macrocycle as shown in Scheme 3.16.¹⁸² In this reaction, the amount of Grubbs catalyst was between 4 and 8 molar percent.



Scheme 3.16 – Grubbs' catalyst mediated metathesis in the presence of phenolic moieties, achieved by McKervery and co-workers.¹⁸²

The cross-coupling reaction of unprotected **3.18** was attempted twice; once in dry CH_2Cl_2 at reflux with 10% of the catalyst, and in dry toluene, again at reflux temperature. Each reaction was allowed to proceed for 16h. At the time, Grubbs first generation catalyst was not commercially available, thus the reaction was carried out using its derivative, known as the second generation. The latter differs from the first generation (shown in Scheme 3.12) by presence of a dimesityl *N*-heterocyclic carbene, in place of one of the triphenylphosphine moieties. This catalyst has generally higher activity than the first-generation catalyst.¹⁸³ In each case, the catalyst was removed by filtration through a pad of silica. Neither effort was deemed to be successful when the reaction mixtures were analysed by ^1H NMR spectrometry. No further dimerisation reactions using this catalyst were attempted. It was decided instead to investigate the reactivity of the allyl moiety towards epoxidation reactions.

A trial epoxidation of the lower-rim allyl derivative using sodium chlorite was then attempted, to investigate whether this group would be amenable to further derivatisation.¹⁸⁴ Complete decomposition of the calix[4]arene to a black, intractable oil was observed. This may, in part be attributed to the reactivity of phenol moieties towards the oxidising power of NaClO_2 .¹⁸⁵



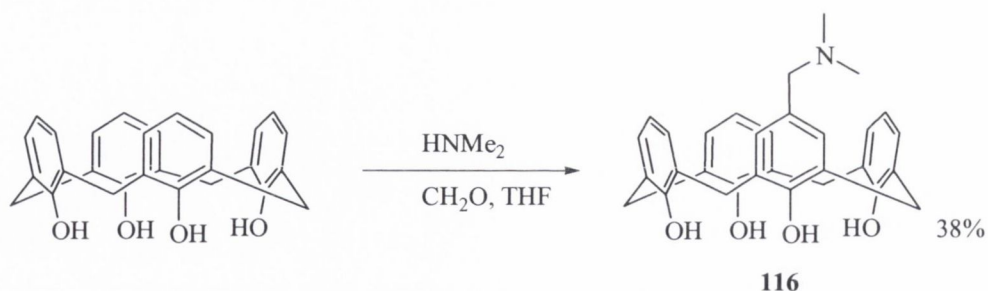
Scheme 3.17 - Attempted epoxidation of calix[4]arene mono-allyl ether **111** to epoxide **115**.

This was repeated using the more traditional method of epoxidation (*m*-CPBA). On this occasion, decomposition of the reaction mixture to a green residue was observed. It was therefore decided not to pursue the use of allyl derivatives further. Instead, a literature method which allowed direct mono-functionalisation at the upper rim, with no side-products was investigated. This will be outlined in the following section.

3.3.5 Gutsche's Quinone Methide Route: Cyanomethyl calix[4]arene

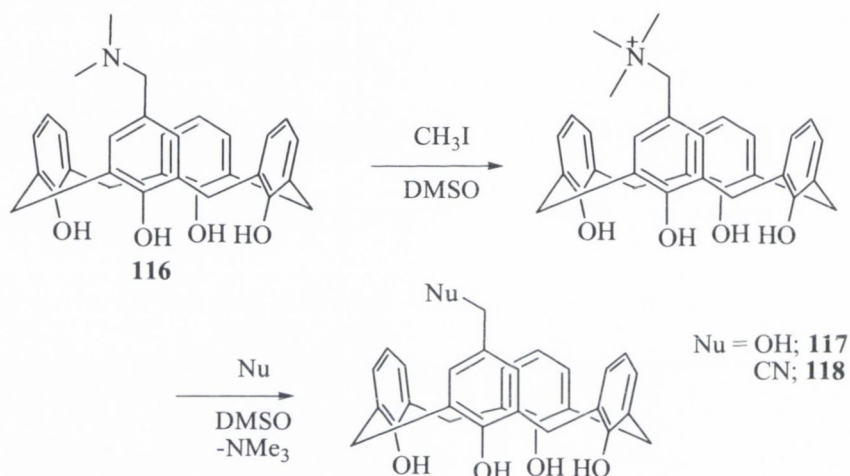
The quinone methide route to mono- and tetra- substituted calix[4]arenes was introduced by Gutsche and co-workers in 1994.³⁹ Using this methodology, Mannich bases of calix[4]arene can be readily prepared, and their reactions with simple nucleophiles (OMe, OEt, CN, OH and phenoxide) were probed. The most significant aspect of this work is that the procedure introduces a single substituent at the upper rim, in high yield (reported 95%), with no purification stages required. Despite such potential synthetic value, to-date this method has received little attention, with only fourteen citations as of late 2006. Some of the reported reactions were repeated to synthesise the 5-cyanomethyl and 5-hydroxymethyl derivatives of calix[4]arene, with a view to their further derivatisation for bioconjugative application

Stirring of calix[4]arene in THF with two equivalents of both aqueous formaldehyde and dimethylamine (40% in CH₃OH) for two hours yields the product as a thick precipitate, which is collected by filtration. Washing with CH₃OH and water, followed by trituration with acetone provided the pure product; a singly aminomethylated calix[4]arene (**3.22**) in a low yield of 38%, as shown in Scheme 3.18.



Scheme 3.18 - Preparation of calix[4]arene Mannich Base.

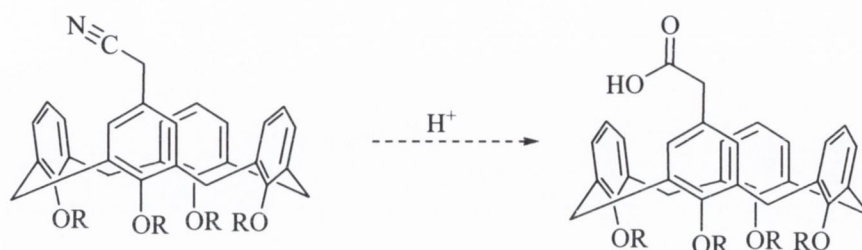
The presence of the secondary amine at the benzylic position allows for formation of quaternary salt using methyl iodide. The resultant trimethylamine is then easily displaced using an appropriate nucleophile, such as hydroxide, cyanide or a halide. This is indicated schematically in Scheme 3.19.



Scheme 3.19 – Quaternisation of Mannich base, followed by nucleophilic attack displacing trimethylamine.

In following the Gutsche procedure, we unsuccessfully attempted the synthesis of the hydroxymethyl analogue **3.39**, using OH as a nucleophile. Use of CN as an attacking nucleophile was undertaken, and the desired product, **3.40** was successfully prepared. In the case of the **3.39**, the nucleophile was delivered as either KOH or CsOH. The cyanation reaction involved treating a DMSO solution of Mannich base **3.22** with excess NaCN in DMSO. The reaction workup required acidification using 1 M HCl, followed by filtration of the resulting solid. Crystallisation from methanol/chloroform, as reported³⁹ was unsatisfactory; purification could only be achieved by using chromatography on silica gel. Due to the severe health risks associated with the use of DMSO solutions of sodium cyanide, and the exposure of cyanides to acid in work-up, this method not repeated or scaled up. It was decided instead to attempt to further derivatise the hydroxyl positions at the lower-rim of the sample in hand. It was anticipated that once lower-rim functionality

was in place, hydrolysis of the upper-rim nitrile would furnish the corresponding carboxylic acid (Scheme 3.20), which would provide a suitable handle for macromolecular conjugation through peptide coupling techniques. Alternatively, reduction of the nitrile would provide the aminoethyl moiety, which would also be of synthetic value.



Scheme 3.20 - Potential acid-catalysed hydrolysis of calix[4]arene nitrile to yield carboxyl derivative.

In order to introduce diverse functionality, esterification was then attempted. As has been outlined in Section 3.3.4 for the allyl analogue **3.18**, esterification is a much-used reaction in calixarene chemistry for the introduction of further functionality, this has been extensively discussed in Chapter 2. The presence of an cyanomethyl group at the upper rim was not expected to impart any changes in reactivity to the phenolic oxygens, so standard conditions of alkylation were used. Stirring **3.22** in CH_3CN at reflux temperature with ethyl bromoacetate with K_2CO_3 base failed to provide any alkylated product. Acylation with either acyl chloride or acetic anhydride also failed to provide us with products. Both of these acylating agents are highly reactive and are expected to readily react.

At this point, it was decided to revert attention to the nitrated tetraester prepared in Section 3.3, and to apply some of the reactions which had been developed in Chapter 2, notably the aminolysis reaction. The following section will detail the reactions which were undertaken to synthesise 5-nitro calix[4]arenes with lower-rim amide functionality.

3.3.6 Aminolysis of nitrated tetraester

The protocols for aminolysis reactions have been discussed in Chapter 2, where the ester moiety is replaced with an amide by nucleophilic attack with an amine. Use of this method has allowed rapid preparation of calix[4]arene derivatives from the tetraethyl ester, as discussed in Chapter 2. This approach was hence adopted also for the synthesis of a number of amides, starting from the mono-nitrated tetraester of calixarene (**3.11**), which was prepared as outlined in Section 3.3.1. For purposes of clarity of analysis, the four rings of calixarene will be discussed as A, B, C and D. A is the nitrated ring, which is proximal to rings B and D, and distal to C. This is denoted in Figure 3.5.

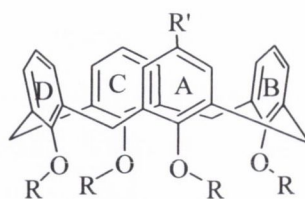
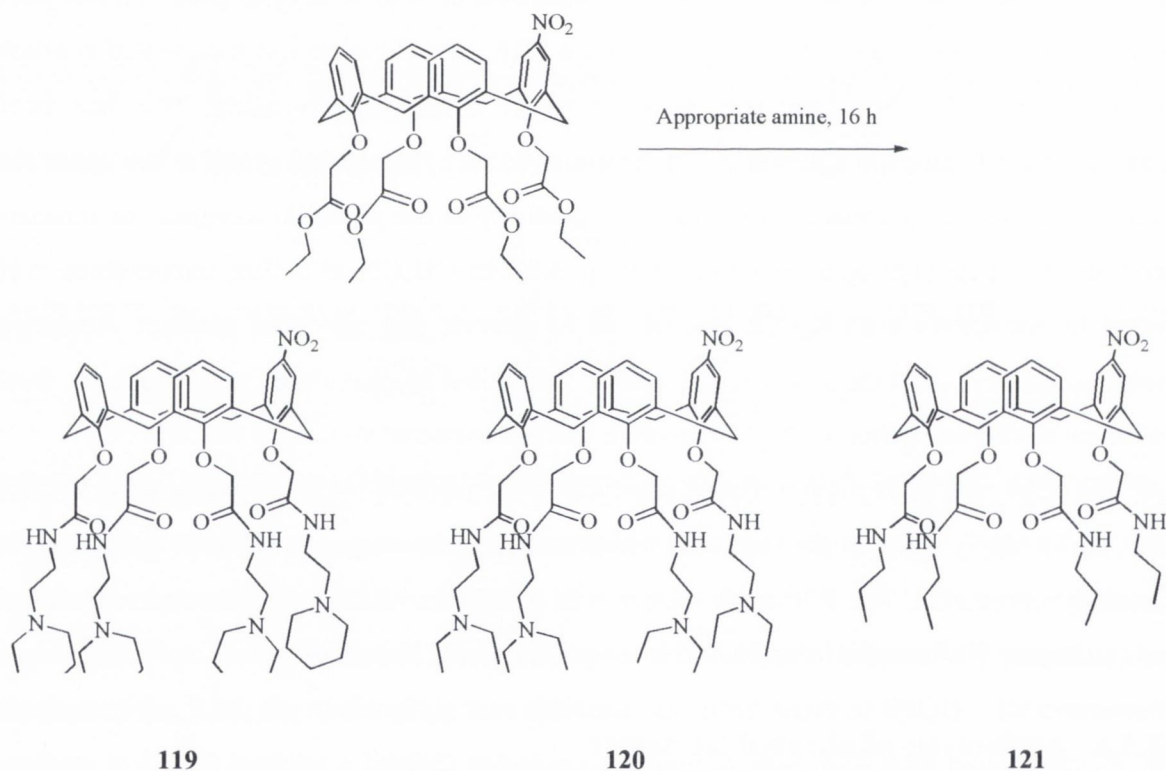


Figure 3.5 - Ring numbering system for desymmetrised calix[4]arene derivatives.

When a simple amine (propylamine) was used in a trial reaction, the reaction proceeded to completion. The tetraamide was isolated by evaporation of the amine, followed by trituration with diethyl ether. The resulting solid was recrystallised from acetonitrile. It was decided to prepare some other analogues of more diverse lower-rim functionality. The analogues prepared using this direct method are summarised in Scheme 3.21.



Scheme 3.21 - Aminolysis of mononitrated tetraethylester of calix[4]arene.

As anticipated, and as seen already in the case of the monobenzyl ether of calix[4]arene **96**, the ^1H NMR spectra of desymmetrised systems are complicated, and full assignment was possible through both high-field one- and two-dimensional NMR experiments. Each of these analogues is similar, thus several regions of the NMR spectra are common to all of the molecules synthesised. The ^1H NMR spectra obtained for each of these compounds is shown in Figure 3.4.

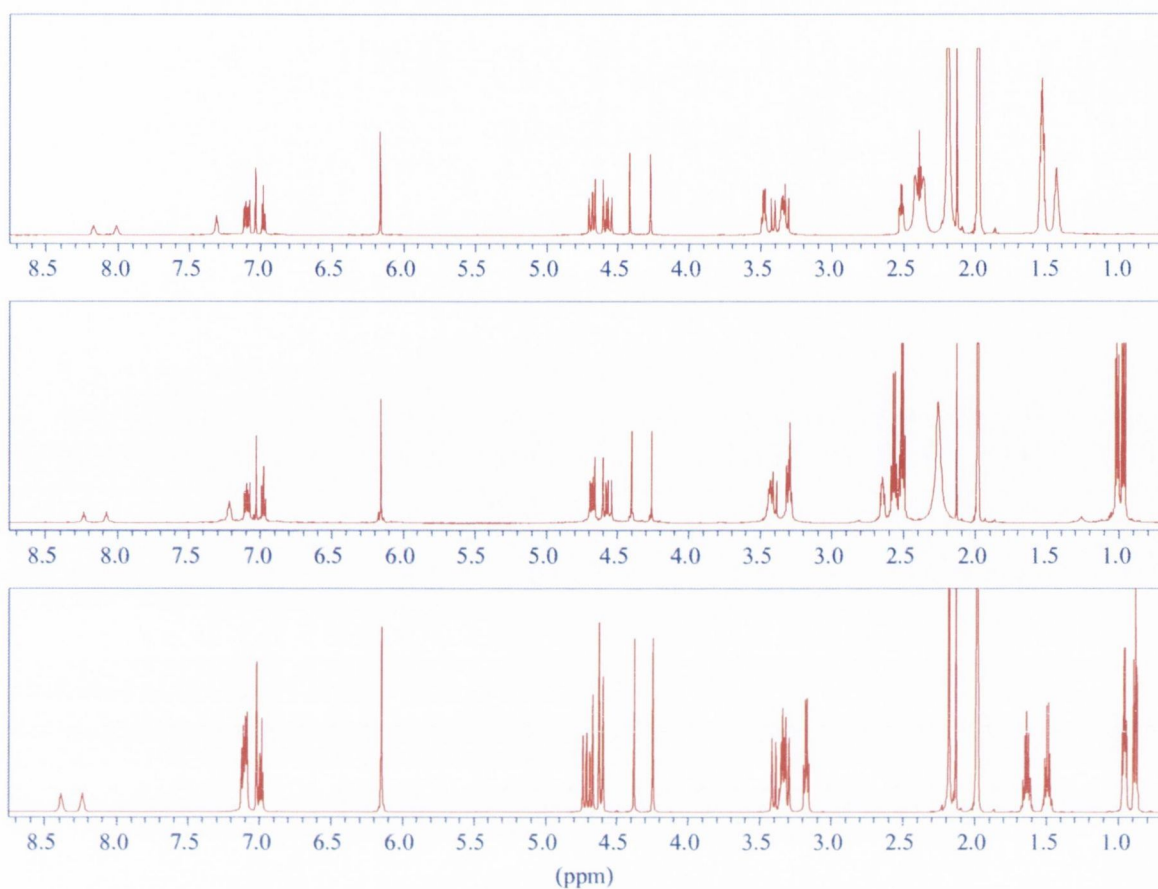


Figure 3.6 – ¹H NMR (600 MHz, CD₃CN) spectra of products obtained upon aminolysis of mono-nitrated tetraethyl ester with: (i) 1-(2-aminoethyl)piperidine (**119**); (ii) *N,N*-diethyl ethylenediamine (**120**); (iii) propylamine (**121**).

In each case, the amide protons are visible as two signals: two broad singlets which are seen furthest downfield. These were assigned using the ¹⁵N-¹H HSQC NMR experiment, whereby ¹⁵N nuclei are inversely detected by virtue of their coupling with directly bound ¹H nuclei. This experiment also detected coupling of the NO₂ moiety to the upper rim protons *ortho*- to the nitro substitution (those on ring A). The ¹⁵N-¹H spectrum obtained for the *N*-propyl analogue is shown in Figure 3.7.

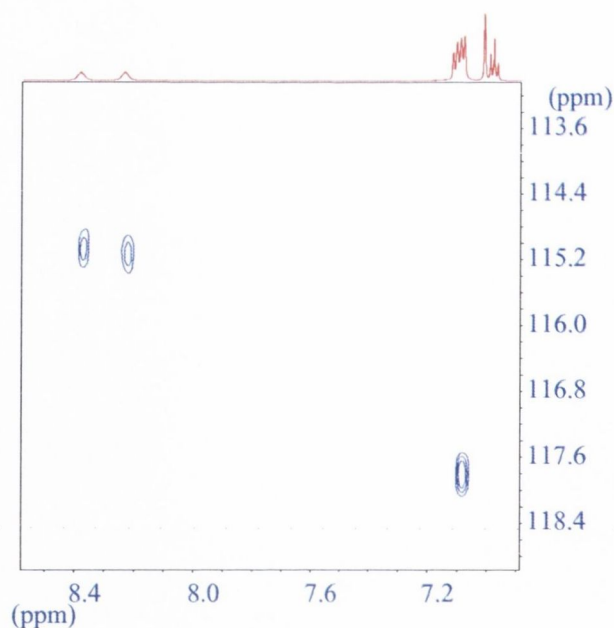


Figure 3.7 – HSQC ^{15}N - ^1H (14.1 T, CD_3CN) indicating presence of three environments of proton-coupled ^{15}N nuclei in **121** ^{15}N resonances were not directly observed in a separate 1-D experiment.

Further high-field NMR experiments were undertaken to fully assign the spectra of this, and the analogous compounds. The H-H COSY obtained for the propylamide analogue (**3.23**) is shown in Figure 3.6. From this spectrum it can clearly be seen how the NH protons couple strongly with alkyl protons (verified through DEPT- ^1H COSY to both CH_2 and CH_3 of the propyl chains). Two environments of terminal CH_3 A, (B,D), C are seen, as a double triplet, centred at 0.95 ppm, and a triplet at 0.87 ppm, each integrating to 6H. The former is assigned as that attached to both of the two non-equivalent phenol rings, thus two triplets appear superimposed. The second resonance corresponds to the terminal methyl groups of the propyl moieties which are appended to the two equivalent rings. Inspection of the C-H cosy allows assignment confirmation of the calixarene doublets. The methylene bridges resonate in the ^{13}C NMR spectrum in two different environments, 30.5 and 30.3 ppm respectively. Correlated to these in the ^1H NMR are four doublets at 4.72, 4.60, 3.39 and 3.30, each integrating to 2H. The full assignment of the methylene moieties α - to the phenolic oxygen is also possible through this experiment; three ^{13}C signals are seen at 73.3, 73.5 and 73.7. By correlation, these correspond to the expected singlets in the ^1H NMR spectrum at 4.65, 4.37 and 4.24 ppm respectively. The C-H COSY obtained for these assignments is shown in Figure 3.8.

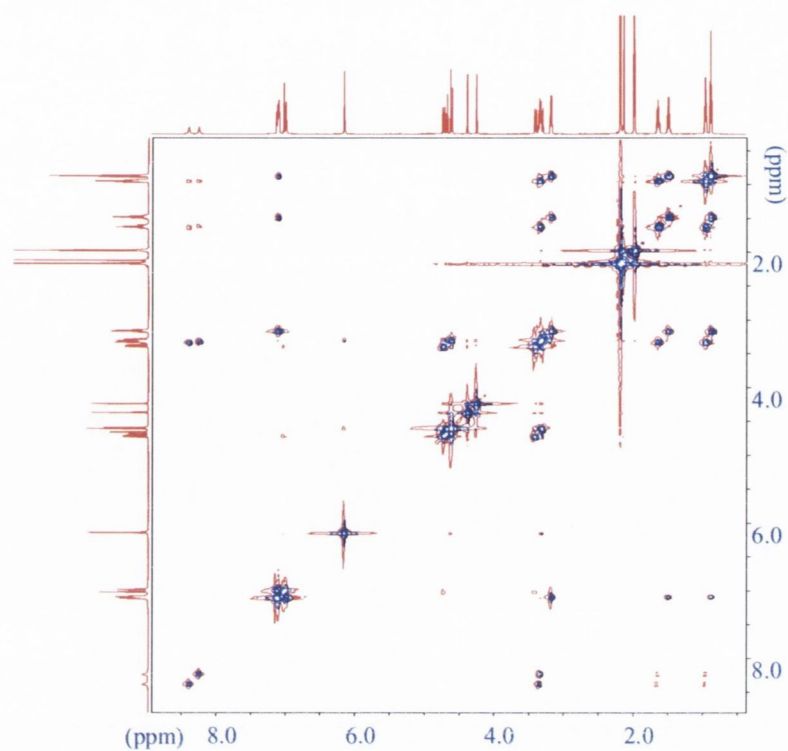


Figure 3.8 – ^1H - ^1H COSY (600 MHz, CD_3CN) obtained for singly nitrated tetrapropylcalix (**121**).

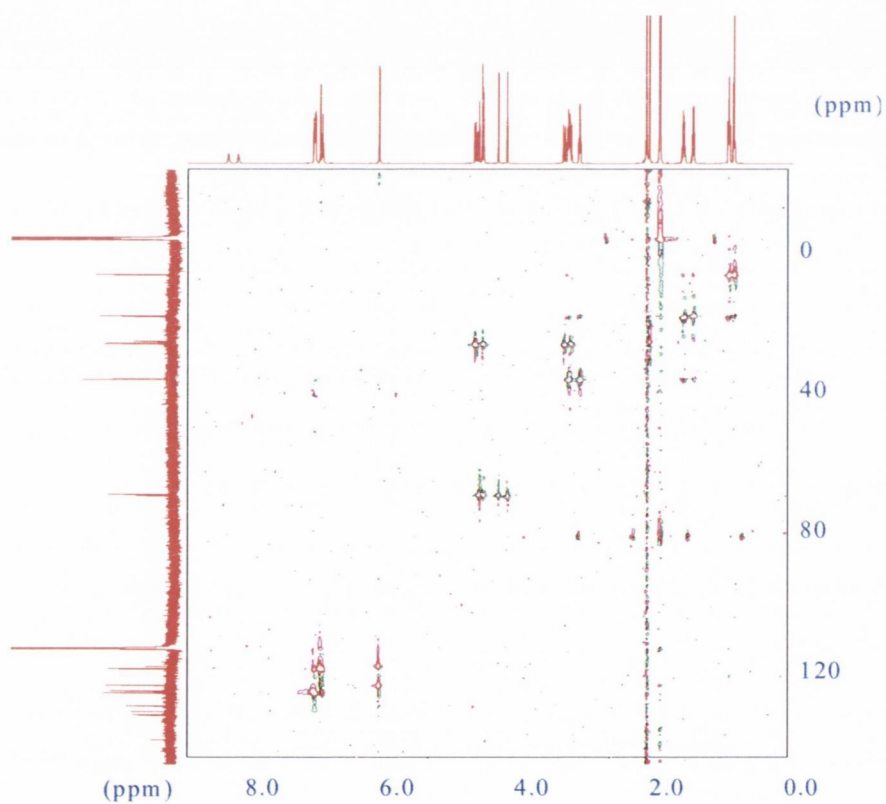
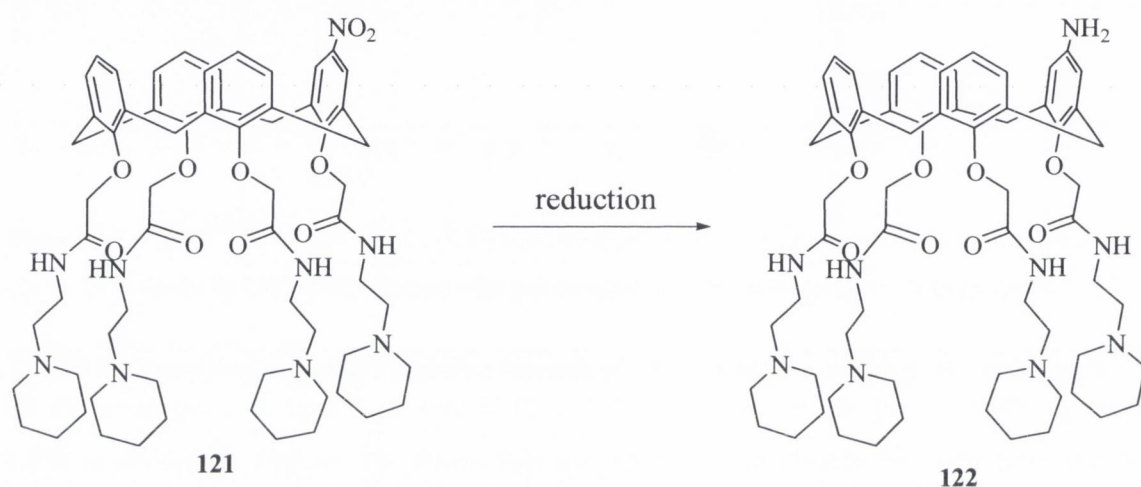


Figure 3.9 – ^{13}C - ^1H COSY (14.1 T, CD_3CN) of **121**

3.3.7 Reduction of the nitro moiety

The aforementioned molecules provide both of the requisite features of the molecules which are to be prepared in this study: upper rim functionality at a single position, and an amide-containing potential binding array at the lower rim. However, further derivatisation is required to enable this species to be incorporated into any further motifs. The amino group is the most accessible derivative available from a nitrated starter. Interconversion is by means of reduction which may be carried out in a number of ways. This interconversion is shown in Scheme 3.22.



Scheme 3.22 – Intended reduction of 3.24; unsuccessful using H₂/Pd/C or H₂N₂H₂/Pd/C.

According to a literature precedent, where the mono-nitrated tetraester (**3.11**) was reduced to the corresponding aniline,¹⁷⁴ tetraamide (**3.23**) was reacted with hydrazine hydrate and Pd/C (10%), in ethanol. The authors of this study noted that both hydrogenation and Raney nickel reduction were unsuccessful. Hydrazinolysis was carried out, allowing the reaction proceed for three hours, after which the catalyst was removed by suction filtration through Celite[®]. Evaporation of all liquid reagents and solvents left an oil to which ethyl acetate was added. This was then left to stand overnight, which yielded a solid, which when analysed by ¹H NMR did not indicate the presence of the product. The reduction of the nitro group of the *N,N*-diethyl analogue was also attempted using hydrogenation, which is not expected to react with either amide or ester moieties. Reaction in a Parr shaker (2.2 atm. H₂, 10% Pd/C, overnight) again did not lead to successful formation of the desired product. Due to time constraints, no further reduction attempts were undertaken.

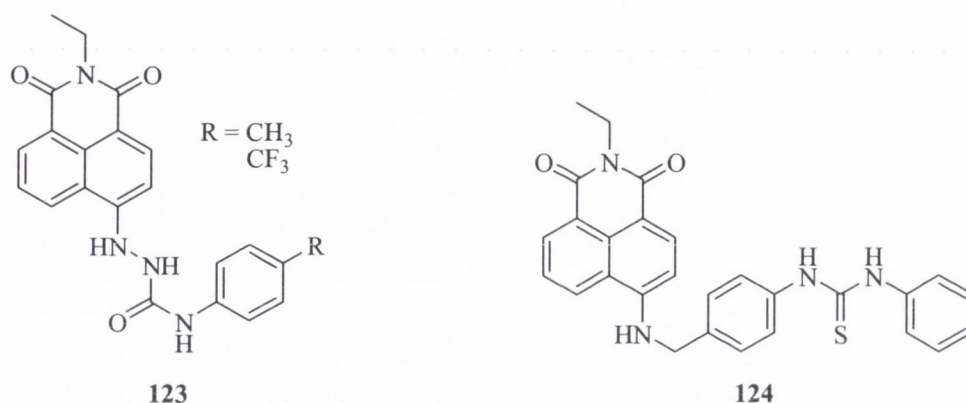
3.4 Conclusion

This chapter has discussed the various approaches which were taken in the course of this study to introduce upper-rim nitro/amino “handles” onto the potential metal-binding chelates which were synthesised in Chapter 2. This approach has largely been stepwise in nature, relying on the introduction of functionality (the nitro group) to an intermediate in a pathway which involved prior lower-rim functionality. Alkylation or acylation of derivatives of calix[4]arene which were accessible using literature precedents, and which contained functionality (either cyanomethyl or allyl groups) at the upper rim were unsuccessful.

Arguably, the most fruitful result of this study has been the extension of the aminolysis reactions which were developed in Chapter 2, to the mononitrated tetra ester (**3.11**). This has allowed access to several compounds with complex lower-rim functionality, with the requisite nitro moiety at the upper rim. While the synthesis and characterisation three such hosts has been discussed, it is envisaged that this reaction type may be applied to any amine, with the proviso of high amine nucleophilicity and steric accessibility. Regrettably, in the course of this latter study, reduction to the amino group, and the further derivatisation of these compounds has not met with success. It is anticipated that the reduction and subsequent stages will be further investigated within the group in the near future.

4.1 Introduction

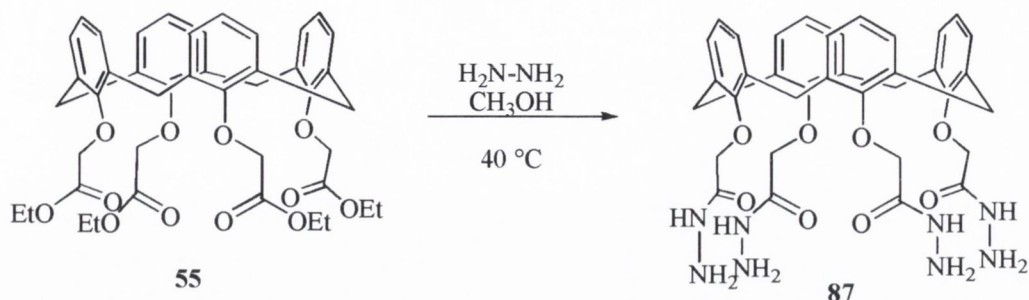
Recent success within our group has involved the synthesis of semicarbazide, or hydrazine-based ureas and thioureas which extend from a naphthalimide chromophore motif,⁹⁴ such as **123**. This built upon earlier work which had been developed, where a urea or thiourea moiety was incorporated closer to the naphthalimide core,⁹⁵ that is, onto the aromatic amine as **124**. The sensors which are based on the semicarbazide subunit complement and build upon the work reported by groups such as those of He¹⁸⁶, Costero¹⁸⁷ and Gale.^{188,189}



In these cases, upon hydrogen bonding of the ureido protons to an anion, internal charge transfer (ICT) causes delocalisation of charge on the 4-amino moiety, and a colour change ensues; from yellow to purple. These sensors have been found to be versatile and selective for AcO^- in a variety of solvents, including competitive aqueous media. Further efforts within our group led to the incorporation of thiourea moieties into a [3]polynorbornane scaffold, allowing for the construction of an anion-binding cleft, possessing strong affinity towards the biologically relevant phosphate and pyrophosphate anions.⁹⁷ As a successful and efficient synthesis of semicarbazide-containing calix[4]arene, as outlined in Chapter 2 had been devised, it was decided to prepare some corresponding urea analogues and assess their potential as anion receptors, as these calix[4]arene-based structures, like their [3]polynorbornane counterparts would present a preorganised binding cavity which would be expected to show affinity to large anions such as phosphate or the simple dianion, pyrophosphate.

The calix[4]arene tetrahydrazide **3** shown in Scheme 4.1 was initially synthesised as part of our ongoing interest in developing potential hosts for lanthanides, as discussed in Chapter 2. Upon attempted complexation of the hydrazide with lanthanide salts, however, no metal

chelate appeared to form. The hydrazide was also used in diazotisation reactions, which have also been discussed in Chapter 2.



Scheme 4.1 - Formation of calix[4]arene tetrahydrazide **87** from calix[4]arene tetraethyl ester

Having developed the direct and efficient synthesis of this compound by aminolysis of calix[4]arene tetraethyl ester using hydrazine hydrate, it was decided to exploit this readily accessible motif for anion binding. The calix[4]arene scaffold offers rigidity and the potential to pre-organise multiple urea moieties, forming an anion-binding motif, which potentially allows for the binding of large anions such as chloride or bromide. In addition, the regioselective and conformation-specific derivatisation chemistry of the calix[4]arenes allows investigation of the effects of both multiple anion-binding sites, and the incorporation of anion-recognition motifs such that allosteric effects may duly be studied. The aim of this work therefore, was to synthesise tetra-ureido calix[4]arenes, such as that shown in Figure 4.1, and to assess their affinity towards anions, principally for AcO^- , halides and H_2PO_4^- . The ease of derivatisation of calix[4]arenes opens the potential to prepare anion receptors with differing substitution patterns and with various conformations. This would allow 1,3-disubstituted and further arrays to be prepared, thus allowing elucidation of both binding mode and strength.

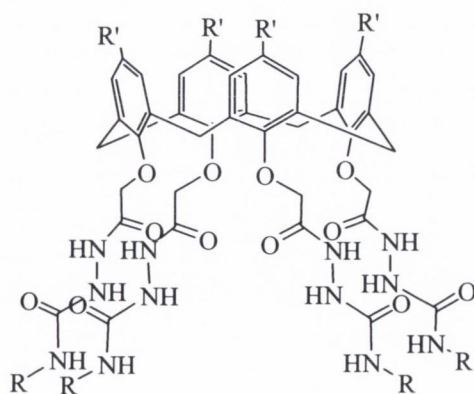
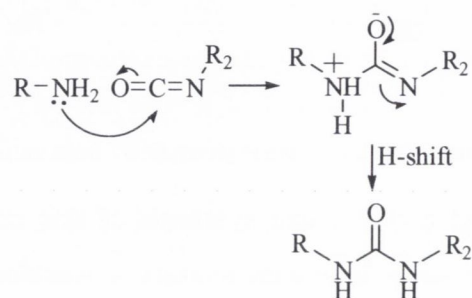


Figure 4.1 – Generic structure of tetrasubstituted calix[4]arene hydrazine-urea; R = alkyl, aromatic; R' = ^tBu,

H

4.2 Synthesis of ureas

The conversion of an amine to a urea or thiourea is generally straightforward; it involves treatment of the amine with an isocyanate, to prepare a urea, or with an isothiocyanate to produce the thiourea analogue. This proceeds for ureas according to the mechanism shown in Scheme 4.2.



Scheme 4.2 – Formation of ureas by reaction of an amine with an isocyanate

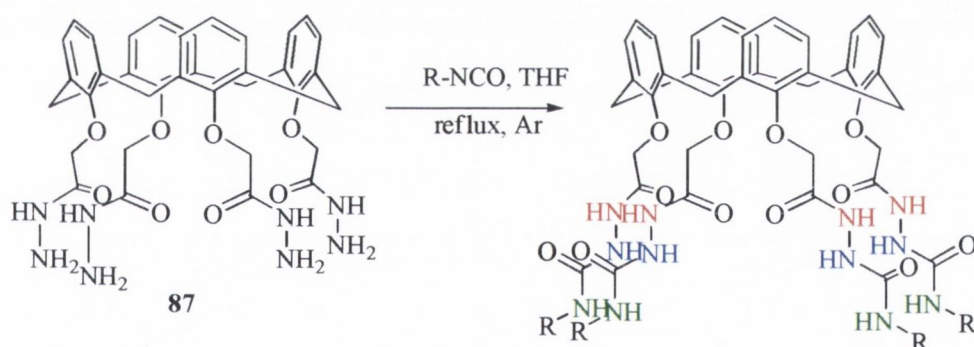
Reaction will potentially occur in any appropriate dry, non-electrophilic organic solvent, with the exception of the alcohols, as isocyanates readily react with nucleophilic alcohols to form urethanes. The calix[4]arene hydrazide **87** was found to be insoluble in organic solvents of moderate polarity (CH_2Cl_2 , THF, Et_2O). In these studies, it was decided to synthesise and investigate two different families of ureas: phenyl ureas which could be studied using ^1H NMR spectroscopy, and nitrophenyl ureas which contain the electron-withdrawing nitro functional group, and are amenable to study by UV-vis spectroscopy.

The reaction of **87** with 4-nitrophenyl isocyanate was initially attempted in dry CHCl_3 , using a small amount of DMF to solubilise the reaction mixture. This gave a bright yellow solid, which appeared to be a mixture of compounds, but which contained the desired, tetrasubstituted product, when analysed in $\text{DMSO}-d_6$ by ^1H NMR. However, quite like the starting hydrazide, the product of this reaction was insoluble in routine solvents (CH_2Cl_2 , CHCl_3 , EtOAc, EtOH, MeOH, CH_3CN), thus purification methods were limited. Reverse-phase preparative layer chromatography, for example was employed to attempt to purify this product. However, adsorption using DMF, followed by elution of the crude sample using CH_3OH on C-18 preparative-layer plates was unsuccessful. It was decided instead that an alternative approach to this reaction was required to enable isolation of these compounds.

The insolubility of 4-nitrophenyl isocyanate contrasts with the liquid nature of the analogous phenyl isocyanate. It was found that reaction of a suspension of hydrazide in

chloroform with phenyl isocyanate occurred by simply stirring overnight under an inert atmosphere. This gave a pearly suspension which was concentrated under reduced pressure, and to which excess methanol was added. Filtration, followed by methanol and water washes gave the desired product, requiring no further purification. To overcome the problem of insolubility of 4-nitrophenyl isocyanate in chloroform, it was found to be sufficient to dissolve four equivalents (for tetrahydrazide **87**) of this material in dry THF. This solution was then added, with stirring, to one equivalent of the hydrazide, also in THF, and the mixture was stirred at reflux overnight. The urea generally was seen to precipitate from solution once the reaction had run to completion. The workup procedure was simple, requiring concentration of the reaction solvent under reduced pressure, followed by addition of methanol. The solid urea was then collected by filtration. Where necessary, trituration of the product in hot methanol was found to be a satisfactory method of purifying the product.

This method, investigated for **125**, the *de*-^tBu analogue was then successfully applied to the ^tBu calixarene analogue **127** and to the disubstituted compound **128**. Attempts to purify the product of the reaction which hoped to yield the 1,3-alternate conformer were unsuccessful.



Scheme 4.3 – Formation of semicarbazide-containing calix[4]amidoureas; R = 4-nitrophenyl (**125**), phenyl (**126**)

A representative ¹H NMR spectrum of one of the tetrasubstituted ureas (**126**) prepared is shown in Figure 4.2, showing the *C*₄ symmetry of the compound and resultant simplicity. The ureas were found to be soluble only in polar aprotic organic solvents, such as DMSO and DMF, and attempts to prepare crystals for X-ray study were unsuccessful. Such insolubility may be attributed to strong intramolecular hydrogen bonds, which are accepted by the ureido carbonyl moiety. It was found that addition of anions to suspensions of these compounds led to their immediate solubilisation in a range of medium-to-high polarity

organic solvents, such as CH_2Cl_2 , THF, Et_2O and CH_3CN . It is believed that perturbation of this hydrogen-bonding motif by the anions is responsible for this effect. Böhmer has extensively reported the formation of capsules which, are present in solution, stabilised through their hydrogen bonding arrays.¹⁹⁰⁻¹⁹² We believe that a similar process of strong hydrogen bonding effects, are occurring in this case. Slow evaporation of the solutions containing anions led to the formation of oils.

These semicarbazide-based systems give rise to three environments of N-H proton, as shown in Scheme 4.3; those at the amide carbonyl (red), and those at the urea moiety (blue and green). The most downfield proton, shown in red will be referred to as the amide proton. Those of the urea moiety, shown in red and blue, it is believed, cooperate in anion binding. While it has been shown previously that the N-N bond of neutral hydrazines is twisted,¹⁹³ and that this twist serves as a conjugation stopper,¹⁹⁴ the methylene group of calix[4]arene serves as a natural conjugation stopper, and as such the electronic properties of the calix[4]arene core are not expected to be perturbed upon anion binding.

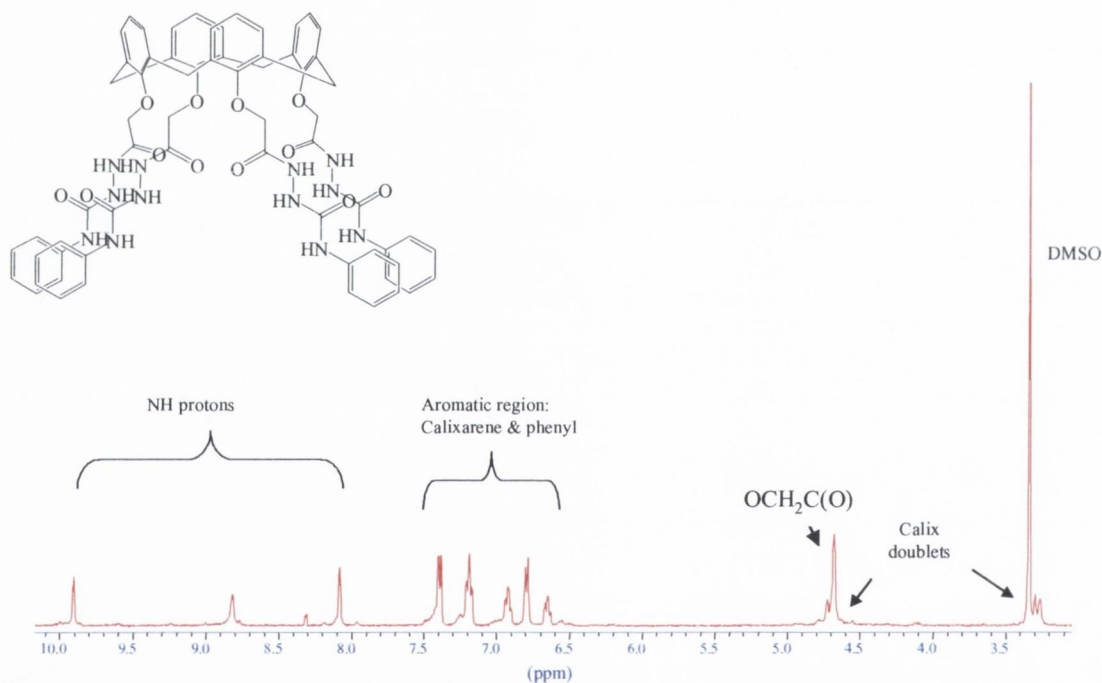
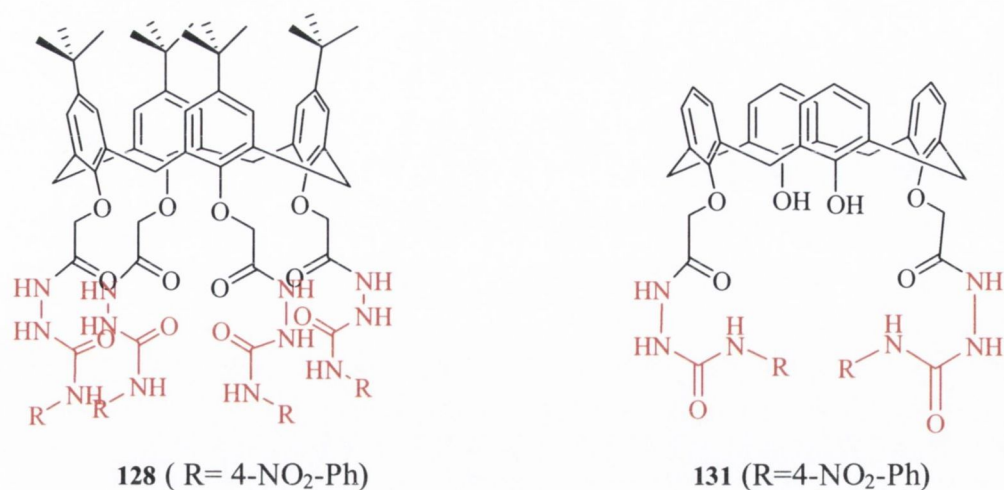


Figure 4.2 – ^1H NMR spectrum of tetraphenylurea **126** recorded in $\text{DMSO-}d_6$ (400 MHz)

The analogues which were synthesised from the t -butyl tetrahydrazide (**127**) and the 1,3-disubstituted hydrazide (**130**, synthesised from 1,3-diester **129**) respectively are shown below.



In addition to the preparation of derivatives in the cone conformation, it was intended also to investigate the 1,3-alternate conformation. This was undertaken as it would provide the host with inherent potential for allostery; either positive or negative. Binding could then occur at two separate identical binding sites, rather than the convergent binding which is anticipated in the cone conformation. However, upon recognition of an anion at one site, the geometry of the second site may change to provide a different recognition environment. This is outlined in cartoon format in Figure 4.3.

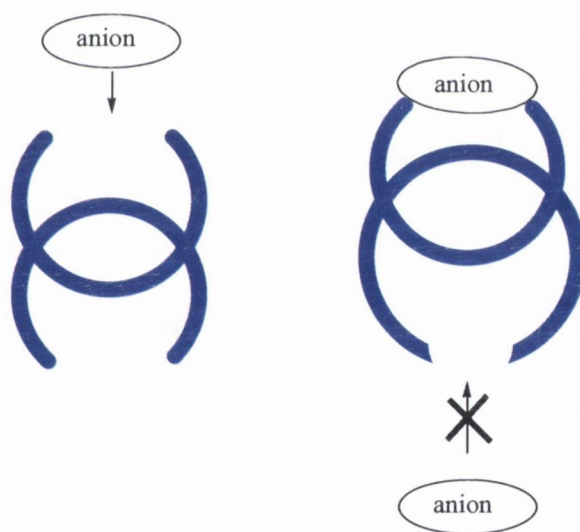
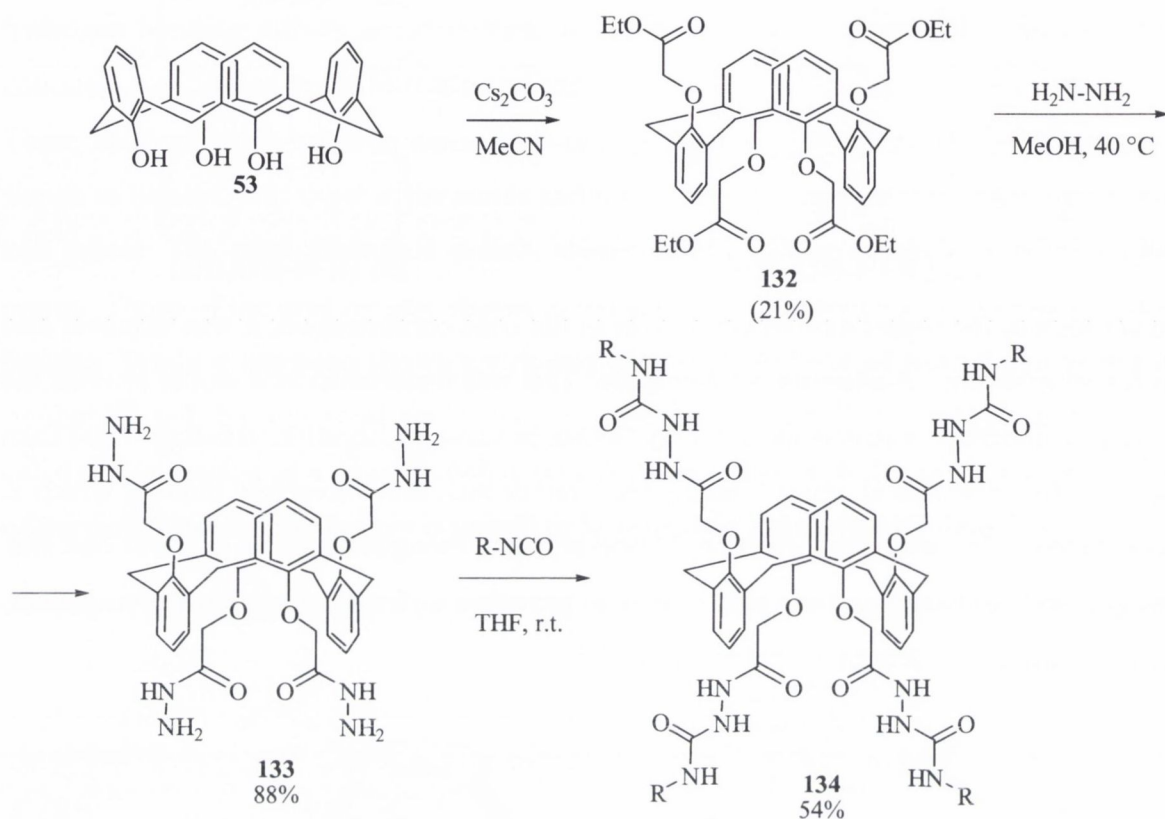


Figure 4.3– Potential negative allosteric inhibition of second binding event; a possible outcome in calix[4]arene-based anion receptor in 1,3-*alt* conformation.

The desired tetraphenyl urea was synthetically accessible from the 1,3-*alt* tetraester, which was formed by alkylation of calix[4]arene with ethyl bromoacetate in the presence of the larger base, caesium carbonate.¹⁹⁵ This was subjected to aminolysis with hydrazine hydrate to furnish the desired hydrazide, which was subsequently treated with 4-nitrophenyl or phenyl isocyanate. This synthetic pathway is outlined in Scheme 4.4. As already noted, this

reaction was not successful for the 4-nitrophenyl analogue. In the case of the phenyl urea, however, the reaction proceeded to completion. As discussed in Chapter 1, the conformation of calix[4]arenes can easily be determined by examination of the signals for the bridging methylene protons.



Scheme 4.4 - Formation of ureas in 1,3-*alt* conformation, where R = Phenyl

The ¹H NMR (400 MHz) spectra for the 1,3-*alt* tetraester (CDCl₃), 1,3-*alt* tetrahydrazide (DMSO-*d*₆) and the 1,3-*alt* tetra phenyl urea (DMSO-*d*₆), 134 are shown in Figure 4.4. The bridging methylene protons are now represented by a singlet, rather than two doublets seen for the cone conformation which has been extensively evidenced in Chapters 2 and 3. This is because both protons of the methylene bridge now point away from the annulus, with no *exo-endo*-differentiating environments. This is seen for the ester and holds true for both the hydrazine and urea, indicating no change in conformation upon further derivatisation. This is as expected as the substituents are sufficiently bulky to impede rotation of the *O*-functionality through the annulus.

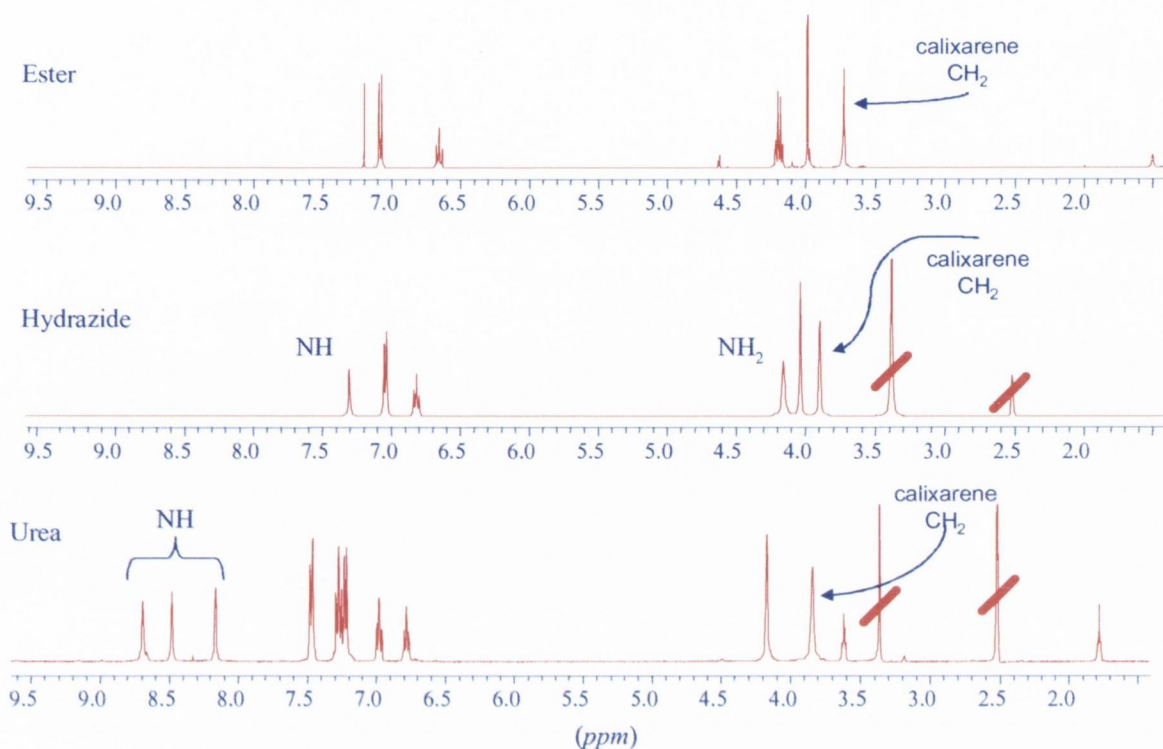


Figure 4.4 - ^1H NMR spectra (400 MHz, CDCl_3 (ester); $\text{DMSO}-d_6$ (hydrazide, urea)) of the reaction stages in 1,3-*alt* conformations leading to 1,3-alternate urea **134** (ethyl CH_3 at 1.26 ppm of ester moiety omitted).

The appearance of three sharp singlets at 8.89, 8.48 and 8.16 ppm in the downfield region, corresponding to the NH protons is a feature which is common to all the ureas that have been synthesised in this study. It is these protons which we propose that participate in hydrogen bonding with anionic guests.

Once these compounds had successfully been prepared, and satisfactorily characterised, a preliminary method of assessment of their affinities towards some anions was conducted. An efficient and expedient method of analysis of these potential binding interactions is by ^1H NMR shift titration, where change in ^1H NMR resonances of significance on the host is monitored as a function of added guest, and from resonance changes, thermodynamic data can be derived.

4.3 Determination of binding constants, K

Binding constants are the equilibrium constants, K , of the reaction between a host and guest, for example **125** and an anion, as seen in Equation 4.1 for a 1:1 binding equilibrium, followed by the corresponding K_2 , seen upon complexation of a second anion (Equation 4.2).



where K_1 and K_2 represent the stepwise binding constants, as seen in Equations 4.3 and 4.4

$$K_1 = \frac{[\text{HA}^-]}{[\text{H}][\text{A}^-]} \quad \text{Equation 4.3}$$

$$K_2 = \frac{[\text{A}_2\text{H}^{2-}]}{[\text{HA}^-][\text{A}^-]} \quad \text{Equation 4.4}$$

The overall equilibrium constant, β , can also be determined (Equation 4.5). This is the product of the stepwise formation constants of K_1 and K_2 (Equation 4.6).



$$\beta_2 = \frac{[\text{A}_2\text{H}^{2-}]}{[\text{A}^-]^2 [\text{H}]} = K_1 \cdot K_2 \quad \text{Equation 4.6}$$

$$\therefore \log \beta_2 = \log K_1 + \log K_2 \quad \text{Equation 4.7}$$

For dynamic processes such as binding equilibria, equilibrium constants are determined by fitting of the acquired data to a model, by a process of non-linear, least-squares regression analysis. SPECFIT, a commercially available software package, was used to manipulate titration data which were obtained by absorption spectroscopy.¹⁹⁶ SPECFIT fits experimental data, from absorbance (or emission) measurements to a global model, where multiple datasets, which share common parameters are simultaneously fitted. This operation yields binding constant data as cumulative $\log \beta$ values (shown for a 1:2 binding equilibrium in Equation 4.7). By subtraction of successive $\log \beta$ values for a multistep equilibrium, $\log K$ for the respective binding events may be evaluated.

SPECFIT cannot accurately fit data when individual $K \geq 10^7 \text{ dm}^3 \text{ mol}^{-1}$, because, at equilibrium, the ratio of the guest-anion complex ion concentration to that of the

precursors, becomes large, and consequently, the overall error in the determined K becomes prohibitively excessive.

For purposes of data treatment herein, equilibrium constants will be reported as $\log K$. WinEQNMR was used to fit NMR data,¹⁹⁷ which, when fitted are also reported as $\log K$ values.

4.4 Assessment of anion binding affinity by ¹H NMR methods

As stated above, by monitoring the change of the resonance of proton(s) of interest of a host, as a function of equivalents of added guest, it is possible to obtain information about the solution equilibrium between host and guest. This is formally done as NMR shift titration. In carrying out such an NMR titration, small aliquots of a solution containing a guest are added to an NMR tube containing a solution of the host. A ¹H NMR spectrum is acquired after each addition. It is expected that once saturation of guest has occurred, there will be no further change in the host's binding proton shift and that the binding isotherm can be established.

In general, anion titrations, including the ¹H NMR method are carried out using bulky cations, to prevent any counterion interactions, thus preventing electrostatic interaction, and allowing anions to be free in solution for binding to the host. These studies were conducted using dry tetrabutylammonium (TBA) salts of the desired guests.

It was decided that **126** would be used to initially screen anions by the NMR technique. This is because it offers a simple, convergent array of urea moieties, which are phenyl substituted. The ¹H NMR spectrum of **126** in DMSO-*d*₆ was recorded at room temperature (insolubility of the host precludes measurement in less protic solvents), and the positions of the hydrazine proton and the two urea protons were examined. It is expected that the urea protons would certainly participate in hydrogen bonding to a guest anion. The role of the amide protons at this point was still uncertain. To **126** was then added solutions containing excesses chloride and nitrate. These were chosen for their differing geometries. Chloride is spherical, while nitrate has a more complex geometry of trigonal planarity. The ¹H spectra that resulted are shown in Figure 4.5.

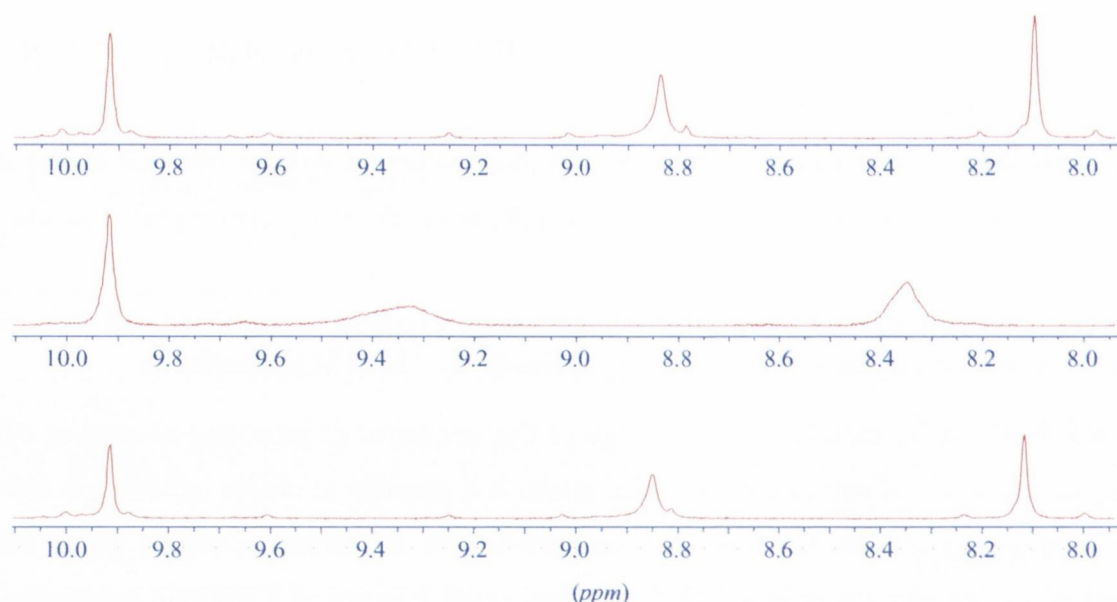


Figure 4.5 – ^1H NMR spectra of NH protons of **126** in presence of excesses of different anionic guests; 1: U1, 2: U1 + Cl^- ; 3: U1 + NO_3^- (anions delivered as TBA salts)

As can be seen from the spectra, there is a significant change in both urea proton resonances upon addition of TBA chloride. There is, however no change in any of the signals when TBA nitrate is added. On the basis of this result, it was decided to perform a full ^1H NMR shift titration on host **126** using Cl^- . From this preliminary result, it can be concluded that the downfield amide proton is not involved in the binding process. Even in the presence of excess chloride, it is not seen to change.

4.4.1 ^1H NMR titration of **126** with TBACl

As mentioned previously, the NMR titration technique involves addition of small aliquots of guest to a tube containing the host. This is typically done such that 2 mg of host in 800 μL of deuterated NMR solvent in the NMR tube can be gradually titrated against 5 μL volumes of a solution of guest, which has been prepared to contain 0.1 equiv. of the anion guest in each addition.

When this was attempted using **126**, the results did not concur with the preliminary measurement discussed above. Unlike the shift change seen above for the downfield urea proton of approximately 0.5 ppm, the successive addition of guest equivalents was accompanied by cumulative shift change of only 0.14 ppm. For the more upfield urea proton H_1 , a change of approx. 0.25 ppm contrasts with the more precisely measured cumulative shift change of 0.08 ppm. This change is significantly smaller than that previously observed, and may be attributed to the addition of the anion as a stock solution,

rather than its solid form as in the preliminary measurement. The overall magnitude of the change is usually insignificant. Of interest is the rate of change, with respect to added guest at which this change occurs. The change in proton H₂ (downfield) is shown in Figure 4.6.

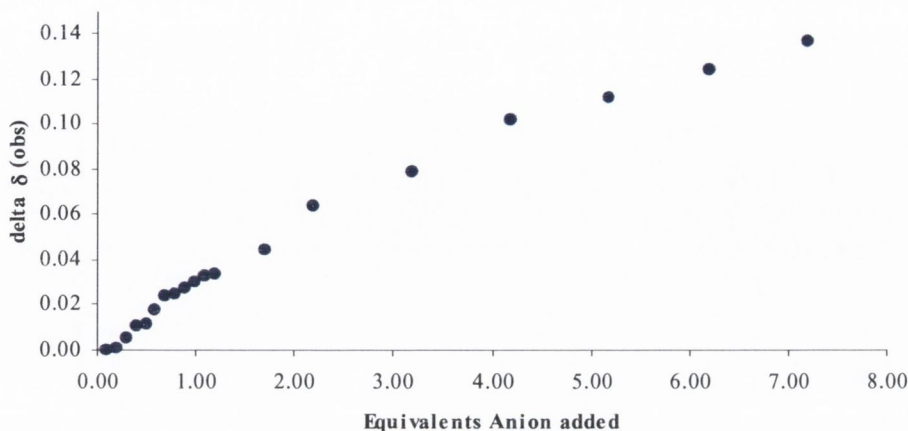


Figure 4.6 - ¹H NMR (400 MHz, DMSO-*d*₆) titration of **126** with Cl⁻ (observing H₂)

Despite seeing a minor inflection at approximately 1.2 equivalents, the trend appears to continue in a roughly linear fashion beyond seven equivalents. It is possible that no binding is occurring, and that the small shift change may be attributed to the change of dielectric constant of the solvent incurred by addition of the TBA solute. More precise conclusions could only be drawn following further measurements, for example, by using UV-vis titrations, which will be discussed in Section 4.8.

4.4.2 NMR titration of **126** with dihydrogenphosphate

The tetrahedral nature of the phosphate anion, as discussed in Chapter 1 is of interest to us, given the size and shapes of the cavities formed by these compounds. Phosphate receptors based on both a charged and a neutral calix[4]arene platform have been reported. In most cases, moderately weak binding associations have been reported.

As described above for Cl⁻, titration on **126** using TBA.H₂PO₄ was undertaken. Upon successive additions of aliquots of a solution of TBA H₂PO₄⁻ to **126**, the proton resonances shifted, indicating binding of the anions to the urea protons. The change in shift of urea proton H-2 is shown in Figure 4.7.

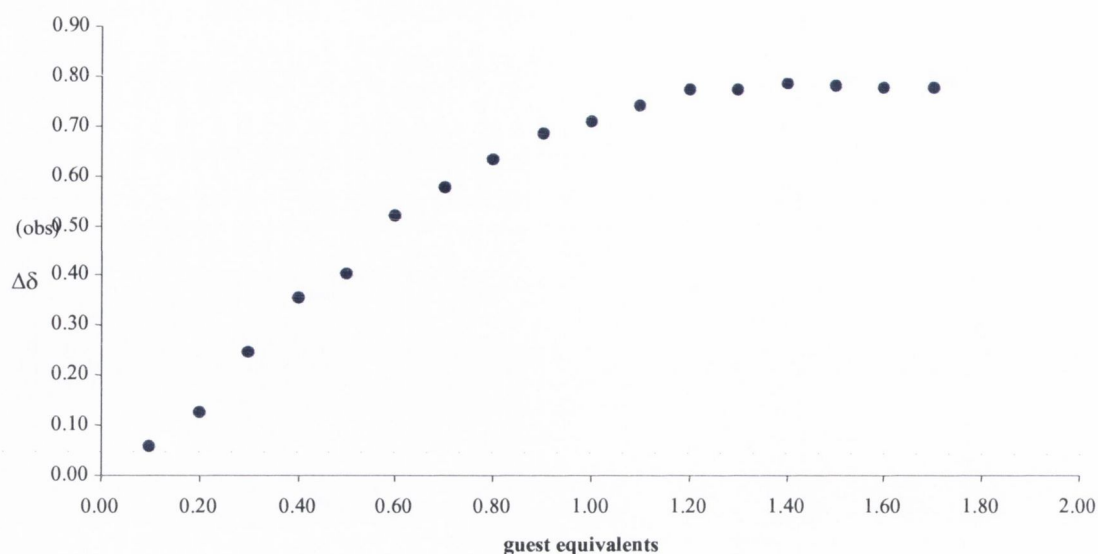


Figure 4.7 - ^1H NMR titration of **126** with H_2PO_4^- ; H-2 proton observed

As seen from Figure 4.7, $\Delta\delta$ of H-2 stabilises at approximately 1 equivalent of added H_2PO_4^- anion, which indicates that the compound is binding one of these anions in a 1:1 host-guest relationship. This is as expected, due to the bulky size and charge distribution of phosphate. The data obtained (change in ^1H shift v. amount of guest added) were processed using WinEQNMR, which calculates equilibrium constants based on NMR shift data.¹⁹⁷ Fitting of the data gave binding constant data of $K = 1 \times 10^4 \pm 4 \times 10^3$. The isotherm and fit as generated using WinEQNMR is shown in Figure 4.8. This binding constant comes with an exceptionally large error of >40%, which is beyond the 15% error margin of the technique, as estimated by Gale.¹⁹⁸

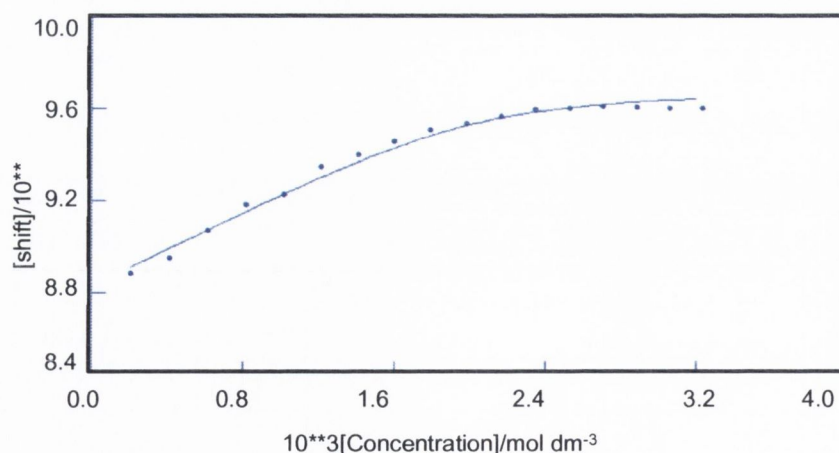


Figure 4.8 - Binding isotherm and fit of ^1H NMR titration of **126** with $\text{TBA}\cdot\text{H}_2\text{PO}_4^-$ in DMSO-d_6 , obtained using WinEQNMR.¹⁹⁷

4.4.3 ^1H NMR titration of **125** with hydrogenpyrophosphate

A titration was undertaken with 4-nitrophenyl-containing host, **125** using TBA pyrophosphate as guest, in $\text{DMSO-}d_6$. Upon addition of 0.1 equiv. guest to the host, the NH resonances appeared to quickly lose resolution. This situation deteriorated through the titration, and therefore no signal could be successfully used to track the changes which were occurring upon binding. A more sensitive technique was therefore sought for this binding study. The next sections will detail the use of UV-Vis spectrophotometry to account for anion-binding interactions.

4.5 Study of anion binding by UV-Vis titration

The NMR titration technique is a useful method of analysis owing to the sensitivity of proton NMR, and its ability to study a wide range of processes and reactions, since the principal requirement is simply the presence of protons. NMR titrations are however, not without fault. It is reported that it is an inefficient method of studying complex equilibria, that is equilibria with >2 states.¹⁹⁷ In addition, errors are inherently large, owing to high signal-to-noise ratios in NMR spectra. As the hosts under study are large, with potential for multiple binding sites, we decided to focus our attention on a more sensitive spectroscopic technique. The presence of the nitrophenyl moieties in the ureas under study allows for this chromophore to be readily observed by UV-vis spectroscopy, and for this to be used as a reporting unit for the anion-binding activity.

4.5.1 UV spectroscopy and the Beer-Lambert law

UV-visible absorption spectroscopy involves measuring electronic transitions that occur when a sample of an analyte is irradiated with light, of a spectrum across the UV and visible regions. When a sample is exposed to light, some is absorbed by the sample, while some passes through. The ratio of the intensity of the light to which the sample is exposed, and the light which passes through, is called transmittance, I/I_0 . Deviance of this value from a value of 1 or 100% (complete transmission) is described by the Beer-Lambert law, which essentially relates concentration of sample to the light absorbed. It is shown in Equation 4.8.

$$-\log_{10} \frac{I}{I_0} = A = \epsilon.c.l \quad \text{Equation 4.8}$$

Where:

A is the absorbance, ϵ is termed the extinction, or absorption coefficient, at a given wavelength, this value is independent of sample concentration or size and carries the unit $\text{cm}^{-1} \text{dm}^3 \text{mol}^{-1}$, or $\text{cm}^{-1} \text{M}^{-1}$. c is concentration, in moles per litre, and l is the length of the sample in centimetres. Absorbance is stated without a unit.

Due to the linear relationship between concentration and absorbance, it follows that the concentration of a solute at any particular absorbance can readily be determined, once the extinction coefficient has been established. The implication of this is that changes in absorbance reflect changes in concentration, thus allowing equilibria between species to be studied.

UV-Vis spectroscopy allows for the study and accounting of stoichiometric states. Where two spectra, that of a host and a host-guest complex overlap, the crossover point is termed the isosbestic point. The presence of isosbestic points can be used to provide elementary information about the equilibrium. A single isosbestic point, observed over a wide range of composition, will indicate two states; starting state and product state. Where no isosbestic point is observed, or the isosbestic point is seen to shift in either intensity or wavelength, this can be interpreted as evidence of presence of a more complex equilibrium.^{199,200}

In contrast to NMR methods, UV-vis spectroscopy is a more sensitive technique, with detection limits of approximately 10^{-8} or $10^{-9} \text{ g mL}^{-1}$, compared to NMR with routine experiments having a much greater limit of detection at approximately $10^{-3} \text{ g mL}^{-1}$. UV-vis is also capable of studying fast exchange processes, due to the timescale of the process (transitions take $\sim 10^{-15} \text{ s}$), compared to NMR which is slow (10^{-2} s) technique.

4.5.2 UV-Vis Titration of **125** with anionic guests

Ureas such as the tetrasubstituted **125** and disubstituted **128** contain nitrophenyl moieties which have a significant absorption band at approximately 340 nm. In addition, the electron withdrawing effect of the nitrophenyl group increases the acidity of the urea protons. This makes this proton more likely to accept electron density, thus increasing the overall affinity of the system towards anions – this effect is illustrated in Figure 4.9.

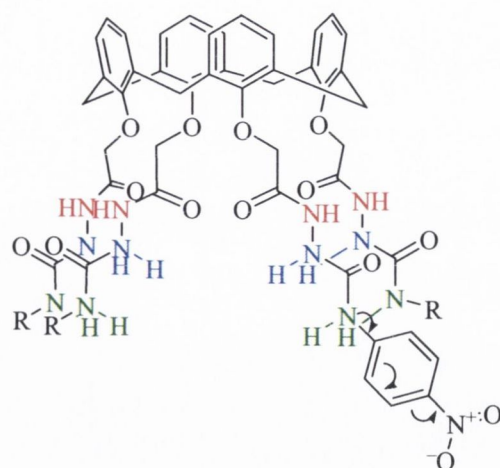


Figure 4.9 - Electron withdrawal effect on urea acidity

The initial interest was to exploit this strong visible absorption as a potential naked-eye colorimetric sensor. This would manifest itself as a compound which upon addition of a guest presents a colour change which can be seen by the human eye, without the use of further instrumentation or detection apparatus. Addition of excess guest to a DMSO solution (10^{-3} M) of **125**, for example showed an immediate colour intensity change. This is shown in Figure 4.10 for a variety of anionic guests (delivered as their TBA salts).



Figure 4.10 - Colorimetric effect upon addition of excess TBA salts of anions to DMSO solutions ($\sim 10^{-3}$ M) of **125**; left to right: free host, F^- , Cl^- , $H_2PO_4^-$, $HP_2O_7^{3-}$, AcO^- and NO_3^-

With evidence of such significant changes, in particular the striking colorimetric responses exhibited by fluoride and pyrophosphate, in addition to the substantial colour change seen in the case of acetate, it was decided to quantify the relationship between absorption of the nitrophenyl moiety and the presence of anionic guests. Use of chloride and nitrate allowed rapid assessment of both spherical and trigonal planar anions to be made; in both cases no colour change was observed.

UV-vis titrations were carried out by addition of aliquots of guest to a solution of known concentration of host, as for the NMR method. For UV-Vis application, this concentration is typically between 10^{-5} and 10^{-6} . In the case of **125**, its extinction coefficient was determined at 377 nm to be $66346 \text{ M}^{-1}\text{cm}^{-1}$. Initial assessment of titration data was

undertaken by simply examining the overall absorbance changes as the guest was added. Secondly, the absorbance at certain wavelengths was plotted as a function of the concentration and, or equivalents of guest added, to give the binding isotherm. In each case, a slow increase in absorbance was observed over the first several equivalents of guest, eventually stabilising to a plateau once guest saturation had been achieved.

In the case of dihydrogenphosphate, over the course of the titration, the samples gave a slight naked-eye response; the colour change from colourless to a pale straw yellow, as observed qualitatively above in Figure 4.11 This trend was observed for each of the other analytes (pyrophosphate, chloride, acetate) – leading to a conclusion that the colorimetric response was only to be observed at high concentrations of guest.

The UV-vis spectra of the titration **125** with TBA H_2PO_4^- are shown in Figure 4.11.

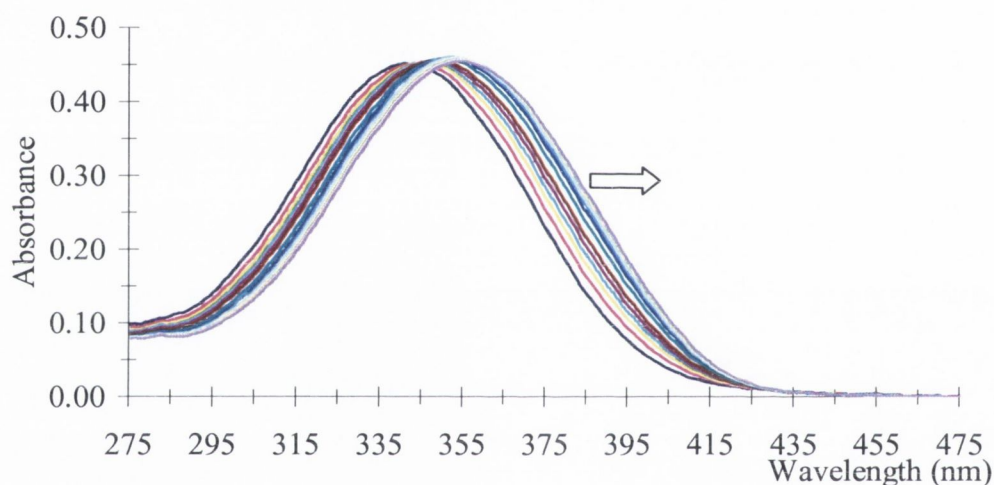


Figure 4.11 - Absorbance spectra observed on titration of **125** with H_2PO_4^- in DMSO

As can be clearly seen, there is red shift (bathochromic shift) of 12 nm. The system lacks a distinct isobestic point, indicating a possibility that there may be a more complex equilibrium than the 1:1 host-guest relationship. The binding isotherm which was extracted from this change is shown in Figure 4.12 A plateau is observed at higher equivalents of anion (>5) than expected for saturation.

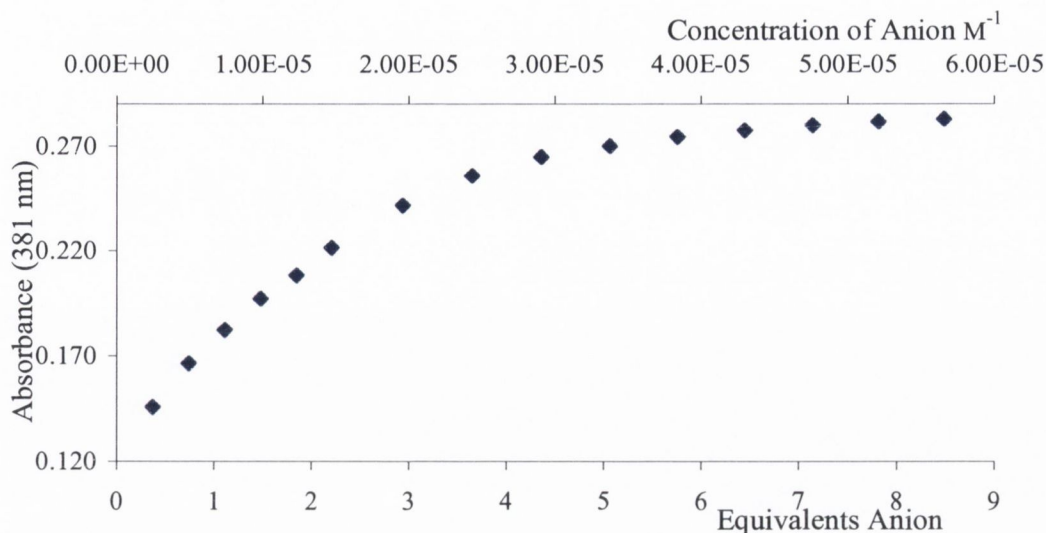


Figure 4.12 - Change in absorbance of **125** at 381 nm upon addition of dihydrogenphosphate – Equivalents of dihydrogenphosphate are shown on the X-axis, concentration of dihydrogenphosphate is shown as a secondary (upper) X-axis.

Secondly, the changes in absorbance was assessed against $-\log_{10}[\text{guest}]$, as shown in Figure 4.13. The relevance of this analysis of data is that it allows a prediction of the binding stoichiometry to be carried out.¹⁹⁹

When the change in absorbance takes place over two log units, it can be inferred that there is a 1:1 binding stoichiometry. However, the established route to determination of the absolute stoichiometry of a host-guest equilibrium is by the method of continuous variation (to construct a Job's plot), which will be discussed in detail in Section 4.5.3. An alternative method of elucidation of complex stoichiometry is by the use of electrospray mass spectrometry. Use of this technique will be discussed in Section 4.6.

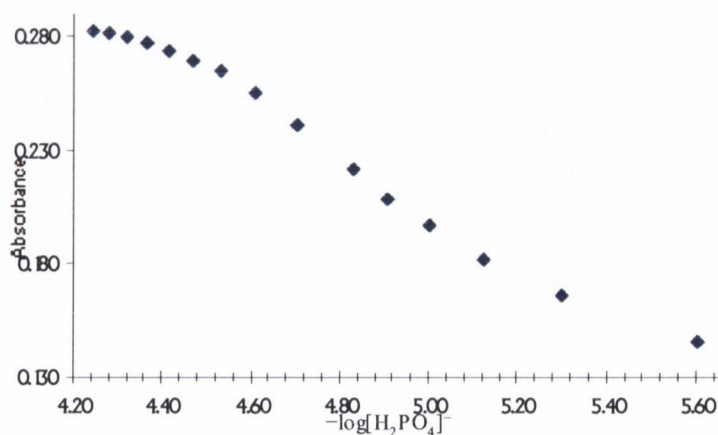


Figure 4.13 - $-\log[\text{anion}]$ v absorbance plot for titration of **125** with dihydrogenphosphate

Once the stoichiometry has been determined, it is then possible to fit the data to an equilibrium model, using SPECFIT. While the fit can be adjusted to account for variation of multiple conditions, including pH and temperature, these parameters were kept constant, performing titrations at 25 °C in DMSO.

Binding constants, $\log \beta$, were determined for each titration that was carried out, and the measurements repeated until a satisfactory repeatability was determined. In accordance with a method reported by Sessler²⁰¹, it was decided to perform titrations within the UV-vis quartz cell. This involved an initial host volume of only 2 mL, and additions were made by means of a microsyringe; aliquots of 2-10 μL . To avoid the loss of any volume that may occur upon mixing, the cell was equipped with a magnetic stirrer bar to ensure mixing of host and guest. Upon each addition of guest, the mixture was allowed to stir for 30 seconds, achieving sample homogeneity before the spectrum was recorded. Stirring was stopped while the spectrum was being acquired, as DMSO is viscous and motion of the solvent and its solutes may cause undesirable noise and inhomogeneity in the spectrum. The binding constants obtained using this method were consistent with those obtained in preliminary measurements, which had been undertaken with mixing performed outside of the cell. However, with the standard deviations reduced from between 0.30 and 0.50, to between $\pm 0.01 - 0.04$, mixing of the solutions within the UV-vis cell, which reduced experimental error, was adopted for all subsequent titrations.

In the titration of **125** with dihydrogenphosphate, the binding data as determined using SPECFIT are shown.

Host	Guest	Method	$\text{Log}K_{11}$	$\text{Log}K_{12}$
125	H_2PO_4^-	UV-vis	5.459 ± 0.174	4.869 ± 0.355

The model to which the data have been fitted is presented alongside the binding isotherm in Figure 4.14 showing very strong agreement between data and fit. A plateau is observed at a guest concentration around 3.5×10^{-5} M, this corresponds to approximately six equivalents of anion. While this appears high, it is significantly lower than the point at which saturation is achieved for most of these studies.

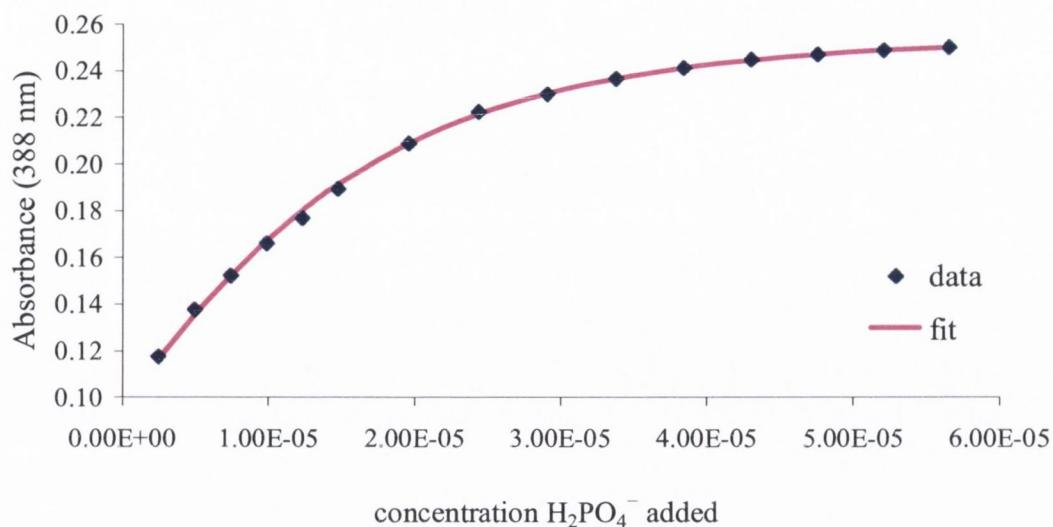


Figure 4.14 – Binding isotherm with fit of titration of **125** with TBA H_2PO_4^- ; $[\text{U}2]_0 = 6.690 \times 10^{-6} \text{ M}$

Further information about a binding equilibrium may be obtained from the speciation plot, which is extracted from SPECFIT data. This is shown in Figure 4.15.

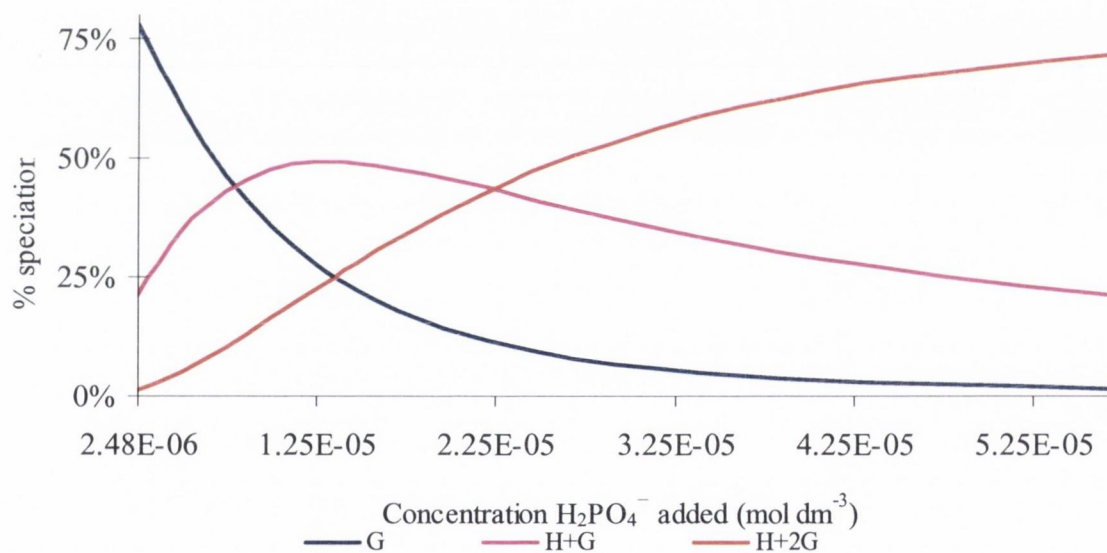
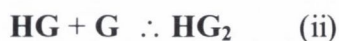


Figure 4.15 - Speciation plot showing composition of titration of **125** with H_2PO_4^-

The speciation plot is a graph wherein the percentage of a constituent of the reaction equilibria is shown as a function of the concentration of added guest. For example, this equilibrium can be represented using the following two-step equilibrium.



The speciation plot for this system indicates the percentage of **H**, **HG**, and **HG₂** which have been formed at any particular concentration of **G**. It is clear that the complex with 1:1

stoichiometry is formed immediately, but this is readily being converted to HG_2 , even at very low concentration of **HG** and **G**. As such, HG_2 is seen to clearly dominate the reaction equilibrium, comprising 78% of the total composition once equilibrium has been reached. Speciation data proves to be of great interest as it allows the assignment of dominant equilibria, and therefore species, in a complex equilibrium system such as this.

The procedure was repeated for several anions, and the data were fitted using SPECFIT. The binding constants which were obtained are shown in Table 4.1. Full titration data, including UV-vis spectra, binding isotherms with corresponding fitting and speciation plots are included in Appendix 2.

Table 4.1 - Binding constants (expressed as $\log K$) obtained for **125** by UV-Vis titration in DMSO, against guests shown; 1:1 stoichiometry as M^{-1} , 1:2; 2:1 stoichiometry as M^{-2} . Values are quoted with standard deviations. Data were processed using SPECFIT.

	1:1 stoichiometry	2:1 (guest to host) stoichiometry
H_2PO_4^-	5.45 ± 0.17	4.84 ± 0.35 (HG_2)
<i>Pyr</i>	5.34 ± 0.04	-
Cl^-	n.d.	-
AcO^-	5.10 ± 0.04	4.29 ± 0.12 (HG_2)
F^-	5.68 ± 0.20	4.79 ± 0.39 (HG_2)
Br^-	4.15 ± 0.05	-

As can clearly be seen from these binding constants, there exists strong binding between each of these guests with host **125**. In the case of chloride, however, a binding isotherm was extracted, but this could not suitably be fitted to a model. It is possible that the binding value may lie between that observed for smaller and larger halides fluoride and bromide respectively. These titrations and the corresponding binding constants reveal that the cavity can strongly accommodate not only spherical halides, but also oxoanions H_2PO_4^- , pyrophosphate and acetate. Each of the oxoanions had a similar binding constant for the formation of 1:1 complexes (within standard deviation).

4.5.3 Determination of host-guest complex stoichiometry

As can be clearly seen from Table 1, there exists the potential for multiple binding equilibria for many of these systems. While binding equilibrium analysis software such as SPECFIT provides insight into the speciation and complexation equilibria that may be

occurring in a host-guest interaction, this is based on fitting the experimental data to a theoretical model. It is therefore desirable to experimentally determine the stoichiometry of the host-guest complex before accepting binding constants beyond the simple 1:1 ratio. The experimental method that is used to determine reaction stoichiometry is called Job's method, which is a method of continuous variation.

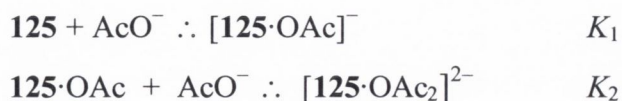
For the equilibrium shown in Equation 4.9 for example, there exists in solution at any point different concentrations of host, guest and the host-guest complexation product. In the course of a titration, this is referred to as speciation, as has been shown in the SPECFIT-derived speciation plots in Sections 4.5.2.



Job's method (which culminates in a "Job plot") requires there to be present, across a range of solutions of different mole fractions, the same number of combined moles of host and guest. This means that the combined number of moles of host and guest must remain constant over a range of samples containing increasing H, and decreasing G, or *vice versa* ($n_{\text{H}} + n_{\text{G}} = k$).

Once the ratio of H to G in the sample has passed the stoichiometric ratio, the amount of either H or G will then be limiting, and no further complex can be formed. In addition, once past the stoichiometric ratio, the amount of either reagent is decreasing (due to the initial condition of keeping $n_{\text{H}} + n_{\text{G}}$ constant). This leads to a decline in the formation of complex HG, rather than a plateau which is observed in simple binding isotherms. The result of this method therefore, is that a maximum of complex is observed at the stoichiometric point. As a method of observing the amount of complex formed, appropriate absorbance or other spectroscopic data may be used; we chose to determine the stoichiometry by UV-vis spectroscopy.

In the case of the binding of acetate by **125**, two complexes have been hypothesised: HG, and HG₂. These are represented by the following equilibria:



The values of K_1 and K_2 are derived from titration measurements, and in this case $\log K_1$ was shown to be 5.10 ± 0.04 , and $\log K_2$ to be 4.29 ± 0.12 . Due to the strong colorimetric response, changing from pale straw to deep yellow, expressed by **125** in the presence of

acetate, we were keen to establish more data supporting this complex. This therefore, became the first candidate for determination of stoichiometry. Eleven absorbance measurements were made at 0.0, 0.1, 0.2, 0.3, 0.4, 0.5, 0.6, 0.7, 0.8, 0.9 and 1.0 mole fractions (χ_H , where $\chi_H = [H]/[H]+[G]$) of host, with the remainder of the mole fraction as guest. When absorbances of each of the solutions were determined and plotted against mole fraction, a roughly linear relationship was observed. This was re-plotted at several wavelengths. This is shown in Figure 4.16.

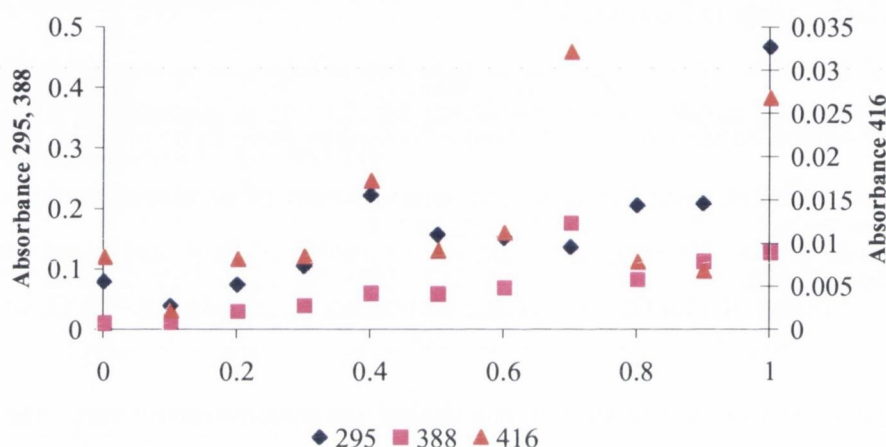


Figure 4.16 – Attempted Job plot for binding by **125** of acetate, as determined by UV-vis spectroscopy, no clear peak can be discerned at any of the wavelengths shown

From this measurement, no useful information regarding the binding states can be obtained. A similarly unsuccessful Job plot was obtained in the case of **125** with pyrophosphate. It is possible that this is due to the fact that both binding constants for each of the equilibria are close (within one order of magnitude). This presents a limitation on the method meaning that it should be adopted for relatively simple systems. No further attempts to determine stoichiometry by Job's method were undertaken.

A further method which would have provided crucial insight into the binding mode is X-ray crystallography. Solid state evidence of a host-guest complex is indisputable, and thus is highly desirable. Several attempts to grow crystals of the complexes were made, varying solvents and concentration of host and guest. The host-guest complexes were found to be soluble in a number of organic solvents (as opposed to the host, **125** which is soluble only in non-volatile, polar solvents such as DMSO). Evaporation of solutions containing combined host and guest in CH_3CN , CH_2Cl_2 and CHCl_3 gave, on all occasions, oils.

In assessing potential binding modes and stoichiometries, it came clear that substituents appended to the lower rim may also have the option of *endo*- or *exo*- binding, that is, that the binding can take place within the cavity formed, or outside this cavity, following free rotation in solution of the urea moieties. The difference between *endo*- and *exo*- binding sites is outlined in Figure 4.17. The existence of these modes or indeed a mixture of both types of binding may possibly lead to unexpected stoichiometry.

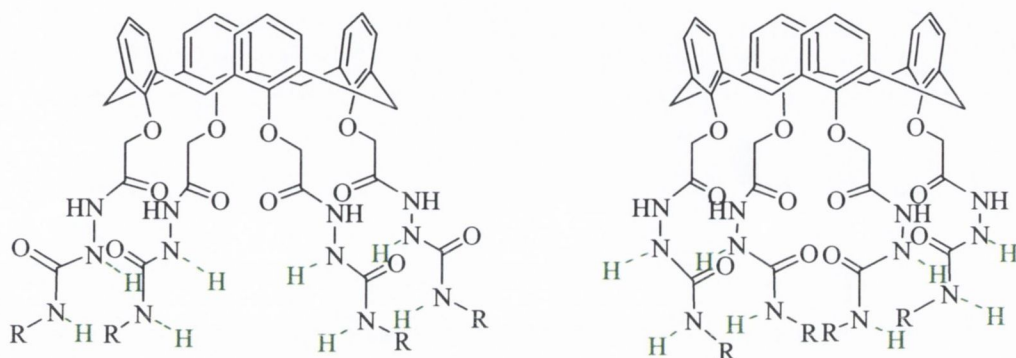


Figure 4.17 – *Endo*- and *exo*- (indicated in green) binding sites which may occur in calix[4]arenes such as **125** (R = 4-nitrophenyl)

The *endo*- binding array, where the anions are encapsulated by the cooperation of all urea moieties, is both the intuitive and the desirable conformation in light of the inherent rigidity of calix[4]arenes. This would provide us with a convergent anion binding array, offering eight ureido protons for anion binding; the participation of amido NH moieties would not be anticipated. However, the *exo*- binding mode may also lead to strong binding of anions, where the calixarene scaffold would merely provide several, non-cooperative binding sites. *Exo*-binding may also provide a contribution from the amido protons. There exists also an upper cavity with amido carbonyls, which have been shown to have great affinity towards small alkali metals (sodium, potassium). This gives rise to the potential for a ditopic receptor. Such a receptor was investigated and will be discussed in the following section.

4.5.4 A potential ditopic receptor for sodium halides²⁰²

Calix[4]arenes have gained much of their appraisal as host molecules from the study of their interaction with alkali metals, most typically Na⁺ and K⁺. As discussed in Chapter 1, alkali metals are bound tightly in the cavity of lower-rim ester and amide substituted species. The calix[4]hydrazides, and the subsequently prepared ureido calixarenes generated in this work retain this motif. It was decided to assess the potential for binding

sodium cations in the “upper cavity” while an anion or anions could then be sequestered by the “lower cavity”. This is shown schematically in Figure 4.18.

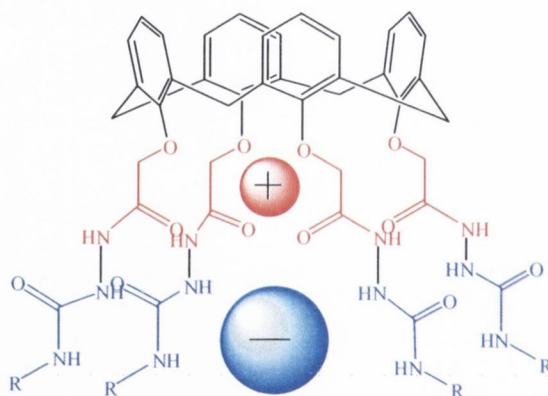


Figure 4.18 – Potential ditopic receptor based on calix[4]arene-based hydrazine urea. The cation -binding motif is coloured red, and the anion binding sites are coloured blue

As the cation must enter the cavity through the lower of the two cavities, it must be in place prior to the addition of anion. It is also hoped that the presence of the cation, such as Na^+ , in the upper cavity will cause preorganisation of the lower substituents (the anion-binding urea moieties). The presence of a positive charge in the host may also assist interaction with an anionic guest by electrostatic interaction.

Titration were undertaken for both Cl^- and Br^- , in the presence of one equivalent of Na^+ . The UV-vis spectra obtained for the Cl^- titration are shown in Figure 4.19.

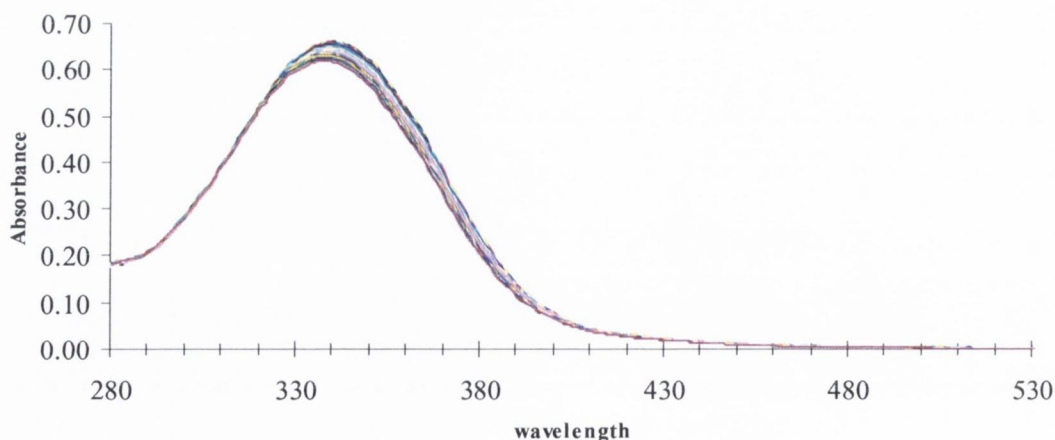


Figure 4.19 - UV-vis spectra obtained for titration of **125** with Cl^- in the presence of 1 equiv. Na^+ (as PF_6^-)

The red shift which is observed is small at 3 nm, and overall hypochromic changes are weak. The extraction of a binding isotherm from these data is difficult. However, fitting of the data with SPECFIT gave a $\log K$ value 4.49 ± 0.15 . This value is not believed to

represent any enhancement over the binding seen without Na^+ (which could not be fitted). When repeated for bromide, a similar spherical, though larger halide, a small shift was again observed. To this binding event, an equilibrium constant $\log K$ of 4.42 ± 0.24 was fitted. Within the standard deviation, this does not represent enhanced binding over the receptor **U2** to Br^- in the absence of Na^+ ($\log K = 4.15$). It can therefore be concluded that Na^+ does not provide enhancement to anion binding either through inducement of preorganisation, or by the introduction of charge to the otherwise neutral anion receptor.

4.5.5 Study of 1,3-disubstituted receptor **131**

As promising results were obtained in the case of **125**, it was postulated on the basis of data-fitting that the strong 1:2 host to guest (for acetate) binding is due to the guest binding to two proximal moieties. To further establish evidence of binding modes, we felt it was necessary to study binding by the 1,3-disubstituted nitrophenyl urea, the synthesis of which was discussed in Section 4.2. This species does not possess proximal binding motifs. Similar colorimetric responses to those observed for **125** were observed for this host. DMSO solutions containing host with excess anion are shown in Figure 4.20.

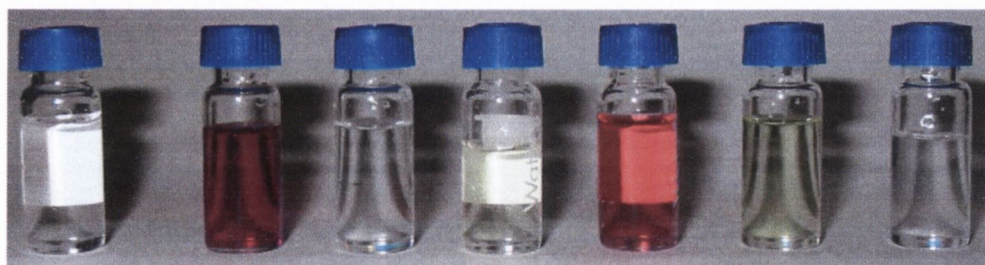


Figure 4.20 - Colorimetric effect observed upon addition of TBA salts of anions to DMSO solutions of **131**; left to right: free host, F^- , Cl^- , H_2PO_4^- , $\text{HP}_2\text{O}_7^{3-}$, AcO^- and NO_3^-

131 was therefore subjected to titration against the noteworthy anions which had been studied for **U2**; OAc^- , $\text{HP}_2\text{O}_7^{3-}$, H_2PO_4^- and F^- , in order to observe similarities or differences in binding behaviour. As was observed in the naked-eye tests (Figure 22), these anions all had a colorimetric effect on **131**. Titrations were performed using the method which had been established for **125**, observing similar UV-vis spectra in each titration (the nitrophenyl moiety gives rise to a very similar nitrophenyl band at ~ 340 nm, which is irrespective of the calix[4]arene scaffold).

In the case of H_2PO_4^- , the UV-vis spectra which were obtained are shown in Figure 4.21. No clear isosbestic point is observed, while the small shift in wavelength is consistent with

the less intense colour change observed in the naked-eye tests. These data were subjected to fitting with SPECFIT, giving a $\log K = 4.86 \pm 0.03$, for a 1:1 complex only.

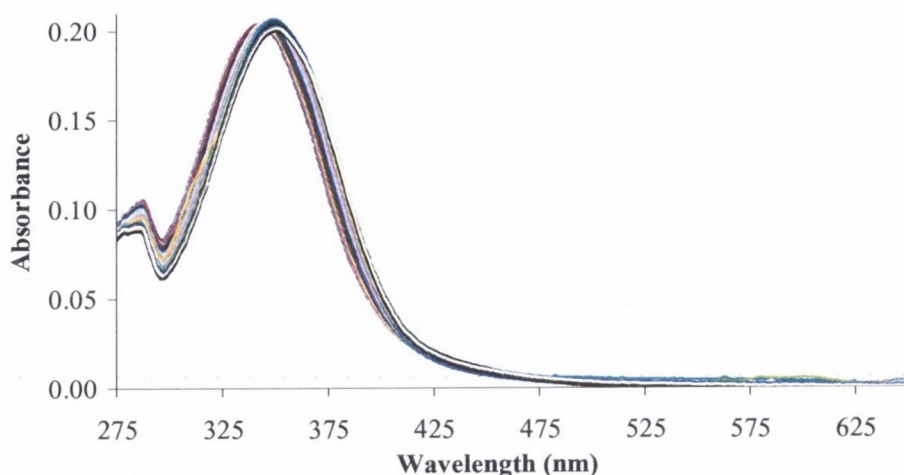


Figure 4.21 – Titration of **131** with H_2PO_4^- ; $[\text{H}]_0 = 6.905 \times 10^{-6}$ M.

Using SPECFIT, no binding model could be found that supported more complex stoichiometry. In this case, it is reasonable to hypothesise that both urea moieties cooperate in binding, given the potential of the calix[4]arene to assemble around its guest. The binding isotherm and its fit are shown in Figure 4.22.

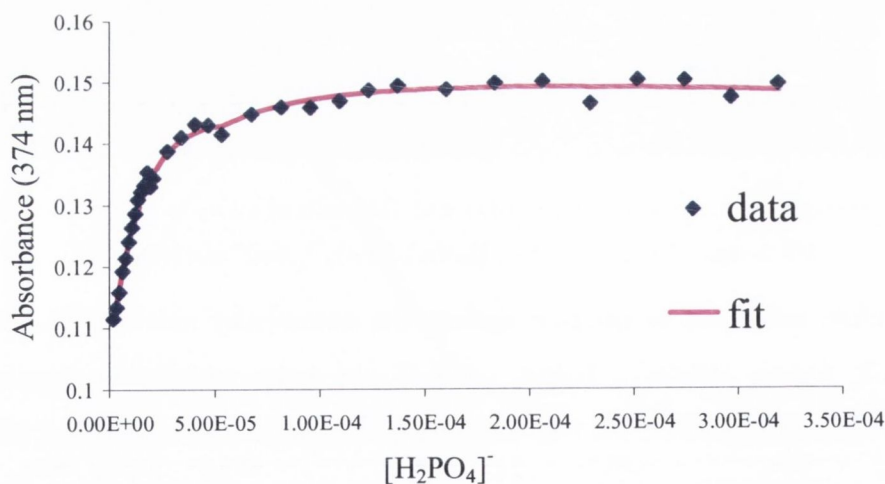


Figure 4.22 – Experimental data v fit of **131** v dihydrogenphosphate

This supports the binding of H_2PO_4^- by two urea subunits. Where proximal ureas are available for binding (as in **125**) they do so, and bind with strong association (a 2:1 guest to host complex is formed with overall $\log \beta = 10.32 \pm 0.18$). However, where the

substituents are not arranged in a proximal manner, the flexibility of the calix[4]arene substituents allows for distal groups to cooperate in binding, albeit with diminished overall stability.

Anion-binding studies were also undertaken using TBA acetate as guest. Here, the smaller anion can potentially bind to both urea moieties. SPECFIT analysis of the UV-vis data provided the binding fit as shown in Figure 4.23.

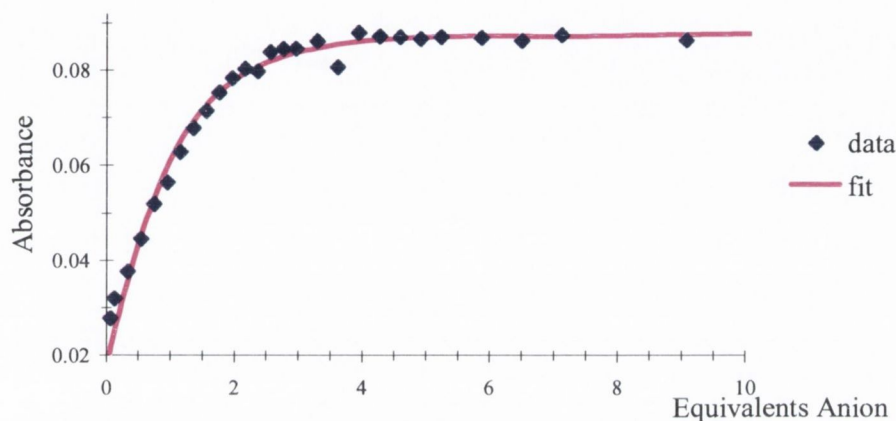


Figure 4.23 – Absorbance Data v Fit for **128**/TBA acetate

The binding constant data derived from this study are presented below. Fitting these data to a HG_2 equilibrium gave strong overall binding, with $\log K_{11}$ established to be 5.64 ± 0.07 , while the second binding event gives rise to $\log K_{21} = 4.39 \pm 0.28$. In this example strong binding is observed, with overall equilibrium lying to the right with $\log \beta > 10$. No deprotonation was observed upon addition of excess anion, the plateau was maintained. Comparison of these binding constants with those obtained for **U2** show little difference, with $\log K_{11}$ and $\log K_{21}$ for **125** found to be 5.11 ± 0.04 and 4.29 ± 0.11 respectively. It can therefore be deduced that in the case of AcO^- , no enhancement, or indeed diminishment of binding is observed upon changing from four binding motifs to two. This leads us to believe that in the case of **125** binding AcO^- , it is probable that binding also occurs in a distal fashion. This is shown schematically in Figure 4.24.

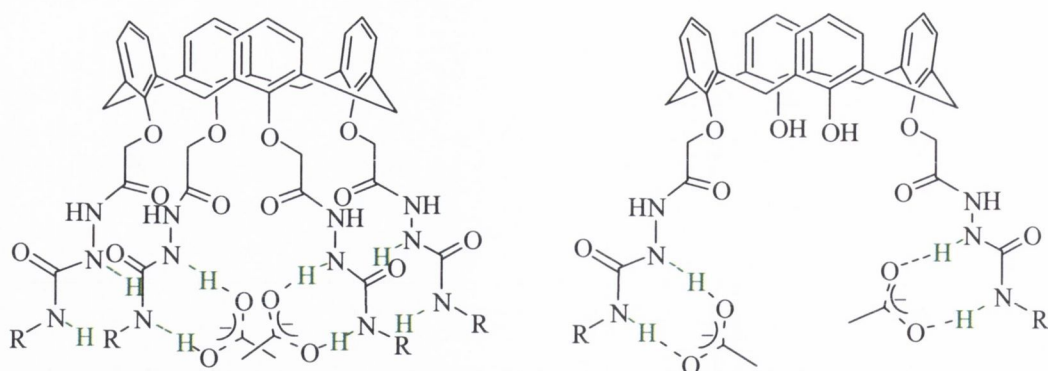


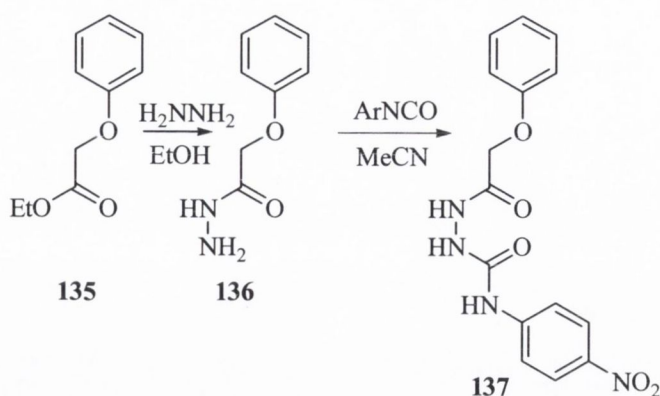
Figure 4.24 – Proposed binding by **125** and **131** of acetate anion, R = 4-nitrophenyl

Receptor **131** was found to also bind F^- and $HP_2O_7^{3-}$. Applying the data obtained for $HP_2O_7^{3-}$ to a model containing a 2:1 guest/host complex provided the most satisfactory fit, of $\log K_{11} = 5.72 \pm 0.11$, and $\log K_{21} = 3.83 \pm 0.30$, while a similar 2:1 guest/host equilibrium was also established for F^- , with $\log K_{11} = 5.07 \pm 0.03$ and $\log K_{21} = 2.91 \pm 0.15$. In both of these titrations, the speciation diagrams showed the 1:1 complex to be the dominating species in solution.

At this point it is unclear whether the remaining urea moieties of **125**, or the free phenolic hydroxyl moieties of **131** play a role in binding of the anions such as AcO^- . It was decided to undertake a study of the anion-binding functionality on a smaller scale, that is, to prepare the semicarbazide binding motif without any effects that may be afforded by calix[4]arene scaffold.

4.5.6 Anion binding using acyclic amidoureas

As has been discussed, the calix[4]arene macrocycle provides rigidity and pre-organisation in the quest for anion sensors. However, in order to assess the benefit of the effects of these factors, if any, it will prove useful to prepare the acyclic analogues of the ureas prepared, and to study the binding of these species. These were synthesised firstly by reaction of ethyl phenoxyacetate with hydrazine hydrate, to yield the corresponding hydrazide. The hydrazide was then reacted with 4-nitrophenyl isocyanate to yield the desired urea. This is outlined in Scheme 4.5.



Scheme 4.5 – Synthesis of acyclic urea **137** for comparative purposes

The product, **137** was characterised by ^1H and ^{13}C NMR, ESMS and elemental analysis. The ^1H NMR spectrum showed similar splitting patterns to those seen for calix[4]arene analogues **125** and **131**. The ^1H NMR spectrum of this potential host is shown in Figure 4.25.

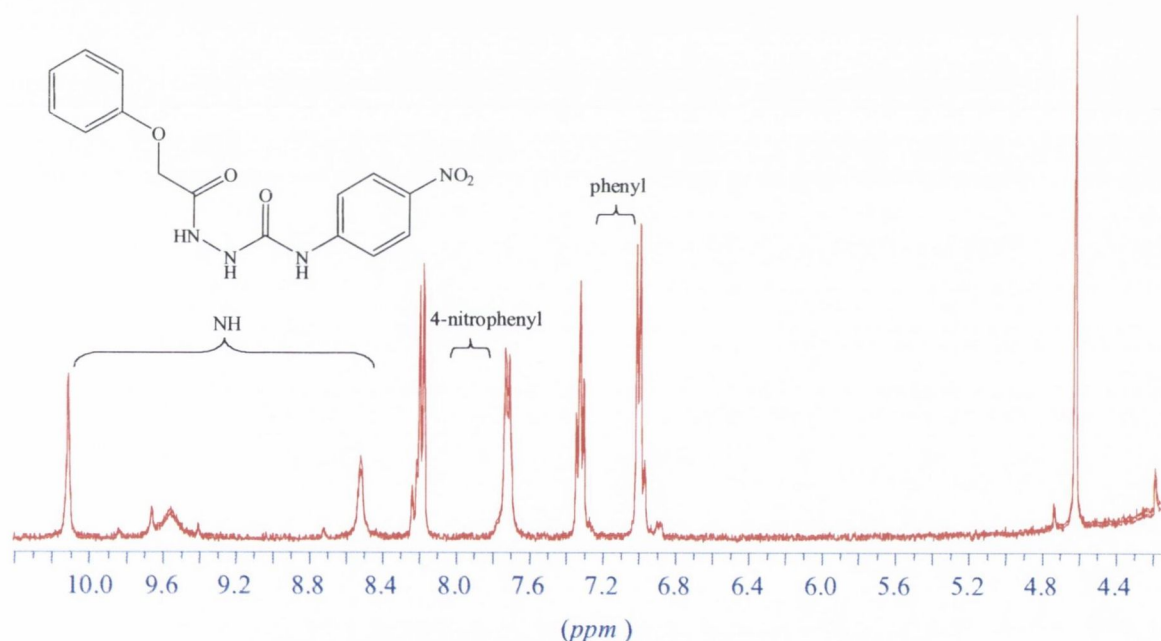


Figure 4.25 - ^1H NMR spectrum of **137** (400 MHz, DMSO-d_6)

Naked-eye tests were also performed with this nitro-containing compound, to determine if there was to be any apparent colour change upon addition of excess anion. The DMSO solution changed from a straw-yellow colour to deep, opaque purple upon addition of F^- or $\text{HP}_2\text{O}_7^{3-}$, and changed its intensity to a yellow-orange, when either AcO^- or H_2PO_4^- were added. This, once again concurs with the changes observed for both **125** and **131**. While it is likely, based on our and literature precedents, in addition to the formation of HF_2^- that

the colour change observed with F^- can be attributed to deprotonation, it was clear that these compounds also possessed capacity to bind anions, without the pre-imposed presence of multiple binding arrays for calixarene derivatives. The colour changes are shown in Figure 4.26



Figure 4.26 - Colorimetric effect upon addition of TBA salts of anions to DMSO solutions of **137**; left to right: free host, F^- , Cl^- , $H_2PO_4^-$, $HP_2O_7^{3-}$, AcO^- and NO_3^-

The nitrophenyl analogue was first titrated against TBA $HP_2O_7^{3-}$, as its colour change (also seen for the calix[4]arene derivatives) was so intense. Upon titration of **137** with $HP_2O_7^{3-}$, two isosbestic points, at 291 nm, and 365 nm were observed, with very little shift from the 340 nm absorbance maximum as guest was added. Moreover, the shape of absorbance changed from the symmetric peak of host alone, to a broad, wide band, trailing off at over 500 nm. The spectra recorded as a function of added anion are shown in Figure 4.27.

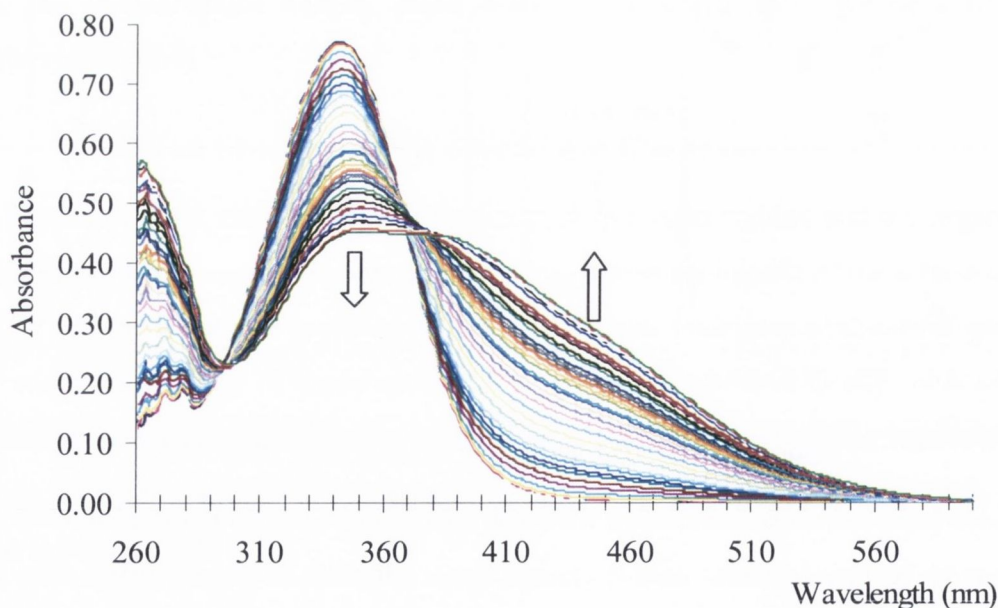


Figure 4.27 – Titration of nitrophenyl acyclic urea **137** with TBA $H_2PO_4^-$.

The change in the spectrum in this case is much more pronounced than observed for the tetrasubstituted or disubstituted calixarene derivatives. From these changes, the binding isotherm shown in Figure 4.28 was extracted.

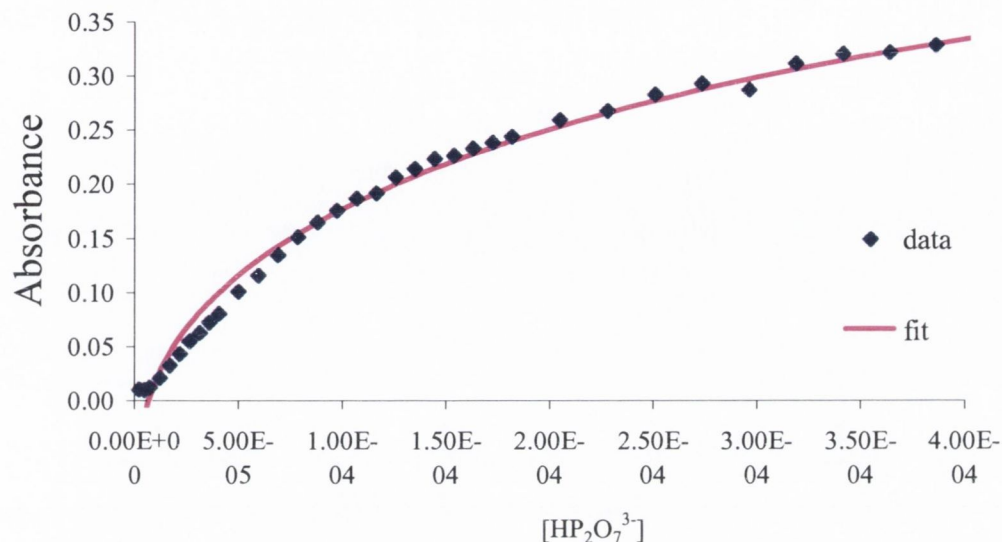


Figure 4.28 - Binding Isotherm and fit of titration of **137** with H_2PO_4^- .

When these data were treated using SPECFIT, the binding constants were consistent with the model of two guests binding one host, this gave $\log K_{11}$ of 5.79 ± 0.30 , with a $\log K_{12} > 7^1$.

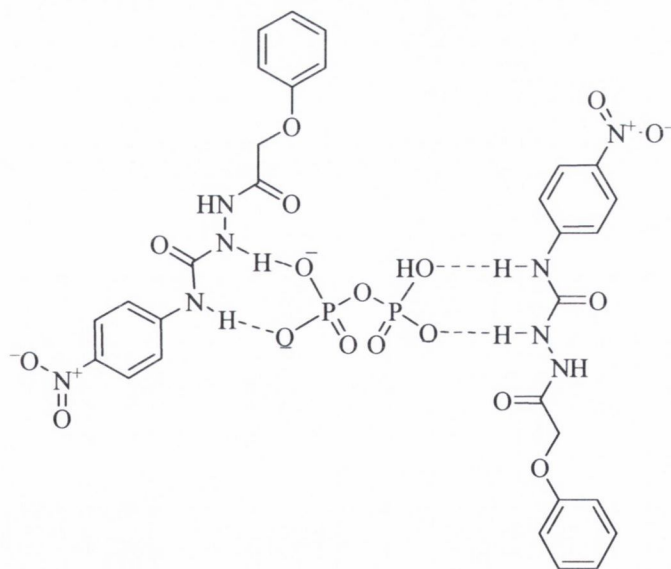


Figure 4.29 – Schematic representation of proposed mode of interaction of acyclic **137** with hydrogen pyrophosphate ($\text{HP}_2\text{O}_7^{3-}$) anion

¹ High binding constants ($\log K > 7$) are beyond the limit of determination using spectroscopic methods, it can be stated that there is a strong binding interaction, but it cannot be precisely affirmed.

The 1:2 stoichiometry can be attributed to a cooperative effect exerted by two host molecules upon one dianionic guest species.

This titration was carried further to larger excess of hydrogenpyrophosphate. As shown in Figure 4.30, in each of the cases of the 4-nitrophenyl amidourea motif, a visible colour change is observed upon addition of hydrogenpyrophosphate. This was studied spectrally for **137**, with the spectra shown in Figure 4.30

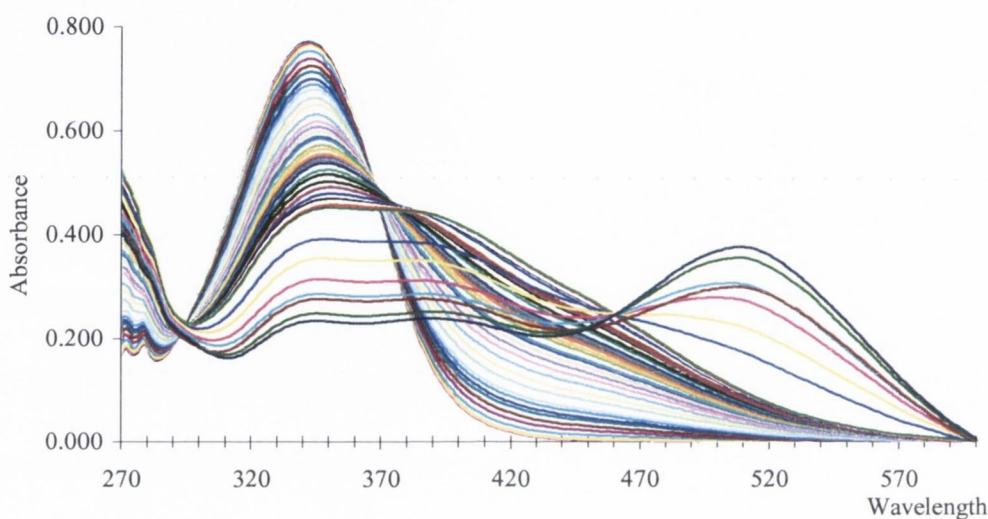


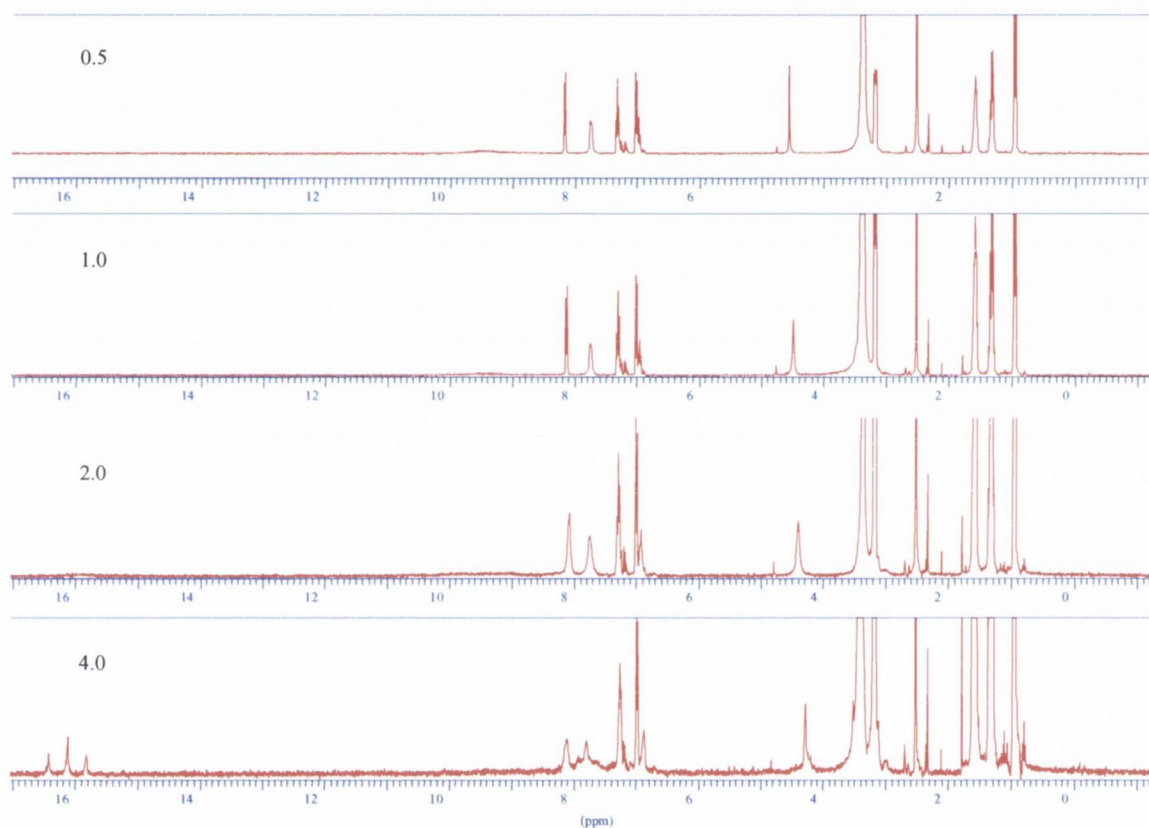
Figure 4.30 - Titration of **137** with $\text{HP}_2\text{O}_7^{3-}$; upon addition of excess guest, the presence of a new band centred at approximately 510 nm is clearly observed

This behaviour cannot be fitted to a single binding model, as it no longer only represents a binding interaction, but rather can be attributed to two stages; binding of the anion, followed by deprotonation of the urea moiety by the anion. Delocalisation of the resultant negative charge gives rise to a highly conjugated species, which accounts for colour change from pale-yellow to deep purple.

This behaviour is well documented in the case of fluoride binding, where deprotonation is frequently observed. Upon deprotonation by fluoride, the abstracted proton forms bifluoride, $[\text{HFH}]^-$, which is observed in ^1H NMR as a triplet at ~ 16 ppm. We have previously shown that bifluoride can be fixed by atmospheric CO_2 , that is, that it can be neutralised.⁹⁵ The groups of Gale²⁰³ and Fabbrizzi²⁰⁴ have recently provided further examples of anion-induced deprotonation of ureas. Fabbrizzi observed that proton abstraction was observed upon titration of a urea-containing guest not only with strongly basic fluoride, but also benzoate, acetate and dihydrogenphosphate.²⁰⁴ It was proposed that deprotonation by oxoanions was possible, according to a stepwise equilibrium involving generation of the conjugate acid of the anions, and subsequent H-bonding between anion

and acid. It is believed that this is the case in our example of hydrogen pyrophosphate recognition. Hydrogen pyrophosphate is sufficiently basic to affect deprotonation by initial formation of two directional N–H···O hydrogen bonds, followed by abstraction of one of the urea protons.

Unfortunately, pyrophosphate-mediated deprotonation does not give rise to change in the ^1H NMR signal, as observed for fluoride. Deprotonation by F^- of **137** is confirmed by the formation of a downfield triplet which was observed following addition of four equivalents



of TBA fluoride. The ^1H NMR spectra are shown in Figure 4.31

Figure 4.31 – Stack-plot of ^1H NMR spectra (400 MHz, $\text{DMSO-}d_6$) of **137** with 0.5, 1.0, 2.0 and 4.0 equiv. TBA F^- respectively. Triplet at ~16 ppm observed due to formation of $[\text{HFH}]^-$. TBA resonances visible in aliphatic region.

Titrations of **134** were also carried out with AcO^- and H_2PO_4^- . The binding constants for all of the anions under study are presented in Table 4.2.

Table 4.2 - Binding constants (expressed as $\log K$) obtained for **137** by UV-Vis titration in DMSO, against guests shown; 1:1 stoichiometry as M^{-1} , 1:2; 2:1 stoichiometry as M^{-2} . Values are quoted with standard deviations. Data were processed using SPECFIT.

	1:1 stoichiometry	2:1 stoichiometry
Dihydrogenphosphate	4.73 ± 0.17	3.56 ± 0.27
Acetate	4.20 ± 0.03	3.21 ± 0.10 (HG ₂)
Fluoride	3.31 ± 0.03	-
Hydrogen pyrophosphate	5.78 ± 0.30	>7 (H ₂ G)

4.6 Electrospray mass spectrometry study of host-guest interactions

Electrospray mass spectrometry (ES-MS) is considered to be a “soft” ionisation technique, as opposed to the more traditional method of electron ionisation mass spectrometry. This softness is due to the technique of ionisation, whereby droplets of a solution of the compound under study are ionised by subjecting a mist of the solution to an electric charge. Columbic forces repel the now ionised analyte, which, in conjunction with the a carrier system (typically an inert gas such as nitrogen), drive the ion to the mass analyser, allowing m/z to be assessed. This contrasts with electron ionisation mass spectrometry (EI-MS), wherein a stream of electrons is used to ionise the analyte, and in this process, the molecule is subjected to fragmentation, and the generation of radical ions. The softness of the electrospray technique has opened it up to supramolecular chemists, allowing the utilisation ES-MS not only for characterisation of synthesised compounds, but also for probing supramolecular interactions by means of the accompanying changes in molecular mass.²⁰⁵ It was decided to undertake a study of anion binding interactions of the compounds reported in this Chapter, using ES-MS.

This study was conducted in collaboration with Dr Dilip Rai of the Centre for Synthesis and Chemical Biology at University College Dublin, and utilised electrospray negative detection mode (ES⁻). Samples were prepared to give a final concentration of approximately 1 mg/mL of complex in acetone. In the case of calixarene-containing ureas which were insoluble in acetone, they were seen to disperse evenly. Dispersions were solubilised upon addition of guest. This investigation initially looked at the acyclic urea **137**, and its interaction with hydrogen pyrophosphate. The mass spectrum was run, and in positive ion detection mode (ES⁺), only a peak at $m/z = 242$ was observed (corresponding

to the tetrabutylammonium cation). In negative detection mode, (ES⁻), the following peaks were observed, where each anion carries a -1 charge.

m/z = 177	HP ₂ O ₇ ³⁻
329	137 - 1
507	134 + HP ₂ O ₇ ³⁻
659	2 × 137
837	2 × 137 + 1 HP ₂ O ₇ ³⁻

These results were as expected, in agreement with the UV-Vis titration measurements and fitting which had been otherwise deduced. It also indicates the formation of dimers of the urea, which is testament to the strong hydrogen bonding offered by the urea moieties, and further accounts for the insolubility of these analytes in organic solvents.

When the interaction of **131** with the hydrogen pyrophosphate anion was probed, the major peaks of interest, again in negative detection mode were:

m/z = 177	HP ₂ O ₇ ³⁻
895	131 - 1
1073	131 + HP ₂ O ₇ ³⁻

No peak corresponding to the complexation of a second hydrogenpyrophosphate anion was observed in this study. This leads us to believe that the hydrogenpyrophosphate anion is indeed bridging the calix[4]arene cavity. A schematic depiction of the bridging by pyrophosphate of the calixarene cavity is shown in Figure 4.32.

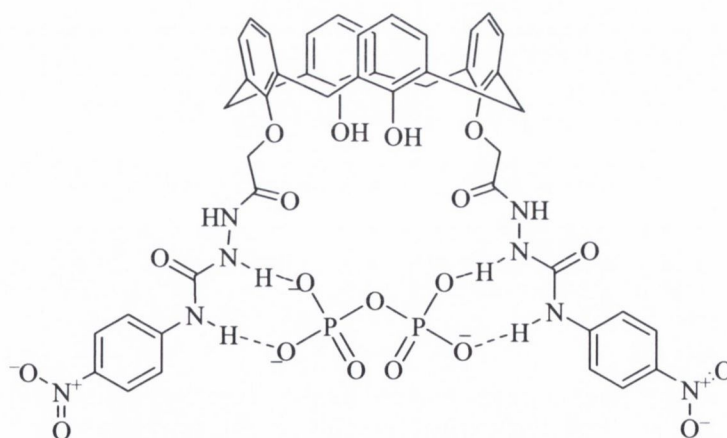


Figure 4.32 – Hydrogen-bonded complex of **131** with HP₂O₇³⁻: a proposed bridging effect

This ESMS study was further extended to host **125** and to further anionic guests, F⁻, AcO⁻ and H₂PO₄⁻. Less encouraging results than those observed for pyrophosphate were obtained. However, some desirable peaks could be discerned. In the case of **125**, a peak at

$m/z = 732$ implied the existence of **125** + H_2PO_4^- , while for **137**, one equivalent of the same anion was seen to be binding by peak at $m/z = 427$. Binding of AcO^- with either **125** or **128** did not present conclusive molecular ion peaks, while the interaction with **137** was implied by the peak at $m/z = 193$, which was assigned to $(\text{137} + \text{AcO}^-)/2$. This study has been preliminary in nature yet has confirmed several binding interactions. It is possible also that the ionisation voltage of the electrospray instrument plays a role in this binding interaction, as postulated by Salter.²⁰⁶ At this point, this factor has not been further investigated.

4.7 Conclusions

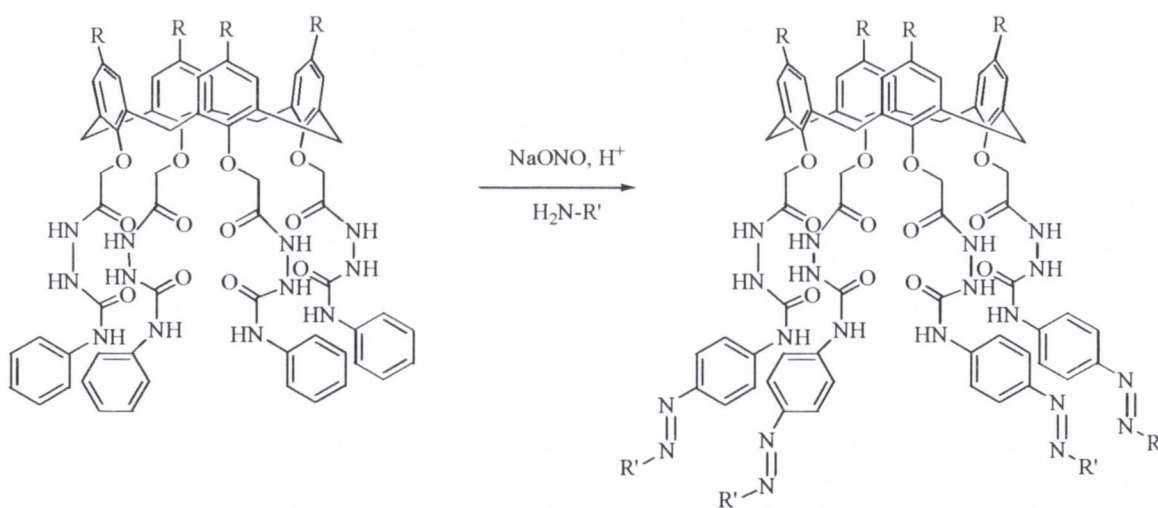
This chapter has outlined the successful synthesis, characterisation, and study of a series of colorimetric anion sensors, based on calix[4]arene. Building upon the precedents as set out in the calixarene literature and beyond, and discussed in Chapter 1, several compounds were assessed, principally using the sensitive technique of UV-Vis spectroscopy, in addition to ^1H NMR and ESMS, for binding affinities towards halides and oxoanions. Strong binding (overall $\beta > 10^4$) was observed in all but one case. The development of an acyclic analogue, used as a model, has allowed the more detailed study of conformation and binding modes within the macrocyclic calixarene analogue. From the comparison of binding data observed for each of tetrasubstituted **125**, disubstituted **131**, and monourea **137**, bridging binding modes have been proposed for the di-anion hydrogenpyrophosphate. Preparing a disubstituted calixarene based receptor, in addition to an acyclic, phenol-based receptor has enabled us to further postulation about the binding modes within the tetrasubstituted compound. Study of the binding of the simple carboxylate anion acetate, in addition to dihydrogenphosphate was undertaken, fitting the UV-vis data using SPECFIT. Insightful results have been obtained following the study on pyrophosphate, which provided stark colour change upon interaction with the urea moiety. It was believed that its size, in addition to its separation of charge would allow it to bridge the calix[4]arene cavity. As such, binding 1:1, in a bridging mode was proposed for **131**, and this species was seen to be the dominant species in solution, despite the transient formation of a 2:1 (guest:host) complex. Pyrophosphate, is thus favourably bound by two ureido moieties, and again this behaviour was seen in solution in the case of **137**, which is less rigid than the calix[4]arene-immobilised counterpart. For this host, two equivalents were required to fully complex pyrophosphate. Both of these proposed stoichiometries were confirmed by ESMS. Finally, in the case of calix[4]arene **125**, the tetrasubstituted ligand, only a single

binding event was seen to occur. This is attributed to the size of the cavity, and the need of the anion to bridge, binding distal ureido moieties, rather than proximal monomer units. Through the synthetic protocols which have been established in the course of this study, it is expected that such analogues may be readily accessible in future studies, to further elucidate the binding modes and stoichiometry of this semicarbazide motif.

4.8 Future Work

This chapter has discussed the synthesis and detailed characterisation of three host systems prepared in the course of this study. Future work remains to answer questions regarding the binding modes of phenyl and other derivatives, in addition to thiourea analogues of each of the species under analysis. Furthermore study of the 1,3-alternate systems will elucidate further the binding modes of these species and investigate to potential allosteric effects. Commercial availability, and synthetic accessibility of isocyanates will enable more diverse analogues to be prepared, ultimately fine-tuning selectivity and enhancing affinity towards anions of interest.

The phenyl analogue will also be further derivatised by diazotisation reactions thus introducing diazo moieties which will act as colorimetric reporting tethers. Such a system is outlined in Scheme 4.6.

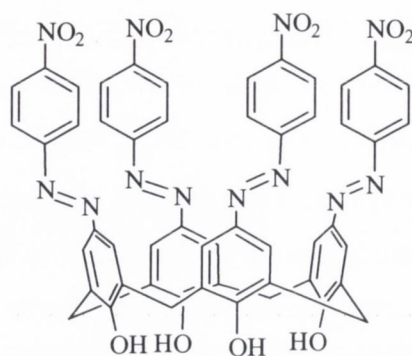


138

Scheme 4.6 – Diazocoupling of U1 to incorporate a chromophore for further colorimetric study.

Preliminary synthesis of a tetraaza calix[4]arene **139** for the purpose of anion recognition was undertaken during these studies, however purification of this compound was not successfully achieved, and its characterisation is therefore not reported in this thesis. This compound utilises the O-H donors of lower-rim unsubstituted calix[4]arenes to bind

anions, and the use of a diazo moiety at the upper rim affects significant colorimetric reporting properties. Hydrogen bonding at the phenolic moiety causes significant change in the dipole of the molecule to clearly affect large changes in the dipole and thus strong changes to the absorption spectrum.



139



Figure 4.33 - Colorimetric effect upon addition of TBA salts of anions to DMSO solutions of crude **139**;
left to right: free host, F^- , Cl^- , $H_2PO_4^-$, $HP_2O_7^{3-}$, AcO^- and NO_3^-

It is anticipated that full synthesis, purification and colorimetric study of this compound and its analogues will be a future project within the group.

5.1 General Experimental Details

All chemicals were purchased from Sigma-Aldrich Ireland Ltd. (Aldrich, Sigma and Fluka/Riedel de Haën brands), Lancaster or Acros Organics and unless specified, were used without further purification. Deuterated solvents for NMR use were purchased from Apollo Scientific Ltd.

Dry solvents, when required, were prepared using standard procedures, according to Vogel, with distillation under dry nitrogen or argon prior to each use.²⁰⁷ Commercial triethylamine and pyridine were dried over potassium hydroxide and distilled before use.

Analytical TLC was performed using Merck Kieselgel 60 F₂₅₄ silica gel plates. Visualisation was by UV light (254 nm), by exposure to iodine vapour, immersion in aqueous alkaline KMnO₄ solution, or with 2% ninhydrin in ethanol spray reagent. Preparative column chromatography was performed on silica gel 60, 230-400 mesh.

NMR spectra were recorded at 273 K, except when stated otherwise, using a Brüker DPX-400 Avance spectrometer, operating at 400.13 MHz (proton) and 100.6 MHz (carbon), or a Brüker AV-600 spectrometer, operating at 600.1 MHz (proton), 150.2 MHz (carbon) and 60.6 MHz (nitrogen). Shifts are referenced relative to the solvent deuterium lock resonance signal. NMR data were processed using Brüker Win-NMR 5.0 software.

Electrospray mass spectra for characterisation purposes were recorded on Micromass LCT spectrometer, running Mass Lynx NT V 3.4, using a Waters 600 controller connected to a 996 photodiode array detector, with HPLC-grade CH₃OH, water or CH₃CN as carrier solvents. Detection was in positive (ES⁺) mode only. Accurate molecular masses were determined by a peak-matching method, using leucine enkephalin (H-Tyr-Gly-Gly-Phe-Leu-OH) as the standard internal reference ($m/z = 556.2771$), and are reported when experimental values are within 5 ppm of the expected mass. Samples were prepared in appropriate non-chlorinated solvents.

UV-Vis titration measurements were performed on a Varian Cary-50 UV-Vis spectrometer. Compounds for titration were dissolved in DMSO until an absorbance in the range 0.1 – 0.5 had been achieved. Titration mixings were performed internally, adding 3-10 μ L aliquots of guest using a microsyringe to a quartz cuvette containing 2.000 mL of host solution equipped with a magnetic stirrer. Fluorescence spectra were recorded on a Varian Cary Eclipse fluorescence spectrophotometer.

Melting points were measured using a Electrothermal 9100 melting-point apparatus and are reported uncorrected. Infrared spectra were recorded using a Perkin-Elmer Spectrum One FTIR spectrometer fitted with an ATR sampler.

Electrospray mass spectrometry studies of anion-binding interactions were recorded at the Centre for Synthesis and Chemical Biology, University College Dublin. Measurements were carried out in collaboration with Dr Dilip Rai, CSCB using a Waters Quattro *micro*TM LC-MS/MS machine. Solutions were made to approximately 1 mg/mL of combined complex in HPLC-grade acetone, and run using 100% CH₃CN as carrier.

Crystals for X-ray diffraction were analysed and solved by Dr Tom McCabe at Trinity College, Dublin using a Brüker SMART APEX single crystal CD diffractometer. Crystallographic data summaries are provided in Appendix 1. Elemental analysis service was provided by Ms. Ann Connolly at the Microanalysis Laboratory, School of Chemistry and Chemical Biology, University College Dublin.

5.2 Nomenclature of calix[4]arenes

In place of *Chemical Abstracts* or IUPAC systematic nomenclature for cyclophanes, calixarenes have an accepted atom-numbering scheme. The atom-numbering system for the carbon skeleton of calix[4]arene derivatives as referred to in the synthetic procedures and text is indicated in Figure 5.1

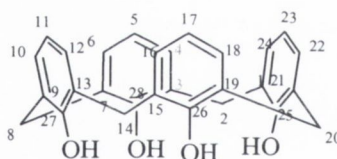
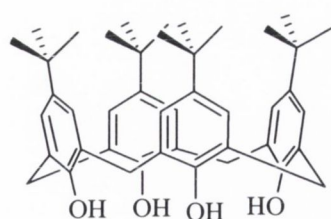


Figure 5.1 – Carbon numbers of 25,26,27,28-tetrahydroxycalix[4]arene and its subsequent derivatives

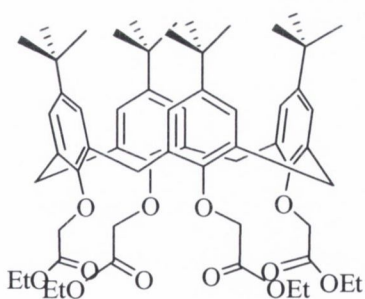
5.3 Synthetic Procedures



Tetra[4-*tert*-butyl]calix[4]arene²⁵ (1)

In a 3 L flange-topped flask, 4-*tert*-butyl phenol (200 g 1.33 mol), NaOH (1.2 g, 30 mmol) and formaldehyde (37% in water, 128 mL) were combined and the contents heated to 120 °C with mechanical stirring over 2 h. A dry, brittle, yellow solid formed which was then crushed and dissolved in diphenyl ether (750 mL). Water of condensation was removed by distillation under a stream of compressed air, after which the solution was heated at reflux for 2 h. Upon cooling to ~60 °C, ethyl acetate (1.5 L) was added through a condenser to precipitate the crude product, which was collected by filtration, washed with ethyl acetate (2 × 100 mL), acetic acid (2 × 100 mL) and water (4 × 100 mL). The off-white crystalline solid was collected and dried by suction filtration, and oven-dried at 80 °C to yield the title calix[4]arene as an off-white microcrystalline solid. (119 g, 55%), m.p. 352 °C (lit. 344 – 346 °C). ¹H NMR (400 MHz, CDCl₃, δ_H): 10.35 (s, 4H, Ar-OH), 7.07 (s, 8H Ar-H) 4.26 (br. s 4H, Ar-CH₂-Ar) 3.51 (br. s, 4H, Ar-CH₂-Ar). 1.24 (s, 36H, -C(CH₃)₃). ¹³C NMR (100 MHz, CDCl₃, δ_C): 146.1, 143.9, 127.2, 125.4, 33.5, 32.1, 30.9.

5,11,17,23-Tetra-*tert*-butyl-25,26,27,28-tetrakis[(ethoxycarbonyl)methoxy]-calix[4]arene (7)

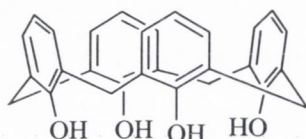


Prepared according to a modified procedure to that of McKervey.⁶⁵

To *tert*-butyl-calix[4]arene (1) (12.5 g, 19.26 mmol) in CH₃CN (80 mL) was added K₂CO₃ (13.3 g, 96 mmol). The suspension was stirred at 60 °C for 30 minutes to affect deprotonation. Ethyl bromoacetate (16.08 g, 96 mmol) was added, and the resulting mixture was heated at reflux for a further 16 h. Solvent was removed at reduced pressure, and the oily residue taken up into CH₂Cl₂/water. The solvents were separated, and the aqueous layer washed with further ethyl acetate (30 mL). Combined organics were then washed with water (2 × 50 mL), and dried (MgSO₄). The solvent was removed at reduced pressure, and ethanol (100 mL) added. This solution was allowed to stand in a freezer overnight, upon which the product (11.40 g, 60 %) crystallised as white needles (m.p.: 121 °C, lit 154-155 °C) ¹H NMR (400

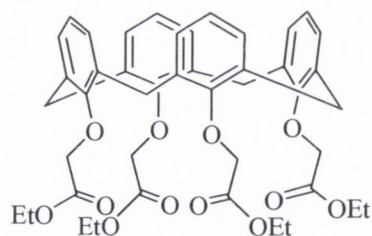
MHz, CDCl_3 , δ_{H}): 6.80 (s, 8H, Ar-H), 4.86 (d, $J = 13.1$ Hz, 4H, Ar- CH_2 -Ar), 4.82 (s, 8H, $\text{OCH}_2\text{C}(\text{O})$), 4.22 (q, $J = 7.5$ Hz, 8H, OCH_2CH_3), 3.20 (d, $J = 13.1$ Hz, 4H, Ar- CH_2 -Ar), 1.31 (t, $J = 7.0$ Hz, 12H, OCH_2CH_3), 1.09 (s, 36H, $\text{C}(\text{CH}_3)_3$). ^{13}C NMR (100 MHz, CDCl_3 , δ_{C}): 170.1, 152.5, 144.7, 133.0, 124.9, 70.9, 70.9, 59.9, 33.4, 31.4, 30.9. **Accurate MS** (m/z): Calculated for $\text{C}_{60}\text{H}_{80}\text{O}_2 + \text{Na}$: 1015.5547, found: 1015.5533.

Calix[4]arene²⁰⁸ (53)



4-*tert*-Butyl calix[4]arene (**1**) (30.00 g, 46 mmol) was suspended in toluene (250 mL) and stirred for 20 minutes at room temperature. Phenol (21.15 g, 225 mmol) was then added, followed by the cautious addition of finely powdered aluminium(III) chloride (32 g, 228 mmol). The mixture was stirred overnight in an inert atmosphere of argon. The resulting brown solution was then poured into ice-water (450 mL) and the phases separated. The pink organic layer was removed, and the aqueous layer washed with CH_2Cl_2 (2×50 mL). Organic layers were combined and the solvent was removed under reduced pressure. To the resulting oily residue, was added methanol (200 mL) to precipitate, upon stirring, calix[4]arene, which was collected by suction filtration to yield a white powder (13.75 g, 72%), m.p. 308 °C (lit. 312 – 315 °C). ^1H NMR (400 MHz, CDCl_3 , δ_{H}) 10.23 (s, 4H, Ar-OH), 7.08 (d, $J = 7.5$ Hz, 8H Ar-H), 6.76 (t, $J = 6.5$ Hz, 4H, Ar-H), 4.29 (bs, 4H, Ar- CH_2 -Ar), 3.58 (bs, 4H Ar- CH_2 -Ar). ^{13}C NMR (100 MHz, CDCl_3 , δ_{C}): 148.4, 128.6, 127.8, 121.9, 31.3.

25,26,27,28-Tetrakis[(ethoxycarbonyl)methoxy]calix[4]arene⁶⁵ (55)



(*cone conformation*)

Calix[4]arene (**53**) (10.0 g, 23.6 mmol) was suspended in CH_3CN (100 mL) with anhydrous K_2CO_3 (19.5 g, 0.14 mol). The suspension was heated for 30 min. to affect deprotonation of the calixarene. Ethyl bromoacetate (13 mL, 0.12 mol) was added and the mixture was stirred at reflux temperature overnight. Solvents were then removed under reduced pressure, and the residue partitioned between CH_2Cl_2 (200 mL) and water (200 mL). The organic layer was removed, the aqueous layer was washed with further CH_2Cl_2 (100 mL) and the combined organic layers washed again with water and brine (100 mL). The organic layer was dried over MgSO_4 and evaporated under reduced pressure. Ethanol was added to the resultant oily residue, and the solution was

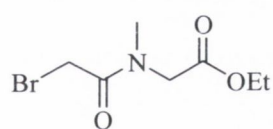
allowed to stand overnight in a freezer ($-19\text{ }^{\circ}\text{C}$). The white crystalline solid which resulted was collected by suction filtration and washed with cold EtOH. Where necessary, this product was further recrystallised from hot ethanol, yielding the title compound as a crystalline solid (12.9 g, 71%), m.p. $98\text{ }^{\circ}\text{C}$ (lit. $108 - 109\text{ }^{\circ}\text{C}$).

$^1\text{H NMR}$ (400 MHz, CDCl_3 , δ_{H}): 6.67-6.72 (m, 12H, Ar-H), 4.95 (d, $J = 14.1\text{ Hz}$, 2H, Ar- CH_2 -Ar), 4.81 (s, 8H, $\text{OCH}_2\text{C}(\text{O})$), 4.28 (q, $J = 7.0\text{ Hz}$, 8H, OCH_2CH_3), 3.31 (d, $J = 13.6\text{ Hz}$, 4H, Ar- CH_2 -Ar), 1.36 (t, $J = 7.0\text{ Hz}$, 12H, OCH_2CH_3). $^{13}\text{C NMR}$ (100 MHz, CDCl_3 , δ_{C}): 169.8, 155.5, 134.2, 128.1, 122.4, 70.9, 60.1, 31.0, 13.8 **Accurate MS:** (m/z) Calculated for $\text{C}_{44}\text{H}_{48}\text{O}_{12}\text{Na}$ ($\text{M}+\text{Na}$): 791.3043; found 791.3024.

General Procedure for Synthesis of α -bromoamides

The procedure shown below, for the α -bromoamide of sarcosine ethyl ester hydrochloride is representative, and is followed for other amines. Where free amines were introduced, one equivalent of base was required; for hydrochloride salts of amines, a second equivalent of base was engaged. CAUTION: α -Bromoamides synthesised herein are irritant and lachrymatory. Due care must be exercised in their preparation and handling.

Ethyl 2-(2-bromo-*N*-methylacetamido)acetate (58)

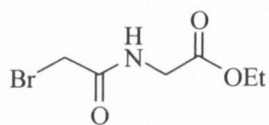


To sarcosine ethyl ester hydrochloride (25.0 g, 0.16 mol) in CH_2Cl_2 (300 mL) was added two equivalents of NEt_3 (45 mL, 0.32 mol, two equiv.). A thick precipitate formed, and this suspension was cooled,

with stirring to $-10\text{ }^{\circ}\text{C}$. Bromoacetyl bromide (15 mL, 0.17 mol, one equiv.) was added in CH_2Cl_2 (150 mL) drop-wise, over 2 hours. The resulting reaction mixture was then stirred at room temperature overnight and filtered to remove unwanted triethylammonium salts. The organic layer was washed with water (100 mL), 1 M HCl (100 mL) and again with water (100 mL). Following drying with CaCl_2 , the organic solvent was removed under reduced pressure to yield the compound as an oil that was used without further purification. A pure sample for characterisation was obtained by distillation under reduced pressure. $^1\text{H NMR}$ (400 MHz, CDCl_3 , δ_{H}): 4.20 (s, 2H, $\text{BrCH}_2\text{-C}(\text{O})$), 4.09 (s, 2H, $\text{NCH}_2\text{C}(\text{O})$), 4.04 (q, $J = 7.0\text{ Hz}$, 2H, OCH_2CH_3), 3.08 (s, 3H, NCH_3), 1.20 (t, $J = 7.0\text{ Hz}$,

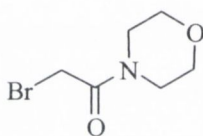
3H, OCH₂CH₃). **Accurate MS** (*m/z*): Required for C₇H₁₂NBrO₃+Na: 259.9898, found 259.9893.

Ethyl 2-(2-bromoacetamido) acetate (59)



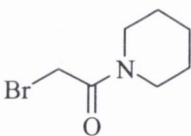
Using the above procedure, glycine ethyl ester hydrochloride (5.56 g, 25.5 mmol) was combined with NEt₃ (51 mmol) and bromoacetyl bromide (25.5 mmol) at -78 °C and when allowed to warm to room temperature and subjected to workup yielded the title compound as an oil which solidified upon standing, yielding an off-white solid, 3.43 g, 38% (m.p.: 71 °C) **¹H NMR** (400 MHz, CDCl₃, δ_H): 7.02 (s, 1H, NH), 4.25 (q, *J* = 8Hz, 2H, OCH₂CH₃), 4.07 (d, *J* = 6 Hz, 2H, NCH₂C(O)), 3.94 (s, 2H, BrCH₂C(O)), 1.31 (t, *J* = 7 Hz, OCH₂CH₃). **IR** (ν/cm⁻¹): 3262, 3084, 1736, 1643, 1562, 1375, 1197, 1028, 871, 733, 707. **Accurate MS** (*m/z*): Calculated for C₆H₁₀NO₃Na⁷⁹Br: 245.9742; found 245.9735.

2-Bromo-1-morpholinoethanone (60)

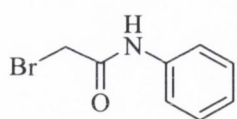


Using the above procedure, morpholine (25 mL, 0.29 mol) was combined with NEt₃ (40 mL, 0.29 mol) and bromoacetyl bromide (25 mL, 0.29 mol) and when subjected to workup yielded the title compound as an oil in quantitative yield, which was used without further purification. **¹H NMR** (400 MHz, CDCl₃, δ_H): 3.87 (s, 2H, Br-CH₂-C(O)), 3.76 (m, 2H, N(CH₂CH₂)₂O), 3.72 (m, 2H, N(CH₂CH₂)₂O), 3.65 (m, 2H, N(CH₂CH₂)₂O), 3.54 (m, 2H, N(CH₂CH₂)₂O). **¹³C NMR** (100 MHz, CDCl₃, δ_C): 165.1, 66.0, 65.8, 46.6, 41.9, 25.0. **IR** (ν/cm⁻¹): 3444, 2901, 1729, 1601, 1461, 1275, 1114, 1039, 929, 582, 456.

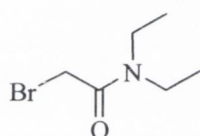
2-Bromo-1-(piperidin-1-yl)ethanone (61)



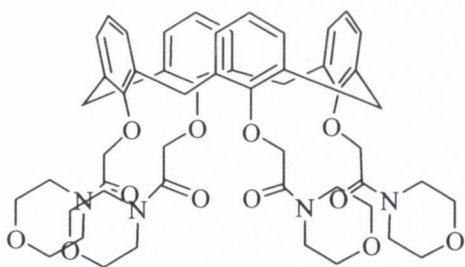
Using the above procedure, in dry CH₂Cl₂ (200 mL) piperidine (10 mL, 0.1 mol) was combined with NEt₃ (14 mL, 0.1 mol) and bromoacetyl bromide (8.8 mL, 0.1 mol), and when subjected to workup yielded the title compound as an oil, which was used without further purification. (quantitative yield). **¹H NMR** (400 MHz, CDCl₃, δ_H): 3.87 (s, 2H, Br-CH₂-C(O)), 3.75-3.76 (m, 2H, piperidine), 3.70 - 3.72 (m, 2H, piperidine), 3.64 - 3.66 (m, 2H, piperidine), 3.52 - 3.55 (m, 2H, piperidine). **¹³C NMR** (100 MHz, CDCl₃, δ_C): 164.5, 47.4, 42.7, 25.8, 25.6, 24.8, 23.7. **IR** (ν/cm⁻¹): 2939, 2858, 1728, 1609, 1448, 1273, 1022, 616, 466.

2-Bromoacetanilide (62)

Using the above procedure, aniline (5.11 mL, 54 mmol) was combined with NEt₃ (7.48 mL, 54 mmol) and bromoacetyl bromide (4.48 mL, 54 mmol), and when subjected to workup yielded the title compound as a brown solid, which was recrystallised from ethanol to give the desired product as an off-white solid (8.30 g, 72%) m.p. 124 °C (lit. 129 – 131 °C). (CARE! – product is severely irritant and lachrymatory). ¹H NMR (400 MHz, CDCl₃, δ_H): 8.23 (s, 1H, NH), 7.55 (d, *J* = 8 Hz, 2H, Ar-H), 7.38 (t, *J* = 7 Hz, 2H, Ar-H), 7.19 (t, *J* = 7 Hz, 1H, Ar-H), 4.04 (s, 2H, BrCH₂C(O)). ¹³C NMR (100 MHz, CDCl₃, δ_C): 164.3, 137.7, 128.0, 123.4, 119.0, 29.2.

2-Bromo-*N,N*-diethylacetamide (63)

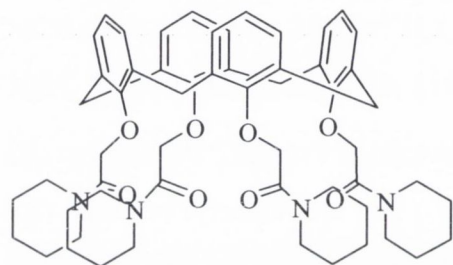
Using the above procedure, *N,N*-diethylamine (10 mL, 96 mmol) was combined with NEt₃ (13.5 mL, 96 mmol) and bromoacetyl bromide (8.4 mL, 97 mmol), and when subjected to workup yielded the title compound as a straw-coloured oil in quantitative yield. ¹H NMR (400 MHz, CDCl₃, δ_H): 3.80 (s, 2H, BrCH₂C(O)), 3.32 (q, *J* = 7.0 Hz, 4H, N(CH₂CH₃)₂), 1.20 (t, *J* = 7.5 Hz, 3H, NCH₂CH₃_{cis}), 1.07 (t, *J* = 7.5 Hz, 3H, NCH₂CH₃_{trans}). ¹³C NMR (100 MHz, CDCl₃, δ_C): 165.7, 42.7, 40.3, 26.3, 14.2, 12.3.

25,26,27,28-Tetrakis(((*N*-morpholino)carbonyl)methoxy)calix[4]arene (64)

To a suspension of calix[4]arene (**53**) (1.0 g, 2.36 mmol) in acetonitrile (50 mL), was added K₂CO₃ (1.95 g, 14 mmol) and 2-bromo-1-morpholinoethanone (**60**) (2.94 g, 14.1 mmol). The suspension was stirred at reflux overnight, resulting in a brown suspension. Solvents were removed, and the residue was partitioned between water (100 mL) and CH₂Cl₂ (100 mL). The organic layer was removed, and the water layer extracted again with CH₂Cl₂ (50 mL). The combined organic layers were then further washed with water (100 mL), dried (Na₂SO₄), and the solvent removed under reduced pressure. The resulting solid was recrystallised from ethanol to give the title compound (1.44 g, 66%) (m.p.: 218 °C). ¹H NMR (400 MHz, CDCl₃, δ_H): 6.60 – 6.67 (m, 12H, Ar-H), 4.98 (d, *J* = 14 Hz, 4H, Ar-CH₂-Ar), 4.91 (s, 4H, ArO-CH₂-C(O)), 3.49 – 3.69 (m,

32H, N(CH₂CH₂)₂O), 3.26 (d, $J = 14$ Hz, Ar-CH₂-Ar). ¹³C NMR (100 MHz, CDCl₃, δ_C): 167.6, 155.4, 134.1, 128.1, 122.2, 70.8, 66.4, 66.2, 44.4, 41.2, 31.1. IR (ν/cm⁻¹): 3445, 2967, 2912, 2863, 1676, 1658, 1466, 1448, 1466, 1358, 1299, 1274, 1213, 1236, 1196, 1112, 1095, 1068, 1026, 998, 911, 852, 778, 754. ESMS (m/z): 955.38 (M+Na). **Analysis:** Required for C₅₂H₆₀N₄O₁₂·H₂O: C, 65.67; H, 6.57; N, 5.89. Found: C, 65.88; H, 6.49; N, 5.65.

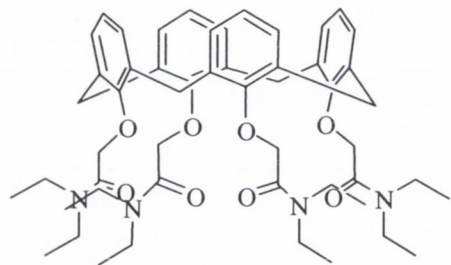
25,26,27,28-Tetrakis(((*N*-piperidiny)carbonyl)methoxy)calix[4]arene (65)



Prepared analogously to **64** in CH₃CN (30 mL), treating calix[4]arene (**53**) (500 mg, 1.18 mmol) with 2-bromoacetyl piperidine (**61**) (1.1 g, 5.34 mmol) and K₂CO₃ (1.0 g, 7 mmol). Heating at reflux temperature overnight gave a coffee-coloured suspension. Workup followed by crystallisation from CH₃OH gave the

title compound as a cream solid (523 mg, 48%) m.p.: 291 °C (dec.). ¹H NMR (400 MHz, CDCl₃, δ_H): 6.64-6.60 (m, 12H, Ar-H), 5.11 (d, $J = 14.1$ Hz, 4H, Ar-CH₂-Ar), 4.90 (s, 8H, OCH₂C(O)), 3.52 (t, $J = 5.0$ Hz, 8H, N[CH₂CH₂]CH₂), 3.43 (t, $J = 5.0$ Hz, 8H, N[CH₂CH₂]CH₂), 3.26 (d, $J = 13.8$ Hz, 4H, Ar-CH₂-Ar), 1.64 (m, 8H, N[CH₂CH₂]CH₂), 1.56 (bs, 16H, N[CH₂CH₂]CH₂). ¹³C NMR (100 MHz, CDCl₃, δ_C): 167.3, 155.9, 134.3, 128.0, 121.8, 71.2, 45.2, 42.1, 31.4, 25.9, 25.1, 24.2. IR (ν/cm⁻¹): 2919, 2848, 1663, 1464, 1204, 1008, 761, 752. ESMS (m/z): 947.46 (M+Na). **Analysis:** Required for C₅₆H₆₈N₄O₈: C, 72.70; H, 7.41; N, 6.06; Found: C, 72.49; H, 7.43; N:5.99.

25,26,27,28-Tetrakis(((*N,N*-diethyl)carbonyl)methoxy)calix[4]arene (66)

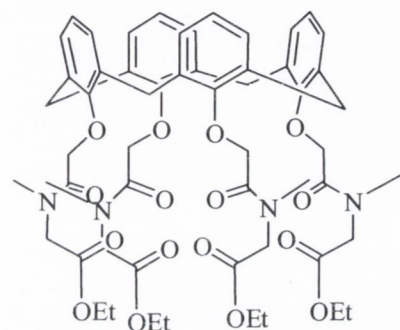


Calix[4]arene (**53**) (2.0 g, 4.7 mmol) was suspended in CH₃CN. To this suspension was added K₂CO₃ (3.9 g, 28 mmol) and **63** (7.25 g, 38 mmol). Following heating at reflux overnight, the mixture was filtered, washed with acetone and solvents were removed under reduced pressure. 1 M H₂SO₄ (10 mL) and water

(30 mL) were added to precipitate a solid which was collected by suction filtration, triturated with Et₂O and collected by suction filtration to yield the product as a buff solid (3.08 g, 74%). ¹H NMR (400 MHz, CDCl₃, δ_H): 6.72 (d, $J = 7.0$ Hz, 8H, Ar-H), 6.65 (t, $J =$

8.0 Hz, 4H, Ar-H), 5.20 (d, $J = 13.6$ Hz, 4H, Ar-CH₂-Ar), 4.98 (s, 8H, OCH₂C(O)), 3.35 – 3.40 (m, N(CH₂CH₃)₂), 3.28 (d, $J = 13.6$ Hz, Ar-CH₂-Ar), 1.11 – 1.20 (m, N(CH₂CH₃)₂). ¹³C NMR (100 MHz, CDCl₃, δ_C): 168.2, 155.9, 134.4, 128.1, 122.0, 71.1, 40.5, 39.6, 31.4, 13.8, 12.6. **Accurate MS** (m/z): Calculated for C₅₂H₆₈N₄O₈+Na: 899.4935, found 899.4970

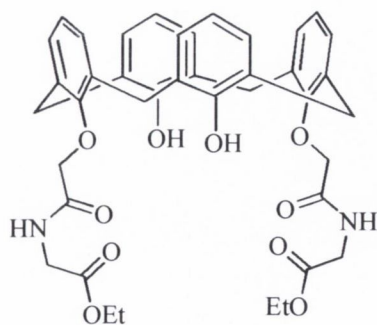
25,26,27,28-Tetrakis(*N*-sarcosiny)calix[4]arene tetraethyl ester (67)



Prepared analogously to **64**, alkylating calix[4]arene **53** (1.0 g, 2.4 mmol) with **58** (4.2 g, 9.6 mmol) in the presence of excess K₂CO₃ (3.0 g, 21 mmol) in CH₃CN (25 mL). The solvents were removed under reduced pressure, and the resulting residue partitioned between CH₂Cl₂ (50 mL) and water (50 mL). The layers were separated, the aqueous layer was washed with further

CH₂Cl₂, and organics were combined and dried (CaCl₂). Solvent was removed at reduced pressure to yield an oil which was dissolved in minimal CH₂Cl₂. Precipitated from EtOAc/Et₂O and recrystallised from EtOH to give **67** as a yellow powder in 11% yield. ¹H NMR (400 MHz, CD₃CO₂D, 70 °C): 7.21 (d, $J = 7.5$ Hz, 8H, Ar-H), 6.89 (t, $J = 7.5$ Hz, 4H, Ar-H), 4.82 (bs, 8H, OCH₂C(O)), 4.63 (d, $J = 12.5$ Hz, 4H, Ar-CH₂-Ar), 4.30 (s, 16H, OCH₂CH₃, NCH₂C(O), overlapping.), 3.47 (d, $J = 12.5$ Hz, 4H, Ar-CH₂-Ar), 3.08 (bs, 12H, NCH₃), 1.35 (bs, 12H, OCH₂CH₃). ¹³C NMR (100 MHz, CD₃CO₂D, δ_C): 169.8, 169.7, 152.6, 135.2, 128.7, 125.4, 73.3, 60.9, 49.0, 34.1, 29.2, 13.1.

25,27-Di(glyciny) calix[4]arene ethyl ester (71)

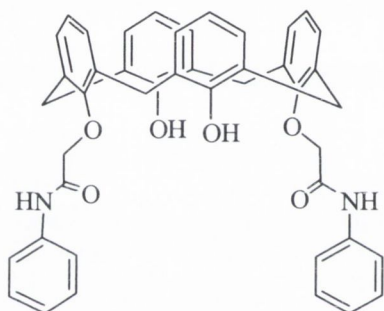


To calix[4]arene (**53**) (0.5 g, 1 mmol) in CH₃CN (40 mL) was added dry K₂CO₃ (0.69 g, 5 mmol). The suspension was stirred at 50 °C for 30 minutes to affect deprotonation. Ethyl 2-(2-bromoacetamido) acetate (1.32 g, 5 mmol) (CAUTION – irritant), was added in one portion, and the resulting suspension was heated at reflux overnight. Solvent was removed at reduced pressure, to yield a brown residue

which was partitioned between CH₂Cl₂ (100 mL) and water (100 mL). The organic layer was removed and washed with water (100 mL), 0.1 M HCl (1 × 50 mL) and once again with water (50 mL). This solution was dried (Na₂SO₄), and CH₂Cl₂ was removed under

reduced pressure, yielding a brown oily residue. To this was added ethanol, which was stirred at room temperature to precipitate a solid, which was collected as a buff powder by suction filtration (0.61 g, 86%). (m.p.: 222 °C) $^1\text{H NMR}$ (400 MHz, CDCl_3 , δ_{H}): 9.28 (bs, 2H, NH), 8.23 (s, 2H, OH), 7.13 (d, $J = 7.1$ Hz, 4H, Ar- H_{ortho}), 6.96 (d, $J = 7.5$ Hz, 4H, Ar- H_{ortho}), 6.74-6.82 (m, 4H, Ar- H_{para}), 4.68 (s, 4H, $\text{OCH}_2\text{C}(\text{O})$), 4.28 (d, $J = 13.1$ Hz, 4H, Ar- CH_2 -Ar), 4.21 (q, $J = 7.0$ Hz, 4H, OCH_2CH_3), 4.17 (s, 4H, $\text{NCH}_2\text{C}(\text{O})$), 3.51 (d, $J = 13.6$ Hz, 4H, Ar- CH_2 -Ar), 1.27 (t, $J = 7.5$ Hz, 6H, OCH_2CH_3). $^{13}\text{C NMR}$ (100 MHz, CDCl_3 , δ_{C}): 168.7, 168.7, 151.9, 151.0, 132.4, 129.2, 128.5, 127.0, 126.0, 119.7, 74.5, 61.1, 41.0, 31.3, 13.6. **IR** (v/cm^{-1}): 3311, 1743, 1682, 1464, 1207, 1044, 775, 768, 753. **ESMS** (m/z): 733.26 (M+Na). **Analysis:** Required for $\text{C}_{40}\text{H}_{42}\text{N}_2\text{O}_{10}$: C, 67.59; H, 5.96; N, 3.94. Found: C, 66.70; H, 5.85; N, 3.92.

25,27-Bis(((*N*-phenyl)carbonyl)methoxy)calix[4]arene (72)

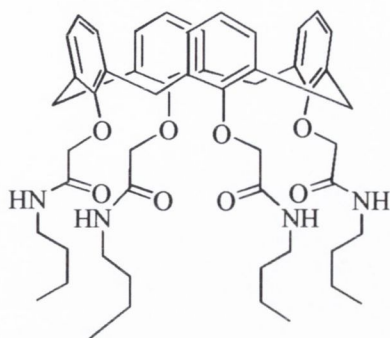


To a suspension of calix[4]arene (**53**) (1.0 g, 2.4 mmol) in CH_3CN (50 mL) was added K_2CO_3 (3.03 g, 14.2 mmol) and 2-bromoacetanilide (**62**) (14.2 mmol). The suspension was heated at reflux overnight, following which the solvent was removed *in vacuo*. The residue was then partitioned between CH_2Cl_2 (100 mL) and water (100 mL), and the organic residue extracted into CH_2Cl_2 . Following washes

($2 \times \text{H}_2\text{O}$, 50 mL), the organic layer was dried (Na_2SO_4), and the solvent removed at reduced pressure. The resultant oil was stirred with ethanol, giving the desired product as a white precipitate, which was collected by suction filtration as a white powder, m.p.: 297 °C (dec.) (1.23 g, 75%). This compound was crystallised for X-ray crystallography studies by adding CH_2Cl_2 , drop-wise, to a suspension of the compound in CH_3OH until a solution formed. This was then allowed to stand overnight, during which crystals which were suitable for X-ray analysis formed. $^1\text{H NMR}$ (400 MHz, CDCl_3 , δ_{H}): 10.25 (s, 2H, OH), 8.41 (s, 2H, NH), 7.39 (d, $J = 8$ Hz, 4H, Ar-H), 7.38 – 7.11 (m, 10H, Ph-H), 7.18 (d, $J = 8$ Hz, 4H, Ar-H), 6.94 (t, $J = 8$ Hz, 2H, Ar-H), 6.82 (d, $J = 7$ Hz, 2H, Ar-H), 4.67 (s, 4H, ArO- CH_2 -C(O)), 4.26 (d, $J = 14$ Hz, 4H, Ar- CH_2 -Ar), 3.62 (d, $J = 14$ Hz, 4H, Ar- CH_2 -Ar). $^{13}\text{C NMR}$ (100 MHz, CDCl_3 , δ_{C}): 164.5, 151.3, 149.9, 136.7, 132.2, 129.5, 128.7, 128.3, 127.0, 126.6, 124.1, 120.6, 118.7, 74.4, 31.4. **IR** (v/cm^{-1}): 3309, 1698, 1533, 1435, 1040,

758, 750, 690. **ESMS** (m/z): 713.27 (M+Na). **Analysis:** Required for $C_{44}H_{38}N_2O_6$: C, 76.50; H, 5.54; N, 4.06. Found: C, 74.08; H, 5.64, N, 4.28.

25,26,27,28-Tetrakis[*(N*-butyl)carbonyl]methoxy]calix[4]arene (75)

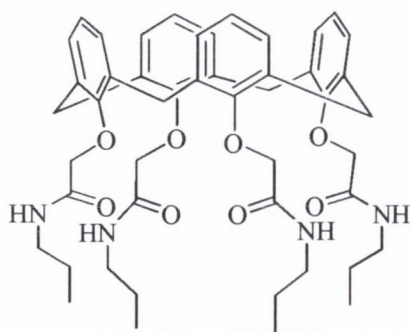


Using the procedure for the synthesis of 25,26,27,28-tetrakis[*(N*-propyl)carbonyl]methoxy] calix[4]arene, aminolysis of the ester, 25,26,27,28-tetrakis[(ethoxycarbonyl)methoxy]calix[4]arene, (**55**) (0.205 g, 0.26 mmol) using *n*-butylamine (2.0 mL, 20 mmol) afforded upon trituration with diethyl ether, the desired product as a white powder. (212 mg, 91%). Crystals suitable for X-ray

diffraction were grown by evaporation of a CH_2Cl_2 /methanol solution. (m.p.: 244–247 °C).

1H NMR (400 MHz, $CDCl_3$, δ_H): 7.39 (bs, 4H, NH), 6.61 (m, 12H, ArH), 4.49 (d, $J = 14$ Hz, 4H, Ar- CH_2 -Ar), 4.45 (s, 8H, ArO- CH_2 -C(O)), 3.36 (q, $J = 8$ Hz, $NCH_2CH_2CH_2CH_3$), 3.25 (d, 4H, Ar- CH_2 -Ar), 1.56 (m, 8H, $NCH_2CH_2CH_2CH_3$), 1.35 (m, 8H, $NCH_2CH_2CH_2CH_3$), 0.94 (t, $J = 7$ Hz, 12H, $NCH_2CH_2CH_2CH_3$). **^{13}C NMR** (100 MHz, $CDCl_3$, δ_C): 169.1, 133.8, 128.4, 122.8, 73.6, 38.7, 31.2, 30.5, 19.7, 13.4. **IR** (ν/cm^{-1}): 3280, 2953, 2929, 1654, 1547, 1460, 1438, 1089, 1052, 772. **ESMS** (m/z): 899.47 (M+Na). **Analysis:** Required for $C_{52}H_{68}N_4O_8 \cdot \frac{1}{2}CH_3OH$: C, 70.60; H, 7.90; N, 6.27. Found: C, 70.48; H, 7.84; N, 6.20.

25,26,27,28-Tetrakis[*(N*-propyl)carbonyl]methoxy]calix[4]arene (76)



To a solution of 25,26,27,28-tetrakis[(ethoxycarbonyl)methoxy]calix[4]arene (**55**) (500 mg, 0.6 mmol) in ethanol (20 mL) was added *n*-propylamine (5 mL, 61 mmol). The solution was heated at reflux for 48 h, and cooled to room temperature. Solvent and excess amine were removed under reduced pressure to yield an oily residue, which was trituated with diethyl ether. The

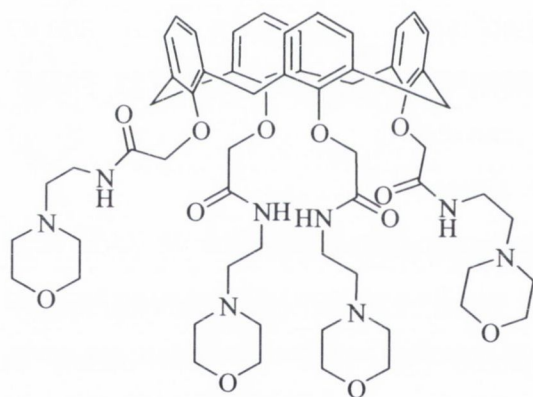
product, a fine white powder was collected by suction filtration and washed with cold diethyl ether. (453 mg, 85%), m.p.: 274 °C). Crystals suitable for X-ray diffraction were grown by evaporation of a CH_2Cl_2 /methanol solution. **1H NMR** (400 MHz, $CDCl_3$, δ_H): 7.38 (s, 4H, NH), 6.63 (m, 12H, ArH), 4.51 (d, $J = 14$ Hz, Ar- CH_2 -Ar), 4.45 (s, 8H, ArO- CH_2 -C(O)), 3.33 (m, 8H, $NCH_2CH_2CH_3$), 3.36 (d, $J = 14$ Hz, 4H, Ar- CH_2 -Ar), 1.61 (m,

8H, NCH₂CH₂CH₃), 0.95 (t, $J = 7$ Hz, 12H, NCH₂CH₂CH₃). ¹³C NMR (100 MHz, CDCl₃, δ_C): 169.1, 155.4, 133.8, 128.5, 122.8, 73.6, 40.7, 30.5, 22.4, 11.0. IR (v/cm⁻¹): 3289, 2965, 2925, 1658, 1551, 1459, 1445, 1083, 1052, 771, 760. **Accurate MS** (m/z): Calculated for C₄₈H₆₀N₄O₈Na (M+Na): 843.4309; found 843.4340. **Analysis:** Required for C₄₈H₆₀N₄O₈: C, 70.22; H, 7.37; N, 6.82. Found: C, 70.34; H, 7.37; N, 6.71.

General procedure for synthesis of ethylamino compounds

To **55** (500 mg, 0.65 mmol) was added the appropriate amine (3 – 10 mL, excess). The mixture became homogeneous after ~5 minutes. The solution was stirred under argon overnight. Excess amine was removed under reduced pressure by vacuum distillation, and the resultant residue triturated with diethyl ether. The solid was collected by suction filtration, washed with cold diethyl ether and air-dried, to give the desired compounds.

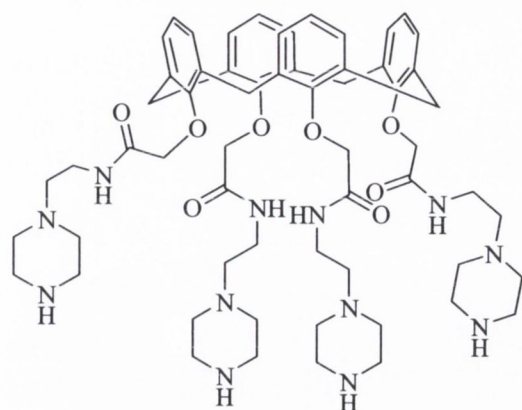
25,26,27,28-Tetrakis-*N*-((4-morpholino)-2-aminoethyl)carbamoyloxymethoxy calix[4]arene (**82**)



calix[4]arene (**82**)

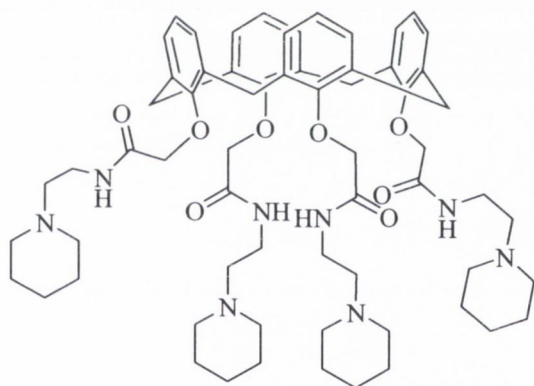
Yield: 640 mg, (89%) white powder. (m.p.: 137 °C). ¹H NMR (400 MHz, CDCl₃, δ_H): 7.57 (bs, 4H, NH), 6.63 (m, 12H, ArH), 4.48 (d, $J = 14$ Hz, 4H, Ar-CH₂-Ar), 4.48 (s, 8H, ArO-CH₂), 3.66 (bs, 16H, N[CH₂CH₂]O), 3.48 (q, 8H, NHCH₂CH₂), 3.26 (d, $J = 14$ Hz, 4H, Ar-CH₂-Ar), 2.54 (t, $J = 6$ Hz, 8H, NHCH₂CH₂), 2.46

(bs, 16H, N[CH₂CH₂]O). ¹³C NMR (100 MHz, CDCl₃, δ): 168.9, 133.7, 128.5, 122.9, 73.7, 66.4, 56.8, 53.0, 35.5, 30.6. IR (v/cm⁻¹): 3299, 2918, 2850, 2809, 1659, 1545, 1444, 1302, 1245, 1197, 1090, 1048, 1008, 867, 761. **MS** (m/z): 1128.39 (M+Na) **Accurate MS:** calculated 1106.6052 (M/2)+H; found 1106.6052. **Analysis:** Required for C₆₀H₈₀N₈O₁₂·1½H₂O: C, 63.64; H, 7.39; N, 9.90. Found: C, 63.76; H, 7.19; N, 10.18.

25,26,27,28-Tetrakis-*N*-((4-piperazinyl)-2-aminoethyl)carbamoyloxymethoxy

calix[4]arene (83)

Yield: 314 mg (44%), hygroscopic white powder; m.p: 98 °C. $^1\text{H NMR}$ (400 MHz, CDCl_3 , δ_{H}): 7.64 (s, 4H, NH), 6.63 (m, 12H, ArH), 4.51 (d, 4H, ArCH₂Ar), 4.48 (s, 8H, ArO-CH₂-C(=O)N), 3.48 (q, $J = 6$ Hz, H[NCH₂CH₂N]), 3.46 (d, $J = 14$ Hz, 4H, Ar-CH₂-Ar), 2.90 (m, 16H, N[CH₂CH₂N]), 2.54 (t,

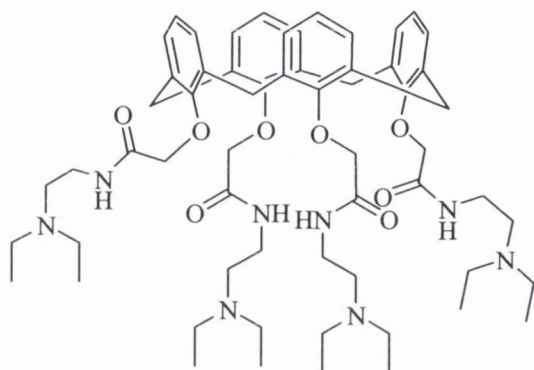
$J = 6$ Hz, HN[CH₂CH₂N]), 2.42 (m, 16H N[CH₂CH₂N]). $^{13}\text{C NMR}$ (100 MHz, CDCl_3) δ : 169.1, 133.7, 128.4, 122.8, 73.6, 57.1, 53.9, 45.6, 45.4, 35.6, 30.6. **IR** (v/cm^{-1}): 3301, 3062, 2912, 2850, 2809, 1659, 1538, 1439, 1244, 1194, 1115, 1094, 1009, 867, 852, 778, 761. **Accurate MS** (m/z): calculated 1102.6730 (M/2)+H; found 1102.6692

25,26,27,28-Tetrakis-*N*-(piperidiny-2-aminoethyl)carbamoyloxymethoxy-calix[4]arene (84)


Yield: 556 mg (78%), white powder. (m.p.: 201 °C) $^1\text{H NMR}$ (400 MHz, CDCl_3 , δ_{H}): 7.63 (bs, 4H, NH), 6.61 (m, 12H, Ar-H), 4.49 (d, $J = 13.8$ Hz, 4H, Ar-CH₂-Ar), 4.46 (s, 8H, ArO-CH₂-CO), 3.47 (q, $J = 6.5$ Hz, 8H, -NH-CH₂-CH₂), 3.26 (d, $J = 13.8$ Hz, 4H, Ar-CH₂-Ar), 2.50 (t, $J = 6.5$ Hz, 8H, NH-CH₂-CH₂),

2.39 (bs, 16H, N(CH₂CH₂)CH₂), 1.52 (m, 16H, N(CH₂CH₂)₂CH₂), 1.43 (m, 8H, N(CH₂CH₂)₂CH₂). $^{13}\text{C NMR}$ (100 MHz, CDCl_3 , δ_{C}): 169.0, 133.8, 128.4, 122.7, 73.7, 57.2, 54.0, 35.9, 30.6, 25.5, 23.9. **IR** (v/cm^{-1}): 3284, 2930, 2949, 2773, 1657, 1550, 1440, 1350, 1319, 1304, 1245, 1198, 1159, 1130, 1087, 1053, 1036, 1011, 831, 770, 758. **Accurate MS** (m/z): calculated 1098.6876 (M/2)+H; found 1098.6882 **Analysis** (%): Required for C₆₄H₈₈N₈O₈ ½ Et₂O: C, 69.87; H, 8.26; N, 9.88. Found: C, 69.90; H, 8.08; N, 10.24.

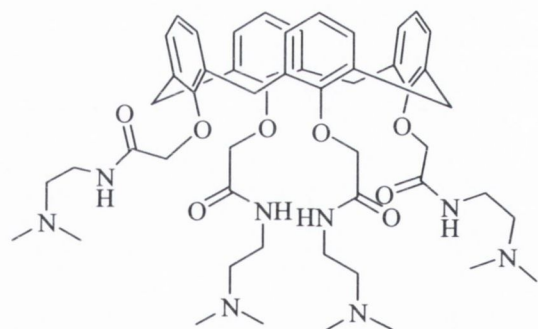
25,26,27,28-Tetrakis-*N*-(*N,N*-diethyl-2-aminoethyl)carbamoyloxymethoxycalix[4]-arene (85)



Yield: 424 mg, (62%) white powder. (m.p. 170 °C (dec.)). $^1\text{H NMR}$ (400 MHz, CDCl_3 , δ_{H}): 7.58 (bs, 4H, NH), 6.60 (m, 12H, Ar-H), 4.49 (d, $J = 14$ Hz, $J=14$ Hz, Ar- CH_2 -Ar), 4.46 (s, 8H, ArO- CH_2 -CO), 3.42 (q, $J = 6.5$ Hz, -NH- CH_2 - CH_2), 3.25 (d, $J = 14$ Hz, Ar- CH_2 -Ar), 2.61 (t, $J = 6.5$ Hz, 8H, -NH- CH_2 - CH_2 -), 2.53 (q, $J = 7$ Hz, 16H, $\text{N}(\text{CH}_2\text{CH}_3)_2$, 0.99 (t, $J = 7$

Hz, 24H, $\text{N}(\text{CH}_2\text{CH}_3)_2$. $^{13}\text{C NMR}$ (100 MHz, CDCl_3 , δ_{C}): 168.9, 133.8, 128.3, 122.7, 73.74, 51.2, 46.3, 36.7, 30.5, 11.2. **IR** (ν/cm^{-1}): 3299, 2966, 2934, 2794, 1685, 1649, 1543, 1457, 1432, 1383, 1353, 1295, 1247, 1203, 1186, 1091, 1067, 1046, 760. **Accurate MS** (m/z): calculated 1050.6882 (M/2)+H; found 1050.6882 **Analysis**: Required for $\text{C}_{60}\text{H}_{88}\text{N}_8\text{O}_8$: C, 68.87; H, 8.45; 10.68; Found: C, 67.01; H, 8.17; N, 10.44.

25,26,27,28-Tetrakis-*N*-(*N,N*-dimethyl-2-aminoethyl)carbamoyloxymethoxycalix[4]arene⁹² (17)



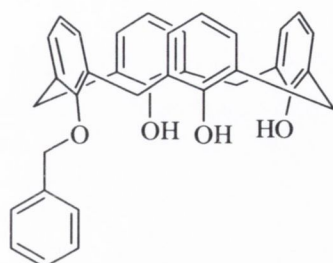
Yield: 536 mg, 88%, white powder, m.p: 208 °C. $^1\text{H NMR}$ (400 MHz, CDCl_3 , δ_{H}): 7.59 (bs, 4H, NH), 6.62 (m, 12H, Ar-H), 4.50 (d, $J = 14$ Hz, Ar- CH_2 -Ar), 4.47 (s, 8H, ArO- CH_2 -CO), 3.45 (q, $J = 6$ Hz, 8H, -NH- CH_2 - CH_2 -), 3.36 (d, $J = 14$ Hz, 4H, Ar- CH_2 -Ar), 2.46 (t, $J = 6$ Hz, 8H, -NH- CH_2 - CH_2 -), 2.21 (s, 24H, $\text{N}(\text{CH}_3)_2$).

$^{13}\text{C NMR}$ (100 MHz, CDCl_3 δ_{C}): 169.0, 155.4, 133.8, 128.4, 122.7, 73.7, 57.6, 44.9, 36.6, 30.6. **IR** (ν/cm^{-1}): 3301, 3006, 2983, 2944, 2776, 1653, 1546, 1459, 1441, 1276, 1260, 1189, 1157, 1086, 1054, 1043, 764, 751. **Accurate MS** (m/z): calculated 938.5608 (M/2)+H; found 938.5630.

General procedure attempted for complex formation

To a solution of the ligand in CH_3CN was added a solution of the appropriate lanthanide trifluoromethanesulfonate, chloride, nitrate or perchlorate salt (1 equiv.) in CH_3CN , and

the combined solution was allowed to stand at room temperature or reflux overnight. The flask contents were concentrated *in vacuo* and poured into a large excess of diethyl ether. The precipitate which formed was collected by suction filtration, and dried under high vacuum.

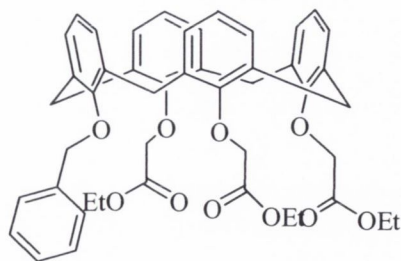


25-Benzyloxy-26,27,28-trihydroxy calix[4]arene^{171,173,175}

(96)

Calix[4]arene (53) (10.0g, 23.6 mmol) was suspended in CH₃CN. Anhydrous potassium carbonate (1.64, 11.88 mmol) was added and the mixture stirred for 30 minutes to afford deprotonation. Benzyl bromide (2.83 mL, 23.58 mmol) was then added and the contents refluxed overnight. The solvent was removed at reduced pressure and the remaining flask contents partitioned between water (30 mL) and CH₂Cl₂ (30 mL) the layers were separated and the aqueous layer washed with CH₂Cl₂ (10 mL). The combined organic layers were evaporated at reduced pressure affording a brown oil. Diethyl ether (100 mL) was added and the mixture stirred for 45 minutes. The product, a fine white powder was collected by filtration (8.17 g, 68%) (m.p.: 217-218 °C, lit.²⁰⁹ 235 °C). ¹H NMR (400 MHz, CDCl₃, δ_H): 9.56 (s, 1H, OH), 9.21 (s, 2H, OH), 7.49-7.76 (m, 5H, Ar-H), 7.12 (d, *J* = 7.6 Hz, 4H, Ar-H), 7.06 (d, *J* = 7.6, 2H, Ar-H), 6.99 (t, *J* = 7.5 Hz, 2H, Ar-H), 6.91 (t, *J* = 7.8 Hz 1H, Ar-H), 6.68 (m, 3H, Ar-H), 5.22 (s, 2H, O-CH₂-Ph), 4.39 (d, *J* = 13 Hz, 2H, Ar-CH₂-Ar), 4.27 (d, *J* = 14 Hz, 2H Ar-CH₂-Ar), 3.45 (d, *J* = 9 Hz, 4H, Ar-CH₂-Ar).

25-Benzyloxy-26,27,28-tris(methoxycarbonyl)ethoxy calix[4]arene^{171,173,175}(97)

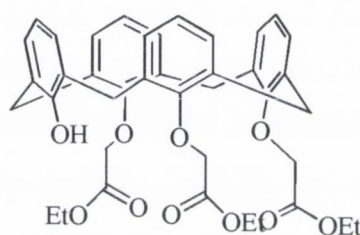


25-Benzyloxy-26,27,28-trihydroxy calix[4]arene (96) (3.0 g, 5.83 mmol) was suspended in CH₃CN (30 mL) with potassium carbonate (1.82 g, 13 mmol) and the mixture stirred for 30 minutes to initiate deprotonation. Ethyl bromoacetate (3.33 mL, 30 mmol) was added and the mixture refluxed overnight. The flask contents were

cooled and the solvent was removed under reduced pressure. The resultant oil was stirred with CH₂Cl₂ (30 mL) and water (30 mL) for 30 minutes. The solvents were separated, with washing of the aqueous layer with further CH₂Cl₂ (2 × 10mL). The combined organic layers were evaporated and the residue stirred with diethyl ether (30 mL) for 30 minutes.

The resulting solid was filtered off and discarded. The filtrate was evaporated at reduced pressure to yield an oil, which, when stirred in ethanol (100 mL) precipitated the desired product which was collected by filtration. (2.23 g, 49%) (m.p.: 98-100 °C, lit.^{171,173}: not reported). ¹H NMR (400 MHz, CDCl₃, δ_H): 7.73 (m, Ar-H), 7.42 (m, Ar-H), 6.62 (m, Ar-H), 5.02 (s, 2H, O-CH₂-Ph), 4.85 (d, *J* = 12 Hz, 2H, Ar-CH₂-Ar), 4.69 (s, 4H, Ar-O-CH₂-C(O)OEt), 4.61 (s, 2H, Ar-O-CH₂-C(O)OEt), 4.44 (d, *J* = 13.5 Hz, 2H, Ar-CH₂-Ar), 4.18 (q, *J* = 4 Hz, 2H, OCH₂CH₃), 3.73 (q, *J* = 7 Hz, 4H, OCH₂CH₃), 3.25 (d, *J* = 13.5 Hz, Ar-CH₂-Ar), 3.07 (d, *J* = 13.5 Hz, 2H, Ar-CH₂-Ar), 1.24 (t, *J* = 7 Hz, 12H, OCH₂CH₃). ESMS (*m/z*): 795.28 (M+Na).

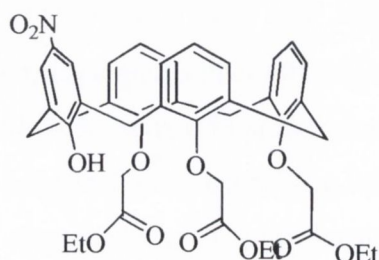
26,27,28-Tris(methoxycarbonyl)ethoxy calix[4]arene^{171,173,175} (98)



25-Benzyloxy-26,27,28-tris(methoxycarbonyl)ethoxy calix[4]arene (97) (2.0g 2.5 mmol), ammonium formate (575 mg, 9 mmol) and palladium/charcoal (10%, 100 mg) were refluxed in ethanol (30 mL) for 3 hours. The solution was poured into CH₂Cl₂ (30 mL) and filtered with suction

through Celite[®], and washed twice with CH₂Cl₂ (20 mL). The solvents were removed at reduced pressure. The resultant oil was dissolved in minimal CH₂Cl₂. Ethanol (30 mL) was added, and the mixture stirred for 30 minutes. The product, a white precipitate was then collected with suction (1.26 g, 72%) (m.p.: 131 °C, lit.^{171,173}: not reported). ¹H NMR (400 MHz, CDCl₃, δ_H): 7.12 (d, *J* = 7.5 Hz, 2H, Ar-H), 7.06 (d, *J* = 7.5 Hz, 2H, Ar-H), 6.93 (t, *J* = 8 Hz, 1H, Ar-H), 6.71 (t, *J* = 7.6 Hz, 2H, Ar-H), 6.51 (m, Ar-H), 6.19 (s, OH), 4.96 (d, *J* = 13 Hz, 2H, Ar-CH₂-Ar), 4.62 (d, *J* = 16 Hz, 4H, ArO-CH₂-C(O)OEt), 4.54 (d, *J* = 16 Hz, 2H, ArO-CH₂-C(O)OEt), 4.37 (d, *J* = 13 Hz, 2H, Ar-CH₂-Ar), 4.28 (q, *J* = 7 Hz, 2H, OCH₂CH₃), 4.14 (q, *J* = 7 Hz, 4H, OCH₂CH₃), 3.34 (d, *J* = 7 Hz, 2H, Ar-CH₂-Ar), 3.32 (d, *J* = 7 Hz, 2H, Ar-CH₂-Ar), 1.33 (t, *J* = 7 Hz, OCH₂CH₃), 1.26 (t, *J* = 7 Hz, 6H, OCH₂CH₃).

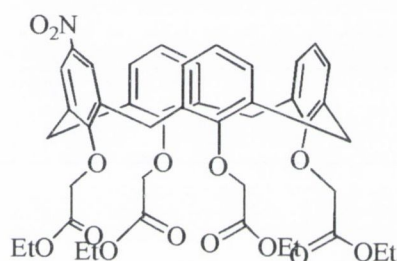
5-Nitro-27,28,29-tris(methoxycarbonyl)ethoxy calix[4]arene^{171,173,175} (99)



26,27,28-Tris(methoxycarbonyl)ethoxy calix[4]arene (98) (1.0 g, 1.38 mL) was dissolved in CH₂Cl₂ (20 mL). Ammonium nitrate (2.0 g, 25 mmol), dissolved in H₂O (10 mL) and HCl (35%, 6 mL) was added to the CH₂Cl₂

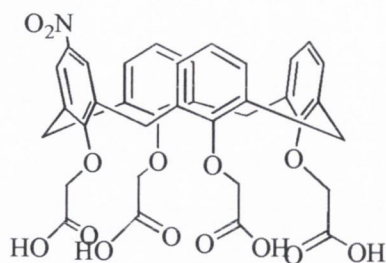
solution. Two drops of acetic anhydride were added and the mixture stirred vigorously for 15 minutes. The layers were separated, and the organic solvent removed *in vacuo*. The residue was dissolved in minimal CH_2Cl_2 and ethanol added to precipitate a fine yellow powder as product (390 mg, 41%), m.p.: 168 °C (lit.¹⁷⁴ 157-159 °C). $^1\text{H NMR}$ (400 MHz, CDCl_3 , δ_{H}): 8.02 (s, 1H, OH), 7.96 (s, 2H, Ar-H), 7.04 (d, $J = 7.5$ Hz, 2H, Ar-H), 6.81 – 6.89 (t, $J = 7.5$ Hz, 2H, Ar-H), 6.61 – 6.65 (m, Ar-H), 5.03 (s, 2H, $\text{OCH}_2\text{C}(\text{O})\text{OEt}$), 4.91 (d, $J = 14$ Hz, Ar- CH_2 -Ar), 4.75 (d, $J = 16$ Hz, 2H, $\text{OCH}_2\text{C}(\text{O})\text{OEt}$), 4.47 (d, $J = 16$ Hz, 2H, $\text{OCH}_2\text{C}(\text{O})\text{OEt}$), 4.43 (d, $J = 14$ Hz, 2H, Ar- CH_2 -Ar), 4.31 (q, $J = 7$ Hz, 4H, OCH_2CH_3), 4.18 (q, $J = 7$ Hz, 2H, OCH_2CH_3), 3.42 (d, $J = 14$ Hz, 2H, Ar- CH_2 -Ar), 3.32 (d, $J = 14$ Hz, 2H, Ar- CH_2 -Ar), 1.36 (t, $J = 7$ Hz, 6H, CH_2CH_3), 1.28 (t, $J = 7$ Hz, 3H, CH_2CH_3).

5-Nitro-26,27,28,29-tetra(methoxycarbonyl)ethoxy calix[4]arene^{171,173,175} (100)



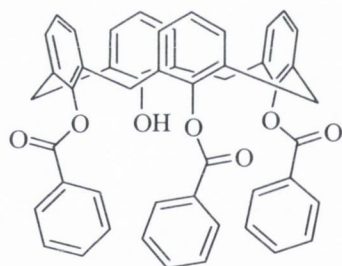
5-Nitro-27,28,29-tris(methoxycarbonyl)ethoxy calix[4]arene (**99**) (300 mg, 0.41 mmol) was dissolved in CH_3CN (10 mL) and potassium carbonate (500 mg, 3.62 mmol) was added. The mixture was stirred for 30 minutes to afford deprotonation. Ethyl bromoacetate (240 μL , 2.1 mmol) was added and the mixture refluxed overnight.

Solvent was removed at reduced pressure and the residue stirred with water/ CH_2Cl_2 for 10 minutes. The layers were separated and the aqueous layer washed with CH_2Cl_2 . Organic layers were combined and solvent evaporated. The residue was stirred in 2-propanol (15 mL) for 3 hours and the resulting precipitate removed by filtration to yield the product as a fine yellow powder (240 mg, 71%). m.p.: 122-124 °C, lit. value not reported. $^1\text{H NMR}$ (400 MHz, CDCl_3 , δ_{H}): 7.26 (s, 2H, Ar-H), 6.84 – 6.91 (m, 4H, Ar-H), 6.38 (s, 2H, Ar-H), 5.01 (d, $J = 14$ Hz, 2H, Ar- CH_2 -Ar), 4.84 (d, $J = 16$ Hz, 4H, $\text{ArOCH}_2\text{C}(\text{O})\text{OEt}$), 4.78 (s, 2H, $\text{ArOCH}_2\text{C}(\text{O})\text{OEt}$), 4.66 (d, $J = 14$ Hz, 2H, Ar- CH_2 -Ar), 4.61 (s, 2H, $\text{ArOCH}_2\text{C}(\text{O})\text{OEt}$), 4.19 – 4.29 (m, 8H, OCH_2CH_3), 3.33 (d, $J = 14$ Hz, 2H, Ar- CH_2 -Ar), 3.27 (d, $J = 14$ Hz, 2H, Ar- CH_2 -Ar), 1.27 – 1.34 (m, 12H, OCH_2CH_3). **Accurate MS** (m/z): expected for $\text{C}_{44}\text{H}_{47}\text{NO}_{14}\text{Na}$ (M+Na): 836.2894; found: 836.2892.

5-Nitro-26,27,28,29-tetra(hydroxycarbonyl)methoxy calix[4]arene¹⁷⁴ (102)

5-Nitro-26,27,28,29-tetra(methoxycarbonyl)ethoxy calix[4]arene (**100**) (2.0 g, 2.46 mmol) was dissolved in THF. Tetramethylammonium hydroxide pentahydrate (4.45 g, 25 mmol) was dissolved in methanol (10 mL) and water (40 mL). The solutions were combined and refluxed overnight.

The solvents were removed at reduced pressure to leave a yellow residue to which 10% HCl (20 mL) was added. The precipitate which formed was collected by suction filtration and purified by column chromatography (95:5 CH₂Cl₂/CH₃OH) to yield an oil which when triturated with methanol yielded the product as a fine yellow crystalline solid (1.05 g, 60%). ¹H NMR (400 MHz, CDCl₃, δ_H): 7.27 (s, 2H, Ar-H), 6.93 – 6.85 (m, 6H, Ar-H), 6.40 (s, 3H, Ar-H), 4.82 (s, 2H, ArOCH₂C(O)OH), 4.78 (d, *J* = 14Hz, 2H, Ar-CH₂-Ar), 4.64 (s, 2H, ArOCH₂C(O)OH), 3.77 (s, 4H, ArOCH₂C(O)OH), 3.34 (d, *J* = 14 Hz, 2H, Ar-CH₂-Ar), 3.24 (d, *J* = 14 Hz, 2H, Ar-CH₂-Ar).

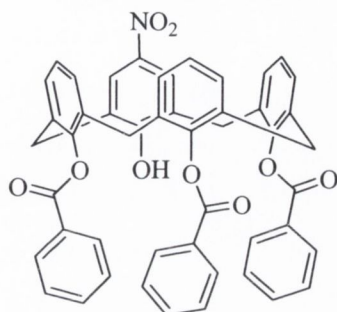
25,26,27-Tribenzoyl-28-hydroxy calix[4]arene (103)

Calix[4]arene (**53**) (4.24 g, 10 mmol) was dissolved in dry pyridine (50 mL) and the solution was cooled to 0 °C. Benzoyl chloride (9.4 mL, 81 mmol) was added by syringe and the solution was stirred for 1h, after which it was allowed to warm to room temperature and stirred for a further 1h. The solution was poured into water (400 mL) and stirred with

trituration to disperse any particles which persisted. The solid which precipitated from the slightly fluorescent solution was collected by suction filtration and crystallised from CHCl₃/CH₃OH as a pale yellow crystalline solid (5.30 g, 72%). ¹H NMR (400 MHz, CDCl₃, δ_H): 8.08 (d, *J* = 7.0 Hz, 4H, Ar-H), 7.74 (t, *J* = 7.5 Hz, 2H, Ar-H), 7.51 (t, *J* = 8.0 Hz, 5H, Ar-H), 7.22 (m, 4H, Ar-H), 7.05 (d, *J* = 7.5 Hz, 2H, Ar-H), 7.00 (dd, *J* = 6.5 Hz, 2H, Ar-H), 6.90 (d, *J* = 7.5 Hz, 2H, Ar-H), 7.52 (dt, *J* = 7.5, 2H, Ar-H), 6.60 (m, 4H, Ar-H), 3.90 (d, *J* = 14.5 Hz, 2H, Ar-CH₂-Ar), 3.83 (d, *J* = 15.5 Hz, 2H, Ar-CH₂-Ar), 3.73 (d, *J* = 15.6 Hz, 2H, Ar-CH₂-Ar), 3.51 (d, *J* = 14.0 Hz, 2H, Ar-CH₂-Ar). ¹³C NMR (100 MHz, CDCl₃, δ_C): 164.1, 163.6, 152.3, 147.8, 146.2, 133.4, 133.1, 132.7, 132.4, 132.1, 130.9,

130.1, 129.9, 129.1, 128.8, 128.5, 128.3, 128.2, 127.6, 127.3, 125.6, 124.7, 119.3, 37.0, 31.9. **Accurate MS** (m/z): Expected for $C_{49}H_{36}O_7Na$ ($M+Na$): 759.2359; found: 759.2396.

5-Nitro-25-hydroxy-26, 27, 28-tribenzoyloxycalix[4]arene¹⁷⁶ (104)

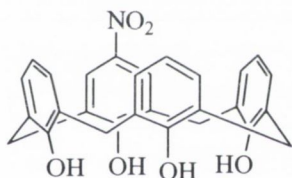


To **103** (2.0 g, 2.7 mmol) in CH_2Cl_2 (50 mL), was added AcOH (1.5 mL) and HNO_3 (85%, 0.2 mL) and the solution was allowed to stir at room temperature for 1 h. Aqueous NaOH (1 M, 50 mL) was added and the resulting two phases were separated. The organic phase was dried (Na_2SO_4), evaporated to dryness under reduced pressure and triturated

with hot methanol. The resulting yellow solid was collected by suction filtration, and identified in accordance with literature characterisation to be the product (1.32 g, 62%).

¹H NMR (400 MHz, $CDCl_3$): 8.04 – 6.66 (m, 26H, Ar-H), 3.94-3.51 (m, 8H, Ar- CH_2 -Ar).

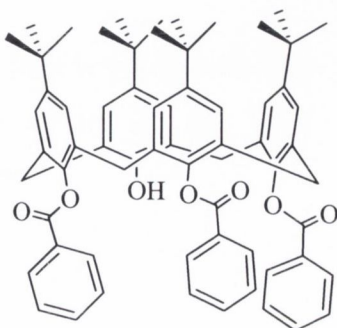
5-Nitro-25, 26, 27, 28-tetrahydroxycalix[4]arene¹⁷⁶ (105)



To **104** (980 mg, 1.3 mmol) in THF (20 mL) and EtOH (20 mL) was added NaOH (3.0 g, 75 mmol) in water (15 mL). The combined solution was heated at reflux for 6 h. HCl (conc.) was added dropwise to acidify the solution, and the resulting

precipitate was collected by suction filtration, and washed successively with water and diethyl ether to yield the desired product as a yellow powder (306 mg, 52%), m.p. 311 °C (dec.), lit. >300 °C (dec.). ¹H NMR (400 MHz, $CDCl_3$): 10.18 (s, 4H, OH), 8.01 (s, 2H, ArH), 7.15 (d, $J = 7.52$, 2H, ArH), 7.15 (d, $J = 8.0$ Hz, 2H, ArH), 7.07 (d, $J = 8.0$ Hz, 2H, ArH), 6.82 (t, $J = 8.0$ Hz, 2H, ArH), 6.75 (t, $J = 7.5$ Hz, 1H, ArH), 4.28 (bs, 4H, Ar- CH_2 -Ar), 3.62 (bs, 4H, Ar- CH_2 -Ar).

5,11,17,23-Tetra-*tert*-butyl-25,26,26-tribenzoyl-28-hydroxycalix[4]arene (106)

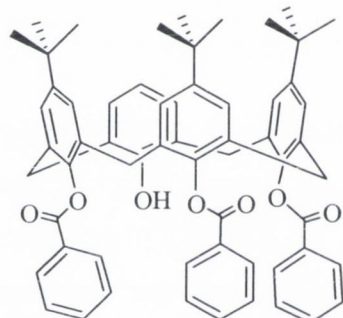


A modification to the procedure of Berthalon¹⁷⁷

*t*Bu calixarene (**1**) (5.0 g, 7.7 mmol), *N*-methylimidazole (3.0 mL, 37 mmol), and benzoyl chloride (2.4 mL, 21 mmol) were combined in dry THF (50 mL) and heated at reflux for 1 h. The solution was cooled and a further quantity of benzoyl chloride (1 mL, 9 mmol) was added. The flask contents were

stirred overnight. Further *N*-methylimidazole (1 mL) and benzoyl chloride (1 mL) was added and the solution was stirred for a further 2h. The mixture was poured into water (50 mL) and stirred. The crude product was collected by filtration, and was triturated with CH₃CN to give a white powder (5.78 g, 78%), m.p. 328 °C, lit. 335-336 °C. ¹H NMR (400 MHz, CDCl₃, δ_H): 8.07 (d, *J* = 7.6 Hz, 4H, ArH), 7.53 (t, *J* = 7.5 Hz, 2H, Ar-H), 7.27 (s, 2H, Ar-H), 7.18 (t, *J* = 8.0 Hz, 5H, Ar-H), 6.96 (s, 2H, Ar-H), 6.92 (s, 2H, Ar-H), 6.29 (m, 3H, Ar-H), 6.53 (m, 3H, Ar-H), 4.18 (d, *J* = 13.5 Hz, 2H, Ar-CH₂-Ar), 4.04 (d, *J* = 16.6 Hz, 2H, Ar-CH₂-Ar), 3.83 (d, *J* = 17.0 Hz, 2H, Ar-CH₂-Ar), 3.47 (d, *J* = 13.6, 2H, Ar-CH₂-Ar), 1.43 (s, 9H, C(CH₃)₃), 0.85 (s, 9H, C(CH₃)₃), 0.70 (s, 18H, C(CH₃)₃). ¹³C NMR (100 MHz, CDCl₃, δ_C): 164.5, 162.8, 149.5, 148.1, 147.5, 143.6, 142.4, 132.6, 132.1, 131.6, 131.2, 129.9, 129.5, 128.9, 128.6, 127.9, 127.4, 127.4, 126.1, 125.6, 125.1, 125.0, 38.5, 33.7, 33.4, 33.2, 31.9, 31.4, 31.0, 30.5, 30.2.

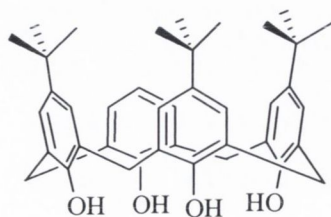
5,11,17-Tris-*tert*-butyl-25,26,26-tribenzoyl-28-hydroxycalix[4]arene¹⁷⁷ (107)



To AlCl₃ (7.8 g, 2.1 mmol) in toluene (200 mL) was added **106** (2.0 g, 2.1 mmol). Following initial warming to drive the suspension into solution, the reaction was allowed to stir at room temperature for 4 h. The solution was poured into HCl (1 M, 250 mL) with stirring, and the phases were separated. The aqueous phase was extracted with CH₂Cl₂ (1 × 100 mL). The organic phases were combined, dried (Na₂SO₄) and

evaporated to dryness under reduced pressure. The resulting residue was triturated with CH₃CN to yield the product as a white powder (1.60 g, 68%). ¹H NMR (400 MHz, CDCl₃, δ_H): 7.95 (d, *J* = 8.5 Hz, 4H, Ar-H), 7.45 (t, *J* = 7.5 Hz, 2H, Ar-H), 7.13 – 7.09 (m, 7H, Ar-H), 6.88 – 6.83 (m, 4H, Ar-H), 6.59 – 6.48 (m, 7H, Ar-H), 4.06 (d, *J* = 13.5 Hz, 2H, Ar-CH₂-Ar), 3.94 (d, *J* = 16.6 Hz, 2H, Ar-CH₂-Ar), 3.74 (d, *J* = 16.6 Hz, 2H, Ar-CH₂-Ar), 3.41 (d, *J* = 14.0 Hz, 2H, Ar-CH₂-Ar), 0.75 (s, 9H, C(CH₃)₃), 0.63 (s, 18H, C(CH₃)₃).

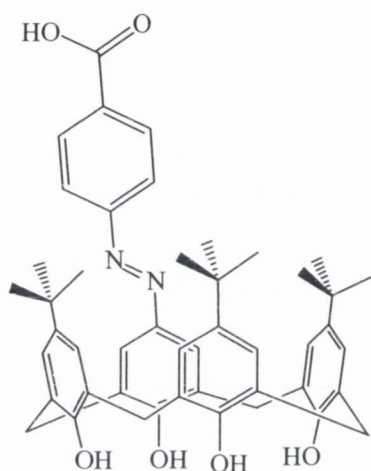
5,11,17-Tris-*tert*-butyl-calix[4]arene¹⁷⁷ (108)



5,11,17-Tris-*tert*-butyl-25,26,26-tribenzoyl-28-hydroxycalix[4]arene (**107**) (2.13 g, mmol) and NaOH (8.5 g, mmol) were combined in EtOH (100 mL) and water (100 mL). The solution was heated at reflux overnight after which a peach-coloured solution remained. This was brought to pH 6 using conc. HCl,

upon which the solution became opaque. The product was extracted into CHCl_3 (3×50 mL), dried (MgSO_4) and the solvent concentrated under reduced pressure. The resulting residue was stirred in CH_3OH , upon which a beige solid precipitated which was collected by filtration (1.22 g, 88%). m.p.: 324°C (dec.); lit. $324\text{--}325^\circ\text{C}$ (dec.). $^1\text{H NMR}$ (400 MHz, CDCl_3 , δ_{H}): 10.31 (s, 4H, OH), 7.10–7.06 (m, 4H, Ar-H), 7.06 (s, 2H, Ar-H), 7.04 (s, 2H, Ar-H), 6.74 (t, $J = 7.5$ Hz, 1H, Ar-H), 4.27 (bs, 4H, Ar- CH_2 -Ar), 3.53 (bs, 4H, Ar- CH_2 -Ar), 1.24 (s, 18H, $\text{C}(\text{CH}_3)_3$), 1.22 (s, 9H, $\text{C}(\text{CH}_3)_3$).

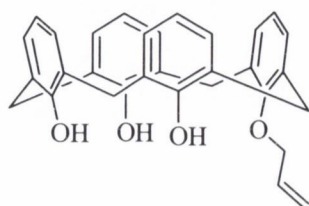
5-(4-Carboxyphenylazo)-11,17,23-tris-*tert*-butyl calix[4]arene (110)



4-Aminobenzoic acid (1.37 g, 10 mmol) and 2 mL of conc. HCl were added to 15 mL water, and the solution was cooled on ice to 2°C . A solution of NaNO_2 (0.8 g, 10 mmol) in water (10 mL) was added dropwise, keeping the temperature $<5^\circ\text{C}$. The resulting suspension was added at 5°C to a solution of 5,11,17-tris-*tert*-butyl calix[4]arene (**108**) (0.59 g, 1 mmol) and $\text{CH}_3\text{CO}_2\text{Na}$ (2.08 g, 20 mmol) in DMF (20 mL). The solution was allowed to warm to room temperature, and stirred for 2 h, and then heated at 60°C for 30 min. The

mixture was acidified with dilute HCl to pH ~ 5 , and the resulting precipitate was collected by filtration and washed with water and methanol. The solid was dissolved in 1 M NaHCO_3 (100 mL), and then the product re-precipitated from solution using conc. HCl. The resulting precipitate was collected by filtration and once again washed with water and methanol, to yield a fine red powder (170 mg, 23%), m.p. $>350^\circ\text{C}$. $^1\text{H NMR}$ (400 MHz, $\text{DMSO-}d_6$, δ_{H}): 10.35 (bs, 4H, OH), 8.22 (d, $J = 8.8$ Hz, 2H, $\text{C}_6\text{H}_4(\text{CO}_2\text{H})$), 7.86 (d, $J = 8.8$ Hz, 2H, $\text{C}_6\text{H}_4(\text{CO}_2\text{H})$), 7.75 (s, 2H, Ar-CH), 7.13 (d, $J = 5.9$ Hz, 4H, Ar-H), 7.06 (s, 2H, Ar-H), 4.32 (m, Ar- CH_2 -Ar), 3.86 (m, Ar- CH_2 -Ar), 1.25 (s, 18H, $\text{C}(\text{CH}_3)_3$), 1.21 (s, 9H, $\text{C}(\text{CH}_3)_3$). $^{13}\text{C NMR}$ (100 MHz, $\text{DMSO-}d_6$ δ_{C}): 166.8, 147.0, 146.5, 143.6, 143.6, 131.6, 130.7, 130.7, 130.5, 128.7, 128.3, 127.1, 125.9, 125.3, 125.2, 124.3, 122.9, 121.7, 48.6, 33.8, 33.7, 31.2, 31.1.

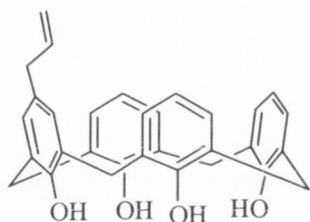
25-Allyloxy-26,27,28-tetrahydroxycalix[4]arene³⁵ (111)



Calixarene (**53**) (10.00 g, 23.5 mmol) was suspended in CH_3CN , and finely powdered sodium methoxide (1.58 g, 27.7 mmol) was added, and the mixture was stirred at 50°C for 30 min. Allyl

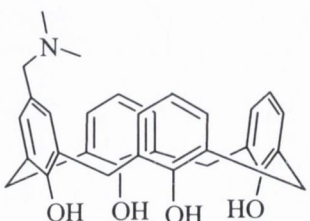
bromide (6.17 mL, 71 mmol) was then added. This mixture was then stirred at reflux temperature overnight. The reaction mixture was cooled to room temperature and quenched by addition of a few drops of 1 M HCl. The solvents were evaporated under reduced pressure and the solid was dissolved in minimal CHCl_3 . This solution was cooled to 0 °C and CH_3OH was added drop-wise, with stirring to precipitate the title compound as small white needles. (7.04 g, 64%), m.p. 205-207 °C (lit. 201 - 202 °C). $^1\text{H NMR}$ (400 MHz, CDCl_3 , δ_{H}): 9.74 (s, 1H, OH), 9.33 (s, 2H, OH), 7.13-7.02 (m, 9H, ArH), 6.91 (t, $J = 7.5$ Hz, 1H, ArH), 6.77-6.67 (m, 4H, ArH), 6.52-6.42 (m, 1H, $\text{CH}=\text{CH}_2$), 5.70 (d, 1H, $J = 18$ Hz, $\text{CH}=\text{CH}_2$ trans), 5.55 (d, $J = 10.5$ Hz, 1H, $\text{CH}=\text{CH}_2$ cis), 4.71 (d, $J = 6$ Hz, 2H), 4.41 (d, $J = 13.0$ Hz, 2H, Ar- CH_2 -Ar), 4.29 (d, $J = 13.5$ Hz, Ar- CH_2 -Ar), 3.51 (s, 2H, Ar- CH_2 -Ar), 3.48 (m, 2H, Ar- CH_2 -Ar). $^{13}\text{C NMR}$ (DEPT 135, 100 MHz, CDCl_3 , δ_{C}): 132.3, 129.4, 129.0, 128.9, 128.8, 128.5, 126.3, 122.3, 122.0, 121.0, 120.4, 77.8, 31.9, 31.6.

5-Allyl-25,26,27,28-tetrahydroxycalix[4]arene³⁵ (112)



25-Allyl-26,27,28-trihydroxycalix[4]arene (**111**) (0.50 g, 1.1 mmol) was suspended in *N,N*-diethylaniline (40 mL), and this mixture was then heated (using a heating mantle and boiling chips) to reflux temperature (>217 °C). After approx. 1 h, a clear pink solution was observed. Heating was continued for a further 3 h, and the solution was then cooled to room temperature. 1 M HCl was added with vigorous stirring until the pH was < 7, and the solid was collected by suction filtration, and washed with CH_3OH , to give a brown-grey solid (0.18 g, 35%). Due to decomposition on repeating this reaction, this product has been characterised (in agreement with the literature³⁵) by $^1\text{H NMR}$ only. $^1\text{H NMR}$ (400 MHz, CDCl_3 , δ_{H}): 10.22 (s, 4H, OH), 7.07 (dd, $J = 7.5$ Hz, 6H, Ar-H), 6.83 (s, 2H, Ar-H), 6.75 (dt, $J = 7.5$ Hz, 3H, Ar-H), 5.88 (m, 1H, $\text{CH}=\text{CH}_2$), 5.07 (m, 1H, $\text{CH}=\text{CH}_2$), 5.04 (m, 1H, $\text{CH}=\text{CH}_2$), 4.27 (bs, 4H, Ar- CH_2 -Ar), 3.52 (bs, 4H, Ar- CH_2 -Ar), 3.19 (m, 2H, Ar- CH_2 -CH=CH₂).

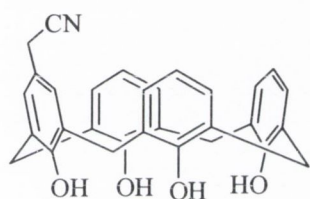
5-[(*N,N*-Dimethylamino)methyl]-25,26,27,28-tetrahydroxycalix[4]arene³⁹ (116)



Calix[4]arene (**53**) (9.45 g, 22 mmol) was dissolved in THF (200 mL). To this solution, with stirring, was added 37% formaldehyde (2 mL, 22 mmol) and dimethylamine (5.5 mL, 1 M CH_3OH solution). After 2 h, a thick white precipitate had

formed which was collected by suction filtration and washed with water and methanol. The solid was then triturated with acetone and collected by suction filtration to yield the title compound as a white powder. (4.07 g, 38%), m.p. >350, dec. (lit. 350 °C, dec.). $^1\text{H NMR}$ (400 MHz, CDCl_3 , δ_{H}): 7.04 (s, 2H, Ar-ortho- $\text{CH}_2\text{N}(\text{CH}_3)_2$), 6.98 (d, $J = 7.0$ Hz, 2H, Ar-H), 6.94 (d, $J = 7.0$ Hz, 4H, Ar-H), 6.43-6.38 (m, 3H, Ar-H), 4.31-4.38 (m, 4H, Ar- CH_2 -Ar), 3.91 (s, 2H, Ar- CH_2 - $\text{N}(\text{CH}_3)_2$), 3.24 (d, $J = 11.0$ Hz, 4H, Ar- CH_2 -Ar), 2.62 (s, 6H, $\text{N}(\text{CH}_3)_2$). $^{13}\text{C NMR}$ (100 MHz, CDCl_3 , δ_{C}): 157.7, 154.6, 153.8, 130.9, 130.8, 130.7, 130.4, 130.0, 127.8, 127.6, 118.4, 118.0, 118.0, 60.3, 41.6, 32.8, 32.1. **ESMS** (m/z): 437.16 ($[\text{M}-\text{N}(\text{CH}_3)_2]^+$).

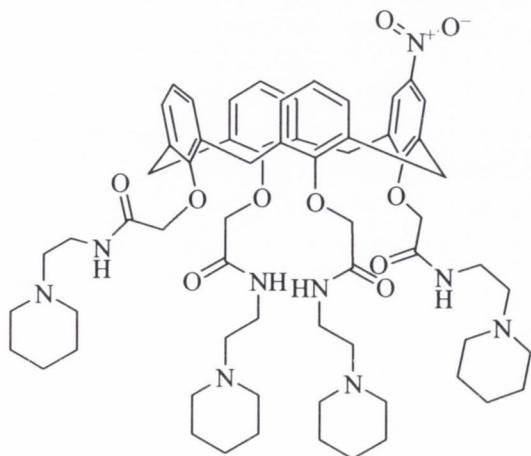
5-(Cyanomethyl)25,26,27,28-tetrahydrocalix[4]arene³⁹ (118)



5-[(*N,N*-Dimethylamino)methyl]-25,26,27,28-tetrahydrocalix[4]arene (**116**) (5.00 g, 10.4 mmol) was dissolved in DMSO (150 mL). Methyl iodide (2.1 g, 14.7 mmol) was then added and the solution was stirred for 1 h. Powdered NaCN (7.4 g, 14 mmol) was added and the reaction mixture stirred for 24 h at room temperature. The solution was poured into 1 M HCl (**CAUTION**), collecting liberated HCN in a series of gas-scrubbing solutions of NaOCl. The solid was collected by suction filtration, and purified by column chromatography (flash SiO_2 , CH_2Cl_2), to yield the desired product.

(0.21 g, 4%), m.p. >350 °C (dec.) (lit. 365 – 366 °C). $^1\text{H NMR}$ (400 MHz, CDCl_3 , δ_{H}): 9.84 (bs, 4H, OH), 7.04-6.85 (m, 8H, ArH), 6.62-6.69 (m, 3H, Ar-H), 3.84 (bs, 4H, Ar- CH_2 -Ar), 3.54 (s, 2H, Ar- CH_2 -CN). $^{13}\text{C NMR}$ (100 MHz, CDCl_3 , δ_{C}): 148.6, 148.3, 148.1, 128.8, 128.6, 128.5, 128.0, 127.9, 127.5, 123.3, 121.7, 121.7, 117.9, 30.9, 30.9, 22.0.

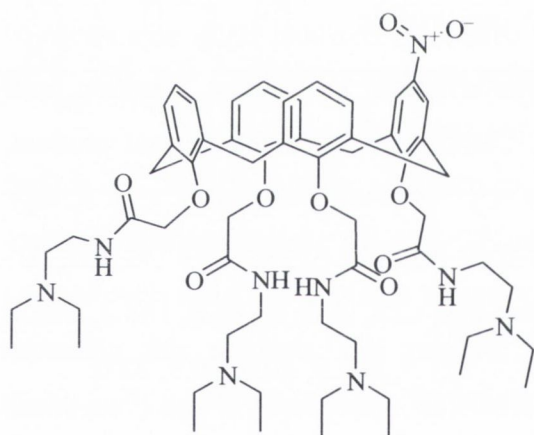
5-Nitro-25,26,27,28-tetrakis-*N*-(piperidinyl-2-aminoethyl)carbamoyloxymethoxy-calix[4]arene (119)



To 5-nitro-26,27,28,29-tetra(methoxycarbonyl)-ethoxy calix[4]arene (**100**) (200 mg, 0.26 mmol) was added 1-(2-aminoethyl)piperidine (3 mL, 21 mmol). The resulting solution was stirred in an argon atmosphere for 16 h. Excess amine was removed by distillation at reduced pressure, and the resulting residue was triturated

with Et₂O. The resulting solid was collected by suction filtration to yield the desired product in 40% yield. ¹H NMR (CD₃CN, 600 MHz, δ_H): 8.17 (bs, 1H, NH), 8.01 (bs, 1H, NH), 7.31 (bs, 2H, NH), 7.11-7.07 (m, 4H, ArH), 7.03 (s, 2H, ArH), 6.97 (t, *J* = 7.5 Hz, 2H, Ar-H), 6.16 (s, 2H, Ar-H), 4.68 (d, *J* = 12.0 Hz, 2H, Ar-CH₂-Ar), 4.66 (d, *J* = 11.6 Hz, 2H, Ar-CH₂-Ar), 4.58 (d, *J* = 14.0 Hz, 2H, Ar-CH₂-Ar), 4.54 (d, *J* = 13.9 Hz, 2H, Ar-CH₂-Ar), 4.40 (s, 2H, ArO-CH₂-C(O)), 4.26 (s, 2H, ArOCH₂-C(O)), 3.46 (q, *J* = 7 Hz, 4H, HNCH₂CH₂N_{pip.}), 3.40 (d, *J* = 14.0 Hz, 2H, Ar-CH₂-Ar), 3.34-3.29 (m, 8H, HNCH₂CH₂N_{pip.}), 2.50 (t, *J* = 7.14, 2H), 2.41-2.35 (m, 16H, N(CH₂CH₂)₂CH₂), 1.54-1.51 (m, 16H, N(CH₂CH₂)₂CH₂), 1.42 (m, 8H, N(CH₂CH₂)₂CH₂) ¹³C NMR (CD₃CN, 150 MHz): 169.5, 168.4, 167.7, 156.9, 154.7, 142.9, 136.1, 135.8, 134.9, 133.4, 129.8, 129.2, 127.7, 123.0, 122.9, 122.1, 73.8, 73.5, 73.5, 57.7, 57.4, 54.3, 54.1, 36.4, 36.4, 30.7, 30.5, 29.7, 25.7, 25.6, 24.1, 24.0. IR (ν/cm⁻¹): 3301, 2940, 2809, 1659, 1538, 1459, 1439, 1295, 1194, 1115, 868, 778, 761. ESMS (*m/z*): 1142.62 (M). Analysis: Required for C₆₄H₈₇N₉O₁₀·2H₂O: C, 65.23; H, 7.78; N, 10.70. Found: C, 65.57; H, 7.44; N, 10.71.

5-Nitro 25,26,27,28-tetrakis-*N,N*-diethyl-2-aminoethyl)carbamoyloxymethoxy-calix[4]arene (120)



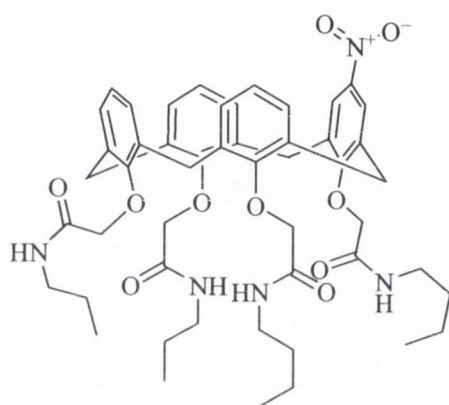
calix[4]arene (120)

To 5-nitro-26,27,28,29-tetra(methoxycarbonyl)ethoxy calix[4]arene (**100**) (200 mg, 0.26 mmol) was added *N,N*-diethyl ethylenediamine (3.0 mL, 21 mmol). The solution was stirred under argon overnight, following which the amine was removed under reduced pressure to leave an oily residue. Trituration of this residue with diethyl ether yielded a fine yellow powder

which was collected by suction filtration (35%), (m.p.: 244 °C (dec.)). ¹H NMR (CD₃CN, 600 MHz, δ_H): 8.23 (t, *J* = 5.6 Hz, 1H, NH), 8.07 (t, *J* = 5.6 Hz, 1H, NH), 7.21 (t, *J* = 4.9 Hz, 1H, NH), 7.06-7.10 (m, 4H, ArH), 7.02 (s, 2H, Ar-H (NO₂)), 6.97 (t, *J* = 7.6 Hz, 2H, ArH), 6.15 (s, 2H, ArH), 4.67 (d, *J* = 14.0 Hz, 2H, Ar-CH₂-Ar), 4.66 (d, *J* = 13.9 Hz, 2H, Ar-CH₂-Ar), 4.58 (d, *J* = 13.8 Hz, 2H, Ar-CH₂-Ar), 4.54 (d, *J* = 13.9 Hz, 2H, Ar-CH₂-Ar), 4.39 (s, 4H, ArOCH₂-C(O)), 4.25 (s, 4H, ArOCH₂-C(O)), 3.37 - 3.42 (m, 8H, N(CH₂CH₂)NEt₂), 3.27-3.30 (m, 4H, N(CH₂CH₂)NEt₂), 2.61-2.65 (m, 4H), 2.55 (q, *J* = 6.8 Hz, 8H, NCH₂CH₃), 2.49 (q, *J* = 7.1 Hz, 8H, NCH₂CH₃) 2.49 (q, *J* = 7.1 Hz, 4H,

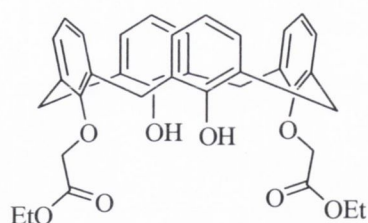
$\text{N}(\text{CH}_2\text{CH}_2)\text{NEt}_2$, 1.00 (t, $J = 7.1$ Hz, 12H, NCH_2CH_3), 0.96 (t, $J = 7.1$ Hz, 12H, NCH_2CH_3). ^{13}C NMR (CD_3CN , 150 MHz): 169.5, 167.7, 156.7, 154.6, 142.9, 136.1, 135.9, 134.9, 133.4, 129.8, 129.2, 127.7, 123.0, 122.9, 122.1, 73.8, 73.6, 73.5, 51.8, 51.6, 46.8, 46.8, 46.5, 37.2, 37.1, 30.6, 30.4, 29.7, 11.3, 11.1 IR (v/cm^{-1}): 3301, 3075, 2968, 2933, 2806, 1651, 1583, 1539, 1516, 1460, 1438, 1342, 1245, 1199, 1093, 1039, 796, 778. ESMS (m/z): 1094.63 (M). Analysis: Required for $\text{C}_{60}\text{H}_{87}\text{N}_9\text{O}_{10}\text{H}_2\text{O}$: C, 64.78; H, 8.06; N, 11.33. Found: C, 64.84; H, 7.83; N, 11.38.

5-Nitro 25,26,27,28-tetrakis-*N*-(propyl)carbamoyloxymethoxycalix[4]arene (121)

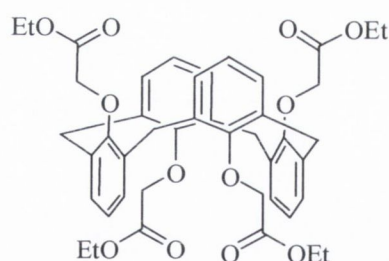


To 5-nitro-26,27,28,29-tetra(methoxycarbonyl)ethoxy calix[4]arene (**100**) (200 mg, 0.26 mmol) was added propylamine (3 mL, 21 mmol). The resulting solution was stirred in an argon atmosphere for 16 h. Excess amine was removed by distillation at reduced pressure, and the resulting residue was triturated with Et_2O . The resulting solid was collected by suction filtration to yield the desired product. (77%, fine

yellow crystals). ^1H NMR (CD_3CN , 600 MHz, δ_{H}): 8.38 (bs, 2H, NH), 8.24 (bs, 2H, NH), 7.09 (m, 4H, Ar-H), 7.01 (s, 2H, ArH), 6.98 (t, $J = 7.5$ Hz, 2H, ArH), 6.14 (s, 2H, Ar-H), 4.71 (d, $J = 14.3$ Hz, 2H, Ar- CH_2 -Ar), 4.68 (d, $J = 13.9$ Hz, 2H, Ar- CH_2 -Ar), 4.61 (s, 2H, $\text{OCH}_2\text{-C}(\text{O})\text{N}$), 4.59 (s, 2H, $\text{OCH}_2\text{-C}(\text{O})\text{N}$), 4.37 (s, 2H, $\text{OCH}_2\text{-C}(\text{O})\text{N}$), 4.24 (s, 2H, $\text{OCH}_2\text{-C}(\text{O})\text{N}$), 3.39 (d, $J = 14.3$ Hz, 2H, Ar- CH_2 -Ar), 3.30 (q, $J = 7.2$ Hz, 4H, $\text{NCH}_2\text{CH}_2\text{CH}_3$), 3.28 (d, $J = 13.1$ Hz, Ar- CH_2 -Ar), 3.16 (q, $J = 6.78$ Hz, 4H, $\text{NCH}_2\text{CH}_2\text{CH}_3$), 1.63 (m, 4H, $\text{NCH}_2\text{CH}_2\text{CH}_3$), 1.47 (m, 4H, $\text{NCH}_2\text{CH}_2\text{CH}_3$), 0.95 (t, $J = 7.14$ Hz, 3H, $\text{NCH}_2\text{CH}_2\text{CH}_3$), 0.95 (t, $J = 7.5$ Hz, 3H, $\text{NCH}_2\text{CH}_2\text{CH}_3$), 0.87 (t, $J = 7.6$ Hz, 6H, $\text{NCH}_2\text{CH}_2\text{CH}_3$). ^{13}C NMR (CD_3CN , 150 MHz, δ_{C}): 169.6, 159.7, 156.7, 154.5, 143.0, 136.2, 135.9, 134.9, 133.5, 129.8, 129.2, 127.6, 123.0, 122.9, 122.1, 73.7, 73.4, 73.3, 40.5, 40.5, 40.4, 30.5, 30.3, 29.7, 22.6, 22.6, 22.3, 10.6, 10.5. IR (v/cm^{-1}): 3286, 2928, 2874, 1654, 1539, 1515, 1461, 1437, 1337, 1255, 1200, 1088, 1037, 778. ESMS (m/z): 888.38 (M). Analysis: Required for $\text{C}_{50}\text{H}_{63}\text{N}_5\text{O}_{10} \cdot \frac{1}{3}\text{H}_2\text{O}$: C, 66.11; H, 6.90; N, 8.03. Found: C, 66.13; H, 6.75; N, 8.09.

25,27-Bis[(ethoxycarbonyl)methoxy]-26,28-dihydroxy calix[4]arene (129)²¹⁰

To calix[4]arene (**53**) (10.00 g, 23.6 mmol) in CH₃CN (100 mL) was added K₂CO₃ (3.25 g, 23.5 mmol). The suspension was stirred at reflux for 2 h. Ethyl bromoacetate (5.8 mL, 52.3 mmol) was added and the mixture was stirred for a further 16 h at reflux. The solvent was removed under reduced pressure, and the residue partitioned between water (100 mL) and CHCl₃ (150 mL). The organic layer was removed, and the aqueous layer washed with further CHCl₃ (3 × 150 mL). The combined organic solvents were dried over MgSO₄, and evaporated. The residue was stirred in hot ethanol for 90 min, and cooled. The desired product precipitated at room-temperature overnight, and was collected by suction filtration as a white powder (9.68 g, 70%). m.p.: 171-174 °C. ¹H NMR (400 MHz, CDCl₃, δ_H): 7.55 (s, 2H, OH), 7.07 (d, *J* = 8 Hz, 4H, Ar-H), 6.91 (d, *J* = 8 Hz, 4H, Ar-H), 6.76 (t, *J* = 8 Hz, 2H, Ar-H), 6.68 (t, *J* = 7 Hz, 2H, Ar-H), 4.75 (s, 4H, ArOCH₂C(O)), 4.50 (d, *J* = 13 Hz, 4H, Ar-CH₂-Ar), 4.35 (q, *J* = 7.5 Hz, 4H, OCH₂CH₃), 3.41 (d, *J* = 13 Hz, 4H, Ar-CH₂-Ar), 1.37 (t, *J* = 7 Hz, 6H, OCH₂CH₃). ¹³C NMR (100 MHz, CDCl₃, δ_C): 168.5, 152.6, 151.9, 132.7, 128.7, 128.1, 127.7, 125.2, 118.7, 72.0, 61.0, 31.1, 13.7. ESMS (*m/z*): 619.23 (M+Na).

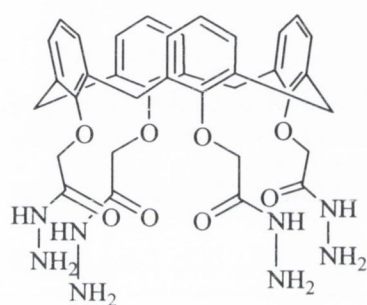
25,26,27,28-Tetrakis[(ethoxycarbonyl)methoxy]calix[4]arene – 1,3-alternate*conformation (132)*

Calix[4]arene (**53**) (2.00 g, 4.7 mmol) was suspended in acetone. To the stirring suspension was added anhydrous Cs₂CO₃ (15.0 g, 46 mmol) and ethyl bromoacetate (11 mL, 99 mmol) and the mixture was stirred overnight at 56 °C. The solvent was evaporated and the residue partitioned between water (100 mL) and CH₂Cl₂ (100 mL). The organic layer was removed, dried (MgSO₄), evaporated to dryness under reduced pressure, and the residue was crystallised slowly (3 – 4 days in freezer) from ethanol to yield the title compound as small fluffy needles (0.76 g, 21%). m.p. 103 °C (lit. 117 – 119 °C). ¹H NMR (400 MHz, CDCl₃, δ_H): 7.53 (d, *J* = 7.5 Hz, 8H, Ar-CH_{meta}), 6.74 (t, *J* = 7.5 Hz, 4H, Ar-CH_{para}), 4.26 (q, *J* = 7.0 Hz, 8H, OCH₂CH₃), 4.06 (s, 8H, OCH₂-C(O)), 3.81 (s, 8H, Ar-CH₂-Ar), 1.35 (t, *J* = 7.5 Hz, 12H, OCH₂CH₃). ¹³C NMR (100 MHz, CDCl₃, δ_C): 169.2, 155.0, 133.1, 130.0, 122.5, 69.2, 60.4, 35.1, 13.8. **Accurate MS** (*m/z*): Calculated for C₄₄H₄₈O₁₂+Na: 791.3043, found: 791.3008.

General Synthesis of calix[4]arene hydrazides

To a solution of the relevant calix[4]arene ethyl ester in methanol was added hydrazine hydrate (2 – 10 mL, large excess), and the solution stirred at 40 °C overnight. The reaction may be monitored by TLC using CH₂Cl₂ as eluent, in which R_f values of the hydrazides are 0. The solvents and excess hydrazine were removed at reduced pressure, giving the crude product as an off-white solid. The residue was triturated sequentially with water and methanol and the product collected by filtration.

25,26,27,28-Tetrakis[(hydrazidocarbonylmethyl)oxy]calix[4]arene – cone conformation (87)



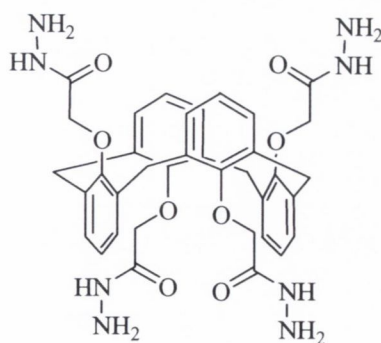
Obtained in 96% yield from **55**. m.p. 201 °C ¹H NMR (400 MHz, methanol-*d*₄, δ_H): 9.50 (s, 4H, NH), 6.85 (d, *J* = 8 Hz, 8H, Ar-H), 6.65 (t, *J* = 8 Hz, 4H, Ar-H), 4.47 (d, *J* = 13 Hz, 4H, Ar-CH₂-Ar), 4.42 (s, 4H, ArO-CH₂-C(O)NH), 3.24 (d, *J* = 13 Hz, Ar-CH₂-Ar). ¹³C NMR (100 MHz, CDCl₃, δ_C): 167.5, 155.1, 134.6, 128.6, 123.4, 73.4, 30.1. IR (ν/cm⁻¹):

3313, 3035, 2920, 1672, 1528, 1459, 1442, 1291, 1248, 1196, 1094, 1006, 982, 730

Accurate MS (m/z): Calculated for C₃₆H₄₀N₈O₈Na (M+Na): 735.2867; found 735.2838.

Analysis: Required for C₃₆H₄₀N₈O₈·H₂O: C, 59.17; H, 5.79; N, 15.33; Found: C, 59.60; H, 5.53; N, 14.63.

25,26,27,28-Tetrakis[(hydrazidocarbonylmethyl)oxy]calix[4]arene – 1,3-alternate conformation (133)

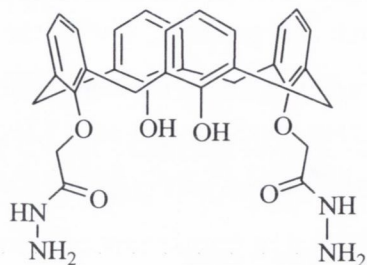


From **129** (750 mg, 0.97 mmol), the desired product was obtained as a white powder (602 mg, 88%), m.p.: 221 °C.

¹H NMR (400 MHz, DMSO-*d*₆, δ_H): 7.30 (s, 4H, CONH), 7.04 (d, 8H, *J* = 7.6 Hz, Ar-H), 6.81 (t, *J* = 7 Hz, Ar-H), 4.15 (s, 8H, NH₂), 4.03 (s, 8H, Ar-O-CH₂C(O)), 3.89 (s, 8H, Ar-CH₂-Ar). ¹³C NMR (100 MHz, DMSO-*d*₆, δ_C): 166.6, 154.8, 133.4, 128.8, 123.0, 68.7, 36.1. IR (ν/cm⁻¹):

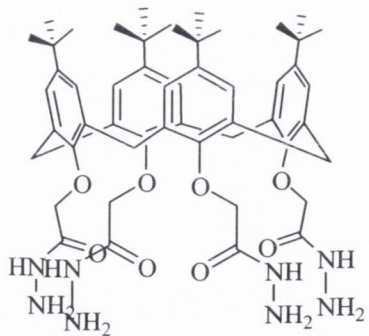
3263, 3233, 1682, 1651, 1598, 1551, 1529, 1493, 1480, 1435, 1369, 1248, 1224, 1168, 1083, 1067, 838, 723, 686. **Analysis:** Required for $C_{36}H_{40}N_8O_8$: C, 60.66; H, 5.66; N, 15.72. Found: C, 63.20; H, 5.37; N, 14.72.

25,27-Bis[(hydrazidocarbonylmethyl)oxy]calix[4]arene (130)



Obtained from 25,27-Bis[(ethoxycarbonyl)methoxy]-26,28-dihydroxy calix[4]arene in 94% yield as a white powder, m.p.: 267 °C. 1H NMR (400 MHz, DMSO- d_6 , δ_H): 9.55 (s, 2H, ArOH), 8.32 (s, 2H, NH), 7.17 (d, $J = 7.6$ Hz, 4H, ArH), 7.07 (d, $J = 7.6$ Hz, 4H, ArH), 6.82 (t, $J = 7.6$ Hz, 2H, ArH), 6.62 (t, $J = 7.0$ Hz, 2H, ArH), 4.54 (s, 4H, ArOCH₂C(O)), 4.20 (d, $J = 12.9$ Hz, 4H, Ar-CH₂-Ar), 3.47 (d, $J = 12.9$ Hz, 4H, Ar-CH₂-Ar). ^{13}C NMR (100 MHz, DMSO- d_6 , δ_C): 165.9, 152.1, 151.6, 133.7, 129.1, 128.8, 127.5, 125.7, 119.5, 73.6, 30.4. **IR** (ν/cm^{-1}): 3312, 2935, 1662, 1586, 1460, 1434, 1334, 1249, 1193, 1156, 1069, 1031, 1006, 985, 896, 785, 752. **Analysis:** Required for $C_{32}H_{32}N_4O_6 \cdot H_2O$: C, 65.52; H, 5.82; N, 9.55. Found: C, 65.73; H, 5.83; N, 9.38.

5,11,17,23-Tetra-*tert*-butyl-25,26,27,28-tetrakis[(hydrazidocarbonylmethyl)oxy]calix[4]arene (127)



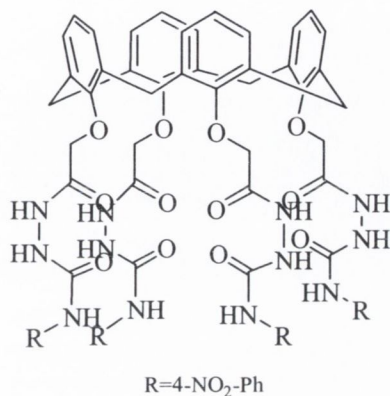
Obtained from 7 as a white powder in 81% yield, m.p.: >310 °C (dec.). 1H NMR (400 MHz, DMSO- d_6 , δ_H): 9.28 (s, 4H, NH), 6.91 (s, 8H, Ar-H), 4.48 (s, 8H, NH₂), 4.40 (d, $J = 13$ Hz, Ar-CH₂-Ar), 4.38 (s, 8H, Ar-O-CH₂-C(O)), 3.19 (d, $J = 14$ Hz, Ar-CH₂-Ar), 1.06 (s, 36H, Ar-C(CH₃)₃). ^{13}C NMR (100 MHz, DMSO- d_6 , δ_C): 167.7, 166.9, 152.2, 144.8, 133.2, 125.5, 124.6, 73.5, 31.1. **IR** (ν/cm^{-1}): 3313, 2953, 1669, 1479, 1361, 1275, 1194, 1124, 1045, 869, 762, 755.

General procedure for the synthesis of ureas

The appropriate hydrazide was suspended in dry THF. Phenyl isocyanate (1.0 equiv. with respect to the free amino moieties) was added neat, while nitrophenyl isocyanate (1.0 equiv. with respect to free amino moieties) was added as a solution in dry THF. The mixture was stirred overnight, giving a thick precipitate. The reaction was quenched by

addition of CH₃OH, and the precipitate filtered, and washed with CH₃OH and water to yield the desired ureas which were suitable for use without further purification.

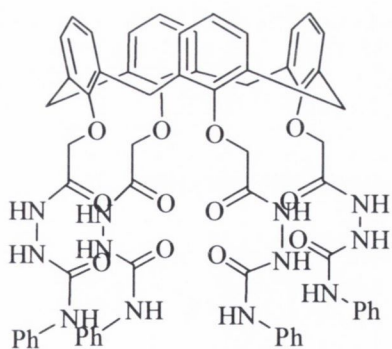
25,26,27,28-Tetra[3-(4-nitrophenyl)ureidocarbamoyl]methoxy calix[4]arene – cone conformation (125)



Obtained from **87** in 72% yield. m.p.: 244 °C. ¹H NMR (400 MHz, DMSO-*d*₆, δ_H): 9.99 (s, 4H, NH), 9.51 (s, 4H, NH), 8.44 (s, 4H, NH), 7.98 (d, *J* = 9.36 Hz, 8H, ArH_{nitrophenyl}), 7.57 (d, *J* = 8.76 Hz, 8H ArH_{nitrophenyl}), 6.78 (d, *J* = 7.00 Hz, Ar-H), 6.67 (t, *J* = 7.00 Hz, Ar-H) ¹³C NMR (100 MHz, DMSO-*d*₆, δ_C): 168.9, 155.5, 154.6, 146.0, 141.0, 134.3, 128.6, 125.4, 124.7, 123.1, 117.7, 72.8, 30.6. IR (ν/cm⁻¹): 3269, 2927, 1709, 1674, 1543,

1500, 1459, 1329, 1228, 1192, 1177, 1111, 1095, 1043, 1007, 852, 840. ESMS (*m/z*, ES⁻): 1369.0, expect 1368.4 (M). **Analysis:** Required for C₆₄H₅₆N₁₆O₂₀·2H₂O: C, 54.70; H, 4.30; N, 15.95. Found: C, 54.66; H, 4.10; N, 15.62.

25,26,27,28-[Tetra(3-phenylureidocarbamoyl)methoxy] calix[4]arene – cone conformation (126)

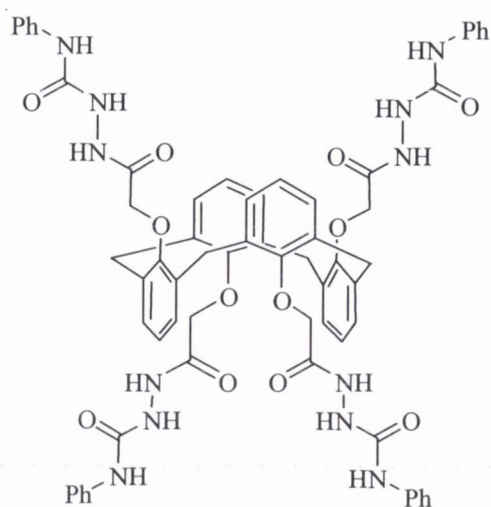


Obtained from **87** in 60% yield. m.p.: 232 °C

¹H NMR (400 MHz, DMSO-*d*₆, δ_H): 9.91 (s, 4H, NH), 8.83 (s, 4H, NH), 8.09 (s, 4H, NH), 7.40 (d, *J* = 7.04 Hz, 8H, Ar-H), 7.20 (t, *J* = 7.04 Hz, Ar-H), 6.92 (t, *J* = 6.52 Hz, 4H, Ar-H), 6.80 (d, *J* = 7.52 Hz, 8H, Ar-H), 6.66 (d, *J* = 7.56 Hz, Ar-H), 4.74 (d, *J* = 12.48 Hz, 4H, Ar-CH₂-Ar), 4.69 (s, 8H, Ar-O-CH₂-C(O)), 3.29 (d, *J* = 13.08 Hz,

4H, Ar-CH₂-Ar). ¹³C NMR (100 MHz, DMSO-*d*₆, δ_C): 168.8, 155.6, 155.4, 139.3, 128.7, 128.6, 123.1, 122.0, 118.7, 72.9, 30.7. IR (ν/cm⁻¹): 3239, 1660, 1541, 1444, 1204, 749, 692. **Analysis:** Required for C₆₄H₆₀N₁₂O₁₂·CH₃OH: C, 63.92; H, 5.28; N, 13.76. Found: C, 63.94; H, 5.14; N, 13.73.

25,26,27,28-[Tetra(3-phenylureidocarbamoyl)methoxy] calix[4]arene – 1,3-alternate



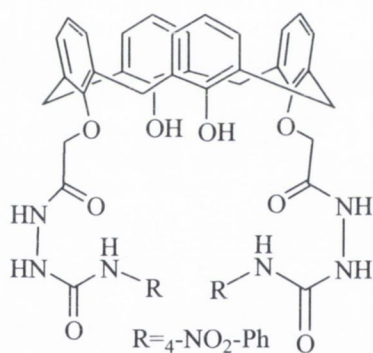
conformation (134)

Obtained from **133** in 54% yield.

m.p.: 214-220 °C $^1\text{H NMR}$ (400 MHz, DMSO- d_6 , δ_{H}): 8.69 (s, 4H, NH), 8.48 (s, 4H, NH), 8.16 (s, 4H, NH), 7.46 (d, $J = 9.0$ Hz, 8H, ArH), 7.28 (t, $J = 8.6$ Hz, 8H, ArH), 7.21 (d, $J = 6$ Hz, 8H, ArH), 6.97 (t, $J = 7.0$ Hz, 4H, ArH), 6.78 (t, $J = 8.0$ Hz, 4H, ArH), 4.16 (s, 8H, ArO-CH₂-C(O)), 3.83 (s, 8H, Ar-CH₂-Ar). $^{13}\text{C NMR}$ (100 MHz, DMSO- d_6 , δ_{C}): 167.8, 55.1, 155.0, 139.5, 133.6,

130.6, 128.7, 122.5, 122.0, 118.5, 69.5, 35.5. **IR** (ν/cm^{-1}): 3278, 1753, 1650, 1596, 1498, 1447, 1314, 1232, 1192, 1094, 1051, 781, 695. **Analysis:** Required for C₆₄H₆₀N₁₂O₁₂·H₂O·CH₃OH: C, 62.89; H, 5.52; N, 13.54. Found: C, 62.68; H, 5.15; N, 13.23.

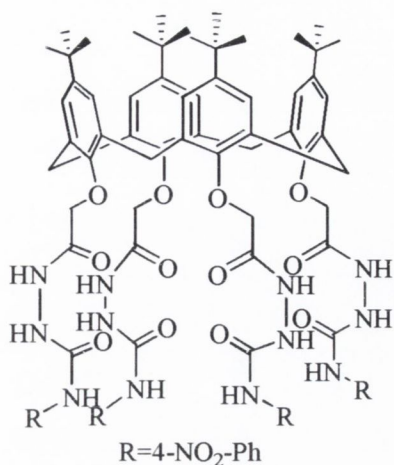
25, 27- Bis[(3-(4-nitrophenyl)ureidocarbamoyl)methoxy] calix[4]arene (131)



Obtained by stirring in dry THF (20 mL), **130** (200 mg, 0.3 mmol) and 4-nitrophenyl isocyanate (115 mg, 0.7 mmol) in 95% yield. m.p.: 242-245 °C $^1\text{H NMR}$ (400 MHz, DMSO- d_6 , δ_{H}): 10.17 (s, 2H, NH_{urea}), 9.59 (s, 2H, NH_{urea}), 8.62 (s, 2H, NH_{amide}), 8.14 (d, $J = 9$ Hz, 4H, Ar-H_{nitrophenyl}), 7.71 (d, $J = 9$ Hz, 4H, Ar-H_{nitrophenyl}), 7.17 (d, $J = 7$ Hz, 4H, ArH), 7.05 (d, $J = 7$ Hz, 4H, ArH), 6.81 (t, $J = 8$ Hz, 2H, Ar-H),

6.62 (t, $J = 7$ Hz, 2H, Ar-H), 4.68 (s, 4H, ArO-CH₂-C(O)), 4.33 (d, $J = 13$ Hz, 4H, Ar-CH₂-Ar), 4.46 (d, $J = 13$ Hz, 4H, Ar-CH₂-Ar). $^{13}\text{C NMR}$ (100 MHz, CDCl₃, δ_{C}): Quaternary not visible, 152.4, 152.3, 146.2, 141.2, 133.5, 129.1, 128.7, 127.5, 125.6, 125.4, 125.0, 119.3, 117.8, 73.3, 30.6. **IR**: (ν/cm^{-1}): 3314, 3097, 1658, 1633, 1595, 1567, 1510, 1466, 1434, 1329, 1302, 1215 **ESMS** (m/z , ES⁻): 895.6 (expect 896.3, M⁻H). **Analysis:** Required for C₄₆H₄₀N₈O₁₂·CH₃OH: C, 60.77; H, 4.77; N, 12.06. Found: C, 60.26; H, 4.48; N, 12.09.

5,11,17,23-Tetra(4-*tert*-butyl)-25,26,27,28-tetra[3-(4-nitrophenyl)ureidocarbamoyl]-methoxy calix[4]arene (127)

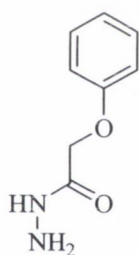


Prepared from corresponding tetrahydrazide (500 mg, 0.5 mmol) and 4-nitrophenyl isocyanate (350 mg, 2 mmol) as a pale yellow powder (0.58 g, 68%) m.p. 218 °C.

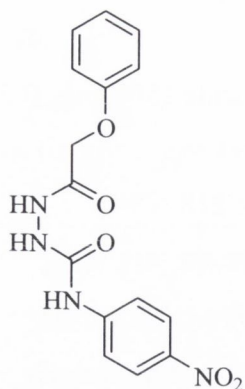
¹H NMR (400 MHz, DMSO-*d*₆, δ_H): 9.99 (bs, 4H, NH), 9.54 (bs, 4H, NH), 8.40 (s, 4H, NH), 7.99 (d, *J* = 9.0 Hz, 12H, nitrophenyl), 7.56 (d, *J* = 8.5 Hz, 12H, nitrophenyl), 6.90 (s, 8H, Ar-H, calixarene), 4.67 (s, 8H, ArO-CH₂-C(O)), 4.59 (d, *J* = 12.6 Hz, 4H, Ar-CH₂-Ar), 3.25 (d, *J* = 12.5 Hz, 4H, Ar-CH₂-Ar). ¹³C NMR (100 MHz, DMSO-

*d*₆, δ_C): 169.2, 154.6, 152.8, 146.0, 144.9, 141.0, 133.1, 125.4, 124.7, 117.8, 73.0, 33.6, 31.1. IR (ν/cm⁻¹): 3277, 2965, 1675, 1570, 1510, 1334, 1189, 1113, 848, 688. **Analysis:** Required for C₈₀H₈₈N₁₆O₂₀·2H₂O: C: 58.96, H: 5.69; N: 13.75; Found: C: 58.49; H: 5.58; N: 13.47.

2-Phenoxyacetohydrazide (136)



Ethyl 2-phenoxyacetate (5.0 mL, 30.5 mmol), was added to a flask containing EtOH (30 mL). To this solution was added hydrazine hydrate (8.0 mL, 0.26 mol), and the solution was heated at reflux for 3 h. The flask contents were cooled to room temperature overnight, upon which a solid crystalline mass formed. These crystals were collected by suction filtration, and dried, furnishing the title product which required no further purification. (4.60g, 91%). m.p. 100 °C (lit. 104-106 °C)²¹¹ ¹H NMR (400 MHz, CDCl₃, δ_H): 7.92 (s, 1H, NH), 7.34 (t, *J* = 8 Hz, 2H, Ar-H), 7.05 (t, *J* = 8 Hz, 1H, ArH), 6.91 (d, *J* = 8 Hz, 2H, ArH), 4.59 (s, 2H, ArOCH₂C(O)), 3.60 (bs, 2H, NH₂) ¹³C NMR (100 MHz, CDCl₃, δ_C): 168.2, 156.6, 129.4, 121.8, 114.1, 66.4. IR (ν/cm⁻¹): 3311, 3202, 3044, 2850, 1663, 1642, 1615, 1598, 1535, 1496, 1433, 1238, 1165, 1036, 1017, 994, 834, 741, 686.

4-(4-Nitrophenyl)-1-(2-phenoxyacetyl)semicarbazide (137)

To 2-phenoxyacetohydrazide (**136**) (0.51 g, 3.1 mmol) in dry THF was added a solution of 4-nitrophenyl isocyanate (0.51 g, 3.11 mmol). The solution was stirred under an argon balloon at room temperature overnight, following which the flask contents were concentrated to approx. one third volume at reduced pressure. Methanol was added, with stirring, to yield the title compound as a pale yellow, fluffy solid, which was collected by suction filtration.

(0.65 g, 64%), m.p. 208-211 °C. ¹H NMR (400 MHz, DMSO-*d*₆, δ_H):

10.11 (s, 1H, NH), 9.55 (s, 1H, NH), 8.54 (s, 1H, NH), 8.18 (d, *J* = 9 Hz, 2H, Ar-H_{nitrophenyl}), 7.73 (d, *J* = 7 Hz, 2H, Ar-H_{nitrophenyl}), 7.32 (t, *J* = 8 Hz, 2H, Ar-H_{ortho}), 7.00 (m, 3H, Ar-H_{meta, para}), 4.63 (s, 2H, OCH₂C(O)) ¹³C NMR (100 MHz, CDCl₃, δ_C): 167.8, 157.7, 146.4, 141.1, 129.5, 125.0, 121.2, 118.0, 117.8, 114.7, 66.0. IR (v/cm⁻¹): 3326, 3228, 3107, 2903, 1728, 1720, 1676, 1660, 1616, 1598, 1567, 1508, 1459, 1412, 1426, 1343, 1333, 1300, 1239, 1202, 1175. ESMS (*m/z*, ES⁻): 329.5 (expect 329.1 M-1).

Analysis: Required for C₁₅H₁₄N₄O₅·¹/₃THF: C: 55.36, H: 4.74; N: 15.81; Found: C: 55.63; H: 4.45; N: 16.32.

References

1. A. Casnati and R. Ungaro, in *Calixarenes in Action*, eds. L. Mandolini and R. Ungaro, Imperial College Press, 2000, 62-84.
2. C. Redshaw, *Coord. Chem. Rev.*, 2003, **244**, 45.
3. D. Diamond and K. Nolan, *Anal. Chem.*, 2001, 23.
4. V. Paquet, A. Zumbuehl and E. M. Carreira, *Bioconjugate Chem.*, 2006, **17**, 1460.
5. K. S. J. Iqbal and P. J. Cragg, *Dalton Trans.*, 2007, 26.
6. V. Sidorov, F. W. Kotch, G. Abdrakhmanova, R. Mizani, J. C. Fettinger and J. T. Davis, *J. Am. Chem. Soc.*, 2002, **124**, 2267.
7. E. Hoppe, C. Limberg and B. Ziemer, *Inorg. Chem.*, 2006, **45**, 8308.
8. R. Cacciapaglia, A. Casnati, L. Mandolini, D. N. Reinhoudt, R. Salvio, A. Sartori and R. Ungaro, *J. Org. Chem.*, 2005, **70**, 5398.
9. R. Cacciapaglia and L. Mandolini, in *Calixarenes in Action*, 2000, 241-264.
10. S. J. Harris, M. A. McKerverey, D. P. Melody, J. Woods and J. M. Rooney, *EP Pat.*, 85-300507;151527, 14 pp, 1985.
11. R. G. Leonard and S. J. Harris, *EP Pat.*, 87-300824; 235935, 12 pp, 1987.
12. S. J. Harris, *EP Pat.*, 87-306963; 259016, 9 pp, 1988.
13. A. Baeyer, *Ber. Dtsch. Chem. Ges.*, 1872, **5**, 25.
14. C. D. Gutsche, *Calixarenes*, First edn., Royal Society of Chemistry, 1989.
15. L. H. Baekeland, *U.S. Pat.*, 942,699, 1908.
16. A. Zinke, E. Ziegler, E. Martinowitz, H. Pichelmayer, M. Tomio, H. Wittmann-Zinke and S. Zwanziger, *Chem. Ber.*, 1944, **77**, 264.
17. B. T. Hayes and R. F. Hunter, *Chem. Ind.*, 1956, 193.
18. J. W. Cornforth, E. D. Morgan, K. T. Potts and R. J. W. Rees, *Tetrahedron*, 1973, **29**, 1659.
19. J. W. Cornforth, P. D'ArcyHart, G. A. Nicholls, R. J. W. Rees and J. A. Stock, *Brit. J. Pharmacol*, 1955, **10**, 73.
20. C. D. Gutsche and R. Muthukrishnan, *J. Org. Chem.*, 1978, 4905.
21. D. R. Stewart and C. D. Gutsche, *J. Am. Chem. Soc.*, 1999, **121**, 4136.
22. D. R. Stewart and C. D. Gutsche, *Org. Prep. Proc. Intl.*, 1993, **25**, 137.
23. V. Böhmer, *Angew. Chem. Int. Ed.*, 1995, **34**, 713.
24. C. D. Gutsche, *Acc. Chem. Res.*, 1983, **16**, 161.
25. C. D. Gutsche and M. Iqbal, *Org. Synth.*, 1990, **68**, 234.
26. T. Gunnlaugsson, J. P. Leonard, S. Mulready and M. Nieuwenhuyzen, *Tetrahedron*, 2004, **60**, 105.

27. T. Gunnlaugsson, R. J. H. Davies, M. Nieuwenhuyzen, J. E. O'Brien, C. S. Stevenson and S. Mulready, *Polyhedron*, 2003, **22**, 711.
28. T. Gunnlaugsson, *Tetrahedron Lett.*, 2001, **42**, 8901.
29. S. E. Matthews, V. Felix, M. G. B. Drew and P. D. Beer, *Org. Biomol. Chem.*, 2003, **1**, 1232.
30. C. D. Gutsche and P. F. Pagoria, *J. Org. Chem.*, 1985, **50**, 5795.
31. E. Pinkhassik, I. Stibor, A. Casnati and R. Ungaro, *J. Org. Chem.*, 1997, **62**, 8654.
32. D. Yuan, W.-X. Zhu, S. Ma and X. Yan, *J. Mol. Struct.*, 2002, 241.
33. I. Yoshida, N. Yamamoto, F. Sagara, K. Ueno, D. Ishii and S. Shinkai, *Chem. Lett.*, 1991, 2105.
34. S. J. Dalgarno, J. L. Atwood and C. L. Raston, *Cryst. Growth Des.*, 2006, **6**, 174.
35. C. D. Gutsche and L.-G. Lin, *Tetrahedron*, 1986, **42**, 1633.
36. P. Lhoták, J. Morávek, I. Stibor and J. Sykora, *Tetrahedron Lett.*, 2002, **43**, 7413.
37. S. Redon, Y. Li and O. Reinaud, *J. Org. Chem.*, 2003, **68**, 7004.
38. S. Kumar, N. Kurur, H. Chawla and R. Varadarajan, *Synth. Commun.*, 2001, **31**, 775.
39. I. Alam, S. K. Sharma and C. D. Gutsche, *J. Org. Chem.*, 1994, **59**, 3716.
40. V. Arora, H. M. Chawla and A. Santra, *Tetrahedron*, 2002, **58**, 5591.
41. A. Sartori, A. Casnati, L. Mandolini, F. Sansone, D. N. Reinhoudt and R. Ungaro, *Tetrahedron*, 2003, **59**, 5539.
42. Y. Hamuro, M. C. Calama, H. S. Park and A. D. Hamilton, *Angew. Chem. Int. Ed.*, 1997, **36**, 2680.
43. N. Kuhnert and A. Le-Gresley, *Tetrahedron Lett.*, 2005, **46**, 2059.
44. N. Kuhnert and A. Le-Gresley, *J. Chem. Soc. Perkin Trans. 1*, 2001, 3393.
45. R. K. Juneja, K. D. Robinson, C. P. Johnson and J. L. Atwood, *J. Am. Chem. Soc.*, 1993, **115**, 3818.
46. A. Dondoni, C. Ghiglione, A. Marra and M. Scoconi, *J. Org. Chem.*, 1998, **63**, 9535.
47. P. A. Scully, T. M. Hamilton and J. L. Bennett, *Org. Lett.*, 2001, **3**, 2741.
48. T. Cairns and G. Eglinton, *Nature*, 1962, **196**, 535.
49. G. D. Andreetti, R. Ungaro and A. Pochini, *J. Chem. Soc. Chem. Commun.*, 1978, 1005.
50. G. D. Enright, E. B. Brouwer, K. A. Udachin, C. I. Ratcliffe and J. A. Ripmeester, *Acta Cryst. Sect. B*, 2002, **58**, 1032.

51. J. A. Ripmeester, G. D. Enright, C. I. Ratcliffe, K. A. Udachin and I. L. Moudrakovski, *Chem. Commun.*, 2006.
52. M. Makka, C. L. Raston, B. W. Skelton and A. H. White, *Green Chem.*, 2004, **6**, 158.
53. S. Shinkai and A. Ikeda, *Pure & Appl. Chem.*, 1999, **71**, 275.
54. Z.-L. Zhong, A. Ikeda and S. Shinkai, in *Calixarenes 2001*, 2001, 476-495.
55. C. J. Pedersen, *J. Am. Chem. Soc.*, 1967, **89**, 2495.
56. B. K. J. Leong, in *Chem. Eng. News*, 1975, p. 5.
57. C. Alfieri, E. Dradi, A. Pochini, R. Ungaro and G. D. Andreotti, *J. Chem. Soc. Chem. Commun.*, 1983, 1075.
58. I. Bitter, A. Grün, G. Tóth, B. Balázs and L. Tőke, *Tetrahedron*, 1997, **53**, 9799.
59. R. Abidi, I. Oueslati, H. Amri, P. Thuery, M. Nierlich, Z. Asfari and J. Vicens, *Tetrahedron Lett.*, 2001, **42**, 1685.
60. I. Oueslati, R. A. SaFerreira, L. D. Carlos, C. Baleizao, M. N. Berberan-Santos, B. deCastro, J. Vicens and U. Pischel, *Inorg. Chem.*, 2006, **45**, 2652.
61. V. Csokai, A. Grün, G. Parlagh and I. Bitter, *Tetrahedron Lett.*, 2002, **43**, 7627.
62. A. Grün, V. Csokai, G. Parlagh and I. Bitter, *Tetrahedron Lett.*, 2002, **43**, 4153.
63. S. O. Kang and K. C. Nam, *Bull. Korean Chem. Soc.*, 2002, **23**, 640.
64. J. K. Choi, S. H. Kim, J. Yoon, K. H. Lee, R. A. Bartsch and J. S. Kim, *J. Org. Chem.*, 2006, **71**, 8011.
65. F. Arnaud-Neu, E. M. Collins, M. Deasy, G. Ferguson, S. J. Harris, B. Kaitner, A. J. Lough, M. A. McKervey, E. Marques, B. L. Ruhl, M. J. Schwing-Weill and E. M. Seward, *J. Am. Chem. Soc.*, 1989, **111**, 8681.
66. M. A. McKervey, E. M. Seward, G. Ferguson, B. L. Ruhl and S. J. Harris, *J. Chem. Soc., Chem. Commun.*, 1985, 388.
67. T. Sakaki, *Japan Pat.*, 94-283728; 08145943, 8, 1996.
68. S. Walsh, F. J. Saez de Viteri and D. Diamond, *Anal. Proc.*, 1995, **32**, 365.
69. M. Telting-Diaz, F. Regan, D. Diamond and M. R. Smyth, *J. Pharm. Biomed. Anal.*, 1990, **8**, 695.
70. M. Telting-Diaz, M. R. Smyth, D. Diamond, E. M. Seward, G. Svehla and A. M. McKervey, *Anal. Proc.*, 1989, **26**, 29.
71. S. E. Matthews, P. Schmidt, V. Felix, M. G. B. Drew and P. D. Beer, *J. Am. Chem. Soc.*, 2002, **124**, 1341.

72. P. Schmitt, P. D. Beer, M. G. B. Drew and P. D. Sheen, *Angew. Chem. Int. Ed.*, 1997, **36**, 1840.
73. S. E. Matthews and P. D. Beer, in *Calixarenes in the Nanoworld*, eds. J. Vicens and J. Harrowfield, Springer, 2006.
74. E. P. Horwitz, D. G. Kalina, H. Diamond, G. F. Vandegrift and W. W. Schulz, *Solv. Extract. Ion Exch.*, 1985, **3**, 75.
75. G. A. Clark, R. C. Gatrone and E. P. Horwitz, *Solv. Extract. Ion Exch.*, 1987, **5**, 471.
76. F. Arnaud-Neu, V. Böhmer, J.-F. Dozol, C. Grüttner, R. A. Jakobi, D. Kraft, O. Mauprivez, H. Rouquette, M.-J. Schwing-Weill, N. Simon and W. Vogt, *J. Chem. Soc. Perkin Trans. 2*, 1996, 1175
77. C. Turro, P. K.-L. Fu and P. M. Bradley, in *Metal Ions in Biological Systems: The Lanthanides and their Interrelations with Biosystems*, eds. A. Sigel and H. Sigel, Dekker, 2003, vol. 40.
78. D. P. Junhua Yu, *Eur. J. Org. Chem*, 2005, **2005**, 4249.
79. J. A. G. Williams, M. Murru, A. Beeby and D. Parker, *J. Chem. Soc. Chem. Commun.*, 1993, 1116.
80. N. Sato and S. Shinkai, *J. Chem. Soc., Perkin Trans. 2*, 1993, 621.
81. J. C. G. Bunzli, *Acc. Chem. Res.*, 2006, **39**, 53.
82. K. Senechal-David, J. P. Leonard, S. E. Plush and T. Gunnlaugsson, *Org. Lett.*, 2006, **8**, 2727.
83. T. Gunnlaugsson and A. J. Harte, *Org. Biomol. Chem.*, 2006, **4**, 1572.
84. J. P. Leonard and T. Gunnlaugsson, *J. Fluoresc.*, 2005, **15**, 585.
85. T. Gunnlaugsson and J. P. Leonard, *Dalton Trans.*, 2005, 3204.
86. T. Gunnlaugsson and J. P. Leonard, *Chem. Commun.*, 2005, 3114.
87. T. Gunnlaugsson, J. P. Leonard, K. Senechal and A. J. Harte, *J. Am. Chem. Soc.*, 2003, **125**, 12062.
88. N. Sabbatini, M. Guardigli, A. Mecati, V. Balzani, R. Ungaro, E. Ghidini, A. Casnati and A. Pochini, *J. Chem. Soc. Chem. Commun.*, 1990, 878.
89. http://www.rad.msu.edu/Education /CourseInfo/CHM_domain/NMS_/JH/Default.htm (accessed January 2007).
90. A. M. Krishnan and R. Lohrmann, *PCT Int. Appl Pat.*, WO9614878 1996.
91. E. M. Georgiev and D. M. Roundhill, *Inorg. Chimica Acta*, 1997, **258**, 93.

92. L. H. Bryant, A. T. Yordanov, J. J. Linnoila, M. W. Brechbiel and J. A. Frank, *Angew. Chem. Int. Ed.*, 2000, **39**, 1641.
93. S. Aime, A. Barge, M. Botta, A. Casnati, M. Fragai, C. Luchinat and R. Ungaro, *Angew. Chem. Int. Ed.*, 2001, **40**, 4737.
94. T. Gunnlaugsson, P. E. Kruger, P. Jensen, J. Tierney, H. D. P. Ali and G. M. Hussey, *J. Org. Chem.*, 2005, **70**, 10875.
95. T. Gunnlaugsson, P. E. Kruger, P. Jensen, F. M. Pfeffer and G. M. Hussey, *Tetrahedron Lett.*, 2003, **44**, 8909.
96. T. Gunnlaugsson, P. E. Kruger, T. C. Lee, R. Parkesh, F. M. Pfeffer and G. M. Hussey, *Tetrahedron Lett.*, 2003, **44**, 6575.
97. F. M. Pfeffer, T. Gunnlaugsson, P. Jensen and P. E. Kruger, *Org. Lett.*, 2005, **7**, 5357.
98. T. Gunnlaugsson, A. P. Davis, J. E. O'Brien and M. Glynn, *Org. Biomol. Chem.*, 2005, **3**, 48.
99. T. Gunnlaugsson, A. P. Davis, J. E. O'Brien and M. Glynn, *Org. Lett.*, 2002, **4**, 2449.
100. T. Gunnlaugsson, A. P. Davis and M. Glynn, *Chem. Commun.*, 2001, 2556.
101. I. V. Korendovych, M. Cho, P. L. Butler, R. J. Staples and E. V. Rybak-Akimova, *Org. Lett.*, 2006, **8**, 3171.
102. J. L. Sessler, D. E. Gross, W. S. Cho, V. M. Lynch, F. P. Schmidtchen, G. W. Bates, M. E. Light and P. A. Gale, *J. Am. Chem. Soc.*, 2006, **128**, 12281.
103. J. L. Sessler, W. S. Cho, D. E. Gross, J. A. Shriver, V. M. Lynch and M. Marquez, *J. Org. Chem.*, 2005, **70**, 5982.
104. J. L. Sessler, D. An, W. S. Cho, V. Lynch, D. W. Yoon, S. J. Hong and C. H. Lee, *J. Org. Chem.*, 2005, **70**, 1511.
105. G. J. Kirkovits, J. A. Shriver, P. A. Gale and J. L. Sessler, *J. Incl. Phenom. Macrocyc. Chem.*, 2001, **41**, 69.
106. C. N. Warriner, P. A. Gale, M. E. Light and M. B. Hursthouse, *Chem. Commun.*, 2003, 1810.
107. C. J. Woods, S. Camiolo, M. E. Light, S. J. Coles, M. B. Hursthouse, M. A. King, P. A. Gale and J. W. Essex, *J. Am. Chem. Soc.*, 2002, **124**, 8644.
108. R. C. Jagessar, M. Shang, W. R. Scheidt and D. H. Burns, *J. Am. Chem. Soc.*, 1998, **120**, 11684.

109. D. H. Burns, K. Calderon-Kawasaki and S. Kularatne, *J. Org. Chem.*, 2005, **70**, 2803.
110. S. Amemiya, P. Buhlmann, Y. Umezawa, R. C. Jagessar and D. H. Burns, *Anal. Chem.*, 1999, **71**, 1049.
111. P. D. Beer, M. G. B. Drew, C. Hazlewood, D. Heseck, J. Hodacova and S. E. Stokes, *J. Chem. Soc. Chem. Commun.*, 1993, 229
112. P. Beer, D. Heseck, K. Nam and M. G. B. Drew, *Organometallics*, 1999, **18**, 3933.
113. M. Dudic, P. Lhoták, I. Stibor, K. Lang and P. Proskova, *Org. Lett.*, 2003, **5**, 149.
114. K. Lang, P. Curinova, M. Dudic, P. Proskova, I. Stibor, V. St'astny and P. Lhoták, *Tetrahedron Lett.*, 2005, **46**, 4469.
115. Y. Morzherin, D. M. Rudkevich, W. Verboom and D. N. Reinhoudt, *J. Org. Chem.*, 1993, **58**, 7602.
116. J. Scheerder, M. Fochi, J. F. J. Engbersen and D. N. Reinhoudt, *J. Org. Chem.*, 1994, **59**, 7815.
117. J. Scheerder, J. F. J. Engbersen, A. Casnati, R. Ungaro and D. N. Reinhoudt, *J. Org. Chem.*, 1995, **60**, 6448.
118. A. J. Evans and P. D. Beer, *J. Chem. Soc. Dalton Trans.*, 2003, 4451.
119. J. Scheerder, J. P. M. v. Duynhoven, J. F. J. Engbersen and D. N. Reinhoudt, *Angew. Chem. Int. Ed.*, 1996, **35**, 1090.
120. G. Tumcharern, T. Tuntulani, S. J. Coles, M. B. Hursthouse and J. D. Kilburn, *Org. Lett.*, 2003, **5**, 4971.
121. T. Yamato, S. Rahman, X. Zeng, F. Kitajima and G. Jeong Tae, *Can. J. Chem.*, 2006, **84**, 58.
122. T. R. Tshikhudo, D. Demuru, Z. Wang, M. Brust, A. Secchi, A. Arduini and A. Pochini, *Angew. Chem. Int. Ed.*, 2005, **44**, 2913.
123. S. Memon, M. Tabakci, D. M. Roundhill and M. Yilmaz, *React. Funct. Polym.*, 2006, **66**, 1342.
124. P. D. Barata, A. I. Costa, P. Granja and J. V. Prata, *React. Funct. Polym.*, 2004, **61**, 147.
125. A. R. Mendes, C. C. Gregorio, P. D. Barata, A. I. Costa and J. V. Prata, *React. Funct. Polym.*, 2005, **65**, 9.
126. Y. Kang and D. M. Rudkevich, *Tetrahedron*, 2004, **60**, 11219.
127. S. E. Matthews, C. W. Pouton and M. D. Threadgill, *Adv. Drug. Del. Rev.*, 1996, **18**, 219.

128. H. Maeda, T. Sawa and T. Konno, *J. Control. Release*, 2001, **74**, 47.
129. Y. Matsumura and H. Maeda, *Cancer Res.*, 1986, **46**, 6387.
130. H. Maeda, *Adv. Drug. Del. Rev.*, 2001, **46**, 169.
131. P. Caravan, J. J. Ellison, T. J. McMurry and R. B. Lauffer, *Chem. Rev.*, 1999, **99**, 2293.
132. R. B. Lauffer, *Chem. Rev.*, 1987, **87**, 901.
133. É. Toth, L. Helm and A. E. Merbach, in *The Chemistry of Contrast Agents in Medical Magnetic Resonance Imaging*, eds. É. Toth and A. E. Merbach, Wiley & Sons, Chichester, 2001, 45-120.
134. S. Aime, M. Botta, M. Fasano and E. Terreno, in *The Chemistry of Contrast Agents in Magnetic Resonance Imaging*, eds. É. Tóth and A. E. Merbach, Wiley & Sons, Chichester, 2001, 193-242.
135. R. M. Izatt, J. D. Lamb, R. T. Hawkins, P. R. Brown, S. R. Izatt and J. J. Christensen, *J. Am. Chem. Soc.*, 1983, **105**, 1782.
136. S. R. Izatt, R. T. Hawkins, J. J. Christensen and R. M. Izatt, *J. Am. Chem. Soc.*, 1985, **107**, 63.
137. R. G. Pearson, *J. Am. Chem. Soc.*, 1963, **85**, 3533.
138. E. Brücher and A. D. Sherry, in *The Chemistry of Contrast Agents in Medical Magnetic Resonance Imaging*, eds. É. Tóth and A. E. Merbach, Wiley & Sons, Chichester, 2001, 243-280.
139. A.-M. Fanning, S. E. Plush and T. Gunnlaugsson, *Chem. Commun.*, 2006, 3791.
140. J. P. Leonard, C. M. G. dos Santos, S. E. Plush, T. McCabe and T. Gunnlaugsson, *Chem. Commun.*, 2006, In Press.
141. L. L. Graham and R. E. Diel, *J. Phys. Chem.*, 1969, **73**, 2696.
142. J. Clayden, N. Greeves, S. Warren and P. Wothers, *Organic Chemistry*, Oxford University Press, 2000.
143. T. D. Harris, T. J. Reilly and J. A. DelPrincipe, *J. Heterocycl. Chem.*, 1981, **18**, 423.
144. T. Gunnlaugsson, D. F. Brougham, A. M. Fanning, M. Nieuwenhuyzen, J. E. O'Brien and R. Viguier, *Org. Lett.*, 2004, **6**, 4805.
145. J. Y. Lee, S. K. Kim, J. H. Jung and J. S. Kim, *J. Org. Chem.*, 2005, **70**, 1463.
146. Y. Wu, H.-B. Liu, J. Hu, Y.-J. Liu, C.-Y. Duan and Z. Xu, *Chin. J. Chem.*, 2000, **18**, 94.

147. Y. Wu, X.-P. Shen, C.-Y. Duan, Y.-J. Liu and Z. Xu, *Tetrahedron Lett.*, 1999, **40**, 5749.
148. J. Scheerder, R. H. Vreekamp, J. F. J. Engbersen, W. Verboom, J. P. M. van Duynhoven and D. N. Reinhoudt, *J. Org. Chem.*, 1996, **61**, 3476.
149. E. A. Alekseeva, V. A. Bacherikov, A. I. Gren', A. V. Mazepa, V. Y. Gorbatyuk and S. P. Krasnoshchekaya, *Russ. J. Org. Chem.*, 2000, **36**, 1321.
150. S. E. Matthews, PhD Thesis, University of Bath, 1995.
151. S. W. Magennis, J. Craig, A. Gardner, F. Fucassi, P. J. Cragg, N. Robertson, S. Parsons and Z. Pikramenou, *Polyhedron*, 2003, **22**, 745.
152. P. D. Beer, G. D. Brindley, O. Danny Fox, A. Grieve, M. I. Ogden, F. Szemes and M. G. B. Drew, *J. Chem. Soc. Dalton Trans.*, 2002, 3101.
153. S. K. Ramalingam and S. Soundararajan, *J. Inorg. Nucl. Chem.*, 1967, **29**, 1763.
154. M. R. Lewis, A. Raubitschek and J. E. Shively, *Bioconjugate Chem.*, 1994, **5**, 565.
155. F. Lecolley, L. Tao, G. Mantovani, I. Durkin, S. Lautru and D. M. Haddleton, *Chem. Commun.*, 2004, 2026.
156. A. Abuchowski, J. R. McCoy, N. C. Palczuk, T. van Es and F. F. Davis, *J. Biol. Chem.*, 1977, **252**, 3582.
157. A. Abuchowski, T. van Es, N. C. Palczuk and F. F. Davis, *J. Biol. Chem.*, 1977, **252**, 3578.
158. F. X. Hu, K. G. Neoh and E. T. Kang, *Biomaterials*, 2006, **27**, 5725.
159. K. S. Soppimath, T. M. Aminabhavi, A. R. Kulkarni and W. E. Rudzinski, *J. Control. Release*, 2001, **70**, 1.
160. M. Brinkley, *Bioconjugate Chem.*, 1992, **3**, 2.
161. G. T. Hermanson, *Bioconjugate techniques*, Academic Press, San Diego ; London, 1996.
162. J. Baranowskakortylewicz and A. I. Kassis, *Bioconjugate Chem.*, 1993, **4**, 300.
163. M. Salmain, M. Gunn, A. Gorfti, S. Top and G. Jaouen, *Bioconjugate Chem.*, 1993, **4**, 425.
164. T.-T. Wang and N. M. Young, *Anal. Biochem.*, 1978, **91**, 696.
165. M. O. Dayhoff, *Atlas of Protein Sequence and Structure, Vol. 5, Suppl. 2*, 1976.
166. R. J. De Lange and T. S. Huang, *J. Biol. Chem.*, 1971, **246**, 698.
167. M. H. B. Grote-Gansey, A. S. d. Haan, E. S. Bos, W. Verboom and D. N. Reinhoudt, *Bioconjugate Chem.*, 1999, **10**, 613.

168. S. Safi, Z. Asfari, L. Ehret-Sabatier, M. Leroy and A. Hagege, *Bioconjugate Chem.*, 2006, **17**, 1346.
169. V. Böhmer, J.-F. Dozol, C. Gruettner, K. Liger, S. E. Matthews, S. Rudershausen, M. Saadioui and P. Wang, *Org. Biomol. Chem.*, 2004, **2**, 2327.
170. S. E. Matthews, P. Parzuchowski, V. Böhmer, A. Garcia-Carrera, J.-F. Dozol and C. Gruttner, *Chem. Commun.*, 2001, 417.
171. J. B. Cooper, M. G. B. Drew and P. D. Beer, *J. Chem. Soc., Dalton Trans.*, 2001, 392.
172. J. B. Cooper, M. G. B. Drew and P. D. Beer, *J. Chem. Soc. Dalton Trans.*, 2000, 2721.
173. P. D. Beer and J. B. Cooper, *Chem. Commun.*, 1998, 129.
174. X. Chen, M. Ji, D. R. Fisher and C. M. Wai, *Synlett*, 1999, 1784.
175. J. B. Cooper, *D. Phil.*, University of Oxford, 1999.
176. L. Wang, X. Shi, P. Jia and Y. Yang, *J. Polym. Sci., Part A: Polym. Chem.*, 2004, **42**, 6259.
177. S. Berthelon, J.-B. Regnouf-de-Vains and R. Lamartine, *Synth. Commun.*, 1996, **26**, 3103.
178. P. Lhoták, *Tetrahedron*, 2001, **57**, 4775.
179. P. Lhoták, J. Morávek and I. Stibor, *Tetrahedron Lett.*, 2002, **43**, 3665.
180. A. K. Chatterjee, T.-L. Choi and D. P. S. H. Grubbs, *J. Am. Chem. Soc.*, 2003, **125**, 11360.
181. S. J. Connon and S. Blechert, *Angew. Chem. Int. Ed.*, 2003, **42**, 1900.
182. M. Pitarch, V. McKee, M. Nieuwenhuyzen and M. A. McKervey, *J. Org. Chem.*, 1998, **63**, 946.
183. M. Scholl, S. Ding, C. W. Lee and R. H. Grubbs, *Org. Lett.*, 1999, **1**, 953.
184. X.-L. Geng, Z. Wang, X.-Q. Li and C. Zhang, *J. Org. Chem.*, 2005, **70**, 9610.
185. Y.-L. Lin, T.-S. Yu, W.-Y. Wang and L.-G. Lin, *Tetrahedron*, 2006, **62**, 6082.
186. L.-H. Wei, Y.-B. He, J.-L. Wu, X.-J. Wu, L.-Z. Meng and X. Yang, *Supramol. Chem.*, 2004, **16**, 561.
187. A. M. Costero, S. Peransi and S. Gil, *Tetrahedron Lett.*, 2006, **47**, 6561.
188. L. S. Evans, P. A. Gale, M. E. Light and R. Quesada, *New. J. Chem.*, 2006, **30**, 1019.
189. L. S. Evans, P. A. Gale, M. E. Light and R. Quesada, *Chem. Commun.*, 2006, 965.
190. M. O. Vysotsky and V. Böhmer, *Org. Lett.*, 2000, **2**, 3571.

191. M. O. Vysotsky, M. Bolt, I. Thondorf and V. Böhmer, *Chem. Eur. J.*, 2003, **9**, 3375.
192. Y. L. Cho, D. M. Rudkevich, A. Shivanyuk, K. Rissanen and J. J. Rebek, *Chem. Eur. J.*, 2000, **6**, 3788.
193. C. F. Wilcox and S. H. Bauer, *J. Mol. Struct.: THEOCHEM*, 2003, **625**, 1.
194. M. Lewis and R. Glaser, *J. Org. Chem.*, 2002, **67**, 1441.
195. K. No, H. J. Lee, K. M. Park, S. S. Lee, K. H. Noh, S. K. Kim, J. Y. Lee and J. S. Kim, *J. Heterocycl. Chem.*, 2004, **41**, 211.
196. M. Maeder and A. D. Zuberbuehler, *Anal. Chem.*, 1990, **62**, 2220.
197. M. J. Hynes, *J. Chem. Soc. Dalton Trans.*, 1993, 311.
198. P. A. Gale, S. Camiolo, G. J. Tizzard, C. P. Chapman, M. E. Light, S. J. Coles and M. B. Hursthouse, *J. Org. Chem.*, 2001, **66**, 7849.
199. K. A. Connors, *Binding Constants*, 1987.
200. J. Brynestad and G. P. Smith, *J. Phys. Chem.*, 1968, **72**, 296
201. J. L. Sessler, V. Roznyatovskiy, G. D. Pantos, N. E. Borisova, M. D. Reshetova, V. M. Lynch, V. N. Khrustalev and Y. A. Ustynyuk, *Org. Lett.*, 2005, **7**, 5277.
202. S. E. Matthews and P. D. Beer, *Supramol. Chem.*, 2005, **17**, 411.
203. L. S. Evans, P. A. Gale, M. E. Light and R. Quesada, *Chem. Commun.*, 2006, 965.
204. M. Boiocchi, L. D. Boca, D. Esteban-Gómez, L. Fabbrizzi, M. Licchelli and E. Monzani, *Chem. Eur. J.*, 2005, **11**, 3097.
205. K.-Y. Ng, A. R. Cowley and P. D. Beer, *Chem. Commun.*, 2006, 3676.
206. P. A. Salter, *D. Phil.*, University of Oxford, 2000.
207. A. I. Vogel, B. S. Furniss, A. R. Tatchell, A. J. Hannaford and P. W. G. Smith, *Vogel's Textbook of Practical Organic Chemistry*, 5th edn., Longman, 1989.
208. C. D. Gutsche and J. A. Levine, *J. Am. Chem. Soc.*, 1982, **104**, 2652.
209. C.-M. Shu, W.-S. Chung, S.-H. Wu, Z.-C. Ho and L.-G. Lin, *J. Org. Chem.*, 1999, **64**, 2673.
210. D. M. Rudkevich, W. Verboom and D. N. Reinhoudt, *J. Org. Chem.*, 1994, **59**, 3683.
211. A. Hamid, H. M., E. S. Ramadan, M. Hagar and E. S. H. El Ashry, *Synth. Commun.*, 2004, **34**, 377.

Appendix

(i) Crystallographic Data

Crystal data for 25,26,27,28-tetrakis(((N-butyl)carbonyl)methoxy)calix[4]arene

Identification code	eq401m	
Empirical formula	C ₅₂ H ₆₈ N ₄ O ₈	
Formula weight	877.10	
Temperature	396(2) K	
Wavelength	0.71073 Å	
Crystal system	Orthorhombic	
Space group	Pna2(1)	
Unit cell dimensions	a = 18.934(5) Å	α = 90°.
	b = 12.940(3) Å	β = 90°.
	c = 19.851(5) Å	γ = 90°.
Volume	4864(2) Å ³	
Z	4	
Density (calculated)	1.198 Mg/m ³	
Absorption coefficient	0.081 mm ⁻¹	
F(000)	1888	
Crystal size	0.55 × 0.50 × 0.50 mm ³	
Theta range for data collection	1.88 to 25.00°.	
Index ranges	-22 ≤ h ≤ 21, -15 ≤ k ≤ 15, -23 ≤ l ≤ 23	
Reflections collected	37232	
Independent reflections	8579 [R(int) = 0.0595]	
Completeness to theta = 25.00°	100.0 %	
Absorption correction	None	
Refinement method	Full-matrix least-squares on F ²	
Data / restraints / parameters	8579 / 1 / 582	
Goodness-of-fit on F ²	1.030	
Final R indices [I > 2σ(I)]	R1 = 0.0463, wR2 = 0.1138	
R indices (all data)	R1 = 0.0490, wR2 = 0.1161	
Absolute structure parameter	0.0(8)	
Largest diff. peak and hole	0.454 and -0.326 e.Å ⁻³	

Crystal data for 25,26,27,28-tetrakis[*N*-propylcarbonyl]methoxy]calix[4]arene

Identification code	EQ403m	
Empirical formula	C ₄₈ H ₆₀ N ₄ O ₈	
Formula weight	821.00	
Temperature	150(2) K	
Wavelength	0.71073 Å	
Crystal system	Triclinic	
Space group	P-1	
Unit cell dimensions	a = 11.807(6) Å	α = 94.070(14)°.
	b = 13.247(7) Å	β = 98.605(10)°.
	c = 16.020(8) Å	γ = 90.167(10)°.
Volume	2471(2) Å ³	
Z	2	
Density (calculated)	1.103 Mg/m ³	
Absorption coefficient	0.075 mm ⁻¹	
F(000)	880	
Crystal size	0.71 × 0.52 × 0.45 mm ³	
Theta range for data collection	1.29 to 23.47°.	
Index ranges	-13 ≤ h ≤ 13, -13 ≤ k ≤ 14, -15 ≤ l ≤ 7	
Reflections collected	8926	
Independent reflections	5972 [R(int) = 0.0333]	
Completeness to theta = 23.47°	81.9 %	
Absorption correction	sadabs	
Refinement method	Full-matrix least-squares on F ²	
Data / restraints / parameters	5972 / 0 / 586	
Goodness-of-fit on F ²	1.206	
Final R indices [I > 2σ(I)]	R1 = 0.0948, wR2 = 0.2720	
R indices (all data)	R1 = 0.1325, wR2 = 0.3278	
Extinction coefficient	0.000(3)	
Largest diff. peak and hole	0.562 and -0.495 e.Å ⁻³	

Crystal data for 25,26,27,28-tetrakis[*(N*-piperidiny)carbonyl]methoxy]calix[4]arene

Identification code	EQ306m	
Empirical formula	C ₅₆ H ₆₈ N ₄ O ₁₈	
Formula weight	1085.14	
Temperature	423(2) K	
Wavelength	0.71073 Å	
Crystal system	Monoclinic	
Space group	C2/c	
Unit cell dimensions	a = 24.495(7) Å	α = 90°.
	b = 11.992(3) Å	β = 124.774(4)°.
	c = 20.256(6) Å	γ = 90°.
Volume	4887(2) Å ³	
Z	4	
Density (calculated)	1.475 Mg/m ³	
Absorption coefficient	0.110 mm ⁻¹	
F(000)	2304	
Crystal size	0.66 × 0.38 × 0.15 mm ³	
Theta range for data collection	1.98 to 22.50°.	
Index ranges	-26 ≤ h ≤ 26, -12 ≤ k ≤ 12, -21 ≤ l ≤ 21	
Reflections collected	14828	
Independent reflections	3197 [R(int) = 0.0223]	
Completeness to theta = 22.50°	100.0 %	
Absorption correction	Lorentz-polarisation, absorption correction	
Refinement method	Full-matrix least-squares on F ²	
Data / restraints / parameters	3197 / 0 / 307	
Goodness-of-fit on F ²	2.078	
Final R indices [I > 2σ(I)]	R1 = 0.1127, wR2 = 0.3963	
R indices (all data)	R1 = 0.1199, wR2 = 0.4148	
Largest diff. peak and hole	1.996 and -0.728 e.Å ⁻³	

Crystal data for 25,27-bis[*(N*-phenyl)carbonyl]methoxy]calix[4]arene

Identification code	EQ340m	
Empirical formula	C ₆₀ H ₅₂ N ₄ O ₈	
Formula weight	957.06	
Temperature	396(2) K	
Wavelength	0.71073 Å	
Crystal system	Triclinic	
Space group	P-1	
Unit cell dimensions	a = 11.3127(10) Å	α = 90.030(2)°.
	b = 13.9727(12) Å	β = 102.141(2)°.
	c = 23.134(2) Å	γ = 90.127(2)°.
Volume	3574.9(5) Å ³	
Z	3	
Density (calculated)	1.334 Mg/m ³	
Absorption coefficient	0.089 mm ⁻¹	
F(000)	1512	
Crystal size	0.50 × 0.50 × 0.50 mm ³	
Theta range for data collection	0.90 to 22.50°.	
Index ranges	-12 ≤ h ≤ 12, -12 ≤ k ≤ 15, -24 ≤ l ≤ 6	
Reflections collected	10231	
Independent reflections	8604 [R(int) = 0.0155]	
Completeness to theta = 22.50°	92.1 %	
Absorption correction	Lorentz-polarisation, absorption correction	
Refinement method	Full-matrix least-squares on F ²	
Data / restraints / parameters	8604 / 0 / 941	
Goodness-of-fit on F ²	1.107	
Final R indices [I > 2σ(I)]	R1 = 0.0444, wR2 = 0.1375	
R indices (all data)	R1 = 0.0488, wR2 = 0.1433	
Largest diff. peak and hole	0.250 and -0.289 e.Å ⁻³	

Crystal data for 25,26,27,28-tetrakis-*N*-(piperidinyl-2-aminoethyl)carbamoxyloxymethoxy-calix[4]arene

Identification code	EQpipidm	
Empirical formula	C ₆₄ H ₈₈ N ₈ O ₈	
Formula weight	1097.42	
Temperature	396(2) K	
Wavelength	0.71073 Å	
Crystal system	Monoclinic	
Space group	Cc	
Unit cell dimensions	a = 19.820(3) Å	α = 90°.
	b = 19.953(3) Å	β = 119.116(3)°.
	c = 18.583(2) Å	γ = 90°.
Volume	6420.4(14) Å ³	
Z	4	
Density (calculated)	1.135 Mg/m ³	
Absorption coefficient	0.075 mm ⁻¹	
F(000)	2368	
Crystal size	0.20 × 0.17 × 0.13 mm ³	
Theta range for data collection	1.60 to 25.00°.	
Index ranges	-23 ≤ h ≤ 23, -23 ≤ k ≤ 14, -20 ≤ l ≤ 22	
Reflections collected	16687	
Independent reflections	9357 [R(int) = 0.0619]	
Completeness to theta = 25.00°	100.0 %	
Absorption correction	None	
Refinement method	Full-matrix least-squares on F ²	
Data / restraints / parameters	9357 / 2 / 764	
Goodness-of-fit on F ²	1.006	
Final R indices [I > 2σ(I)]	R1 = 0.0882, wR2 = 0.2134	
R indices (all data)	R1 = 0.1669, wR2 = 0.2607	
Absolute structure parameter	-2(3)	
Largest diff. peak and hole	0.615 and -0.396 e.Å ⁻³	

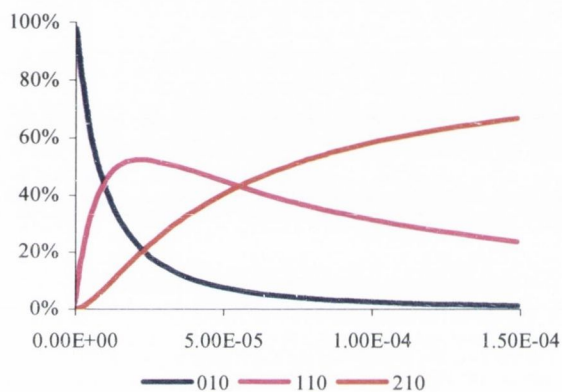
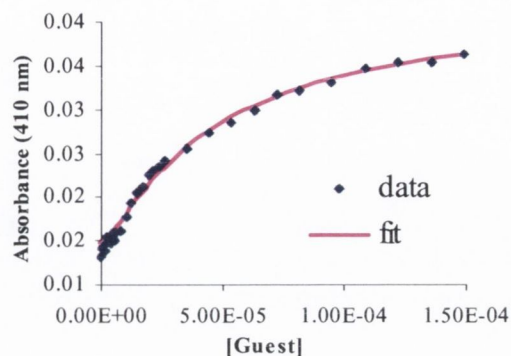
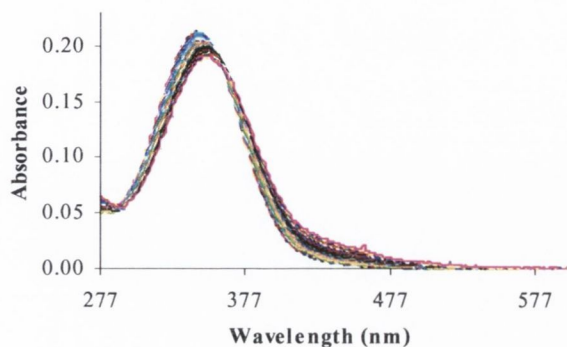
Appendix

(ii) UV-Vis Titration & Speciation Data

Speciation plots: percentage speciation is represented relative to the initial concentration of host.

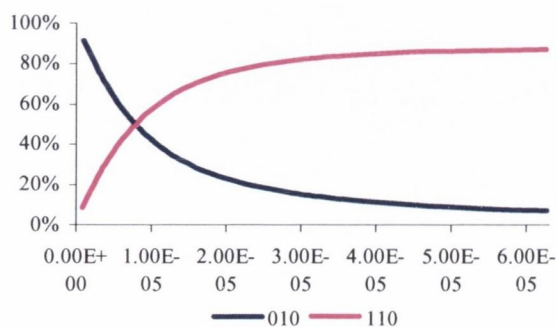
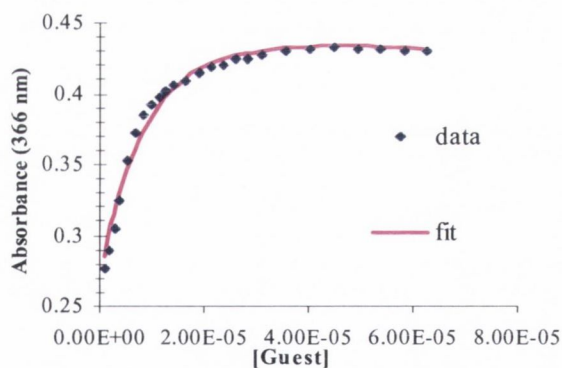
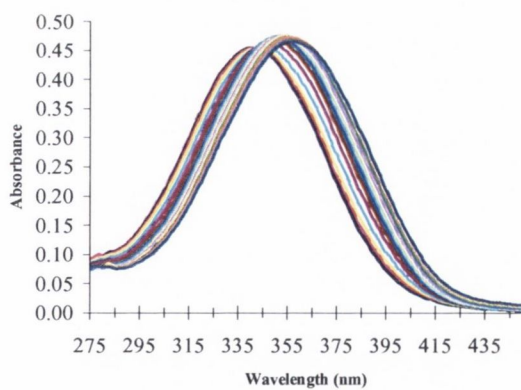
Titration of 125

Acetate; $[H]_0 = 3.218 \times 10^{-6}$



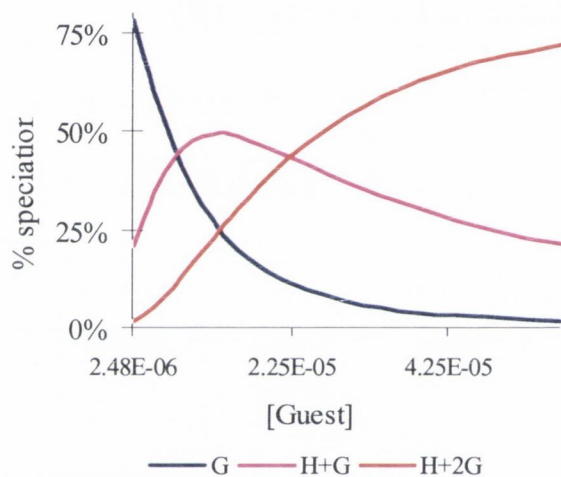
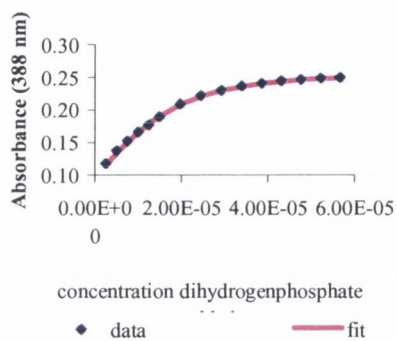
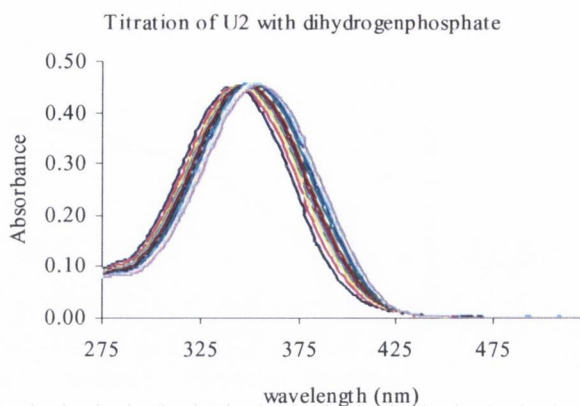
G	H	
1	1	5.10876 ± 0.0440832
2	1	9.39951 ± 0.0762474

Pyrophosphate; $[H]_0 = 6.881 \times 10^{-6}$



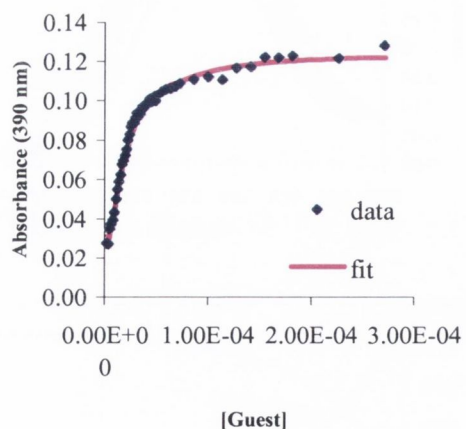
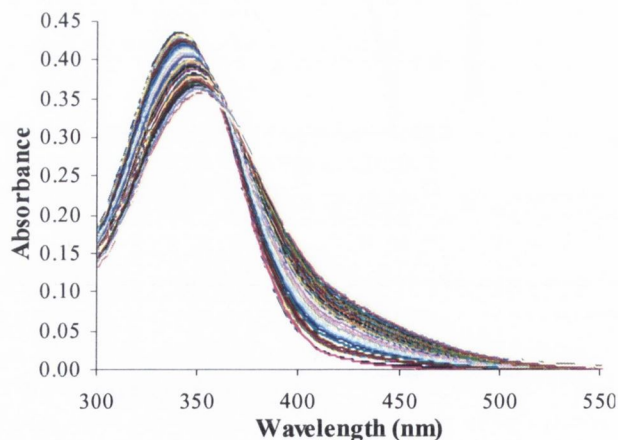
G	H	
1	1	5.34221 ± 0.0406951

Dihydrogenphosphate; $[H]_0 = 6.690 \times 10^{-6} \text{ M}$

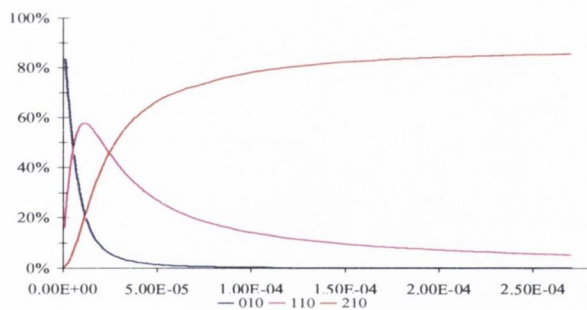


G	H	
1	1	5.45898 ± 0.174353
2	1	10.3277 ± 0.180932

Fluoride; $[H]_0 = 6.562 \times 10^{-6}$

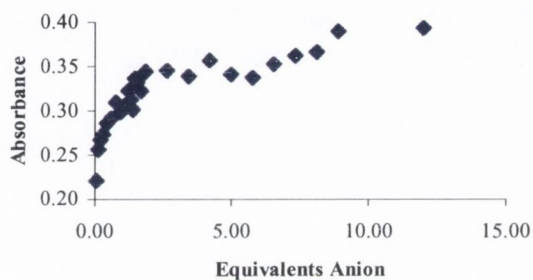
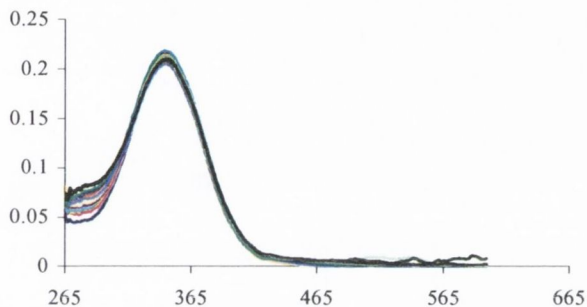


□



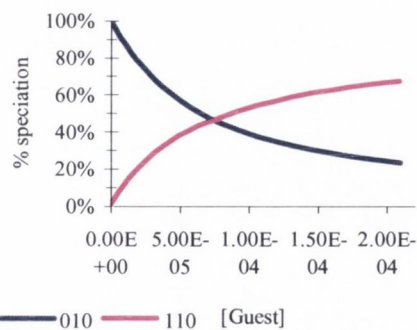
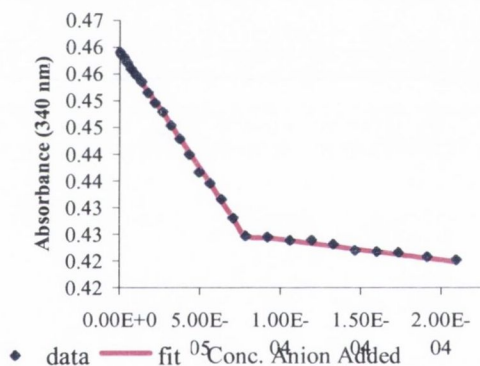
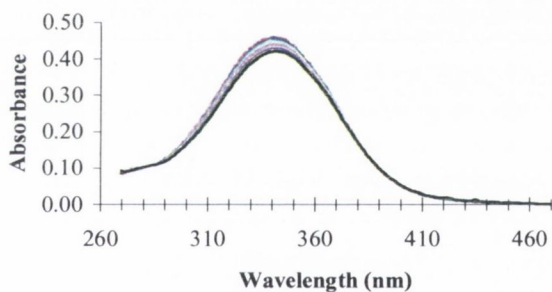
G	H	
1	1	5.68620 ± 0.20143
2	1	10.4748 ± 0.19240

Chloride; $[H]_0 = 3.19537 \times 10^{-6}$



Data could not be fitted to an appropriate model

Bromide; $[H]_0 = 6.915 \times 10^{-6}$

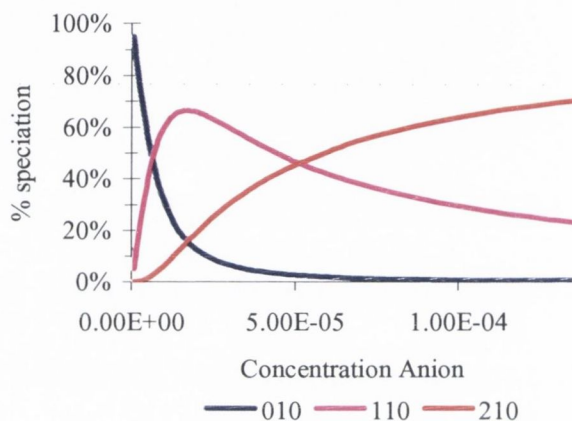
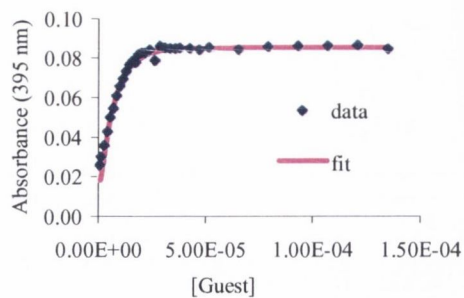
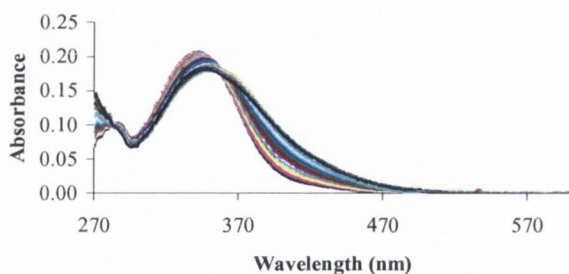


G	H	
1	1	4.14656 ± 0.05497

— 010 — 110 [Guest]

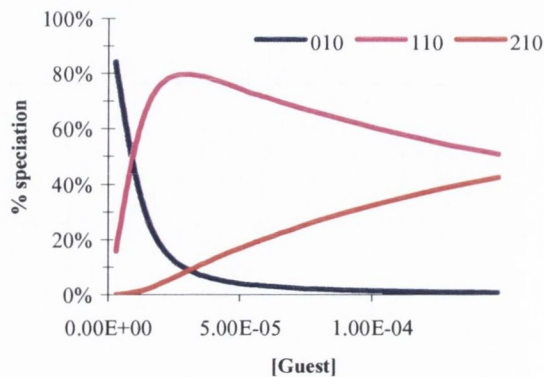
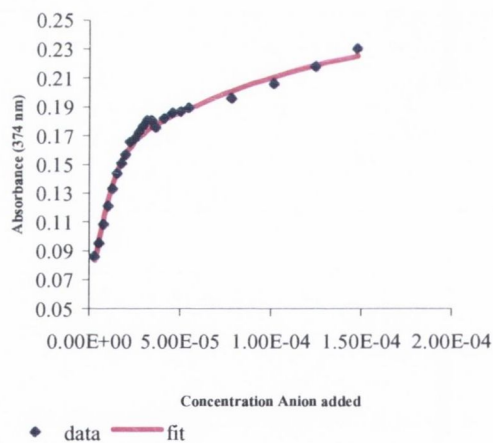
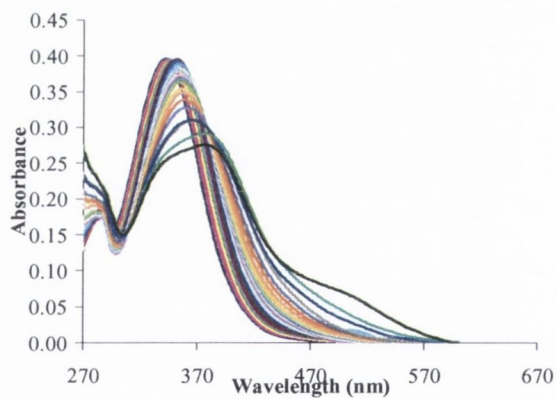
Titration of 131

Acetate; $[H]_0 = 7.178 \times 10^{-6}$



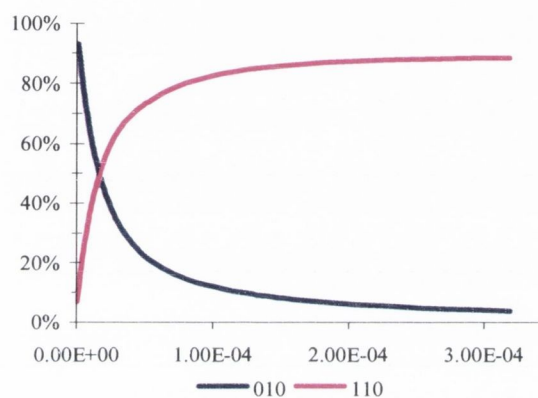
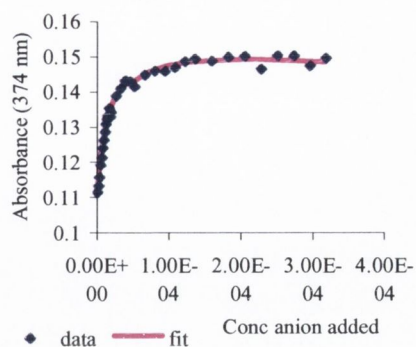
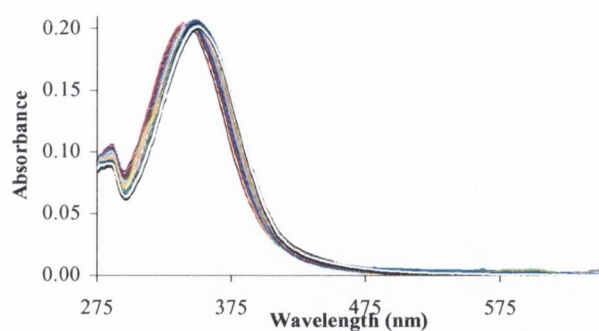
G	H	
1	1	5.636220 ± 0.072531
2	1	10.02550 ± 0.202355

Pyrophosphate; $[H]_0 = 1.355 \times 10^{-5}$



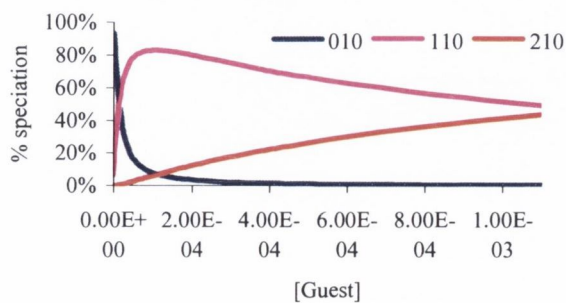
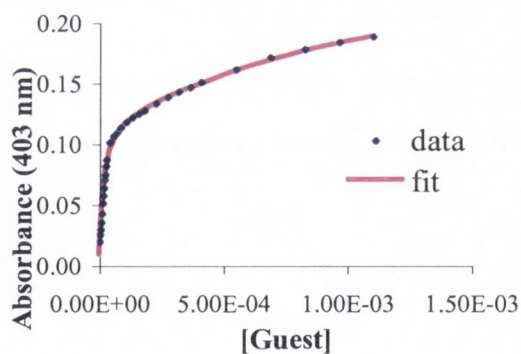
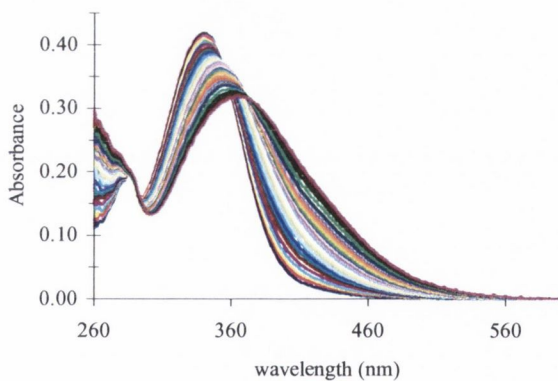
G	H	
1	1	5.72428 ± 0.112998
2	1	9.53577 ± 0.196826

Dihydrogenphosphate; $[H]_0 = 6.905 \times 10^{-6}$



G	H	
1	1	4.86009 ± 0.0346

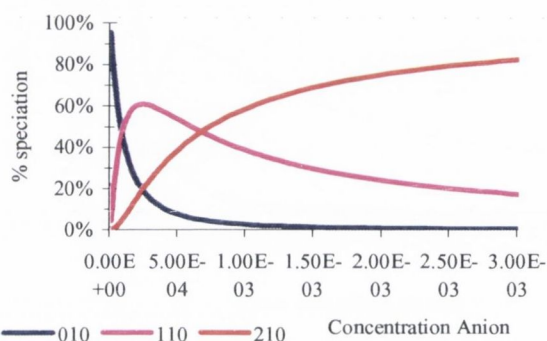
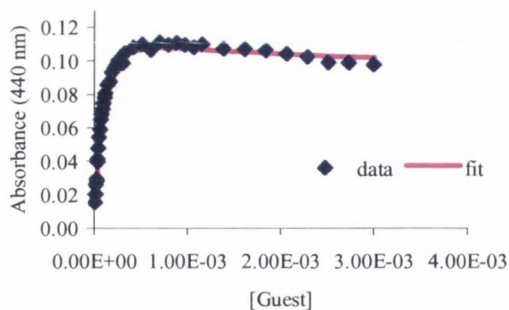
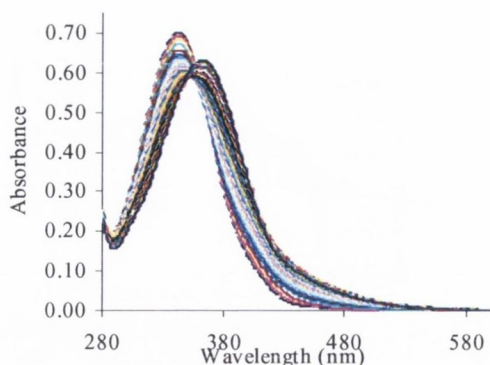
Fluoride; $[H]_0 = 1.441 \times 10^{-5}$



G	H	
1	1	5.07451 ± 0.034139
2	1	7.98720 ± 0.122702

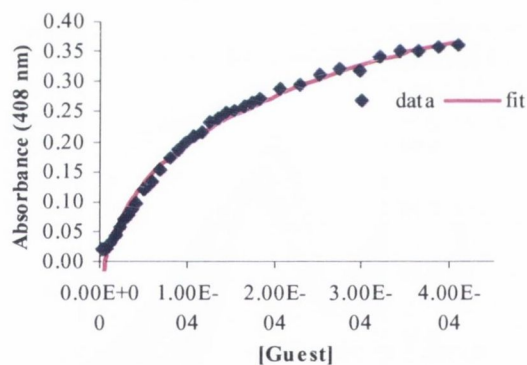
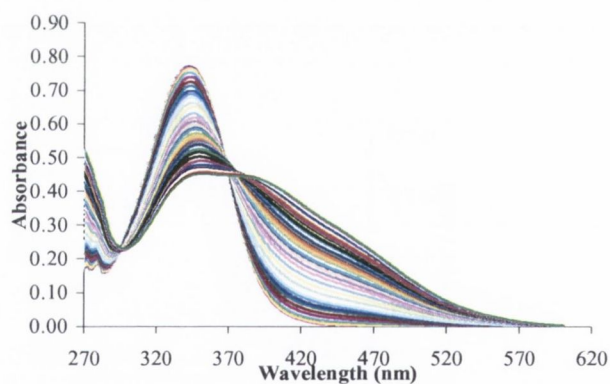
Titration of 137

Acetate; $[H]_0 = 4.33 \times 10^{-5}$

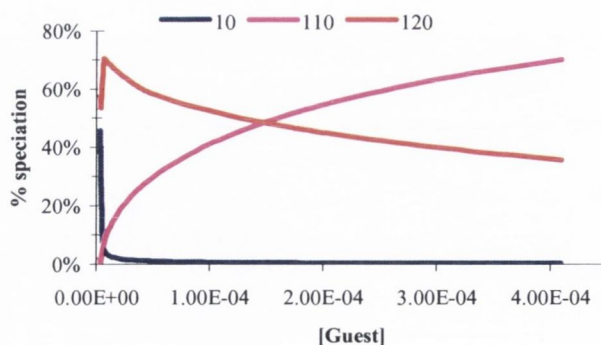


G	H	
1	1	4.20002 ± 0.0294
2	1	7.41278 ± 0.0624

Pyrophosphate; $[H]_0 = 4.555 \times 10^{-6}$

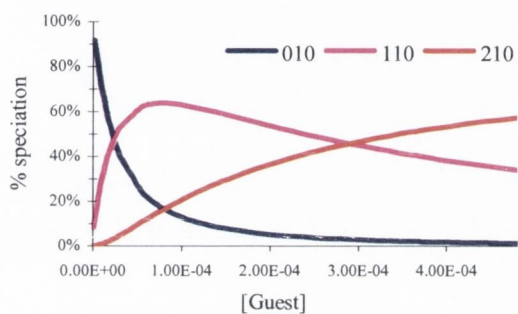
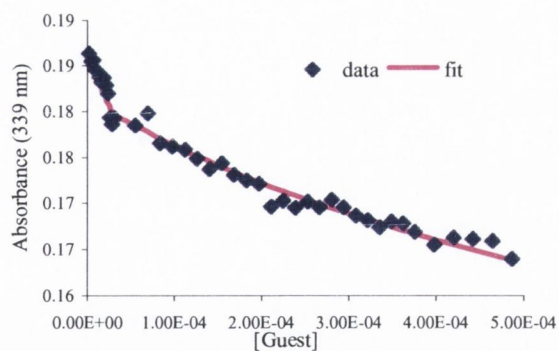
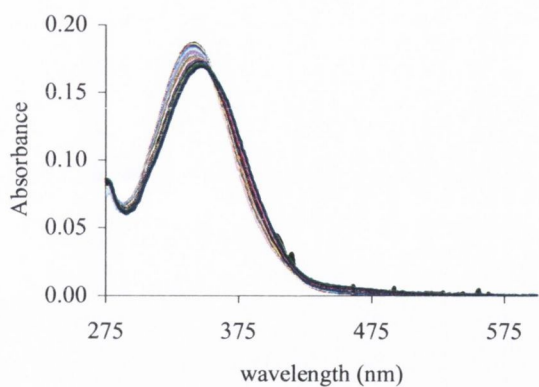


□



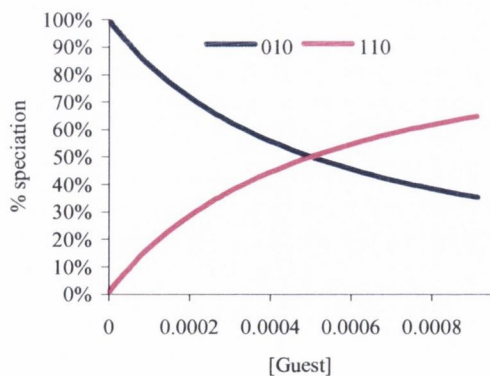
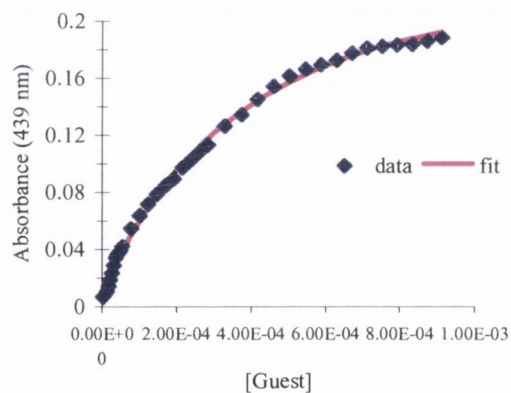
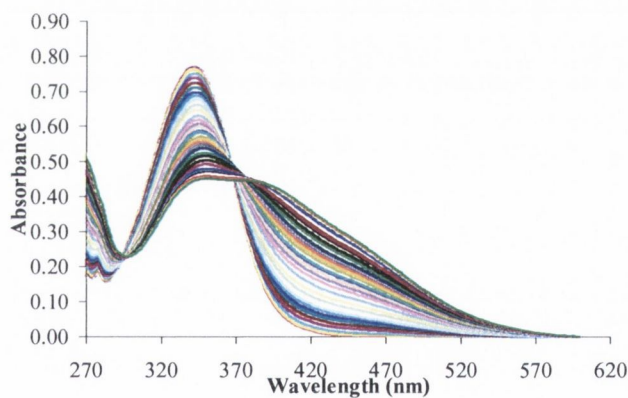
G	H	
1	1	5.78904 ± 0.296696
1	2	13.387 ± 0.491633

Dihydrogenphosphate; $[H]_0 = 1.05 \times 10^{-5}$



G	H	
1	1	4.73172 ± 0.166672
2	1	8.28995 ± 0.113038

Fluoride; $[H]_0 = 3.001 \times 10^{-5}$



G	H	
1	1	3.30948 ± 0.0305511

Anion sensing using colorimetric amidourea based receptors incorporated into a 1,3-disubstituted calix[4]arene

Eoin Quinlan,^a Susan E. Matthews^{b,*} and Thorfinnur Gunnlaugsson^{a,*}

^a*School of Chemistry, Centre for Synthesis and Chemical Biology, Trinity College Dublin, Dublin 2, Ireland*

^b*School of Chemical Sciences and Pharmacy, University of East Anglia, Norwich NR4 7TJ, United Kingdom*

Received 15 August 2006; revised 10 October 2006; accepted 19 October 2006

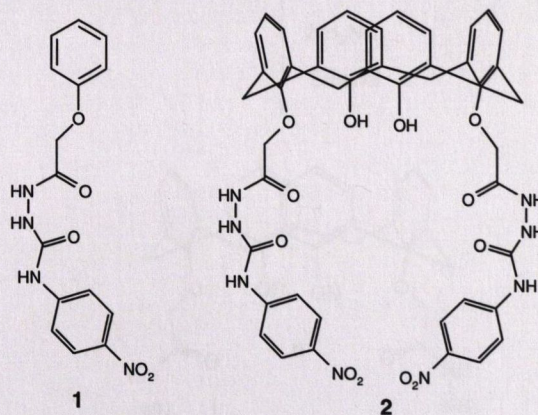
Available online 9 November 2006

Abstract—The synthesis of amidourea-based colorimetric anion sensors **1** and **2** and the evaluation of these sensors using anions such as acetate (CH_3CO_2^-), fluoride (F^-), hydrogen phosphate (H_2PO_4^-) and hydrogenpyrophosphate (*pyr*) in DMSO is described. While **1** has a single amidourea moiety, **2** has two such receptors incorporated into a lower-rim 1,3-disubstituted calix[4]arene scaffold. Whilst both sensors gave rise to red shifts in their absorption spectra upon anion recognition, the sensing of F^- and *pyr* gave rise to large changes with concomitant colour changes from yellow to purple, which were visible to the naked eye.
© 2006 Published by Elsevier Ltd.

The recognition of anions using luminescent or colorimetric methods has become an active area of research.^{1,2} In particular, charged or charge neutral receptors such as metal based macrocycles,³ amides,⁴ carbamides,⁵ ureas⁶ or thioureas⁷ have been employed for the selective recognition of anions in relatively simple structural motifs.⁸ Such binding sites have also been incorporated into structural frameworks such as steroids,⁹ calixarenes¹⁰ and polynorbornanes¹¹ giving rise to more pre-organized anion recognition motifs. Moreover, such designs can give rise to larger supramolecular assemblies as demonstrated elegantly by Gale et al.,¹² Kruger et al.¹³ and Beer et al.¹⁴ to name just a few. Anion receptors have also been employed for medicinal purposes and as biological mimics for the transport of anions or ion pairs across cell membranes.¹⁵

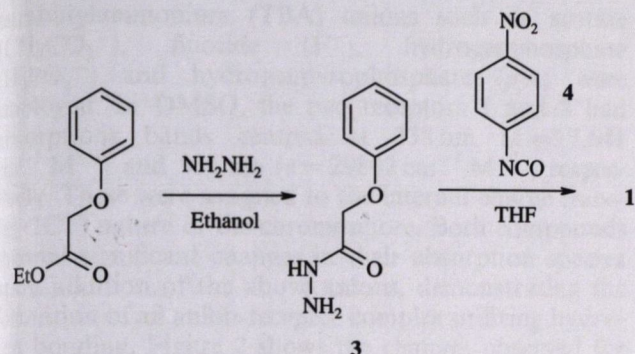
We are interested in the development of sensors for anions and have demonstrated such sensing based on the use of charge neutral photoinduced electron transfer (PET) sensors¹⁶ as well as colorimetric anion sensors based on the use of internal charge transfer chromophores.^{17,18} In this letter, we build upon these earlier successes and present **1**, which can also be incorporated into a preorganized scaffold, such as at the lower-rim of a 1,3-disubstituted calix[4]arene, for example, **2**.¹⁹ Our receptors are based on a simple amidourea structure

that can hydrogen bond to anions such as acetate, phosphate and potentially halides. Furthermore, using 4-nitrobenzene as part of the receptor enables us to monitor this binding spectroscopically in the visible region. We have previously used related amidothioureas as a part of naphthalimide based colorimetric sensors.²⁰ Similarly, both Gale et al., using pyrrolylamidoureas,²¹ and Jiang et al.²² using *N*-benzamido-thiourea, have developed many excellent examples of receptors for anion recognition. However, to the best of our knowledge, **2** is the first example of an amidourea based 1,3-disubstituted calix[4]arene based colorimetric sensor for anions.



The synthesis of **1** was achieved in two steps as shown in Scheme 1. This involved the use of 2-phenoxy-acetohydrazide **3**, which was made from ethyl 2-phenoxyacetate

* Corresponding authors. Tel.: +353 1 608 3459; fax: +353 1 671 2826 (T.G.); e-mail addresses: susan.matthews@uea.ac.uk; gunnlaut@tcd.ie



Scheme 1. Synthesis of 1.

by reaction with hydrazine hydrate in ethanol under reflux for 3 h, followed by cooling to room temperature overnight, upon which a solid was formed. Reacting 3 with 4-nitrophenyl isocyanate 4 under an inert atmosphere at room temperature overnight gave 1 as a light yellow precipitate in a 62% yield after filtration and washing with methanol. The ^1H NMR (400 MHz, in $\text{DMSO}-d_6$) clearly showed the presence of the two urea protons, and the amide urea proton.[†]

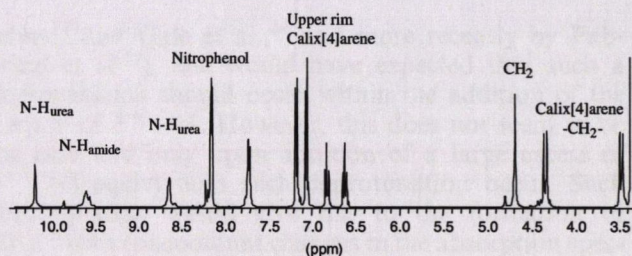
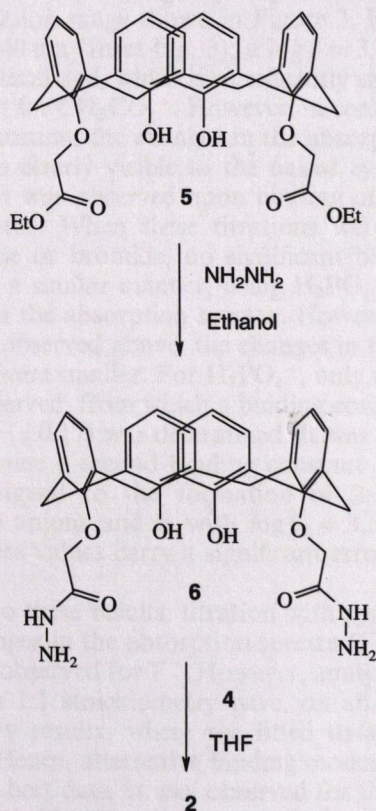
The rationale behind 2 was to incorporate two anion receptors into a single calixarene scaffold with the aim of achieving colorimetric sensing of anions such as phosphate or pyrophosphate, where the binding of the anion would be in a 1:1 stoichiometry. The synthesis of the desired sensor 2, commenced with the synthesis of the hydrazine intermediate 6, which was achieved in one-step from 25,27-bis[(ethoxy-carbonyl)methoxy]-26,28-dihydroxy calix[4]arene, 5, previously synthesized by Reinhoudt et al.,²³ through treatment with an excess of hydrazine hydrate. Following cooling to room temperature, the solution was evaporated to dryness under reduced pressure and the resulting residue triturated with methanol, collected by suction filtration and washed with distilled water providing 6 in a 94% yield

[†]Compound 1: Mp 208–211 °C. Anal. Calcd for $\text{C}_{15}\text{H}_{14}\text{N}_4\text{O}_5 \cdot 0.3\text{THF}$: C, 55.36; H, 4.74; N, 15.81. Found: C, 55.41; H, 4.41; N, 16.24%. ^1H NMR (400 MHz, $\text{DMSO}-d_6$) δ_{H} : 10.11 (s, 1H, NH), 9.55 (s, 1H, NH), 8.54 (s, 1H, NH), 8.18 (d, $J = 9.0$ Hz, 2H, Ar-H(nitrophenyl)), 7.73 (d, $J = 7.0$ Hz, 2H, Ar-H(nitrophenyl)), 7.32 (t, $J = 8.0$ Hz, 2H, Ar-H(ortho)), 7.00 (m, 3H, Ar-H(meta,para)), 4.63 (s, 2H, $\text{OCH}_2\text{C}(\text{O})$). ^{13}C NMR (100 MHz, $\text{DMSO}-d_6$) δ_{C} : 167.8, 157.7, 146.4, 141.1, 129.5, 125.0, 121.2, 118.0, 117.8, 114.7, 66.0. IR ν_{max} (cm^{-1} , solid): 3326, 3228, 3107, 2903, 1728, 1720, 1676, 1660, 1616, 1598, 1567, 1508, 1459, 1412, 1426, 1343, 1333, 1300, 1239, 1202, 1175.

Compound 2: Mp 242–245 °C Anal. Calcd for $\text{C}_{46}\text{H}_{40}\text{N}_8\text{O}_{12} \cdot \text{CH}_3\text{OH}$: C, 60.77; H, 4.77; N, 12.06. Found: C, 60.26; H, 4.48; N, 12.09%. ^1H NMR (400 MHz, $\text{DMSO}-d_6$) δ_{H} : 10.17 (s, 2H, NH_{urea}), 9.59 (s, 2H, NH_{urea}), 8.62 (s, 2H, NH_{amide}), 8.14 (d, $J = 9$ Hz, 4H, Ar-H(nitrophenyl)), 7.71 (d, $J = 9$ Hz, 4H, Ar-H(nitrophenyl)), 7.17 (d, $J = 7$ Hz, 4H, ArH), 7.05 (d, $J = 7$ Hz, 4H, ArH), 6.81 (t, $J = 8.0$ Hz, 2H, Ar-H), 6.62 (t, $J = 7.0$ Hz, 2H, Ar-H), 4.68 (s, 4H, $\text{ArO}-\text{CH}_2-\text{C}(\text{O})$), 4.33 (d, $J = 13$ Hz, 4H, $\text{Ar}-\text{CH}_2-\text{Ar}$), 4.46 (d, $J = 13$ Hz, 4H, $\text{Ar}-\text{CH}_2-\text{Ar}$). ^{13}C NMR (100 MHz, $\text{DMSO}-d_6$) δ_{C} : Quaternary not visible, 152.4, 152.3, 146.2, 141.2, 133.5, 129.1, 128.7, 127.5, 125.6, 125.4, 125.0, 119.3, 117.8, 73.3, 30.6. IR ν_{max} (cm^{-1} , solid): 3314, 3097, 1658, 1633, 1595, 1567, 1510, 1466, 1434, 1329, 1302, 1215.

as a white powder. We have also employed this method for the conversion of the tetra ester of calix[4]arene into the tetra hydrazidocarbonyl in good yield. The synthesis of the desired sensor was then achieved by reacting 6 in dry THF with 2 equiv of 4. The mixture was stirred overnight at room temperature after which it was quenched by the addition of methanol, and the off-yellow precipitate filtered and washed with methanol to yield 2 as a pale yellow powder in a 95% yield.[†] The ^1H NMR (400 MHz, $\text{DMSO}-d_6$) of 2, Figure 1, shows the formation of the desired amidourea sensor with characteristic resonances appearing at 10.17, 9.59 and 8.62 ppm for the three N–H protons. Figure 1 also shows the simplicity of the ^1H NMR caused by the C_2 symmetry of 2 (see Scheme 2).

The ability of both 1 and 2 to recognize anions was evaluated in DMSO by observing the changes in the absorption spectra of both compounds. For the current study,

Figure 1. The ^1H NMR (400 MHz, $\text{DMSO}-d_6$) of 2.

Scheme 2. Synthesis of 2.

tetrabutylammonium (TBA) anions such as acetate (CH_3CO_2^-), fluoride (F^-), hydrogenphosphate (H_2PO_4^-) and hydrogenpyrophosphate (*pyr*) were employed. In DMSO, the two receptors **1** and **2** had absorption bands centred at 338 nm ($\epsilon = 17,641 \text{ cm}^{-1} \text{ M}^{-1}$) and 336 nm ($\epsilon = 29802 \text{ cm}^{-1} \text{ M}^{-1}$), respectively. These were assigned to the internal charge transfer (ICT) nature of the chromophore. Both compounds showed significant changes in their absorption spectra upon addition of the above anions, demonstrating the formation of an anion-receptor complex utilizing hydrogen bonding. Figure 2 shows the changes observed for the titration of **1** with acetate. Here, significant spectral changes were observed for the 336 nm transition, which was hypsochromically shifted upon anion recognition. The changes in the 440 nm wavelength were used to evaluate the binding affinity of **1** and these changes are shown as an inset in Figure 2. Fitting these changes using the nonlinear least squares regression program SPECFIT, gave a good fit, with two binding constants, $\log \beta_1 = 4.20 (\pm 0.03)$ and $\log \beta_2 = 3.21 (\pm 0.09)$. This indicates that the binding of acetate is not a 1:1 stoichiometry as might be expected. Examining the changes in the main transition in Figure 2, it can be seen that no clear isosbestic point is observed, which suggest that there is more than one simple 1:1 binding process occurring. This can possibly be viewed as one of the anions forming linear hydrogen bonds to the urea part of the receptor, with a second binding occurring at the amide.

In a similar manner, the titration of F^- revealed some interesting results, as here the binding was determined to be mostly 1:1. Figure 3 shows the changes observed in the absorption spectra upon the addition of F^- . As can be seen from these changes the absorption band at 338 nm is significantly reduced in intensity, with concomitant formation of a new band centred at ca. 420 nm and an isosbestic point at 369 nm. This signifies a 1:1 binding interaction, which is somewhat surprising.¹⁷ Given the fact that F^- is a strong Lewis base and can deprotonate one, or more, of the N–H protons of the receptor (as previously demonstrated by our-

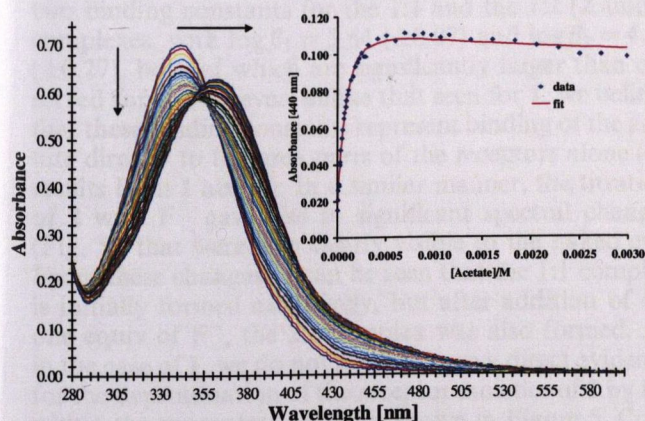


Figure 2. Changes in the absorption spectra upon titration with acetate in DMSO. The arrows show the red shift observed upon anion-complex formation. Inset: The changes at 440 nm and the fitted data observed using SPECFIT.

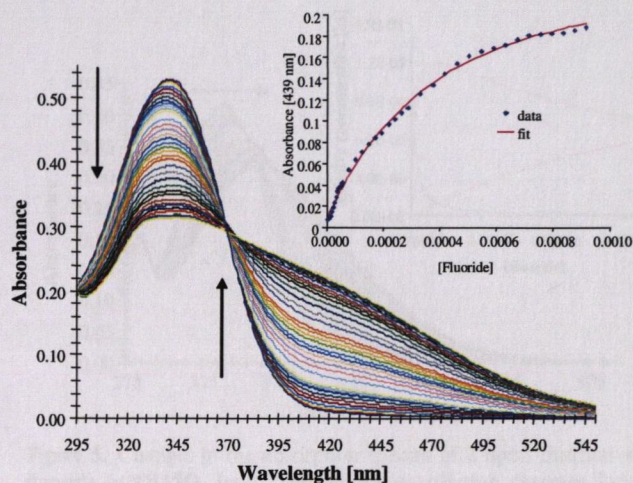


Figure 3. The changes in the absorption spectra of **1** upon titration with fluoride in DMSO. Inset: The changes at 439 nm and the result of fitting the data to 1:1 binding using SPECFIT.

selfes¹⁷ and Gale et al.,²⁴ and more recently by Fabbrizzi et al.²⁵), one would have expected that such a deprotonation should occur within the addition of the 2 equiv of F^- to **1**. However, this does not seem to be the case and only upon addition of a large excess of F^- (>40 equiv) does such deprotonation occur. Such deprotonation would give rise to the formation of HF_2^- with concomitant changes in the absorption spectra, which would be shifted to longer wavelengths.¹⁷ Indeed this was found to be the case for **1** at such high F^- concentrations. Hence, we can conclude that for F^- , the binding occurs only through hydrogen bonding within the concentration range shown in Figure 3. From these changes at 440 nm (Inset Fig. 3), a $\log \beta = 3.31 (\pm 0.03)$ value was determined, which is significantly smaller than that observed for CH_3CO_2^- . However, in contrast to the CH_3CO_2^- titration, the changes in the absorption spectra were also clearly visible to the naked eye, where a yellow colour was observed upon binding of the anion to the receptor. When these titrations were repeated using chloride or bromide, no significant binding was observed. In a similar manner, using H_2PO_4^- gave rise to changes in the absorption spectra. However, in contrast to that observed above, the changes in the absorption spectra were smaller. For H_2PO_4^- , only a small red shift was observed, from which a binding constant value $\log \beta_1 = 4.73 (\pm 0.17)$ was determined. It was also possible to determine a second binding constant from these changes, assigned to the formation of 2:1 complex between two anions and **1**, with $\log \beta_2 = 3.55 (\pm 0.30)$, however, these values carry a significant error.

In contrast to these results, titration with *pyr*, gave rise to large changes in the absorption spectra (Fig. 4), similar to those observed for F^- . However, analysis of these data using a 1:1 stoichiometry gave, on all occasions, unsatisfactory results, where the fitted data carried a large error. Hence, alternative binding modes were considered. The best data fit was observed for the scenario where 2 equiv of **1** and a single anion formed a complex. The speciation distribution diagram for this fitting is

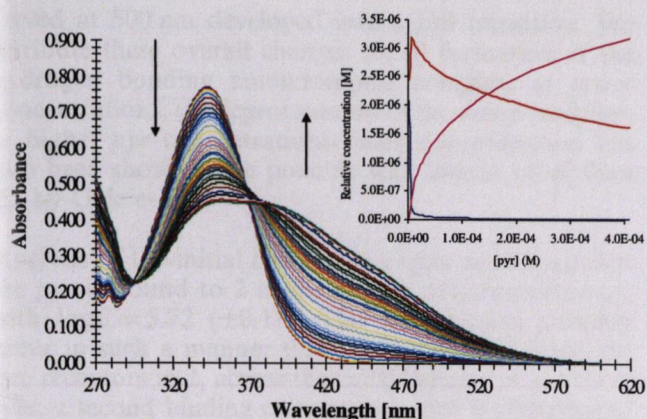


Figure 4. The changes in the absorption spectra of **1** upon titration with *pyr* in DMSO. Inset: Speciation distribution diagram for the titration of **1** with *pyr* in DMSO: — **1**; — 1:1 and — 2:1.

seen as an inset in Figure 4. From this fit, two binding constants can be determined for 2:1 (1:anion) and 1:1 anion binding, where at a lower concentration, the 2 equiv of **1** bind to *pyr*, but with increasing concentration of the anion, the self-assembly brakes down to give the 1:1 complex as the dominant stoichiometry (Fig. 4). For the 1:1 binding, a value of $\log \beta = 5.78 (\pm 0.30)$ was determined, which is quite strong binding; while for the 2:1 self-assembly, a binding constant of $\log \beta = 7.59 (\pm 0.8)$ was determined. However, it is worth pointing out that this latter binding carries a large error.

Having established the ability of **1** to interact with anions in 1:1, 2:1 or 1:2 stoichiometries, we investigated the use of **2** under identical conditions. In the case of **2**, the anion receptors are more preorganized, and as such should be able to bind anions such as H_2PO_4^- or *pyr* in a more cooperative manner, giving rise to an exclusive 1:1 binding of these anions. We first evaluated the ability of **2** to sense CH_3CO_2^- , which would be expected to bind in a 2:1 manner (anion:2) as each of the amidoureas would be expected to act independently. Upon titration with CH_3CO_2^- , the absorption spectrum of **2** was shifted to longer wavelengths in a similar manner to that observed for **1**. Analysis of the changes at 440 nm indeed revealed two binding constants for the 1:1 and the 1:2 (2:anion) complexes, with $\log \beta_1 = 5.64 (\pm 0.07)$ and $\log \beta_2 = 4.39 (\pm 0.27)$, both of which are significantly larger than observed for **1**. However, unlike that seen for **1**, we believe that these binding constants represent binding of the acetate directly to the urea parts of the receptors alone (cf. results from **1** above). In a similar manner, the titration of **2** with F^- gave rise to significant spectral changes (Fig. 5), that were also clearly visible to the naked eye. From these changes, it can be seen that the 1:1 complex is initially formed exclusively, but after addition of ca. one equiv of F^- , the 2:1 complex was also formed. As in the case of **1**, we do not seem to have a direct evidence for the deprotonation of the receptor moieties of **2** by F^- within the concentration range shown in Figure 5. Consequently, we can conclude that F^- is being recognized as the hydrogen bonding complex, mirroring that observed for **1**. From these changes a value of $\log \beta = 5.1 (\pm 0.05)$ was determined for the 1:1 complex formation, with a

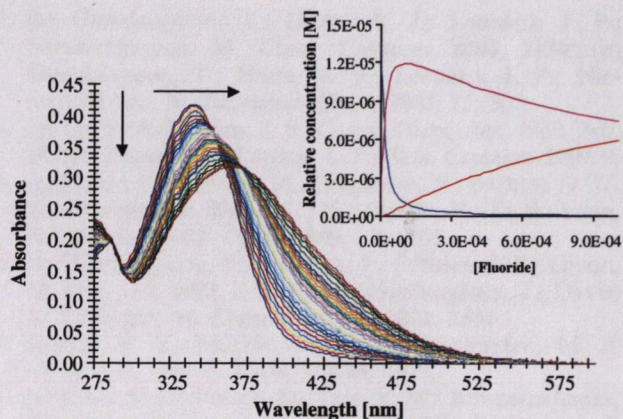


Figure 5. Changes in the absorption spectra of **2** upon titration with fluoride in DMSO. Inset: The species distribution diagram for the titration: — **2**, — 1:1 and — 2:1 (anion:2).

$\log \beta = 3.24 (\pm 0.15)$ value being determined for 2:1 complex.

The titrations of **2** using H_2PO_4^- also gave rise to hypsochromic shifts in the absorption spectra. However, as for the titration of **1**, these changes were not as pronounced as those for CH_3CO_2^- and F^- . However, here the preorganization of the sensor was evident as only 1:1 binding was observed, with $\log \beta = 4.86 (\pm 0.03)$ being determined. This is somewhat stronger binding than that observed for **1**, demonstrating the advantage of the use of the receptors as part of the calix[4]arene scaffold.

The most striking results were however, once again observed for the titration with *pyr*. The changes in the absorption spectra are shown in Figure 6, and clearly show that the band centred at 336 nm is initially shifted to longer wavelengths, in a similar manner to that seen for **1** giving rise to the formation of a new band at ca. 377 nm, and a shoulder at ca. 500 nm. However, at a higher concentration (not shown), the 377 nm absorption gave way to even further changes with the formation of two new bands at 346 and 384 nm, respectively. Moreover, the shoulder previously ob-

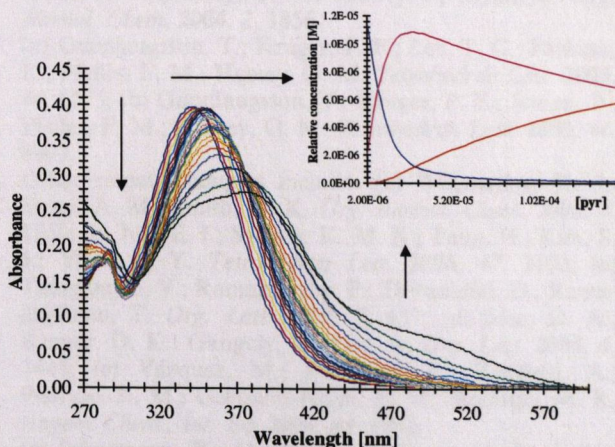


Figure 6. The changes in the absorption spectra of **2** upon titration with *pyr* in DMSO. Inset: The species distribution diagram for the titration of **2** with pyrophosphate: — **2**, — 1:1 and — 1:2 (anion:2).

served at 500 nm developed into a full transition. We attribute these overall changes to: (i) formation of the hydrogen bonding anion:receptor complex, at lower concentrations, (ii) deprotonation of the anion receptors at higher *pyr* concentrations. Such deprotonation has also been shown to be possible with anions other than F⁻ by Gale et al.²¹

Analysis of the initial changes in Figure 6, showed that the *pyr* is bound to **2** in the desired 1:1 stoichiometry, with $\log \beta = 5.72 (\pm 0.11)$. This binding can possibly occur in such a manner that the *pyr* anion bridges the two receptors in **2**, across the calix[4]arene cavity. However, a second binding constant can also be determined from these changes, assigned to the 1:2 (2:anion) stoichiometry, with $\log \beta = 3.81 (\pm 0.31)$. The speciation distribution diagram for the binding of *pyr* to **2** is shown in Figure 6 as an inset. From these changes, it can be seen that the recognition of *pyr* initially involves the formation of a 1:1 self-assembly, with the formation of the 1:1 and the 1:2 binding stoichiometries at higher concentrations. We are currently evaluating these binding possibilities in a greater detail.

In summary, we have developed calixarene **2** as a novel colorimetric sensor for anions, by incorporating amide-urea based receptors, used in model compound **1**, into 1,3-disubstituted calix[4]arene in short and high yielding synthesis. We have demonstrated that these receptors can bind F⁻ in a 1:1 stoichiometry with concomitant colorimetric changes, where the binding occurs through hydrogen bonding and that no deprotonation of the receptors in either **1** or **2** occurs until high F⁻ concentrations are reached. We have also shown that a strong 1:1 binding is observed for H₂PO₄⁻ and *pyr*, where the latter binding occurs by bridging the anion across the lower-rim cavity of the 1,3-functionalized calix[4]arene scaffold **2**. We are currently working towards developing other analogues of **2** with the aim of achieving a more selective anion sensing and the formation of anion template self-assembly structures.

Acknowledgement

We like to thank TCD and Enterprise Ireland for financial support and Dr. John E. O'Brien for assisting with NMR measurements.

References and notes

- (a) Sessler, J. L.; Gale, P. A.; Cho, W. S. *Anion Receptor Chemistry*; Royal Society of Chemistry: Cambridge, UK, 2006; (b) Gunnlaugsson, T.; Glynn, M.; Tocci (née Hussey), G. M.; Kruger, P. E.; Pfeffer, F. M. *Coord. Chem. Rev.* **2006**, doi:10.1016/j.ccr.2006.08.017.
- (a) Steed, J. W. *Chem. Commun.* **2006**, 2637; (b) Martínez-Máñez, R.; Sancenón, F. *Chem. Rev.* **2003**, *103*, 4419; (c) Suksai, C.; Tuntulani, T. *Chem. Soc. Rev.* **2003**, *32*, 192; (d) Gale, P. A. *Coord. Chem. Rev.* **2001**, *213*, 79; (e) Gale, P. A. *Coord. Chem. Rev.* **2000**, *199*, 181; (f) Beer, P. D.; Gale, P. A. *Angew. Chem., Int. Ed.* **2001**, *40*, 486.
- (a) Gunnlaugsson, T.; Harte, A. J.; Leonard, J. P.; Nieuwenhuyzen, M. *Chem. Commun.* **2002**, 2134; (b) Gunnlaugsson, T.; Harte, A. J.; Leonard, J. P.; Nieuwenhuyzen, M. *Supramol. Chem.* **2003**, *15*, 505.
- (a) Davis, A. P.; Joos, J. B. *Coord. Chem. Rev.* **2003**, *240*, 143; (b) Davis, A. P.; Lawless, L. J. *Chem. Commun.* **1999**, 9.
- (a) Pfeffer, F. M.; Seter, M.; Lewcenko, N.; Barnett, N. W. *Tetrahedron Lett.* **2006**, *47*, 5251; (b) Xie, H.; Yi, S.; Yang, X.; Wu, S. *New J. Chem.* **1999**, *23*, 1105.
- (a) Gunnlaugsson, T.; Davis, A. P.; O'Brien, J. E.; Glynn, M. *Org. Lett.* **2002**, *4*, 2449; (b) Gunnlaugsson, T.; Davis, A. P.; Glynn, M. *Chem. Commun.* **2001**, 2556.
- Kruger, P. E.; Mackie, P. R.; Nieuwenhuyzen, M. *J. Chem. Soc., Perkin Trans. 2* **2001**, 1079.
- (a) Kang, S. O.; Powell, D.; Day, V. W.; Bowman-James, K. *Angew. Chem., Int. Ed.* **2006**, *45*, 1921; (b) Linares, J. M.; Powell, D.; Bowman-James, K. *Coord. Chem. Rev.* **2003**, *240*, 57.
- McNally, B. A.; Koulov, A. V.; Smith, B. D.; Joos, J.-B.; Davis, A. P. *Chem. Commun.* **2005**, 1087.
- (a) Matthews, S. E.; Beer, P. D. *Supramol. Chem.* **2005**, *17*, 411; (b) Lhotak, P. *Top. Curr. Chem.* **2005**, *255*, 65; (c) Evans, A. J.; Matthews, S. E.; Cowley, A. R.; Beer, P. D. *Dalton Trans.* **2003**, 4644.
- Pfeffer, F. M.; Gunnlaugsson, T.; Jensen, P.; Kruger, P. E. *Org. Lett.* **2005**, *7*, 5375.
- (a) Gale, P. A. *Acc. Chem. Res.* **2006**, *39*, 465; (b) Gale, P. A. *Chem. Commun.* **2005**, 3761.
- (a) Goetz, S.; Kruger, P. E. *Dalton Trans.* **2006**, 1277; (b) Keegan, J.; Kruger, P. E.; Nieuwenhuyzen, M.; O'Brien, J.; Martin, N. *Chem. Commun.* **2001**, 2192.
- (a) Beer, P. D.; Sambrook, M. R.; Curiel, D. *Chem. Commun.* **2006**, 2105; (b) Sambrook, M. R.; Beer, P. D.; Lankshear, M. D.; Ludlow, R. F.; Wisner, J. A. *Org. Biomol. Chem.* **2006**, *4*, 1529.
- (a) Gale, P. A.; Light, M. E.; McNally, B.; Navakhun, K.; Sliwinski, K. E.; Smith, B. D. *Chem. Commun.* **2005**, 3773; (b) Boon, J. M.; Smith, B. D. *Curr. Opin. Chem. Biomol.* **2002**, *6*, 749; (c) Cotes, S. J.; Frey, J. G.; Gale, P. A.; Hursthouse, M. P.; Light, M. E.; Navakhun, K.; Thomas, G. L. *Chem. Commun.* **2003**, 568.
- (a) Gunnlaugsson, T.; Ali, H. D. P.; Glynn, M.; Kruger, P. E.; Hussey, G. M.; Pfeffer, F. M.; dos Santos, C. M. G.; Tierney, J. J. *Fluoresc.* **2005**, *15*, 287; (b) Pfeffer, F. M.; Buschgens, A. M.; Barnett, N. W.; Gunnlaugsson, T.; Kruger, P. E. *Tetrahedron Lett.* **2005**, *46*, 6579; (c) Gunnlaugsson, T.; Davis, A. P.; O'Brien, J. E.; Glynn, M. *Org. Biomol. Chem.* **2005**, *3*, 48; (d) Gunnlaugsson, T.; Davis, A. P.; Hussey, G. M.; Tierney, J.; Glynn, M. *Org. Biomol. Chem.* **2004**, *2*, 1856.
- (a) Gunnlaugsson, T.; Kruger, P. E.; Lee, T. C.; Parkesh, R.; Pfeffer, F. M.; Hussey, G. M. *Tetrahedron Lett.* **2003**, *44*, 6575; (b) Gunnlaugsson, T.; Kruger, P. E.; Jensen, P.; Pfeffer, F. M.; Hussey, G. M. *Tetrahedron Lett.* **2003**, *44*, 8909.
- Other recent examples include: (a) Winstanley, K. J.; Sayer, A. M.; Smith, D. K. *Org. Biomol. Chem.* **2006**, *4*, 1760; (b) Jun, E. J.; Swamy, K. M. K.; Bang, H.; Kim, S. J.; Yoon, J. Y. *Tetrahedron Lett.* **2006**, *47*, 3103; (c) Thiagarajan, V.; Ramamurthy, P.; Thirumalai, D.; Ramakrishnan, T. *Org. Lett.* **2005**, *7*, 657; (d) Jose, D. A.; Kumar, D. K.; Ganguly, B.; Das, A. *Org. Lett.* **2004**, *6*, 3445; (e) Vázquez, M.; Fabbri, L.; Taglietti, A.; Pedrido, R. M.; González-Noya, A. M.; Bermejo, M. R. *Angew. Chem., Int. Ed.* **2004**, *43*, 1962.
- (a) Schazmann, B.; Alhashimy, N.; Diamond, D. *J. Am. Chem. Soc.* **2006**, *128*, 8607; (b) Cao, Y. D.; Vysotsky, M. O.; Bohmer, V. *J. Org. Chem.* **2006**, *71*, 3429; (c) Lang, K.; Curinova, P.; Dudic, M.; Proskova, P.; Stibor, I.; St'astny,

- V.; Lhotak, P. *Tetrahedron Lett.* **2005**, *46*, 4469; (d) Haino, T.; Nakamura, M.; Kato, N.; Hiraoka, M.; Fukazawa, Y. *Tetrahedron Lett.* **2004**, *45*, 2281; (e) Budka, J.; Lhotak, P.; Michlova, V.; Stibor, I. *Tetrahedron Lett.* **2001**, *42*, 1583.
20. Gunnlaugsson, T.; Kruger, P. E.; Jensen, P.; Tierney, J.; Ali, H. D. P.; Hussey, G. M. *J. Org. Chem.* **2005**, *70*, 10875.
21. (a) Evans, L. S.; Gale, P. A.; Light, M. E.; Quesada, R. *Chem. Commun.* **2006**, 965; (b) Evans, L. S.; Gale, P. A.; Light, M. E.; Quesada, R. *New J. Chem.* **2006**, *30*, 1019.
22. (a) Wu, F. Y.; Li, Z.; Guo, L.; Wang, X.; Lin, M. H.; Zhao, Y. F.; Jiang, Y. B. *Org. Biomol. Chem.* **2006**, *4*, 624; (b) Nie, L.; Li, Z.; Han, J.; Zhang, X.; Yang, R.; Liu, W. X.; Wu, F. Y.; Xie, J. W.; Zhao, Y. F.; Jiang, Y. B. *J. Org. Chem.* **2004**, *69*, 6449.
23. Rudkevich, D. M.; Verboom, W.; Reinhoudt, D. N. *J. Org. Chem.* **1994**, *59*, 3683.
24. Camiolo, S.; Gale, P.; Hursthouse, M. B.; Light, M. E. *Org. Biomol. Chem.* **2003**, *1*, 741.
25. Gómez, D. E.; Fabbri, L.; Licchelli, M.; Monzani, E. *Org. Biomol. Chem.* **2005**, *3*, 1495.